Clemson University
TigerPrints

All Dissertations | Dissertations

8-2008

CUES FOR CELLULAR ASSEMBLY OF VASCULAR ELASTIN NETWORKS

Chandrasekhar Kothapalli
Clemson University, sekhar512@yahoo.com

Follow this and additional works at: https://tigerprints.clemson.edu/all_dissertations

 Part of the Biomedical Engineering and Bioengineering Commons

Recommended Citation
Kothapalli, Chandrasekhar, "CUES FOR CELLULAR ASSEMBLY OF VASCULAR ELASTIN NETWORKS" (2008). *All Dissertations*. 238.
https://tigerprints.clemson.edu/all_dissertations/238

This Dissertation is brought to you for free and open access by the Dissertations at TigerPrints. It has been accepted for inclusion in All Dissertations by an authorized administrator of TigerPrints. For more information, please contact kokeefe@clemson.edu.

CUES FOR CELLULAR ASSEMBLY OF VASCULAR ELASTIN NETWORKS

A Dissertation
Presented to
the Graduate School of
Clemson University

In Partial Fulfillment
of the Requirements for the Degree
Doctor of Philosophy
Bioengineering

---

by
Chandrasekhar R. Kothapalli
August 2008

Approved by:
Dr. Anand Ramamurthi (Committee Chair)
Dr. Naren Vyavahare
Dr. Martine Laberge
Dr. Bryan Toole

ABSTRACT

Elastin, a structural protein distributed in the extracellular matrix of vascular tissues is critical to the maintenance of vascular mechanics, besides regulation of cell-signaling pathways involved in injury response and morphogenesis. Thus, congenital absence or disease-mediated degradation of vascular elastin and its malformation within native vessels due to innately poor elastin synthesis by adult vascular cells compromise vascular homeostasis. Current elastin regenerative strategies using tissue engineering principles are limited by the progressive destabilization of tropoelastin mRNA expression in adult vascular cells and the unavailability of scaffolds that can provide cellular cues necessary to up-regulate elastin synthesis and regenerate faithful mimics of native elastin. Since our earlier studies demonstrated the elastogenic utility of hyaluronan (HA)-based cues, we have currently sought to identify a unique set of culture conditions based on HA fragments (0.756-2000 kDa), growth factors (TGF-β1, IGF-1) and other biomolecules (Cu^{2+} ions, LOX), which will together enhance synthesis, crosslinking, maturation and fibrous elastin matrix formation by adult SMCs, under both healthy and inflammatory conditions. It was observed that TGF-β1 (1 ng/mL) together with HA oligomers (0.2 μg/mL) synergistically suppressed SMC proliferation, enhanced tropoelastin (8-fold) and matrix elastin synthesis (5.5-fold), besides improving matrix yield (4.5-fold), possibly by increasing production and activity of lysyl oxidase (LOX). Though addition of IGF-1 alone did not offer any advantage, HA fragments (20-200 kDa) in the presence of IGF-1 stimulated tropoelastin and soluble elastin synthesis more than 2.2-fold, with HMW HA contributing for ~5-fold increase in crosslinked matrix elastin synthesis. Similarly, 0.1 M

of Cu^{2+} ions, alone or together with HA fragments stimulated synthesis of tropoelastin (4-fold) and crosslinked matrix elastin (4.5-fold), via increases in LOX protein synthesis (2.5–fold); these cues also enhanced deposition of mature elastic fibers (~ 1 μm diameter) within these cultures. Interestingly, instead of copper salt addition, even release of Cu^{2+} ions (~ 0.1 M) from copper nanoparticles (400 ng/mL), concurrent with HA oligomers, promoted crosslinking of elastin into mature matrix, with multiple bundles of highly-crosslinked elastin fiber formation observed (diameter ~ 200-500 nm). These results strongly attest to the potential individual and combined benefits of these cues to faithful elastin matrix regeneration by healthy, patient-derived cells within tissue-engineered vascular constructs.

When these *cues* (TGF-β1 and HA oligomers) were added to TNF-α-stimulated SMC cultures, model cell culture systems mimicking phenotypically-altered cells within aneurysms, they upregulated elastin matrix production, organized elastin protein into fibers, and simultaneously stabilized this matrix by attenuating production of elastolytic enzymes. Similarly these cues also attenuated inflammatory cytokines release within cells isolated from induced-aortic aneurysms in rats, and significantly upregulated elastin synthesis and matrix formation by upregulating LOX and desmosine protein amounts. The cues were also highly effective in organizing the elastin into fibrous matrix structures mimicking the native elastin deposition process. The outcomes of this study might be of tremendous use in optimizing design of HA constructs to modulate vascular healing and matrix synthesis following revascularization, and in enabling repair of elastin networks within diseased or inflammatory (aneurysmal) adult vascular tissues.

ACKNOWLEDGEMENTS

This work would not have been possible without the help of many people. First of all, I would like to express my gratitude to Dr. Anand Ramamurthi, for trusting my abilities and introducing me to the field of cardiovascular tissue engineering, in which I had no prior experience. Dr. Ramamurthi was very helpful and patient in guiding me through this work, besides his encouragement and advice with my career decisions. It would be more appropriate to say that I worked 'with' Dr. Ramamurthi for my PhD, rather than 'for' Dr. Ramamurthi. I would also like to thank my committee members – Prof. Martine Laberge, Prof. Naren Vyavahare and Prof. Bryan Toole, for their guidance and advice in bringing this work to fruition. I really appreciate their flexibility in accommodating my committee meetings, despite their busy schedules.

I would also like to thank members of CTEL, especially Binata for initially showing me how to perform biochemical assays, and Samir for his insights on laboratory techniques. Carol Moskos of the electron microscopy lab at MUSC and Joan Hudson of the microscopy facility at Clemson were very helpful with elastin imaging techniques. I would especially like to thank Prof. Vyavahare's lab for making some of my Clemson trips successful: Jake Isenburg and Dev Raghavan for helping with the atomic absorption spectroscopy measurements, Chaitra Cheluvaraju and LaShan Simpson for their help with rat aneurysm-inducement surgeries. Drs. Dan Simionescu and Agneta Simionescu were also very helpful in training me how to perform gel zymography analysis in their lab. Dr. Rick Visconti's lab at MUSC familiarized me with RT-PCR and allowed me use their facilities for the same. The list would not be complete without thanking my friends

outside the lab (Bala, Abhijit, Glady, Bret, Michael, Sashi, Venkat), who invited me for numerous lunches and dinners. I really had great time with y'all.

I would like to thank my family members who have always supported my decision to attend graduate school. My mom (Annapurna) and dad (Prof. Rao) have always been understanding and appreciative of my efforts, in spite of me visiting them only thrice in eight years. They constantly encouraged me and made me realize the 'philosophy' component of PhD. And last but not least, I want to thank my wife – Smita, for truly understanding the time commitments involved in grad school, and helping me graduate in a timely fashion.

I hope the current and future students have fun working in CTEL as much as they enjoy Charleston life. In case you happen to read this section and did not find your name, please contact me and we can discuss.

DEDICATION

To my Advisor, Parents and Smita

TABLE OF CONTENTS

Page

Table of Contents (Continued)

Page

Table of Contents (Continued)

Page

Table of Contents (Continued)

Page

Table of Contents (Continued)

Page

Table of Contents (Continued)

Page

LIST OF FIGURES

Page

List of Figures (Continued)

Page

List of Figures (Continued)

Page

LIST OF TABLES

Page

CHAPTER 1

INTRODUCTION

1.1. Background

Abdominal aortic aneurysms (AAAs) are pathological conditions wherein segments of elastic arteries dilate and structurally weaken resulting in fatal vessel rupture[1]. AAAs are also frequent outcomes of inherited conditions such as Marfans syndrome – characterized by defects in assembly and stabilization of arterial elastin[2], chronic matrix proteolytic effects by inflammatory cells (e.g., macrophages) that infiltrate in response to calcified lipid deposits within the abdominal aortic wall[3]. In the United States alone, more than 70,000 surgeries are performed annually to treat AAAs[3], and despite this, nearly 16,000 people die every year due to this condition[4]. Specifically, AAs are characterized by arterial dilatation, degeneration of the arterial structure, decrease in medial elastin content, disruption or fragmentation of elastic lamellae, presence of matrix-degrading enzymes such as matrix metalloproteinases (MMPs), inflammatory infiltration, and calcification[5-9]. The rupture of AAs is associated with mortality rates of ~ 80%[10]. Since elastin is a major component of the extracellular matrix (ECM) in vascular connective tissues, these pathological events degrade insoluble crosslinked elastin to soluble peptides[11], which further promotes macrophage-mediated matrix destruction *via* secretion of cytokines, chemokines, interleukins, and proteinases[12, 13]. The pathogenesis of AAs could also arise from enzymatic degradation of healthy elastic fibers and excessive accumulation of proteoglycans[14], leading to loss of elasticity and

strength of the aortic wall, and progressive dilation to form a rupture-prone sac of weakened tissue[1]. Thus, absence or destruction of elastin critically regulates aneurysm formation, progression and fatal rupture, while restoration of elastin in these segments will likely stabilize and restore homeostasis in these tissues.

Current surgical methods for AA treatment have been: *open aneurysm repair* - wherein the weakened aortic segment is replaced with a sutured synthetic mesh graft, and *endovascular abdominal aortic aneurysm repair* - wherein a woven polyester graft mounted on a self-expanding stent is deployed within the aneurysm site[15]. Currently, the elective repair of AAs, which is performed to prevent aortic rupture in nearly 40,000 patients each year, results in about 1500 operative deaths[16]. Standard open surgical repair (aneurysectomy) and endovascular aortic aneurysm repair (EVAR) are the two widely used surgical treatment methods that are currently available[16]. Though these procedures are associated with low mortality rates (< 5%), high operational success rates (> 85%) and short recuperation times, long-term cardiac and pulmonary complications and other surgical and graft-associated complications can cause patient survival rates to drop to ~ 50% at 10 years post-operation[17]. Current pharmacological treatment options are limited for patients with small aneurysms, even though this group makes up the largest percentage of all AAA patients[18]. Several pharmacological approaches have been tested thus far, including anti-inflammatory agents, genetic and pharmacological inhibition of MMPs and proteinase inhibitors, though none of these are completely effective, nor have been tested clinically[19, 20]. Chemical stabilization of existing elastin matrices is yet another promising approach, but is not expected to restore elastin that has

already been degraded[21]. We believe that active cellular-mediated regeneration of lost elastin within the aneurysmal sites could potentially revolutionize AAA treatment via standalone application or by integration with other surgical and non-surgical approaches. However, this is challenging since adult vascular cells do not generate much elastin on their own and mature elastic fibers rarely undergo active remodeling. Thus, regeneration of elastin networks in aneurysmal vessel segments is the focus of next generational therapies targeted at aneurysm treatment.

1.2. Regenerative Strategies

Current efforts at *in vivo* or *in vitro* regeneration of matrix structural networks comprise a recently explored sub-field of regenerative medicine, termed matrix tissue engineering.

Matrix tissue engineering can be defined as the therapeutic approach combining cells, scaffolding materials and biochemical cues, focused on regenerating and restoring the ultrastructure and biochemical roles of extracellular matrix networks, to thereby restore homeostasis in target connective tissues.

Tissue engineering offers a promising approach for the fabrication of a functionally-responsive, living-tissue like constructs with biological and biomechanical properties that mimic native vascular tissue. In recent years, researchers have explored the possibility of effecting elastic tissue repair through regeneration of elastin in situ within elastin-compromised vessels and synthetic or tissue engineered grafts *in vitro* culture systems deployed at the site of vascular disease or injury. Although considerable

progress has been made towards understanding the principles of elastin biosynthesis, and matrix assembly, ultrastructural organization and stabilization *in vivo*, many of the conditions and mechanisms required to replicate the same, with provided cues are still elusive. This is especially challenging in light of the extremely poor elastin regenerative capacity of adult human and other cells, vascular and non-vascular in origin. Thus, identifying elastogenic cues as represented by elastogenic biomaterials scaffolds or growth factors; and further modulating the assembly of the elastin precursors into ultrastructural and functional mimics of native elastin are immense challenges.

1.2.1 Cellular Scaffolds for Elastin Tissue Regeneration

Previous attempts to repair and regenerate elastin *in situ* at disease/ injury sites using synthetic tissue-engineered[22, 23] grafts have not succeeded due to the progressive destabilization of tropoelastin mRNA expression in post-neonatal vascular cells[24]. Though synthetic scaffolds allow precise control over properties such as molecular weight, porosity, microstructure, degradation time and mechanical properties[25], they result in poor cellular interaction, abridged ECM remodeling and inefficient elastin crosslinking[23]. Implants made of synthetic elastomers[26, 27] do not elicit cell signaling pathways, despite restoring mechanical properties; while functionalization of elastic allografts[28] or xenografts[29, 30] are curtailed by the inefficiency of current chemical processes[31] in completely removing native cells and proteins essential to prevent immune rejection[30] and calcification[32] in the host without compromising native elastin architecture[33, 34]. Besides, elastomer-assemblies from natural or synthesized polypeptide

precursors[35-37] and synthetic cell scaffolds that provide elastogenic biomechanical cues *in vitro* or *in vivo*[38-40] only marginally replicated the functional architecture and mechanics of native elastin, especially since they do not incorporate other elastin-associated proteins (e.g., fibrillin, oxytalan) crucial to elastic fiber formation and properties[41, 42]. Recent successes in synthesizing native elastin-like fibers within fibrin-collagen constructs cultured with *neonatal* RASMCs strongly demonstrate the superiority of ECM-based cell scaffolds over synthetic scaffolds for simulating the physical and chemical environment of tissues[22, 43]. As components of native tissues, ECM-based scaffolds are more likely to evoke native integrin-ECM interactions and preserve the native cell phenotype and matrix synthesis capabilities[22]. Thus, a challenge for faithful elastin matrix regeneration by adult cells lies in identifying appropriate cues based on specific ECM molecules, that have been shown to influence and regulate elastin synthesis, maturation, and organization *in vivo*[22, 44].

1.2.2 Hyaluronan Cues for Elastin Regeneration

ECM molecules (e.g. GAGs) have been shown to influence elastin synthesis and organization during development, through their association with proteoglycans[45-47]. Specifically, HA has been suggested to participate in elastogenesis through its strong binding with versican[48], which in turn interacts with elastin-associated microfibrils to form higher-order structures important to elastin fiber synthesis[49-51]. Moreover, it has been suggested that anionic HA chains coacervate soluble tropoelastin and facilitate local crosslinking into a stable elastin matrix[52, 53]. These studies encourage our exploration of

the elastogenicity of HA biomaterials. However, prior studies indicate that the physicochemical and biological properties of HA depend on its size[54]. Studies by our group and others have shown that HA fragments (MW<1 MDa) and oligomers (MW<1 kDa) are more cell-interactive[55] than the relatively bio-inert HMW HA (>1 MDa)[56]. Evanko *et al*., showed that though HA 6-mers do not affect proliferation of healthy vascular SMCs[57], they inhibit SMC proliferation in diseased tissues[57]. Studies by Joddar *et al*.[58] clearly showed enhanced elastogenic responses of RASMCs to HA 4-mers (MW ~ 756 Da), although HMW HA appeared to facilitate elastin crosslinking and matrix deposition *via* purely physical interactions[59]. These studies also mirrored the results of Evanko *et al.*,[57] in that HA oligomers did not influence proliferation of healthy adult vascular SMCs[58, 60]. These prior outcomes therefore suggested that HA fragments may usefully cues for elastin synthesis and stability, and inhibit SMC hyperplasia, common in elastin-compromised, diseased vessels. Thus, optimizing the HA fragment-sizes based on their benefits to elastin synthesis and stabilization by adult vascular SMCs, without stimulating inflammatory cell responses, is vital towards developing cellular-based therapies for regenerating elastin matrices.

1.2.3 Elastogenic Growth Factors and Biomolecules

Biochemical regulators present in ECM have been shown to influence both the cellular phenotype and the amount/ quality of the elastin deposition[61, 62]. Elastin synthesis was reportedly enhanced by stimulating SMCs with growth factors such as TGF-β and IGF-1, which up-regulate cellular tropoelastin mRNA expression[63-65] and

encourage LOX-mediated crosslinking of soluble tropoelastin into a mature, insoluble matrix[66]. Insulin like growth factor (IGF-1) with 500 ng/mL concentration was shown to induce 86 ± 14 and 35 ± 5% increases in tropoelastin and total elastin protein synthesis, respectively, by rat neonatal pulmonary fibroblasts, relative to controls[67]. This was confirmed by a corresponding 95 ± 20% increase in the tropoelastin mRNA/beta-actin mRNA ratio[67]. In addition, a dose dependence of tropoelastin synthesis on IGF-1 concentration was noted. Kahari *et al*. examined the effects of short-time exposure of TGF-β1 on elastin mRNA abundance, promoter activity, and mRNA stability in cultured human skin fibroblasts and found a TGF-β1 dose-dependent increase in elastin mRNA steady-state levels, with a maximum enhancement of ~30-fold attained at a dose of 1 ng/mL[68]. These results demonstrate that TGF-β1 is a potent enhancer of elastin gene expression and that this effect is mediated, at least in part, post-transcriptionally. In addition, TGF-β has been suggested to augment LOX-mediated crosslinking of soluble tropoelastin into a mature, insoluble matrix layer[69, 70]. Metal ions (e.g., copper or Cu^{2+}) in extracellular environment also regulate biologic processes such as minimizing vascular defects[71], promoting angiogenesis[72, 73] and enhancing LOX activity[74]. Thus, from a tissue engineering perspective, exposing healthy cells to suitable combination of biomolecular cues has immense potential to modulate the amount, quality and ultrastructure of the elastin matrix they lay down to engineer constructs that mimic the biologic and functional characteristics of native tissues. However, from the standpoint of in situ regeneration of degraded elastin matrices *in vitro*, it is yet unknown, if and how these biochemical cues will benefit the elastin matrix amount and quality, when therapeutically applied to

chronically-stimulated or injured cells. The purpose of this study is to identity and optimize unique combinations of therapeutic cues that will allow *in vivo* and *in vitro* regeneration of elastin structures that are ultrastructurally-faithful to native elastin tissue structure. Establishment of such guidelines will greatly facilitate development of technologies that can enable tissue engineering of elastin-rich constructs, and/or open up new non-surgical novel therapies that will enable regenerative repair of degraded elastin matrices by cells in situ at disease/injury sites.

1.3. Study Objectives and Aims

Based on the previous background, the objective of this project is to determine:

a) The potential benefits of growth factors (TGF-β, IGF-1) and biomolecules (e.g., Cu^{2+}) together with exogenous HA fragments (0.76-2000 kDa) on elastin matrix synthesis and organization by adult SMCs;

b) The impact of optimized cues (HA fragments and biomolecules) on the quality (amount, ultrastructure, alignment, efficiency, stability) of the synthesized elastin matrix;

c) The benefits of providing optimized cues to chronically-stimulated (aneurysmal) SMCs towards restoring their elastin synthesis and crosslinking abilities.

The **scientific impact** of this work is the ability to tissue-engineer elastin matrices by both healthy and chronically-stimulated adult cells, which inherently do not produce

much elastin, towards restoring homeostasis in de-elasticized vessels. Accordingly, three **specific aims** are proposed:

Specific Aim 1: Investigate the standalone/ combined benefits of exogenous delivery of growth factors (TGF-β or IGF-1) and HA fragments to elastin synthesis, maturation and organization by adult RASMCs.

Rationale: (a) An optimal HA fragment-size exists that maximizes cellular elastin output and yet preserves the non-proliferative cellular phenotype; (b) Concurrent delivery of HA fragments and growth factors will upregulate elastin synthesis, maturation, and stabilization to a greater extent than possible by providing either of these cues separately; and (c) A unique set of cues exists that is conducive to the fabrication of a mimic of native vascular elastin.

Specific Aim 2:

A. Determine the standalone and combined benefits of culturing adult RASMCs with soluble copper sulfate ($CuSO_4.5H_2O$) and HA fragments (0.76-2000 kDa), to elastin matrix synthesis and organization (crosslinking density, composition and ultrastructure).

B. Compare the impact of copper delivery mode, *i.e.*, soluble $CuSO_4$ *vs.* copper nano-particles (CuNP; 80-100 nm) on elastin matrix synthesis and quality.

Rationale: (a) Concurrent delivery of HA fragments and Cu^{2+} ions will upregulate elastin synthesis, maturation and stabilization to a greater extent than possible by providing HA cues alone; (b) HA-Cu^{2+} complex will facilitate coacervation of tropoelastin to enable enhanced lysyl oxidase (LOX)-mediated crosslinking to form elastin networks; and (c) An efficient delivery mode and dose of Cu^{2+} exists that promotes elastin organization and stabilization with no cellular toxicity.

Specific Aim 3:

A. Evaluate the efficacy of cues (HA oligomers, growth factors, Cu^{2+}) optimized in aims 1 and 2 to suppress elastin-degrading enzymes (e.g., MMPs) and promote synthesis of native elastin mimics by chronically-stimulated adult RASMCs.

B. Compare the elastogenic benefits of cues on elastin matrix synthesis by aneurysmal adult RASMCs.

Rationale: (a) Cells subjected to chronic-stimulation respond to the elastin regenerative cues identified in aims 1 and 2 of this project; (b) These cues will suppress MMPs and other elastolytic activity of cells, and restore stimulated RASMCs to a healthier phenotype.

1.4. Organization of Dissertation

In chapter 2, we present a comprehensive overview of elastin, it's location, structure, physiological relevance in blood vessels, biomechanics, pathological

significance in healthy and diseased conditions, and current strategies for restoration of vascular elastin homeostasis.

Chapters 3 and 4 details the effect of growth factors, that of TGF-β1 or IGF-1, alone or together with HA fragments/ oligomers, on elastogenesis by adult RASMCs. The benefits of exogenous delivery of these cues to elastin production, stabilization, crosslinking and maturation by healthy RASMCs were elaborated.

Chapter 5 details the benefits of exogenous copper ion delivery, from copper sulfate or copper nanoparticles (CuNP), concurrent with HA fragments/ oligomers, to elastin crosslinking and fiber formation by RASMCs. The mode of copper ion delivery and the concentration of copper ions which will maximize native elastin mimics formation were optimized. Besides, the benefits of exogenously delivered bovine LOX protein to RASMC-mediated elastin synthesis and crosslinking were evaluated.

Chapter 6 details the utility of optimized cues (from chapter 3) towards restoring elastin output and matrix organization by RASMCs under chronically-stimulated conditions *in vitro*. Chapter 7 details the innate elastin matrix synthesis by SMCs isolated from aneurysmal rat aortic segments, and their release of inflammatory biomolecules. Further, the chapter details our efforts to determine the the utility of elastogenic cues, identified and optimized in chapter 3, for minimizing inflammation and restoring healthy elastin synthesis by these cells.

Finally, chapter 8 will list the overall conclusions we derived from this multi-faceted project, identify future directions for the short and long-term progress of the current work.

CHAPTER 2

LITERATURE REVIEW

2.1 Vascular Anatomy

2.1.1 Structure and Functions

Blood vessels are conduits that distribute blood to bodily tissues and can be broadly classified into two distinct circulating pathways namely: *pulmonary vessels* – which transports blood from the right ventricle to the lungs and back to the left atrium and, *systemic vessels* – which carry blood from the left ventricle to the tissues in all parts of the body and then return the blood to the right atrium. Based on their structure and function, blood vessels are classified as *arteries*, *veins* or *capillaries* (**Figure 2.1**). Arteries carry the blood away from the heart, while veins return blood from tissues back to the heart. Another difference between arteries and veins is that the layers in vein wall are not as distinct as in arteries.

Both arteries and veins have a defined three-layered structure with the *tunica intima* (inner wall of the vessel) adjoining the vessel lumen, the *tunica media* (middle layer) and the *tunica adventitia* (outer layer). The *tunica intima,* the innermost layer of arteries is made up of simple squamous epithelium surrounded by a connective tissue basement membrane. Endothelial cells present in this layer rest on a basement membrane made up of extracellular matrix (ECM) consisting collagen type IV, laminin and heparin sulfate proteoglycans[75]. The *tunica intima* is separated form *tunica media* by a layer of elastin sheets and fibers, called as *internal elastic lamina* (IEL). The *tunica*

media layer is usually the thickest layer in arteries, especially those of large size (> 1 cm; elastic and muscular arteries), which not only provides mechanical support for the vessel but also regulates vessel diameter to accommodate pulsatile blood flow and regulate blood pressure. It contains concentric layers of circumferentially-organized smooth muscle cells (SMCs) alternating with elastin sheets (lamellae) arranged into concentric bundles. SMCs are responsible for the synthesis of elastin, collagen and other ECM components, and also serve to regulate blood flow by constricting and dilating the blood vessel. The *tunica media* extends from the IEL to the *external elastic lamina* (EEL). The *tunica adventitia* layer provides the outer covering of arteries, forming between 10-50% of the arterial wall thickness, and consists predominantly of fibroblasts and longitudinally-aligned collagen-rich ECM[75]. This is the primary load-bearing layer that allows the arteries to stretch and prevent over-expansion due to pressure exerted on the walls by blood flow. The relative thickness and composition of the vascular layers in *media* vary progressively, with vessel size and location. In large vessels such as the aorta, where high blood pressures must be accommodated, the media is thick with concentric fenestrated elastic sheets separated by fibroblast-produced collagen and SMCs; these vessels are thus very elastic. Farther away from the heart, within the distributing muscular arteries, the proportion of smooth muscle to elastin increases dramatically; the media contains 3-40 SMC layers. These cells serve to adjust flow in response to sympathetic nerve stimulation. Further away from the heart, arteries branch into arterioles (< 0.5 mm), wherein the media may be as few as 2-3 concentric smooth

muscle cells. The adventitia is very thin and these arterioles provide major resistance to blood flow.

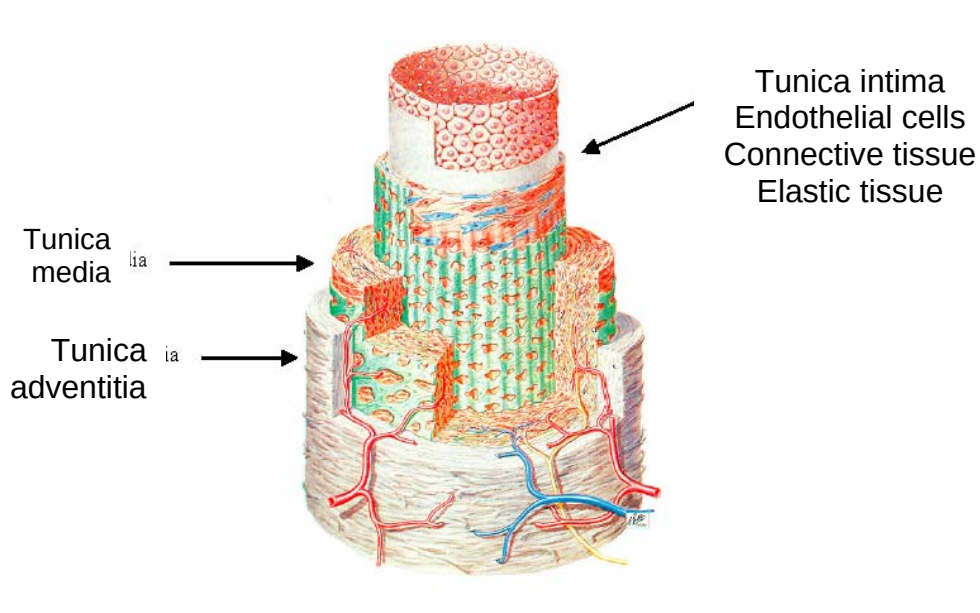

Figure 2.1. Anatomy of blood vessels[76].

2.1.2 Cellular Components of Vascular Tissues

The major cell types found in cardiovascular tissues include cardiac fibroblasts, cardiomyocytes, endothelial cells (ECs), and smooth muscle cells (SMCs) – all of these cells interact dynamically with the ECM in response to mechanical strains during development and disease[77]. Under healthy non-activated conditions these cell regulate numerous processes to maintain homeostasis, but if damaged or diseased, they initiate restorative signaling pathways that can lead to further tissue impairment if prolonged. In this section, we detail in brief, the characteristics and functions of two important cell types in blood vessels, ECs and SMCs, under healthy and diseased conditions.

ECs line the lumen of all blood and lymph vessels and act as a wall between the blood and vascular tissue and therefore, are capable of communicating with both blood and tissue species. ECs act as a semi-permeable layer controlling the transfer of cellular and fluid blood elements into the vessel wall. These cells have a highly specialized surface: the apical surface interacting directly with the blood, the basal surface contains adhesion junctions that attach the EC to the basal lamina, and the lateral surface comprised of junctions responsible for joining ECs together and allowing communication between ECs. Adjacent ECs connect and communicate with each other via three types of cell junctions: tight junctions, anchoring junctions and gap junctions.

ECs secrete a number of types of collagen into their sub-endothelium (basal matrix), the most abundant being collagen IV and V[78]. Type IV collagen is involved in EC adhesion and proliferation, while type V collagen inhibits EC growth[79]. Laminin, a glycoprotein secreted by ECs into the basal lamina, supports growth and adhesion of ECs[80], although ECs do not migrate on laminin coated surfaces[81]. The luminal surface of ECs is covered with a thin layer of heparin sulfate (glycocalyx) synthesized by the cells themselves, while the basal lamina contains numerous other glycosaminoglycans (GAG) components, including dermatan sulfate, heparin sulfate and chondroitin sulfate[82, 83].

SMCs are responsible for vessel contractility and remodeling during growth and pathogenesis. Under homeostasis conditions, vascular SMCs express differentiation markers, remain in contractile phenotype, with low proliferation. They participate in healthy turnover of ECM in the blood vessels and maintain normal signaling mechanisms with the environment they inhabit. *In vivo*, SMCs mainly experience cyclic tensile

strains due to pressure forces of the blood and compression due to thinning of the vessel wall during inflation[84]. These cyclic strains increase cellular collagen and elastin synthesis although synthetic responses are sensitive to strain magnitude, frequency, and duration[85, 86]. However, in response to several physiological and pathological stimuli, mature SMCs can undergo phenotypic modulation (from contractile to synthetic) and reenter the cell cycle. Many growth factors and cytokines have been shown to stimulate vascular SMC proliferation and/or matrix production *in vitro* and *in vivo* [87, 88], which includes but not confined to, platelet-derived growth factor (PDGF), basic fibroblast growth factor (bFGF), tumor necrosis factor-α (TNF-α), insulin-like growth factor-1 (IGF-1), interleukin-1 (IL-1) and transforming growth factor-β (TGF−β). Besides these factors, hypertension and mechanical injury were also found to profoundly influence the SMC phenotype[89]. Abnormal SMC proliferation is thought to contribute to the pathogenesis of vascular occlusive lesions, including atherosclerosis, vessel renarrowing (restenosis) after angioplasty, and graft atherosclerosis after coronary transplantation. Therefore, elucidating the molecular mechanisms governing vascular SMC proliferation, and its implication in cardiovascular disease is of great interest.

From this discussion we can infer that, changes in the intravascular environment, mechanical stimulation of cells within the vascular wall, and complex cellular-signals coordinating the SMC phenotype/ matrix synthesis mechanisms, can lead to activation of SMCs to elicit abnormal biological responses that manifest themselves as the pathology of vascular disease.

2.1.3 Components of Vascular ECM

The extracellular matrix (ECM) is a complex structural entity surrounding and supporting cells that are found within connective mammalian tissues[90]. ECM components are synthesized, organized and remodeled by the cells around and within the matrix. The vascular ECM is primarily composed of three classes of biomolecules namely, (a) structural proteins such as elastin and collagen, (b) fibrous proteins such as fibrillin, fibronectin and laminin, which have both structural and adhesive functions, and (c) proteoglycans, composed of a protein core to which long chains of repeating disaccharide units of GAGs are attached. All these components complex with one another to form high molecular weight macromolecular structural units[91].

Collagen is the most abundant protein found in the ECM, which is primarily responsible for providing support and tensile strength to the tissue structure[92]. There are at least 12 types of collagen, out of which types I-III are the most abundant and predominantly seen in bone, skin, muscle, cartilage and tendon[93]. Type IV collagen is a major component of the basal lamina[94]. Collagens are predominantly synthesized by fibroblasts but epithelial cells also synthesize these proteins[95]. In addition to its structural role, collagen is also believed to be involved in promoting cell attachment and differentiation although the mechanisms are not yet clearly elucidated. Their defining structural feature is a triple-stranded helical structure of three polypeptide chains, which are composed of a series of three amino acid (Gly-X-Y) sequences where typically, X is proline and Y is a post-translationally modified form of proline called 4-hydroxyproline[92]. Once the pro-collagen is secreted, proteolytic enzymes splice the pro-

polypeptides from pro-collagen, allowing it to form much longer collagen fibers in the extracellular space. Aggregations of these fibrils (10–30 nm diameter) form collagen fibers (500–3000 nm in diameter), which are then organized to reinforce the tensile strength of the respective tissue in which they are present.

GAGs are unbranched polysaccharide chains composed of repeating disaccharide units, with one of the two sugars in the repeating disaccharide being a modified amino sugar (*N*-acetylglucosamine or *N*-acetylgalactosamine)[96]. The second sugar is usually uronic acid (glucuronic or iduronic). Because of carboxyl-groups on most of their sugars, GAGs are highly negatively charged. GAGs may be classified as those that are sulfated (e.g., chondroitin sulfate, dermatan sulfate, heparin sulfate) and those that are non-sulfated (hyaluronic acid: HA) (**Figure 2.2**). In aortic tissues, GAGs closely associate with collagen and elastic fibers, which in turn suggests orderly interactions between them and the cellular components[91].

Unique among the GAGs is the sole unsulfated GAG, a very long-chain biopolymer, hyaluronan (HA). HA, composed of repeating GlcNAc β1-3, GlcA β1-4 linkages, is the simplest known GAG and is abundant in skin, synovial fluid and skeletal tissues[97]. In cardiovascular tissues, HA has been implicated in early tissue development (vasculogenesis). In adult tissues, HA is also produced in large quantities during wound healing, including within inflamed blood vessels, where it is thought to precede and modulate synthetic activities of cells leading to matrix deposition. A more detailed explanation of HA synthesis, forms and its implicated mechanisms in vasculogenesis is described in later sections.

Proteoglycans, on the other hand, are complex macromolecules that contain a core protein to which huge clusters of GAG chains are covalently bound. Proteoglycans have extended structures in solution and occupy very large hydrodynamic volumes relative to their molecular weights. This property is critical in the functioning of cartilaginous structures that must act as cushions for variable, compressive loads. Proteoglycans bind various secreted signaling molecules such as fibroblast growth factor (FGF) and transforming growth factor (TGF-β), and can enhance or inhibit their signaling activity, thereby regulating cell behavior and their interactions with one another. They also sterically block the activity of these proteins, and serve as a storage reservoir of the proteins, enabling delayed release.

ECM is composed of other proteins with multiple protein-binding domains, which adhere to the scaffolding molecules and to cell surface receptors, thereby contributing not only to the organization of the ECM but to the cells within it. Fibulins are a family of calcium binding proteins that are found in the ECM, and they play an important role in development. *In vivo* fibulin-1 is found in association with elastic fibers that contain elastin and fibrillin. Fibronectin is a large, secreted glycoprotein dimer (each chain ~270 kD) with the chains joined by disulfide bonds at one end[98]. It exists in multiple isoforms, one of which is a soluble form found in blood and other body fluids where it is thought to be involved with blood clotting and wound healing[99].

2.2 Elastin – An Overview

A network of elastic fibers in the ECM of connective tissues such as skin, blood vessels and lungs, provides them strong resilience and the ability to recoil, after transient stretch. A detailed discussion of the distribution, composition, synthesis, ultrastructure and roles of elastin in the context of maintaining vascular homeostasis, of their mechanisms of turnover, abnormal degradation and current state of science for their restoration follows in this section.

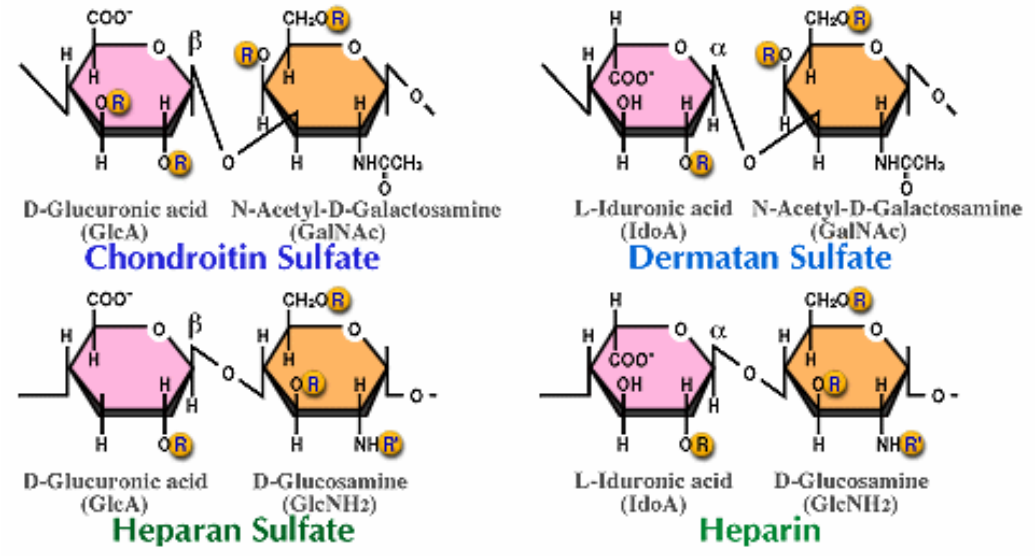

Figure 2.2. Repeating disaccharide units of various glycosaminoglycans[100].

2.2.1 Elastin Distribution

Elastin is distributed in the arterial walls, pulmonary tissues, intestines, and skin, as well as in other tissues where stretching and elasticity are required for normal function of these tissues[101], as given in **Table 2.1**. Elastin is the predominant ECM protein in

arteries, comprising around 30-50% of the dry mass of the aorta. However, the relative amount of elastin varies across a range of tissues and species depending on its function. For example, loose connective tissues such as skin contain sparse distribution of elastic fibers, around 2-5% by weight[102]. Typically, elastic fibers are associated with collagen to prevent excessive tissue stretch and tearing, and are surrounded by an amorphous matrix environment composed of GAGs and proteoglycans[103]. For example, elastic ligaments consist of thick elastin fibers (100 μm) interspersed with collagen fibers in structures such as *ligamenta flava* of the vertebral column and the *ligamentum nuchae* of the neck[103]. In cardiovascular tissues, long inelastic collagen fibrils are generally inter-woven with the elastic fibers to limit the extent of their stretching and to prevent the tissue from tearing at abnormally high loads. Elastic fibers are thinner and straighter than collagen fibers and are arranged in a branching pattern to form a three-dimensional network of fibers, inter-woven fibers, sheets and fenestrated sheets. Recent studies have reported that the form and nature of elastin deposited in connective tissues vary significantly with their aging, with the greatest differences being observed between developing and geriatric tissues, as shown in **Figure 2.3** below.

Tissue	**Percentage of composition**			
	Collagen	**Elastin**	**GAGs**	**Water**
Tendon/ligament	30	1.5	0.03-0.3	65
Skin	30	0.2	0.03-0.35	60-72
Fibrocartilage	20	0.1-0.2	0.6	75
Elastic cartilage	16	5-7	3-4	70
Hyaline cartilage	5-18	< 0.1	5-11	75
Bone	5-20	-	0.4	30-50
Cornea	12-15	-	0.2-1.0	80
Aorta	5-15	7-15	0.2-2.5	70-75
Elastic ligament	9	35	-	55

Table 2.1. Elastin distribution in mammalian tissues[104].

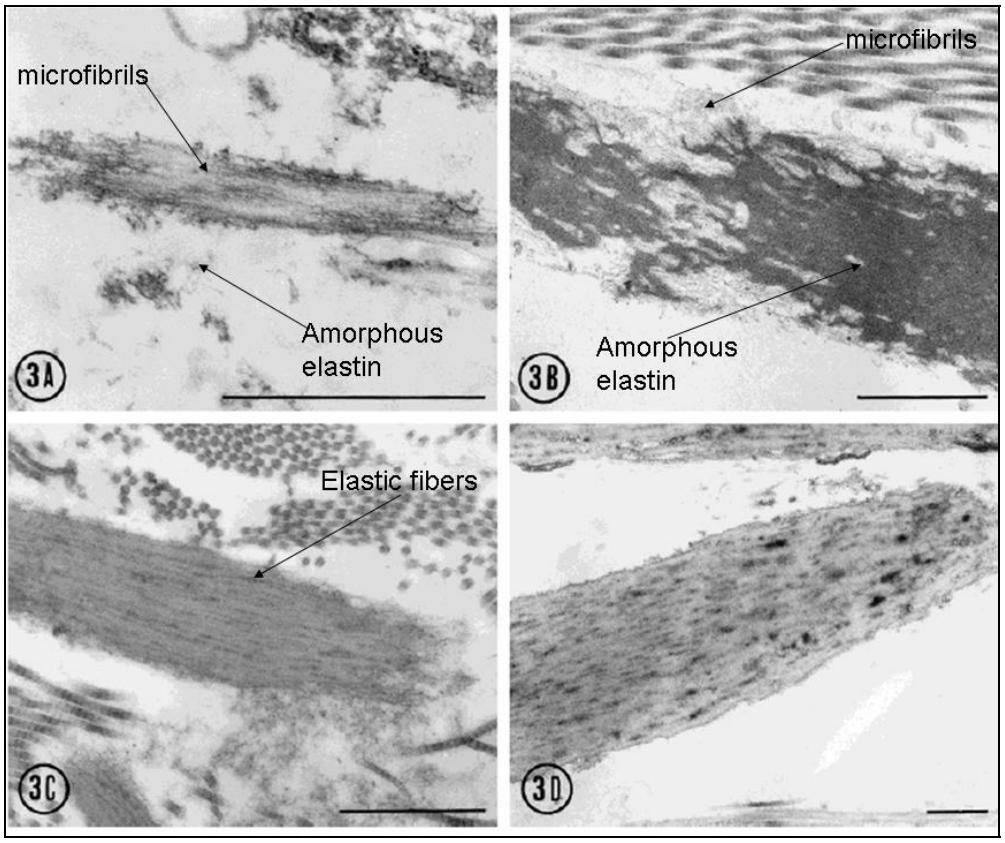

Figure 2.3. Ultrastructural appearance of human dermal elastic fibers during aging[105]. (A) elastic fiber composed of bundles of microfibrils with very little amount of amorphous elastin in five-day-old baby. (B) Elastic fiber is wider and consists of amorphous elastin surrounded by a variable number of microfibrils in a ten-year-old boy. (C) mature elastic fiber mostly consisting of amorphous elastin, containing electron-opaque longitudinal strips, and surrounded by a few microfibrils in a sixteen year-old boy; (D) electron-dense irregular precipitates often seen within the amorphous elastin in a forty-eight-year-old woman. Scale bar: 1 μm.

2.2.2 Composition of Elastin

Elastin, the main component of elastic fibers, is a highly hydrophobic protein consisting of a highly conserved peptide sequence 'VGVAPG', which contributes to the protein being highly rich in proline and glycine amino acids (**Table 2.2**). The typical amino acid composition of elastin is largely conserved across species and is composed of non-polar amino acids with a few polar side chain residues. Elastic fibers formed within tissues by the cellular-mediated deposition process vary in thickness, length and tri-dimensional architecture depending on the direction and magnitude of the forces exerted upon the tissue. Unlike collagen, elastin is not glycosylated and contains some hydroxyproline, but very minimal hydroxylysine. Elastin protein is mainly composed of two types of short segments that alternate along the polypeptide chain: hydrophobic segments, which adopt a β-sheet confirmation that is responsible for the elastic properties of the molecule, and alanine- and lysine-rich α-helical segments, which form cross-links between adjacent molecules (**Figure 2.4**).

Amino acid (AA)	**Residues per 1000 AAs**
Aspartic Acid (Asp)	3.6
Glutamic acid (Glu)	13.9
Serine (Ser)	15.9
Glycine (Gly)	382.1
Histidine (His)	0
Arginine (Arg)	6.6
Threonine (Thr)	10.3
Alanine (Ala)	214.6
Proline (Pro)	104.8
Tyrosine (Tyr)	35.9
Valine (Val)	81.4
Methionine (Met)	0

Cysteine (Cys)	0
Isoleucine (Ile)	24.1
Leucine (Leu)	64.8
Phenylalanine (Phe)	13.9
Lysine (Lys)	1.7
Isodesmosine (Ides)	2.2
Desmosine (Des)	3.4

Table 2.2. Amino acid composition of elastin derived from rat aorta. Values are expressed as residues/1000 total amino acid residues[106].

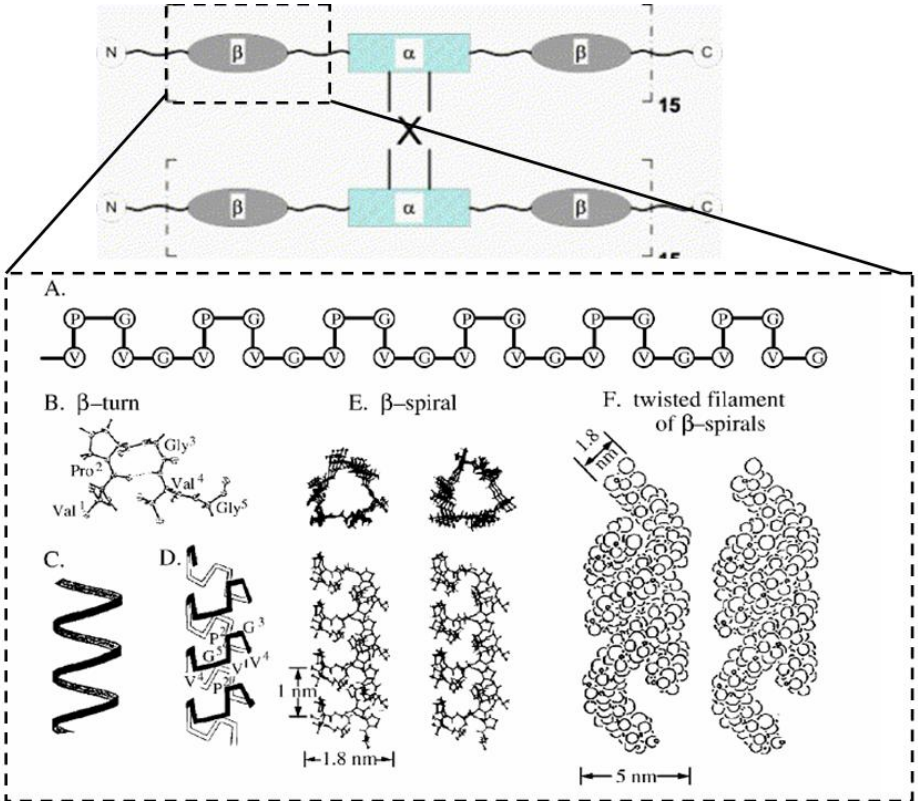

Figure 2.4. Domains of elastin polypeptides (adapted from Vyavahare and Simionescu).

Purified elastin is highly hydrophobic because, ~70% of it's component aspartic and glutamic residues are amidated[107]. The polypeptide chains in elastin, specifically the

α-helical segments, are cross-linked by both disulfide bridges and polyfunctional heterocyclic acids (desmosine and isodesmosine). These internal linkages of desmosine and isodesmosine make elastin a highly stable protein[107]. Due to this reason, elastin is insoluble in conventional solvents commonly used for the extraction and purification of globular and fibrous proteins, typical of biological elastomers such as resilin and abductin[103]. To overcome these limitations, researchers have used combined treatments of harsh solvents and thermal cycles, involving oxalic acid and boiling sodium hydroxide, to isolate elastin from the extracellular components[103]. Also because of its high stability, physiologic elastin turnover is rather slow, extending over a lifetime.

2.2.3 Elastin Ultrastructure

Elastin fibers are made up of two major structural components, a central core of amorphous elastin, and surrounded by microfibrils. During the early stages of elastogenesis, microfibrils first deposit in an organized-fashion in the extracellular space to form a pre-scaffold or template at the periphery of the cell. Amorphous elastin is then deposited on this microfibrillar-scaffold, and then crosslinked[108]. During the elastin deposition process, the microfibrils become displaced to the periphery of the growing fiber. The core of elastic fibers is thus covered with a sheath of microfibrils, each of which has a diameter of about 10 nm and length of < 100 nm[109]. Microfibrils are composed of a number of different glycoproteins, predominantly, the large glycoprotein fibrillin, which is essential both for the integrity of elastic fibers and to cell interaction with these fibers.

Besides elastin, microfibrils can also self-associate to form minor fiber bundles; groups of bundles of microfibrils are termed as *oxytalan fibers*. A fiber that is composed of both elastin and microfibrils is termed an *elaunin fiber*. Only those fibers that are composed mostly of elastin, with only a microfibrillar boundary are called *elastic fibers*. Microfibrils are found in elastin containing tissues as well as in tissues that lack elastin. Structurally, they are made up of repeating globular domains connected by thin fibrillar domains and consist primarily of two proteinaceous components - fibrillin 1 and 2[108]. Tropoelastin, the soluble elastin precursor, has been shown to specifically interact with microfibrillar components, specifically, fibrillin and microfibril-associated glycoproteins (MAGPs), in a step that has been shown to be vitally important to elastin matrix assembly. Another family of proteins shown to associate with elastic fibers is *fibulins*. Fibulins 1-5 bind to tropoelastin and have been localized to elastic fibers in developing tissues.

Transmission electron micrographs show elastin to appear as amorphous clumped masses exhibiting low electron density. Elastic fibers are either seen in cross-section as having rounded clumps of amorphous elastin at their cores (100-800 nm), or as longitudinally-aligned, laterally-associating bundles of elastin fibrils. The microfibrils that surround the amorphous elastin are far more electron-dense and are readily apparent even within TEM images of mature elastin fiber matrices (**Figure 2.5**). As explained above, microfibrils within the elastic fiber are associated with the growth process and hence become entrapped within the newly deposited elastin[108] as the fibers grow. Besides, guiding elastin deposition and fiber formation, microfibrils have also been

shown to mediate SMC interaction with elastin fibers, which critically regulates cell phenotype and behavior, and ensures lack of hyper-proliferation[109].

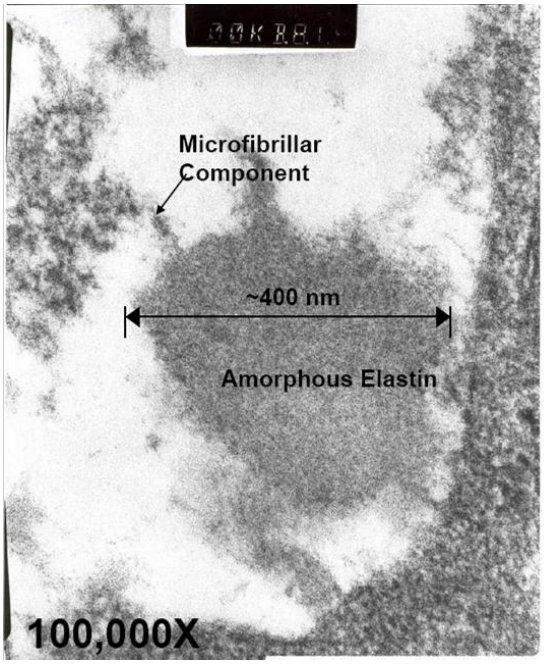

Figure 2.5. High resolution TEM image of elastin and fibrillin fibers in RASMC cultures *in vitro*[110].

2.2.4 Mechanical Properties of Elastin

Elastin is a rubber-like protein that exhibits reversible deformation with very high resilience. The proteins are stretchy, reaching maximal extensions in excess of 100%, with a very low modulus of elasticity[111]. This suite of properties implies that a key function of elastin is to impart tissues low stiffness, high strain and capacity for efficient storage of elastic energy. Elastin functions in association with collagen in vertebrate connective tissues where reversible elasticity is required (e.g., in skin and elastic

cartilage). In addition, elastin is a major component of arteries, where its stretchiness and ability to store elastic-strain energy allow arteries to smoothen the pulsatile flow of blood from the heart, lowering peak blood pressure and the mechanical work of the heart, thereby maintaining a relatively steady flow of blood through tissues.

Despite these general observations, elastin does not behave similarly under all conditions[112]. Stretchy materials like elastin achieve their mechanical properties because they contain flexible molecules that can easily change their shape, or conformation, when stretched. The desirable properties of low stiffness, high extensibility and high resilience that are vital for elastin's normal function rely entirely on the ability of the molecules to change their shape faster than the macroscopic shape change imposed by an external force. As mentioned previously, the mechanical properties of blood vessels stem from their microstructural wall components, such as collagen and elastin fibers, and the SMCs[113]. Since these individual components take up loads at different stress levels, their source-, and location-specific differences, content and distribution within blood vessels, and their alteration in diseased states can render the mechanical properties of blood vessels complex and difficult to predict.

Collagen and elastin affect the mechanical behavior of vessels in different ways. Specifically, collagen contributes mainly to the linear regime of the non-linear stress-strain curve (role in limiting vessel distension), whereas elastin mainly contributes to the toe part of the stress-strain curve. While collagen provides rigidity, elastin allows the connective tissues in blood vessels, cardiac and other elastic tissues, to stretch and then recoil to their original positions[107]. Large arteries have a high degree of elasticity

because they have elastin as the major wall component[114], and for this reason are able to accommodate high systolic blood pressures. It has been shown[115] that axial elastin fibers in the intimal and adventitial layers, and circumferential medial fibers, help distribute tensile stresses during vessel inflation and relaxation, conclusively providing evidence that emphasizes the mechanical importance and indispensability of elastin fibers in the aortal anatomy. The absence or degradation of vascular elastin thus exposes other medial components, i.e., collagen and SMCs to very high tensile stresses to stimulating hyper-proliferation of SMCs, and their transformation into a synthetic phenotype, resulting in exuberant, uncontrolled synthesis and accumulation of collagen and ground substance, leading to pathology of hypertension.

2.2.5 Mechanisms of Elastin Synthesis and Fiber Assembly

As described in earlier sections, elastic fibers comprise a core of amorphous elastin surrounded by peripheral microfibrils. However, the biochemical characteristics of elastic fibers are complex, because they contain numerous other components as well, and exhibit a highly-regulated pattern of deposition, and a multi-step hierarchical assembly process. Briefly, elastin is synthesized as a soluble precursor, 72 kDa tropoelastin, which is post-translationally crosslinked by isodesmosine and desmosine to form an alkali-insoluble elastin matrix (**Figures 2.6**). Biochemical analyses and molecular biology approaches have shown that the tropoelastin molecule is highly hydrophobic and contains alternating hydrophobic and hydrophilic peptide domains which confer on the polymer its peculiar elastic properties and stability[116]. In fact, the

conformation of the hydrophobic sequences is responsible for the elastic recoil in water[117, 118], whereas the hydrophilic alanine-rich portions, exhibiting a-helical conformation, are involved in the intermolecular crosslinking, mediated by lysine residues[119].

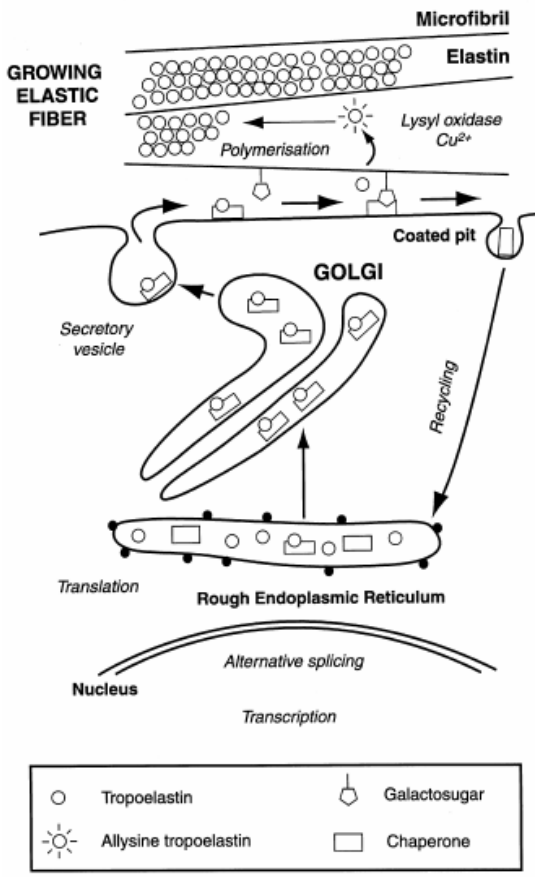

Figure 2.6. Mechanism of elastin synthesis and release from the cells[120].

2.2.5.1 Tropoelastin Synthesis

In humans, the elastin gene is present with a single copy on chromosome-7[121]; the primary transcript undergoes various alternate splicing during development and in different organs[122]. It has been proposed[123] that the tropoelastin protein is secreted post-

transcriptionally by the endoplasmic reticulum and packaged by Golgi apparatus within the cytoplasm, and delivered extracellularly by transcytosis. The tropoelastin protein is secreted by the cell after being hydroxylated on a number of proline residues[124], mainly located on the protein segment corresponding to exon-18. It has been suggested that the carboxy-terminal peptide of tropoelastin encodes the domain directing the cytoskeleton-mediated intracellular transport to the cell membrane[125], and forms a positively charged pocket which could define a binding site for the acidic microfibrillar proteins mediating elastic fiber assembly[126]. The tropoelastin molecule that leaves the Golgi apparatus attaches to the extracellular domain of a membrane protein called the elastin-binding protein (EBP). The EBP intracellularly attaches to tropoelastin and accompanies the precursor to the plasma membrane. The primary function of EBP besides tropoelastin transportation is to protect the molecule from enzymatic degradation[127], as will be discussed later.

2.2.5.2 Elastin Matrix Synthesis

Once the tropoelastin molecule finds its way to the extracellular space, it interacts with glycoprotein microfibrils and becomes oriented in the proper alignment for crosslinking into a growing elastin fiber. The observations that elastic fibers are often in contact with the cell plasma membrane, and that this latter exhibits receptor sites for elastin[127], suggest that elastic fiber assembly may occur at localized regions on the cell surface[128]. This assembly process is mediated at the cell surface by an elastin-binding complex, which has been isolated from elastin-producing cells and consists primarily of three proteins[127]. Two among these proteins are integral membrane proteins (55 and 61

kDa) that form a transmembrane link between the extracellular compartment and the cytoskeleton. The third protein is the detachable 67-kDa EBP, described earlier, which also has galactolectin domain. EBP binds the hydrophobic VGVAPG sequence in elastin, the cell membrane, and galactosugars via three separate sites[129]. Binding of galactosugars to the lectin site of the 67-kDa EBP lowers its affinity for both tropoelastin and for the cell-binding site, resulting in the release of bound elastin and the dissociation of the 67-kDa subunit from the cell membrane[130]. Thus, galactosugar-containing microfibrillar proteins may be involved in the coordinated release of tropoelastin from the 67-kDa binding protein on the cell membrane to the growing elastin fiber[131]. However, an excess of galactose-containing components such as glycoproteins, glycosaminoglycans, or galactolipids in the ECM may adversely affect elastin assembly by inducing premature release of tropoelastin and elastin-binding protein from the cell surface.

2.2.5.3 Elastin Crosslinking

The cross-linking reaction between tropoelastin molecules is initiated by the formation of an δ-aldehyde, allysine, through oxidation of lysyl ε-amino groups present on the α-chain domains of adjacent elastin molecules, by a member of the lysyl oxidase (LOX) enzyme family[132]. Approximately 40 lysine residues in 16 crosslinking domains of tropoelastin have been estimated to eventually participate in forming the bi-, tri-, and tetrafunctional crosslinks of polymer with reversible deformation and high resilience. Crosslinking of elastin is initiated by the action of LOX, one of six variants of a family of a copper-dependant enzymes that catalyze the oxidative deamination of lysine residues

into allysine[69]. In addition to LOX, there are four LOX–like (LOXL1–4) proteins that resemble LOX in containing a conserved amino oxidase domain[133]. Because LOX is critical for elastin and collagen cross-linking, it associates with these proteins early in the assembly phase. For example, LOXL1 has been localized to the elastin globules that form on the cell surface and antibodies to LOX have been localized to microfibrils[134]. LOXL1 has also been shown to interact with fibulin-5, fibrillin, and with tropoelastin in ligand-binding assays. However, inhibition of LOX activity through copper deficiency or through the administration of enzymatic inhibitors results in weakened connective tissue throughout the body[135]. Subsequent formation of the elastin crosslinks by isodesmosine and desmosine occurs as a series of spontaneous condensation reactions[74].

2.2.5.4 Elastic Fiber Assembly

In the extracellular space, newly secreted tropoelastin molecules aggregate on pre-existing elastic fibers or on bundles of electron-dense long microfibrils, which appear to function as scaffolds for elastic fiber assembly (**Figure 2.7**)[136]. Microfibrils appear as long 12-nm-diameter tubules, forming loose bundles in the ECM, and may exist either in association with strands of amorphous elastin or spread among collagen fibrils; in the latter case, they are mostly found in tissues where elastin can not be recognized even by immuno-cytochemistry. During elastin fiber formation, fibrillin microfibrils are found grouped in small bundles near the plasma membrane and within each microfibrillar bundle, amorphous elastin secreted by cells gets deposited in discrete locations, where they gradually coalesce and generate the central core of elastin. The majority of

microfibrils are progressively displaced towards the periphery of the elastic fiber in this process, leading to their maturation in tissue.

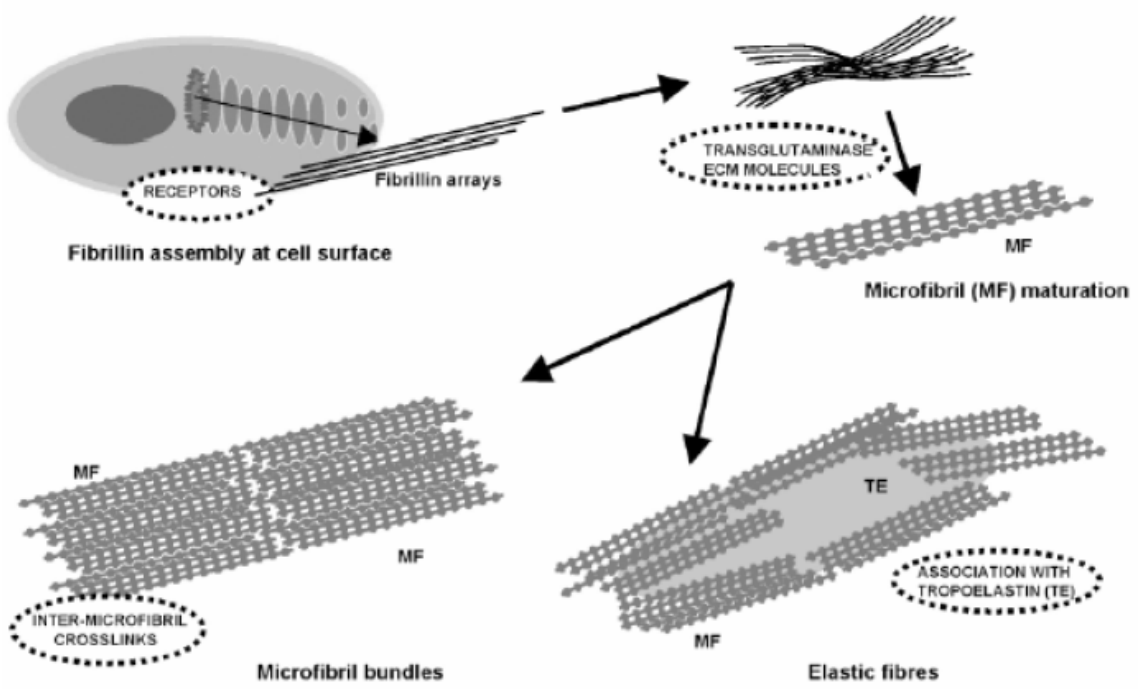

Figure 2.7. Schematic for the formation of elastic fibers[109].

Conventionally, an elastic fiber is described according to its appearance in electron microscope images after fixation and sectioning. Using this technique, it was realized that elastic fibers consist of an electron-lucent amorphous component and electron-opaque longitudinal strips of unidentified materials, surrounded by a discontinuous coat of 10-12 nm wide microfibrils oriented in the direction of the fiber. However, recent studies showed that elastin molecules are organized as 5-nm-thick filaments forming a three-dimensional network along the fiber[137]. Studies have shown that, besides elastin, a number of matrix constituents such as vitronectin, LOX, decorin,

osteopontin and biglycan epitopes are present within normal elastic fibers[138, 139]. Therefore, elastin matrix synthesis can be regarded as a complex sequential process involving aggregation of interconnected fibers, in which the major component is elastin, but whose formation is achieved with the contribution of several other matrix constituents, which are very likely important for their physiology and protection against pathological outcomes. *In vivo* and *in vitro* studies have shown that elastin gene expression and synthesis may be influenced by several factors, among which the dietary regimen[140], cell density in culture[141], hypoxia[142], and cytokines such as IGF-1[143] and TGF-β1[144]. TGF-β has been shown to up-regulate the elastin promoter[145]. These factors are generally released in significant levels during tissue inflammation and repair, to reactivate elastin gene expression during physiologic wound healing[146]. The utility of such growth factor cues to elastin regeneration will be further elucidated in later sections.

2.2.6 Biochemical Roles of Elastin

2.2.6.1 Elastin Modulates Cell Phenotype

In healthy vascular tissues, SMCs in the *tunica media* are quiescent (non-proliferative) and are embedded in a network of elastin-rich ECM that acts as a barrier to their migration[108]. Destruction of the aortic media and supporting lamina through degradation of elastin is an important mechanism in the formation and expansion of aortic aneurysms, floppy sacs of de-elasticized, vascular segments susceptible to rupture. SMCs in the arterial wall are believed to be involved in this vascular remodeling through the production of various proteases. Naturally occurring inhibitors of MMP activity in

the vessel wall, known as tissue inhibitors of metalloproteinases (TIMPs), are produced by SMCs, and upon their interaction with intact elastin regulate the activity of these enzymes and help to prevent elastin degradation under non-injury conditions[147].

SMCs within healthy, mature arteries exist in a quiescent contractile state, but can switch to a synthetic, non-contractile state under circumstances of injury, repair, or regeneration[148, 149]. This phenotype is characterized by an increased rate of proliferation, migration, and exuberant secretion of disorganized fibrous ECM (**Figure 2.8**). Numerous *in vitro* studies have implicated elastin in regulating SMC proliferation, migration, and differentiation. For example, it was reported that in cells cultured in collagen gels, exogenous soluble elastin significantly inhibits the proliferation and migration of vascular SMCs in a dose-dependent manner[150]. When SMCs were cultured on substrates of insoluble elastin, they similarly maintained organized contractile myofilaments and did not undergo phenotypic transition to a synthetic proliferative phenotype[151]. It should however be noted that these inhibitory effects are specific to intact elastin, since elastin peptides (fragments) and other matrix components do not impede SMC proliferation, migration or matrix synthesis. Further, adding intact elastin exogenously to the culture medium has been shown to inhibit the proliferation of SMCs[152] isolated from aortae of patients with congenital, inherited vascular disorders such as Supravalvular Aortic Stenosis (SVAS) and Williams-Beuren Syndrome (WBS). Viewed together, these observations suggest that intact elastin closely regulates SMC behavior in healthy tissues. Thus, homeostatic disturbances in vascular elastin/ elastin matrices can adversely influence SMC phenotype.

2.2.6.2 Elastin Regulates Vascular Calcification

Vascular calcification has been positively correlated with an increased risk of myocardial infarction, due to reduced blood flow resulting from decreased vessel elasticity, a partial outcome of structural or degenerative disorders of elastic fibers[32, 153, 154]. Arterial calcification, a common event in the pathogenesis of arteriosclerosis, generally occurs at two distinct regions within the vessel wall, i.e., the *t. intima* and the *t. media*. Intimal calcification occurs mostly in association with atherosclerosis, subsequent to lipid deposition, macrophage infiltration, and vascular SMC proliferation, whereas medial calcification can exist independently of atherosclerosis and is typically associated with calcium deposits along the elastic lamellae[155]. Genetic or induced aberration of elastic lamellar structure, or the associated microfibrils that mediate SMC interaction with elastin, can interrupt SMC-elastin signaling, to induce SMCs to assume an activated/ inflamed synthetic phenotype, characterized by increased Ca^{2+} influx and subsequent calcium deposition and matrix hardening[102]. The next section details the various disorders of elastin, the mechanisms by which tissue calcium levels are affected, and vascular homeostasis adversely impacted.

2.3 Abnormalities of Vascular Elastin

2.3.1 Elastin Breakdown and Vascular Inflammation

Under normal physiological conditions, turnover of insoluble elastin is very slow, a life-long process, and hence very little remodeling of elastin fibers occurs in adults[108]. This implies that active elastin matrix synthesis is almost a one-time phenomenon and

elastin repair and regeneration are highly limited in adult tissues. It has been shown that some elastin synthesizing cells, such as human skin fibroblasts and adult rat aortic SMCs (RASMCs) possess detectable levels of elastin-degrading enzymes (elastases). Though this basal enzyme activity is very low compared to that generated by inflammatory cells, it is significant because it permits cell migration through the developing ECM and in developing tissues, modulates morphogenesis of newly synthesized elastic fibers[156]. Although tropoelastin has been shown to be very susceptible to proteolytic degradation before it undergoes cross-linking into insoluble elastin, there is no evidence to suggest that significant intra-cellular degradation occurs prior to secretion.

Enhanced elastin destruction however, does occur under certain pathological conditions, either as a result of the release of powerful elastases released by inflammatory cells and bacteria, or due to a genetic deficiency in the naturally occurring elastase inhibitor α1-antitrypsin. Although inflammatory cell-derived elastases are unlikely to play a significant role in normal regulation of the elastic matrix, it is clear that they contribute substantially to the pathogenesis of some human diseases, including atherosclerosis, pulmonary emphysema, pollutional lung disease, and rheumatoid arthritis[156]. Neutrophil- and macrophage-derived elastases are of particular importance in this regard and have been the subject of many studies. Recent studies on the development of aortic aneurysms[156] reveal upregulated synthesis of MMPs in inflamed vascular tissues, which rapidly degrade the collagen and elastin matrix to result in loss of wall tensile strength and elasticity, and leads to progressive increases in vessel diameter[157]. Thus, enhanced secretion and activity of proteolytic enzymes in inflamed

vessels causes accelerated matrix destruction in turn leading to loss of vascular homeostasis. However, recent studies indicate that matrix degradation products, particularly the elastin peptides further exacerbate the cycle of inflammation and matrix destruction, as discussed subsequently.

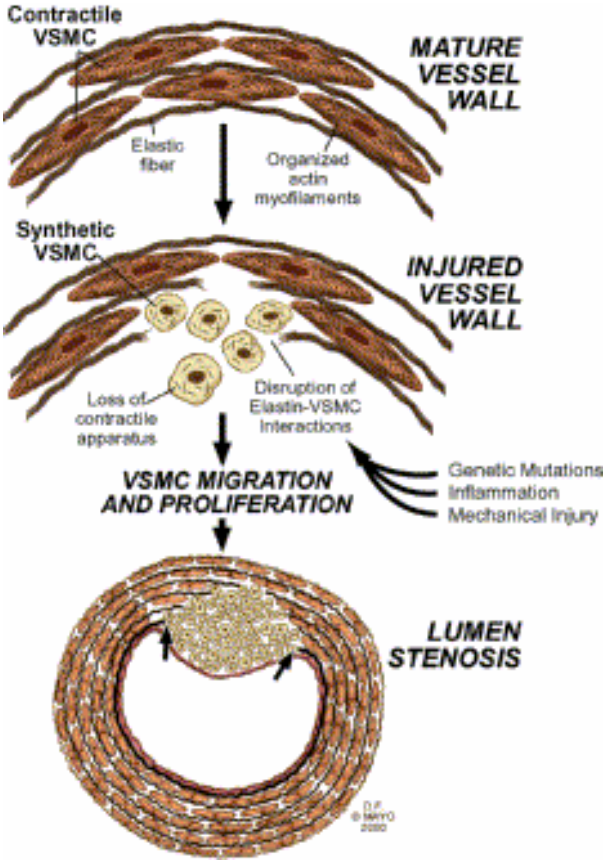

Figure 2.8. Model of elastin–SMC interactions. In healthy, mature elastic tissues, intact elastin fibers interact with SMCs around the elastic lamellae to remain in a quiescent and contractile state. The disruption and destruction of elastic fibers by mechanical injury, genetic mutations, or inflammation interrupts this signaling mechanism and induces SMCs to migrate, hyper-proliferate, and generate a disorganized matrix[102].

Elastin peptides are released by degradation of elastin matrices and are present in human serum and other biological fluids. Through their interaction with elastin-laminin receptors (ELR) present on the surface of fibroblasts, phagocytes, lymphocytes, SMCs and ECs, elastin peptides elicit a variety of biologic effects such as MMPs over-expression, greater Ca^{2+} influx, enhanced vaso-relaxation and chemotactic activity[158] (**Figure 2.9**). These effects are not elicited when these cells interact with intact elastin. The transduction pathway of the ELR receptor involves the activation of phospholipase C (PLC) by a pertussis toxin sensitive G-protein. PLC indirectly induces an increase in intracellular free calcium, and phosphorylates MAP kinase, which triggers off a series of events like increased chemotactic activity, increased ionic fluxes, and overexpression of MMPs[158]. A progressive age-dependent uncoupling of the elastin-laminin receptor also occurs impairing its transduction pathway, which results in alteration of the calcium signaling and loss in ability of cells to maintain calcium homeostasis. With increased aging, these alterations in signal transduction of ELR result in modified activities of parenchymal and phagocytic cells such as enhanced production of free radicals and elastases. Thus, it can be hypothesized that age-related changes in elastin-laminin receptor signal transduction may be involved in initiation of atherogenesis[158]. Non-age related increase in activity of the ELR can result in increased release of degradative enzymes, the MMPs, vascular calcification, and ECM elastin remodeling[157]. Thus, preserving the normal signal transduction pathway adopted by the ELR receptor is of prime relevance in the context of elastin preservation and regeneration.

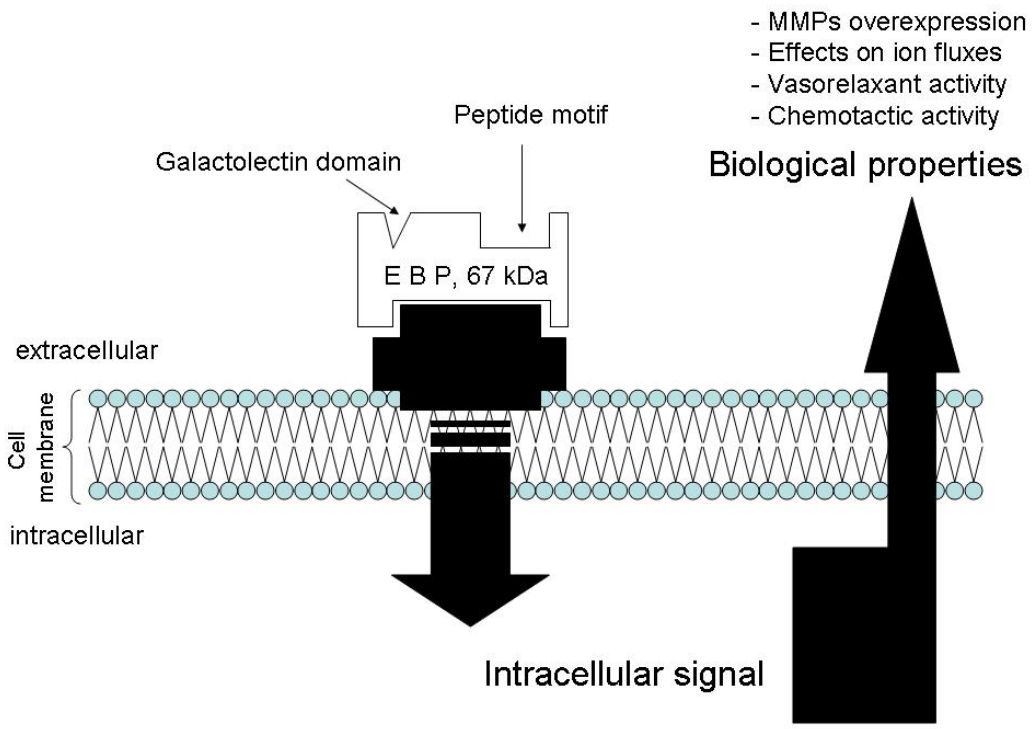

Figure 2.9. Schematic representation of the Elastin Laminin Receptor (ELR). Soluble elastin peptides generated by breakdown of intact matrix elastin bind to the ELR and trigger a series of pathological outcomes (redrawn)[158].

2.3.2. Elastin Disorders

Elastic fibers are complex ECM polymers, composed of at least 19 different proteins that comprise both the microfibrillar and the amorphous components of elastic fibers. Mutations in three of the genes encoding the most abundant of these elastic fiber proteins result in a broad spectrum of elastic tissue phenotypes, ranging from skeletal and skin abnormalities to vascular and ocular defects[2]. Congenital defects in the ELN gene causes impaired deposition of insoluble elastin and accumulation of smaller elastin

peptides, which transduce intracellular signals causing increased cell proliferation. Impaired elastogenesis and increased cell growth could lead to the development of connective-tissue abnormalities, including occlusive arterial lesions[159]. Genetic disorders of the elastic fiber system are typically grouped according to the molecular constituent affected by the underlying mutations. One group of genetic disorders due to mutations in the ELN leads to conditions such as supravalvular aortic stenosis (SVAS) and cutis laxa (CL)[2]. A second group of genetic disorders affecting the microfibril component of the elastic fiber, fibrillin-1 and fibrillin-2 (FBN1 and FBN2) results in Marfan syndrome (MFS) and congenital contractural arachnodactyly (CCA)[2].

2.3.2.1 Supravalvular Aortic Stenosis (SVAS)

SVAS is an inherited obstructive arterial disease caused by point mutations, translocations and deletions in the elastin (ELN) gene[160]. The condition is characterized by congenital narrowing of large elastic arteries with an estimated incidence of 1 in 13,000 live births and extreme clinical variability[161]. Approximately 20% of SVAS patients have diffuse narrowing of the ascending aorta, characterized primarily by medial thickening[162]. While narrowing of the coronary arteries may lead to heart infarcts and sudden death, cerebral artery stenoses are implicated in susceptibility to cerebral infarcts and stroke in childhood[163]. Vascular lesions in SVAS patients show disorganized, irregular and thickened elastic fibers, excessive, clumped and hyper-trophic SMCs, extensive deposition of collagen in the inner media, and intimal fibrosis.

2.3.2.2 Cutis Laxa

Cutis Laxa (CL) is a clinical condition found in a heterogeneous group of acquired and genetic disorders, characterized by redundant, loose, sagging and inelastic skin[164]. Autosomal recessive CL is a severe disorder often accompanied by pulmonary emphysema and cardiovascular complications such as dysfunctional arteries[165], which can lead to death in childhood. Abnormal ultrastructure of dermal elastic fibers, and in some cases reduced elastin synthesis by skin fibroblasts and vascular cells, had been demonstrated previously in cutis laxa patients[166]. The abnormal protein synthesized by the mutant allele may be secreted and interfere with the deposition of normal elastin in a dominant negative fashion[167].

2.3.2.3 Williams-Beuren Syndrome (WBS)

Williams-Beuren syndrome is a complex genetic developmental disorder that is caused by deletion of one allele of the elastin gene[168]. The syndrome manifests itself as cardiovascular, neurobehavioral, facial, connective tissue, metabolic and growth abnormalities, including peripheral arterial stenosis and hypertension. Affected patient populations have unusually thick arterial walls, which are extremely distensible[169]. The abnormal distensibility and extreme thickness of the arterial wall is likely due to abnormal elastic fiber assembly within the media[170]. SMC de-differentiation to a synthetic phenotype, leading to arterial wall hypertrophy, may be a major outcome, as well as a cause of such increases in vascular distensibility.

2.3.2.4 Marfan Syndrome (MFS)

MFS is an autosomal dominant disorder of connective tissues that chiefly affects the ocular, skeletal and cardiovascular systems[171]. It has been firmly established that mutations in fibrillin-1 gene gives rise to MFS[2]. In the majority of cases, FBN1 mutations are unique to an individual or family and these mutations occur throughout the gene. Mutations causing premature translation termination and truncated fibrillin-1 molecules have also been identified, including a mutation that produces a severely shortened fibrillin molecule comprised of only the first 55 amino acids. Thus, disruption of fibrillin structure, or their absence can interrupt elastin-SMC signaling and alter SMC phenotype to a synthetic one[172]. Vascular tissues of MFS patients thus display disorganized and fragmented elastic fibers with excessive accumulation of amorphous matrix. The resulting cardiovascular complications include ascending aortic aneurysms and dissections, and mitral valve prolapse. These complications can lead to a shortened life expectancy if left untreated. The dilated segments can progress to dissection and spontaneous rupture of the vessel wall, which is the leading cause of morbidity and mortality in MFS patients.

2.3.3 Acquired Disorders of Elastin

Vascular proliferative diseases such as atherosclerosis and coronary restenosis lead to arterial narrowing and re-occlusion. Though it is still unclear how atherosclerosis initiates, owing to differences in developmental animal models and advanced human atherosclerotic tissues, the most popular theory involves the development of a fatty streak

and its conversion into a fibrous plaque. Although their etiologies are diverse, these disorders all share common pathologic features such as initial accumulation of SMCs within the intima between the endothelium and medial layer of the vessel wall, their subsequent activation, de-differentiation into proliferative synthetic phenotype, their aggressive migration into the sub-endothelial space, neointima formation. Both *in vitro* and *in vivo* studies have implicated the intact elastin matrix as a negative regulator of SMC proliferative activity within the arterial wall[102]. Thus, proteolytic degradation of vascular elastin matrices by activated/ inflamed SMCs exacerbates the progressiveness and severity of atherosclerotic disease.

As explained previously, elastin biochemically regulates vascular homeostasis by signaling SMCs via defined pathways to remain in a quiescent, contractile state. The disruption of elastin by inflammation, or direct mechanical injury can interrupt cell–matrix signaling and directly activate the SMCs[173]. Elastin degradation by macrophages, T cells, and their proteases during inflammatory disease of vessels, act in concert with the numerous cytokines and growth factors activated during vascular injury to incite SMCs to dedifferentiate, migrate, proliferate, and occlude arteries. Degradation of the elastin component is believed to be the result of a proteolytic cascade that involves the cooperation of several degradative enzyme types such as serine proteases, MMPs, and cysteine proteases[157]. MMPs (e.g., MMPs-2, 9) present in latent forms under normal physiologic conditions, are generally activated following vessel wall injury[174]. Thus, the disruption of elastin is not simply an end product of inflammation and vascular occlusion, but an important contributor to the pathogenesis of occlusive vascular disease. Therefore,

preventing elastin matrix degradation following vascular injury or restoring the lost/ degraded vascular elastin matrix is imperative for restoration of vascular homeostasis[102].

2.4. Aortic Aneurysms (AAs)

Aneurysms are pathological conditions wherein segments of elastic arteries dilate abnormally and weaken structurally, resulting in dissections, which enlarge ultimately leading to vessel rupture. In addition, morphological changes in aortic diameter can also occur as a consequence of prolonged and untreated vascular hypertension, inherent abnormalities in the protein architecture of the aortic wall, trauma, infection, and also due to progressive destruction of aortic proteins by enzymes during chronic vascular inflammation[1]. Aneurysms typically exhibit location-specific differences in their pathologic mechanisms, and can develop anywhere along the vessel, though they predominantly occur in the abdominal section (abdominal aortic aneurysms or AAAs). AAAs develop gradually at the rate of ~ 1 cm/year, exhibiting very few symptoms during their developmental stages, thereby making early detection impossible[1]. Unfortunately, by the time AAs are detected, they are at advanced stages (**Figure 2.10**), wherein they dissect and catastrophically rupture to cause life-threatening internal bleeding, effects of hemorrhagic shock, embolism, and stroke with fatality rates of ~80%[17]. Abdominal AAs are also frequently manifested in inherited conditions such as MFS, characterized by defects in assembly and stabilization of arterial elastin[2].

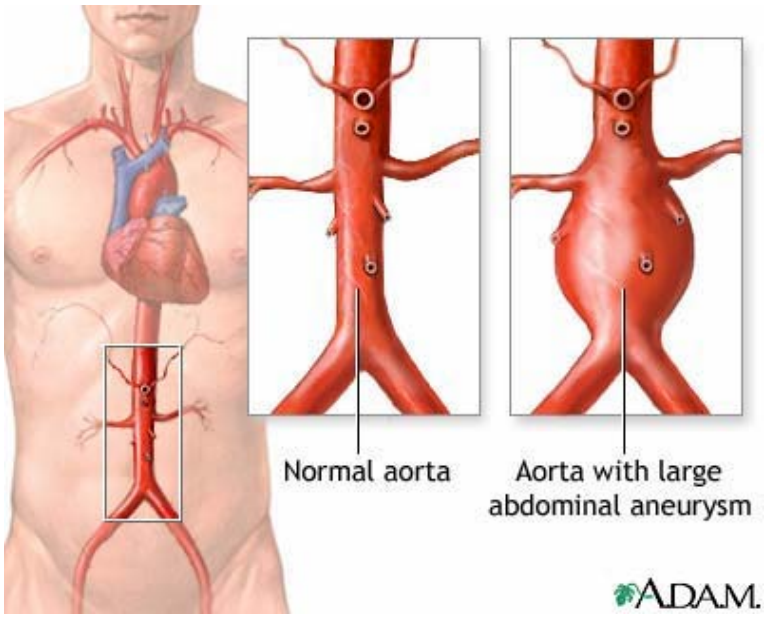

Figure 2.10. Abdominal aortic aneurysm - involves a widening, stretching, or ballooning of the aorta. As the aorta gets progressively larger over time there is increased chance of rupture.

There are several causes for the occurance of AAs, and the most prominent among them being atherosclerotic disease, defects in arterial components, genetic disorders and high blood pressure. AAAs initiate primarily as an infrequent outcome of chronic matrix proteolytic effects of inflammatory cells that infiltrate in response to calcified lipid deposits or atherosclerotic plaques within the abdominal aortic wall[3]. The pathogenesis of AAs might be due to the absence of SMCs, fragmented and diminished density of elastic fibers, and excessive accumulation of proteoglycans in a mostly non-inflammatory environment[14], ultimately resulting in destruction of the aortic wall architecture. AAs also result from gradual enzymatic degradation of structural proteins

such as elastin and collagen, leading to loss of elasticity and strength of the aortic wall and its progressive dilation to form a rupture-prone, balloon-like sac of weakened tissue. Genetic disorders, such as in MFS, that impacts vascular matrix architecture and homeostasis, can also manifest in vascular aneurysms. Since absence or destruciton of elastin critically regulates aneurysm formation, progression and fatal rupture, restoration of elastin in these segments is likely to stabilize and restore homeostasis in these tissues.

2.5 Therapeutic Strategies for Restoring Vascular Elastin

Thus, so far we have detailed the mechanisms of elastin synthesis, matrix assembly and stabilization, the importance of elastin in maintaining vascular homeostasis (cell signaling and biomechanics), and the pathological conditions that compromise cardiovascular elastin. It may be inferred from this discussion that conditions that compromise vascular elastin can severely impair vascular homeostasis and thus must be replaced or preserved as a priority. As will be discussed subsequently, traditionally, the elastin matrix degenerative diseases have been surgically addressed, although next generational in situ elastin restorative strategies are in development, which aim to bypass long-term surgical complications. These strategies may be broadly classified into three categories: (a) *preservation* (e.g., MMP inhibition), (b) *replacement* (e.g., using synthetic elastomers assembled from peptides *in vitro*, allogeneic and xenogeneic grafts, etc), and (c) *regeneration* (e.g., using tissue engineered scaffolds, genetic engineering). This section also details the approaches being used so far and their relative merits and disadvantages.

2.5.1 Treatments of Vascular Aneurysms

2.5.1.1 Non-Surgical Strategies

Based on knowledge of AA etiology and pathology, current treatment procedures can be classified broadly into two catergories, i.e, surgical and non-surgical strategies. Three potential non-surgical AA treatment strategies have been identified which aim to (*a*) inhibit pathological matrix degradation by proteolytic enzymes (e.g., cathepsins, MMPs), (*b*) stabilize existing matrix structures using pharmacological agents, and more recently, (*c*) promote active healing to regress already developed aneurysms through endovascular seeding of healthy cells. However, none of these strategies present an integrated approach to modulating aneurysmal cell phenotype, reinstating healthy matrix architecture, and providing conditions for stabilizing the local vascular environment.

2.5.1.2 Surgical Strategies

The most standard surgical procedure for AA treatment has been open aneurysm repair (*aneurysmectomy*; **Figure 2.11A**), wherein the weakened aortic segment (>5 cm diameter) is flow-excluded and then replaced with a carefully sutured synthetic mesh graft. However, in case the aneurysm is easily accessible and less life-threatening, a minimally-invasive *endovascular abdominal aortic aneurysm repair* (EVAR) technique (**Figure 2.11B**) is employed, wherein a woven polyester graft or Dacron, mounted on a self-expanding stent is deployed within the vessel, at the site of the aneurysm. Though elective open repair carries low mortality rates (5%) and has long-term durability, a large number of the mainly elderly patients are unfit for surgery[175]. In such cases, EVAR is an

attractive alternative that has 1-month success rates of 85%, and short recuperation times[176]. However, it was observed that, long-term cardiac and pulmonary complications (22% vs. 11%), and other surgical (33 vs 45%; neurological wounding, bleeding and stroke) and graft-associated (4% vs. 13%; thrombosis, leaks, tears) complications can cause survival rates to drop to ~50% at 10 years post-op[17], in both the cases. Thus, there is a crucial need to develop nonsurgical approaches to inhibit, preserve matrices against, or regress the complex mechanisms of pathological elastin degradation in vascular aneurysms, about which knowledge is limited.

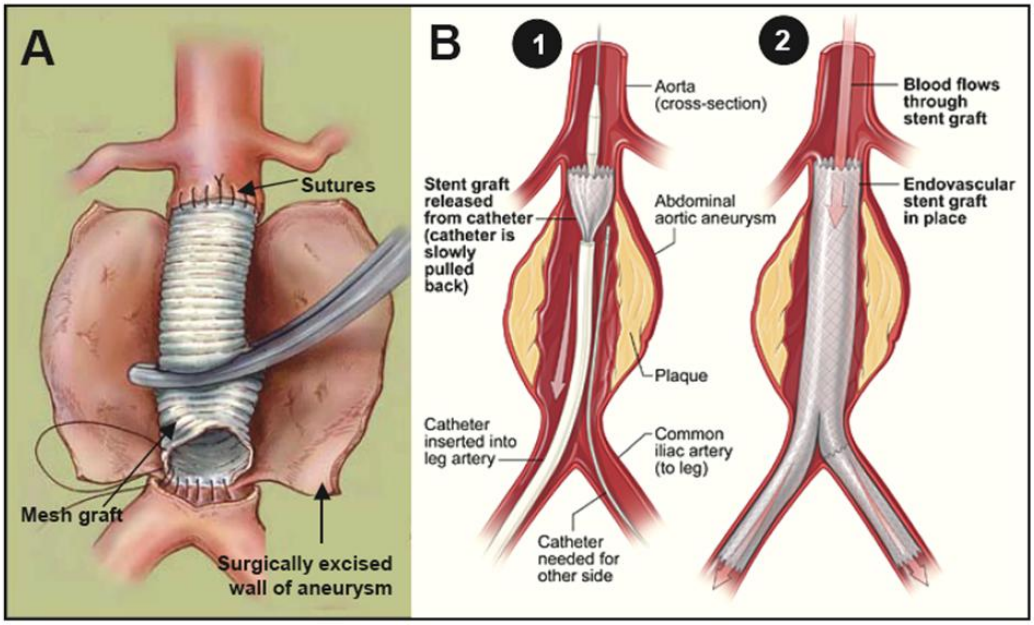

Figure 2.11. Conventional repair (A) and minimally invasive endovascular repair (B) of abdominal AAs.

2.5.2 Elastin Preservative Strategies

These strategies mainly focus on preserving the elastin matrices in the vascular tissues that survive pathological degradation. These strategies seek to arrest or decelerate the enzymatic degradation of the matrices, so as to possibly prolong the time to surgical intervention. At present, most of these preventive strategies involve a pharmacokinetic approach.

MMPs are released by inflammatory cells and then act on the ECM slowly degrading the key components like elastin[147]. The availability and activities of these proteolytic enzymes is tightly regulated in healthy tissues by naturally-occurring factors, -TIMPs[177], to prevent uncontrolled matrix degradation. The MMPs-2 (gelatinase A) and -9 (gelatinase B) have been reported to specifically cause elastin degradation leading to aneurysm formation[178] and subsequent vessel wall weakening[179]. MMP-9 is the most important MMP in the spectrum of aneurysmal pathogenesis, and can cleave several substrates including elastin, collagen and fibrinogen[180]. In light of this information, early pharmacological strategies targeted at elastin preservation focused on inhibiting MMPs[157]. MMP-9 inhibitors such as doxycycline, dexamethasone, green tea catechins and indomethacin are being investigated as therapeutic strategies to inhibit MMP-9 activity, and hence elastin degradation[157]. Doxycycline and trapidil[181] have also been studied in the context of inhibiting MMP-2 activity.

Besides TIMPs, human tissues and peripheral blood contain protease inhibitors (e.g., serine proteinase inhibitors) that bind to elastase enzymes and prevent their action on elastin matrices. Under healthy conditions, these proteins control unchecked

inflammatory responses, coagulation, and regulate tissue repair mechanisms. When the availability of these elastase inhibitors is suppressed or when they are genetically abnormal or absent (e.g., anti-trypsin deficiency), accelerated elastin breakdown and degradation may occur. In such conditions, exogenous delivery of alternative elastase inhibitors, or transfection of vascular SMCs with genes such as α-1 anti-trypsin gene, which codes for one such inhibitor, can help regulate *in vivo* production of these elastase inhibitors and arrest elastin loss[182]. However to date, most of these attempts have succeeded only *in vitro*, because numerous other unknown factors influence their functional activity, and also contribute to alternate mechanisms of elastin degradation process *in vivo*. Thus, alternate non-pharmacological approaches based on replacing degraded elastin matrices with synthetic or biological elastomers have been tested, as detailed below.

2.5.3 Replacement Strategies

2.5.3.1 Allogeneic Grafts

Most early replacement strategies focused on using matrices isolated allogeneically from cadeveric vessels. Allogeneic tissue grafts have attracted much attention as a substitute for replacing damaged, injured or lost vessel segments. This is due to identical structural makeup, mechanical properties and size-matches, between donor and recipient vessels. It has been demonstrated that allogeneic elastin may be sourced from vessels from deceased fetuses, cadavers, and umbilical cords[183]. There is a huge supply-demand gap in terms of these tissues which makes their use very limited,

especially in cases where immediate surgical vessel replacement is required. Another main reason why the success of these implants is limited is their high failure rate owing to donor-specific immune-response, besides graft destruction[184, 185]. To overcome these limitations, researchers have tried to de-cellularize donor vessel segments, and merely graft the matrix that remains. Several methods have been developed to generate completely acellular tissue matrices using multi-step extraction with a combination of detergents and enzymatic agents such as, triton detergent, trypsin/ ethylene-diamine-tetraacetic acid (EDTA), or sodium dodecyl sulfate (SDS) in the presence of protease inhibitors[186-188]. Histological analysis of such tissues indicates that the major structural protein components survive, though their quality and long-term stability may be compromised. Certainly, studies have shown many of these de-cellularized protocols to damage the ECM. Moreover, the transplanted tissue represents a continuous source of (*a*) antigens capable of activating the immune system, and (*b*) overproduced cytokines, to cause early rejection and inflammation., post-transplantation[189]. Therefore, lifelong immuno-suppression is required to ensure long-term allograft survival[190].

2.5.3.2 Xenogeneic Grafts

Since allograft transplantation is limited by shortage of available organs, the use of animals in lieu of human subjects as donors (xenograft transplantation) offers a potentially viable alternative. Though there is no scarcity for organs and tissues available for implantation from animals, previous attempts at using xenogeneic grafts failed miserably because of end-stage organ failure[191], different lifespan of humans from other

xenogeneic sources such pigs, disease transmission[192], lack of antigenic similarity[193], and most importantly permanent alteration to the genetic code of animals used as sources[194]. When transplanted into untreated humans or nonhuman primates, pig organs are rejected hyperacutely within minutes by antibody-mediated complement activation[195, 196]. A number of molecular incompatibilities, physiological and biochemical variations have been identified between pigs and humans, including blood viscosity, liver metabolism, and differences in presence and activities of various enzymes and hormones. Of particular concern has been the incompatibility of coagulation factors that might lead to the development of a pro-coagulant state in the graft with subsequent thrombosis[196]. Moreover, compliance mismatch and mechanical stiffening post-transplantation also contribute for the failure of xenografts in the long-term[194]. Attempts to remove immunoreactive molecules and cells from the xenografts such as porcine arterial segments resulted in poor structural integrity of the resulting matrix.

2.5.3.3 Synthetic Elastomers

To overcome the immune-compatibility limitations of allogeneic and xenogeneic grafts, researchers have fabricated biodegradable/ biocompatible elastomeric scaffolds from polyesters, for vascular replacements. Elastomers are predominantly used in applications that require compliance with soft or cardiovascular tissue[197, 198]. The required properties of polymeric biomaterials are similar to other biomaterials, that is, biocompatibility, sterilizability, adequate mechanical and physical properties, and good processability for ease of manufacturing. Biodegradable elastomers have been shown to

match mechanical properties of cardiovascular tissues, rendering them useful substitutes in their applications[25]. Such matching of biomaterial-tissue properties is vital to ensure that cells perceive bio-mechanical stimuli that mimics the dynamic *in vivo* vascular tissue environment and thus respond likewise[85]. Most of these polymeric scaffolds were designed to mimic the native tissue in terms of porosity and three-dimensional structure, suitable for cell infiltration and matrix synthesis[199]. Current synthetic vessel replacements are limited to large diameter vessels, while there is no satisfactory synthetic small diameter (<6 mm inner diameter) vascular prosthesis[200]. Dacron was the leading material used for vascular reconstruction of all the major large arteries, while nonfabric Teflon grafts, such as expanded poly(tetrafluoroethylene) (e-PTFE) grafts were first used as small arterial substitutes (Gor-Tex).

Two key factors were believed to have caused graft failure[201]: (a) intimal tissue overgrowth (hyperplasia) that develops in the artery just proximal and distal to the artificially created connection between the rigid graft and the compliant artery, (b) the loss of self-cleaning quality as the graft becomes stiff and nonpulsatile, thus no longer preventing deposits of fibril and platelets forming on the walls. Thus, it could be expected that mismatch not only in mechanical, but also in interfacial properties between the graft and host vessel will affect the patency of vascular grafts[202]. To overcome these limitations, the development of biocompatible surface modifications and controlled release modalities for vascular implant materials became essential, for achieving controllable modulation of cellular interactions at the tissue-biomaterial interface. Anti-thrombogenic coatings such as heparin and benzalkonium chloride were developed, as

well as velour-lined vascular patches reinforced with polyester[203]. It was found that compliance mismatch between the graft and host artery also results in differential mechanical strains and haemodynamic wall shear stress, due to pulsatile blood flow and the viscoelastic nature of the blood vessel wall itself[204, 205]. In general, a synthetic graft that is larger than its host vessel creates a state of low velocity blood flow and shear stress, thus promoting failure; while, in smaller grafts, a fibrin layer develops over the artificial surface in the body during healing, obstructing the graft lumen.

2.5.3.4 Elastomers from Elastin Peptides

Elastin has the remarkable property of being able to self-assemble *in vitro* from monomeric units of amino acids into a robust biopolymer, a process which naturally occurs in the elastin polymerization process *in vivo* and termed as coacervation[36, 206]. Coacervation is a reversible phase separation in which a protein in solution forms molecular aggregates upon an increase in temperature, and separates from the solvent as a second phase[207]. The temperature at which coacervation takes place is a measure of the propensity for self-aggregation, and is inversely related to ionic strength of the solution and the concentration of the polypeptide[206]. There is substantial evidence that the hydrophobic domains are necessary for self-aggregation[208], and the interactions of hydrophobic domains align lysine residues for formation of the covalent crosslinks that stabilize the insoluble polymeric matrix[209, 210]. It has been reported that the polymers developed using self-assembling elastin peptides display considerable promise as biomaterials for applications in drug delivery and soft tissue engineering. Attempts by

researchers to genetically alter these polymeric sequences by inclusion of sequences such as GRGDSP for favorable cell attachment yielded positive results with normal complement of collagen and elastic fibers[35], as shown in **Figure 2.12**.

However, it should be noted that, *in vitro* assembled elastin matrices does not include the natural mechanism of elastin deposition and assembly over a pre-existing fibrillin scaffold, which also plays a key role in maintaining SMCs in quiescent state. Besides, repetitive cyclic loading of these materials fabricated using this approach might promote failure of this elastin at very early stages compared to insoluble elastin matrices. Most importantly, since native elastin fibers contain numerous other non-elastin components, such as microfibrils (fibrillin, etc), which are critical to effect the unique interactions of cells with the elastin matrix and thus respond accordingly, their absence within synthetic/ unnaturally assembled elastomers prevents them from vitally regulating vascular cell behavior when implanted *in vivo*. Thus, despite being able to replicate the mechanics of native elastin, elastin matrices assembled *in vitro* using soluble peptides proffer serious drawbacks that limit their clinical utility.

2.5.4 Elastin Regenerative Strategies

Tissue engineering offers a promising approach for the fabrication of a functionally-responsive, living-tissue like constructs with biological and biomechanical properties that mimic native vascular tissue. In recent years, researchers have explored the possibility of effecting elastic tissue repair through regeneration of elastin in situ within elastin-compromised vessels and synthetic or tissue engineered grafts *in vitro*

culture systems deployed at the site of vascular disease or injury. Although considerable progress has been made towards understanding the principles of elastin biosynthesis, and matrix assembly, ultrastructural organization and stabilization *in vivo*, many of the conditions and mechanisms required to replicate the same, with provided cues are still elusive. This is especially challenging in light of the extremely poor elastin regenerative capacity of adult human and other cells, vascular and non-vascular in origin. Thus, identifying elastogenic cues as represented by elastogenic biomaterials scaffolds or growth factors; and further modulating the assembly of the elastin precursors into ultrastructural and functional mimics of native elastin are immense challenges. In the following sections, we will highlight recent developments on this front.

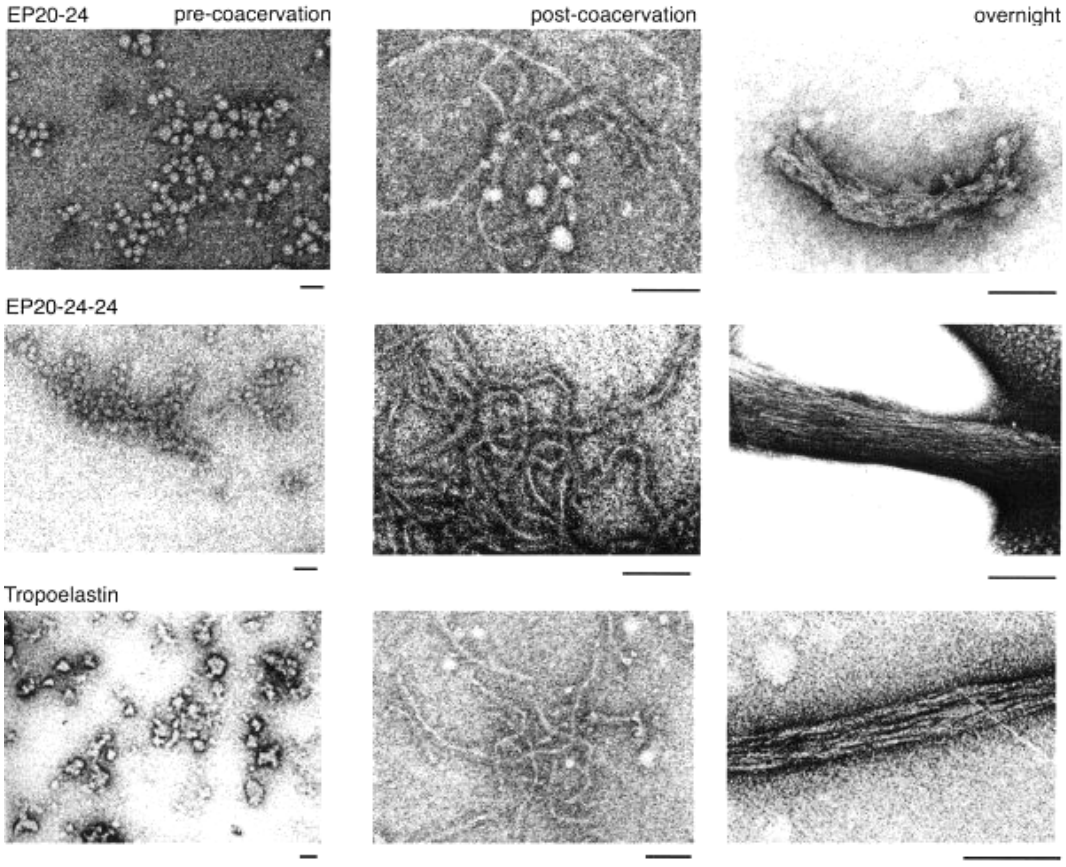

Figure 2.12. Comparison of structures formed from elastin peptides EP20-24, EP20-24-24, and tropoelastin at three stages of coacervation. Prior to and immediately following coacervation, the structures formed by these polypeptides are similar to those formed by the natural elastin precursor, tropoelastin. However, after overnight incubation above the coacervation temperature, the structures formed from EP20-24-24 closely resemble that of tropoelastin, whereas structures formed from EP20-24 are less compact and well-organized. All scale bars represent 100 nm[36].

Tissue-engineered elastin constructs are expected to proffer distinct advantages over synthetic elastomers because elastin is innately non-thrombogenic, and when faithfully regenerated, would contain non-elastin proteinaceous components crucial to signaling cells and regulating their behavior. The potential to heal and remodel their biological matrix depending on the local dynamic environment, elicits relatively attenuated foreign body reaction, since they are only made up of components generated by the patient's own cells. This ensures seamless integration with recipient (patient) tissues. However, the challenges to tissue engineering such constructs are also substantial. These include mimicking native elastin structure, achieving elastin matrix regeneration in a short time frame, matching compliance with native elastin, and to be immediately functional post-implantation, if regenerated *in vitro*; and to ensure that the elastogenic cues/ biomaterials do not incite undesired cell responses such as inflammation and proteolytic activity[38, 211]. Two classes of scaffolds have been most

commonly investigated in the context of upregulating elastin matrix biosynthesis, as described below.

2.5.4.1 Synthetic Scaffolds

Synthetic scaffolds are three-dimensional templates that support cell adhesion, their migration, differentiation, proliferation, and matrix synthesis and deposition to effect guided tissue regeneration. Synthetic scaffolds employed for tissue engineering applications are selected so as to be biocompatible, reproducible with high porosity and inter-connected microstructure to allow cell infiltration and sustenance, and to be so modulated in their chemistry to permit them to be tailored to obtain desired degradation profiles and mechanical properties[212]. Most importantly, scaffolding materials must be selected such that they elicit the desired biological response (e.g., elastin matrix synthesis) from seeded cells. In the context of elastin matrix regeneration, the most widely investigated synthetic scaffolds are poly(lactic acid) (PLA), poly(glycolic acid) (PGA), poly(caprolactone) (PCL) and their copolymers (PLGA)[213]. Though these scaffolds did not exhibit significant SMC attachment, it was reported that they favored elastin deposition on them[214]. In many cases, release of degradation products due to hydrolysis of these polymers result in local changes in pH and other toxic characteristics that might negatively impact cell attachment and proliferation rates, and ultimately their elastin synthesis capabilities[215]. Similar attempts made by seeding SMCs onto polyhydroxyalkanoate scaffolds subjected to blood flow resulted in uniformly aligned elastin and collagen fibers in the direction of flow[216]. However, it was observed that the

elastin synthesized was either insufficiently- or un-crosslinked, leading to permanent elastin breakdown and loss in construct, 6-months post-implantation in lamb carotid arteries[23].

In other studies, synthetic scaffolds were coated with laminin or other ECM-based matrix molecules. However, in these cases, elastin mRNA expression continues to be severely compromised[217]. Opitz et al., employed poly 4-hydroxybutyrate scaffolds seeded with SMCs and subjected to a pulsatile flow bioreactor[218]. Tissue analyses after one month revealed that though elastin was synthesized in these scaffolds compared to controls which received no stimulus, the elastin fibers were poorly organized with a marked decrease in desmosine content compared with the native aorta. These studies showed that quantitatively less elastin was synthesized, and the level of elastin crosslinking was low, which prompted use of other cellular cues such as growth factors and enzymes which might promote better organization and crosslinking of resulting elastin. Thus, it can be postulated that scaffolds made up of naturally available materials might elicit native cell responses more closely than the synthetic scaffolds.

2.5.4.2 Biological Scaffolds

In recent years, biomolecules specifically, ECM components such as collagen, chitosan, fibrin and GAGs have been increasingly studied in the context of fabricating scaffolds for guided tissue regeneration. The use of ECM-based biomaterials proffers distinct potential advantages, such as providing cells biochemical and biomechanical signals they would experience in a healthy tissue *in vivo* environment and thus potentially

and more faithfully evoke a natural, non-exaggerated matrix regenerative cell response. In addition, ECM molecules, due to their origin would be more readily accepted into the body without extreme inflammatory responses. Since ECM molecules are susceptible to proteolytic degradation, scaffolds based on these materials are chemically derivatized or crosslinked to provide long-term stability. However, this concurrently introduces changes in the innate mechanical and biochemical properties of these ECM molecules, and compromises their ability to elicit native cell responses. Thus, a key challenge un the use of ECM scaffolds for effecting tissue regeneration is to develop methods of matrix stabilization that largely do not alter the biochemical and other characteristics of ECM molecucules. Alternately, ECM components that are amenable to such derivitizations without undergoing significant change must be selected. However, overall, the utility of such materials is contingent on their demonstrated ability to upregulate or facilitate the targeted regenerative phenomenon (in our case, elastin matrix regeneration).

Early attempts to use SMC-seeded collagen scaffolds for blood vessel substitutes resulted in no detectable elastin generation[219, 220]. A more recent study reported higher levels of elastin synthesis by neonatal VSMCs seeded onto fibrin scaffolds and within fibrin-collagen constructs than in collagen constructs[43]. In these cases, although complex elastin geometries similar to that in native elastin were observed, the elastin was produced by neonatal RASMCs, and not adult RASMCs[156]. Neonatal cells have higher elastin regenerative capabilities than those of adult SMCs.

In another interesting study, Lee *et al*. demonstrated that the phenotype of SMCs in engineered tissues is strongly regulated by the chemistry of scaffold *in vitro*[38]. This

means that SMCs exhibit a differential cell growth and ECM production depending upon the scaffold on which they are seeded. Their studies also showed that 2-D culture models also provide useful insights into the elastin production mechanism compared to 3-D models, since trends in scaffold-chemistry-dependent variations of cell phenotype and matrix synthesis are maintained, though not necessarily to the same levels in a 3-D culture system. Studies by Ramamurthi *et al.,* using hyaluronic acid based gels with RASMCs cultured on top of them, demonstrated an increased amount of elastin (both soluble and insoluble) production on the hyaluronan gel, compared to polystyrene culture plates[110]. Furthermore, microscopic analysis of the elastin structure isolated by alkali digestion revealed smooth, highly fenestrated sheets composed of fibers, visible at the sheet edges. It can be concluded that the cellular gene expression could be regulated by various scaffold-derived cues including cell adhesion molecules, growth factors, and mechanical stimuli. In this respect, 3-D scaffolds provide more of these cues than the 2-D cultures. Also, ECM-based scaffolds are more likely to evoke native integrin-ECM interactions and preserve the native cell phenotype, thereby influencing their matrix synthesis capabilities.

These studies validate the overall superiority of 3-D, ECM-based cell scaffolds over 3-D synthetic scaffolds or 2-D monolayer cell cultures to efforts to simulate the chemical and physical environment of tissues. This is because, cells within 3-D scaffolds exist in a more natural environment in which they contact other cells and ECM in three dimensions and are therefore expected to more closely evoke native cell responses than 2-D substrates. In addition, successful up-regulation of elastin synthesis and organization

into mature elastic tissue is crucially contingent on the selection of an appropriate scaffold material from among a sub-set of ECM molecules shown to actively facilitate elastogenesis *in vivo*. One class of biological molecules that was proved to have great potential as elastogenic cell scaffolds is glycosaminoglycans (GAGs). A detailed review on GAGs, HA in particular, for the elastin regeneration potential forms the core theme of the following sections.

2.6 Glycosaminoglycans (GAGs)

As explained in section 2.2, GAGs are linear polysaccharides present on all cell surfaces and in the ECM. They are usually found attached covalently to core proteins forming the proteoglycan family. GAGs assume extended structures in aqueous solutions because of their strong hydrophilic nature based on their extensive sulfation patterns, which is further enhanced when they are covalently linked to core proteins. They hold a large number of water molecules in their molecular domain and occupy enormous hydrodynamic space in solution. The high viscosity of GAGs is associated with low compressibility, which renders these molecules ideal as lubricating fluids in bone joints. Simultaneously, their rigidity provides structural integrity to cells and provides passageways between cells, permitting cell migration[221]. These interactions are often crucial to the biological functions of these proteins.

As shown in **Figure 2.13**, GAGs can be classified into four groups: the hyaluronic acid type, the chondroitin/ dermatan sulfate type, the heparan sulfate/ heparin type, and the keratan type[103]. They have molecular masses ranging from few kDa to few million

daltons. GAGs play an important role in the regulation of many processes, such as hemostasis, growth factor control, anticoagulation, cell adhesion, inflammation, and pathogens attachment[222]. **Table 2.3** summarizes the distribution and functions of different GAG types[103].

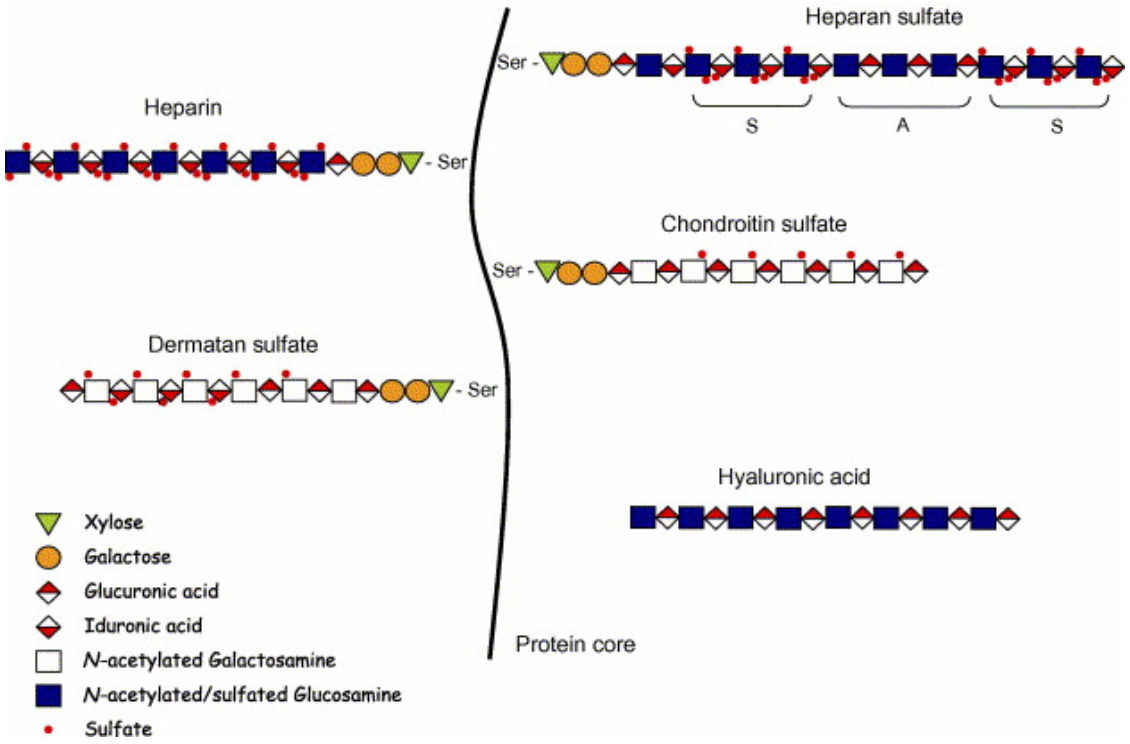

Figure 2.13. Schematic representation of the different GAGs[221].

Though HA does not covalently attach to proteins to form proteoglycans, it forms non-covalent complexes with proteoglycans in the ECM, such as versican. Several recent studies have suggested that GAGs such as HA by themselves, or through their interaction with versican facilitate the synthesis, maturation, and ultrastructural organization of

elastin, and are therefore currently a subject of focused study in the context of developing next-generational natural scaffold materials for elastin regeneration.

Type of GAG	Localization	Comments
Hyaluronan	Synovial fluid, vitreous humor, ECM of loose connective tissue	Large polymers, shock absorbers
Chondroitin sulfate	Cartilage, bone, heart valves	Most abundant GAG
Heparan sulfate	Basement membranes, components of cell surfaces	Contains higher acetylated glucosamine than heparin
Heparin	Component of intracellular granules of mast cells lining the arteries of the lungs, liver and skin	More sulfated than Heparan sulfates
Dermatan sulfate	Skin, Blood vessels, heart valves	-
Keratan sulfate	Cornea, bone, cartilage aggregated with Chondroitin sulfates	-

Table 2.3. Characteristics of glycosaminoglycans.

2.6.1 Hyaluronic Acid: Synthesis and Fragment-Size Effects

HA is a high molecular weight biopolysaccharide[223], which consists of N-acetyl-D-glucosamine (GlcNAc) and D-glucuronic acid (GlcA) linked by a β 1-4 glycosidic bond (**Figure 2.14**). The disaccharides are linked by β 1-3 bonds to form the HA chain[224]. Bacterial production of HA by Streptococcus equi and Streptococcus zooepidemicus enabled it to be produced in larger quantities than could be achieved with the extraction from umbilical cords and rooster combs.

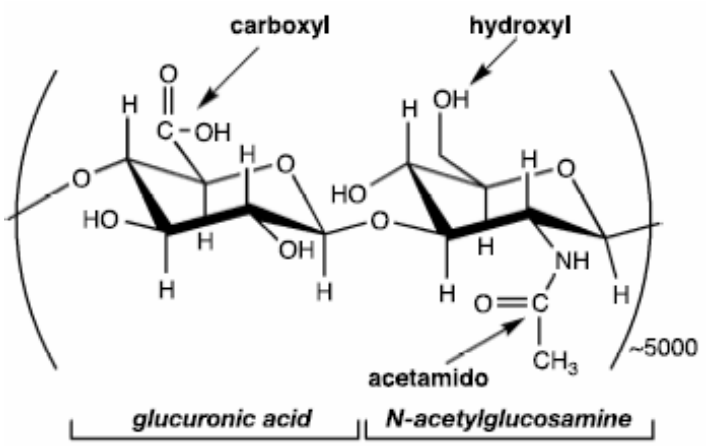

Figure 2.14. Structure of hyaluronic acid (HA).

Trans-membrane glycotransferase enzymes (HA synthases: HAS1, HAS2, HAS3) regulate the biosynthesis of HA. The amino acid sequences of these enzymes are similar but they are produced from genes located at three distinct locations of the chromosome. Each enzyme contains two components (or gylcosyltransferases), one adds GlcNAc and the other is responsible for GlcUA with each addition occurring at the reducing end of the growing chain. The HAS enzymes are transmembrane proteins with an active site on the inner surface of the plasma membrane where HA is pieced together. As the HA chain is being synthesized, it is extruded through the plasma membrane via the HAS complex onto the cell surface or into the ECM. This unrestrained synthesis mechanism allows HA to amass such large chain lengths. HA is synthesized on the inner surface of the plasma membrane, while other GAGs are produced by enzymes within the golgi apparatus of cells[225].

The physiologic cell signaling functions of HA, such as its role in regulating cell aggregation, migration, and differentiation, are achieved through interactions with matrix proteins and cell surface HA receptor proteins, i.e., hyaladherins[226]. Hyaladherin is a term given to a diverse group of proteins capable of binding to HA, via a 100-amino acid sequence called a *link module*, which contains an immunoglobulin domain and two adjacent link modules. It is thought that the link modules mediate protein-HA binding and the immunoglobulin controls protein-proteoglycan interactions. Although there are likely to be several distinct cell surface HA binding proteins, only the cell adhesion molecule CD44 and the receptor for HA-mediated mobility (RHAMM), have been characterized at the molecular level[227]. CD44 is a cell surface glycoprotein with a molecular weight around 85 kDa and plays an important role in HA binding to the cell surface[228, 229]. On the other hand, RHAMM (Receptor for HA-Mediated Motility), has a high molecular weight of 1-2 million Da, that includes a HA binding site and a protein kinase[230]. Upon binding to RHAMM protein, HA induces metabolic changes in the cells, such as stimulation of the protein kinase activity[231]. In contrast to CD44, RHAMM does not display significant homology to the link protein HA binding domain.

Despite its structural simplicity, HA specifically is involved in a wide array of phenomena like morphogenesis, embryonic development, tissue stability, cell proliferation, remodelling, migration, differentiation, angiogenesis, or wound healing. Inflammatory conditions increase HA levels in tissues and body fluids, as with lung fibrosis, rheumatoid arthritis, myocardial infarction and transplant rejection, as well as invasive processes[232].

Recent research throws light on the fragment-size specific effects of HA on the above processes. Native long-chain, high-molecular weight HA (HMW HA) is a stable polymer with MW > 1 million Da, which hydrates the ECM and binds growth factors and smaller GAGs. However, it also causes poor cell interaction because it prevents cell-cell contact. During embryonic development, HMW HA surrounds migrating and proliferating cells, allowing the proliferating cells to develop without being disturbed from the ECM environment, and provides hydrated pathways for migratory cells[233]. HMW HA is inherently anti-inflammatory and immunosuppressive by preventing free radical and infectious organism migration into the tissue. Thus, HMW HA allows tissues to heal without the presence of damaging molecules and organisms resulting in reduced scar formation within the tissues[234]. However, HMW HA must be fragmented in order stimulate a receptor mediated cellular responses.

On the other hand smaller fragments of HA (~100 kDa; LMW HA) and HA oligosaccharides (~ 2-10 kDa) can be pro-cellular, pro-angiogenic and pro-inflammatory[235]. LMW HA is capable of binding to cell surface receptors in a monovalent manner resulting in the stimulation of specific cell signaling cascades, thus influencing their metabolic functions. LMW HA is formed by enzymatic digestion of larger HMW HA and is thought to play a role in wound healing due to their ability to promote angiogenesis *in vivo*[236]. The reason for this occurrence may involve specific receptors such as CD44 and signaling pathways of these cells[237]. In addition, it has been shown that LMW HA stimulates cells to produce angiogenic proteins and enhance the synthesis of collagen types I and VIII. LMW HA has been discovered within

proliferating ECs and SMCs possibly interacting with intracellular receptors[238, 239]. Studies have shown that HA fragments induce the expression of cytokine gene expression in macrophages, which is crucial for initiating and maintaining the inflammatory response[240]. In contrast, studies have also shown that HA oligosaccharides are able to inhibit *in vivo* tumor growth, induce apoptosis, reverse drug resistance in cancer cells and stimulate dendritic cells maturation activating the immune response against tumors[241, 242] (**Figure 2.15**). In various tissue types, HA oligosaccharides have been shown to be more biologically active than long-chain HA, and are likely responsible for eliciting elastogenic responses from cells[110, 243]. Recent studies have reported that HA 4-mer is the minimum size for HA-SMC interaction, which in turn suggests the presence of a receptor for HA 4-mers that does not recognize other sizes of HA[235].

Numerous studies have established that only short oligosaccharides (decasaccharides and hexasaccharides) are necessary for recognition and binding to hyaldherins and CD44 receptor[238]. Cell anchored long-chain HA molecules can prevent cells, particles and large molecules from approaching close to the cell membrane. It can be speculated that larger HA fragments can create a more efficient shield than low molecular weight smaller HA fragments at similar concentrations[235], likely because long-chain HA meshworks overlap and aggregate with HA molecules attached to neighboring cell surface binding sites, while smaller HA fragments contain HA molecules that are not long enough to overlap and reinforce neighboring hyaluronan aggregates, leaving spaces and channels through which particles can approach closely to the cell membrane.

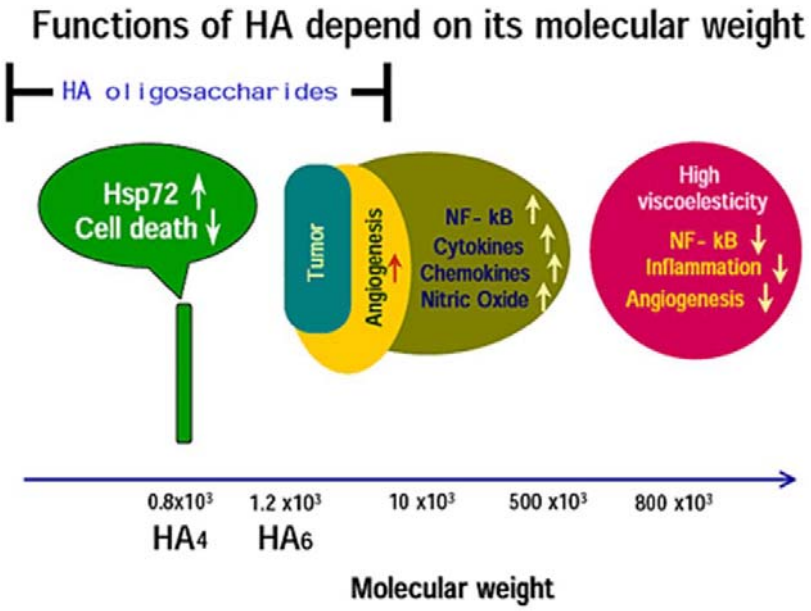

Figure 2.15. Fragment-size specific functions of HA[235].

2.6.2 Applications of HA in Tissue Engineering

The above discussion provides a general idea of how HA can be used as a biomaterial. The intrinsic physicochemical and biological properties of HA made possible its applications in clinical therapies, diagnostics, tissue engineering scaffolds, and drug delivery devices. Initially, HA was used as space filler, lubricating material, and as viscoelastic-ophthalmic filler material to support the implantation of intraocular lenses in cataract patients[244]. However, its current applications span from orthopedic to cardiovascular engineering, wound healing and regeneration of skin, as antiadhesive material in dental applications, and in general tissue engineering and surgical interventions[54, 245]. A list of FDA approved HA products in market are listed in **Table 2.4** below. In recent years, HA has found applicability abroad as a joint lubricant in

arthritic joints, owing to its favorable rheological properties[246]. Recently, Anika, Biomatrix, and Fidia obtained FDA approval for the use of HA as an injectable in the USA[103]. In addition, HA has been used as an implant fluid /film to improve lubricity, and reduce fouling and tissue abrasion and tissue adhesions following surgery, the latter application due to the poor interaction of HA films with cells[103, 247]. In these applications, the long-term success of the product is significantly facilitated by the inherently non-antigenic and non-immunogenic properties of HA, a result of their strong homology of structure across species[248].

Under pathological conditions, as in cancer and atherosclerosis, HA exhibits undesirable properties that can be tailored to provide benefits to tissue engineering[249]. For example, since HA promotes angiogenesis and facilitates tumor growth *in-vivo*, it can be used in neo-vascularization of grafts and vascular scaffolds. HA is also an important component of the cellular microenvironment because it directly affects tissue organization via interactions with cell surface receptors such as CD44[250]. Through a well- studied interaction with CD44, HA promotes the migration of cells, facilitates ECM remodeling, promotes the inflammatory response and can inhibit cell adhesion. Thus, a tissue engineered construct that incorporates HA and/or HA receptors could have enhanced cell-material interactions and improved cell migration. HA plays a vital role in the development of cartilage, the maintenance of the synovial fluid, and the regeneration of tendons[226].

Application	Tradename	Approval type	Company
Osteoarthritis	Hyalgan	Premarket	Fidia
	Synvisc	Premarket	Biomatrix/Genzyme
	Supartz	Premarket	Seikagaku
	Hylashield	510 k	Biomatrix
Ophthalmology	Healon	Premarket	Pharmacia
	Amvisc	Premarket	Bausch and Lomb
	Coease, Shellgel, Staarvisc	Premarket	Anika Therapeutics
	Amo Vitrax, Vitrax	Premarket	Allergan/Medtronic
	Provisc, Viscoat	Premarket	Alcon Laboratories
Wound healing	Bionect	510 k	Fidia
	Ialuset	510 k	IBSA
Postsurgical adhesions	Adcon	Premarket	Gliatech
	Intergel	Premarket	LifeCore Biomedical
	Seprafilm	Premarket	Genzyme
Surgical scaffolding	Hyalomatrix	510 k	Fidia
	Hylasine	510 k	Biomatrix
Gastrourology	Deflux	Premarket	Q-Med

Table 2.4. FDA-approved HA products in market[251].

In previous studies, HA-liposomes have been investigated for their ability to act as site-adherent and sustained-release carriers of epidermal growth factor for the topical therapy of wounds and burns, which in itself involves regeneration of elastic tissues[252]. Composite sponges of hyaluronan and chondroitin sulfate have been used as wound dressings or scaffolds for tissue engineering[253-255]. HA has also been proven to be effective for increasing the blood compatibilities of cardiovascular implants such as vascular grafts and stents. For example, biomaterial surfaces treated with cross-linked HA have been associated with reduced platelet adhesion and thrombus formation[256-258]. Cross-linked HA is also a promising biomaterial for cardiac tissue engineering. **However, very few studies have investigated the matrix regenerative capabilities of HA, in the context of elastin synthesis by adult SMCs, and that is the focus of our current efforts.**

2.7. Role of HA in Elastin Synthesis

Previous studies reported that in pulmonary, vascular and dermal tissues, a close association exists between GAGs such as HA and heparin sulfate, and proteoglycans such as versican and elastin[50, 51, 259, 260]. Though not all GAGs (e.g., dermatan and chondroitin sulfates) support elastic fiber formation[261], HA plays a prominent role in the synthesis and organization of microfibrils (fibrillin), a precursor for elastic fiber deposition[50, 51, 260]. HA has been implicated to play key roles in the synthesis[262], organization, and stabilization[263] of elastin by VSMCs. HA has been suggested to play an indirect role in elastogenesis through its intimate binding of versican, which in turn interacts with microfibrillar proteins (fibulin-1, 2) and elastin-associated proteins to form higher-order macromolecular structures important for elastic fiber assembly[50, 51, 260]. Recent studies provide evidence that some GAGs (e.g., HA) coacervate soluble tropoelastin molecules on their highly anionic surfaces, to facilitate LOX- mediated crosslinking into an insoluble matrix[264], and stabilize elastin fibers against degradation by elastases. These findings encourage further study into the utility of HA biomaterials as scaffolds for elastic tissue regeneration.

Previously, Ramamurthi et al. evaluated the matrix (elastin and collagen) synthesis potential of UV-irradiated, DVS-crosslinked HA gel substrates (hylans; MW > 1.5 MDa), and found that at all assay times, the amounts of elastin was derived from the HA-based cell cultures was 25% or more than that derived from cells cultured on plastic, though no significant differences were found in the two substrates beyond the first two weeks of culture when elastin content was normalized to the cell DNA content (**Figure**

2.16). At early culture times (< 2 weeks), cells cultured atop the irradiated hylans showed a 2.4-fold increase in the ratio of insoluble to soluble matrix elastin relative to those cultured on plastic and a 25% increase in total (i.e., soluble + insoluble) output of matrix elastin. At longer culture times (< 6 weeks), the same trend was maintained. When the DNA-normalized amounts of elastin matrix were compared, significant elastin up-regulation was noted among cells cultured on HA versus those on plastic at 2 weeks but not at later time points. Cells grown on HA deposited an unusual matrix layer, rich in elastin at the HA-cell interface. This elastin was found to be organized into fenestrated sheets and loose elastin fibers, structures that were also isolated from the elastin matrix of the ventricularis layer of porcine cardiovascular tissues (**Figure 2.17**). Cell-synthesized tropoelastin was incorporated and stabilized into an unusually exuberant elastin matrix layer not seen in control cells cultured on plastic or atop gels containing only long-chain HA. The preferential deposition of matrix elastin at this interface may be due to the attraction and coacervation of soluble tropoelastin molecules by the highly anionic HA gel.

This hypothesis is supported by previous studies by Wu *et al*.,[265] and Forneieri *et al*.,[266] which demonstrated that positively charged lysine residues on the tropoelastin molecules bind to negatively charged GAG molecules. The GAGs then induce the tropoelastin molecules to coacervate along their surface. The electrostatic interactions between the GAGs and the tropoelastin molecules are freed only when the lysine residues are modified by cell-derived LOX during crosslinking of the elastin[265]. A comparative study of the biochemical and imaging data suggests that (a) intimate cell contact with the

HA substrate may influence it's direct up-regulatory effects on elastin gene expression (or elastin output), and (b) HA influence elastin matrix deposition through a secondary, post translational mechanism that may involve the preferred coacervation of synthesized tropoelastin on the anionic HA surface, resulting in more efficient crosslinking into an insoluble matrix form. Although UV light introduces some new crosslinks into the gel, the predominant and a highly repeatable effect is the cleaving of a small proportion of HMW HA molecules on the gel surface into shorter, intermediate MW (~100-500 KDa) fragments and shorter oligomer (MW ~5-10 KDa). These results generated the hypothesis that smaller HA fragments induce enhanced cell responses.

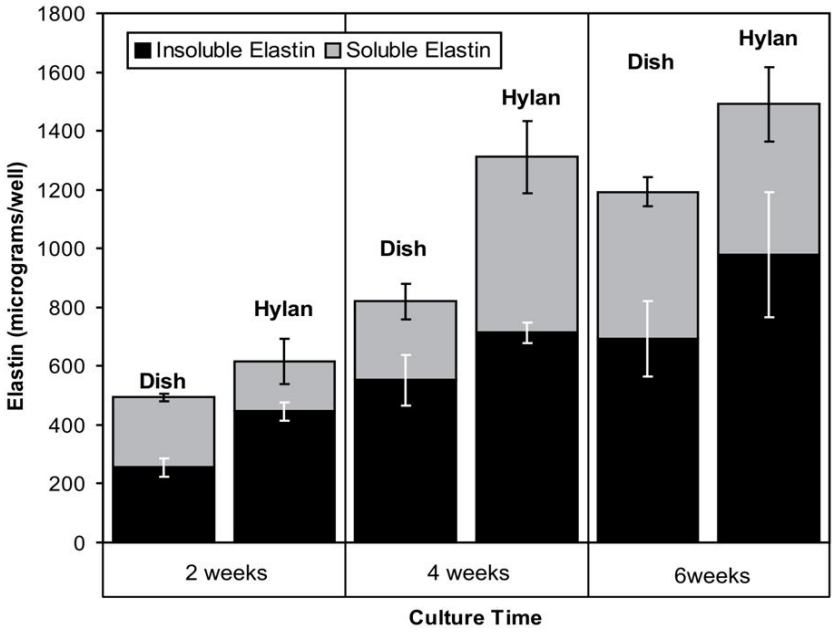

Figure 2.16. Substrate-dependent synthesis of ECM matrix elastin. Shown is the mean ± SD of the amounts of elastin derived from cell layers cultured within plastic dishes and atop irradiated hylan gels for up to 6 weeks ($n = 3$)[110].

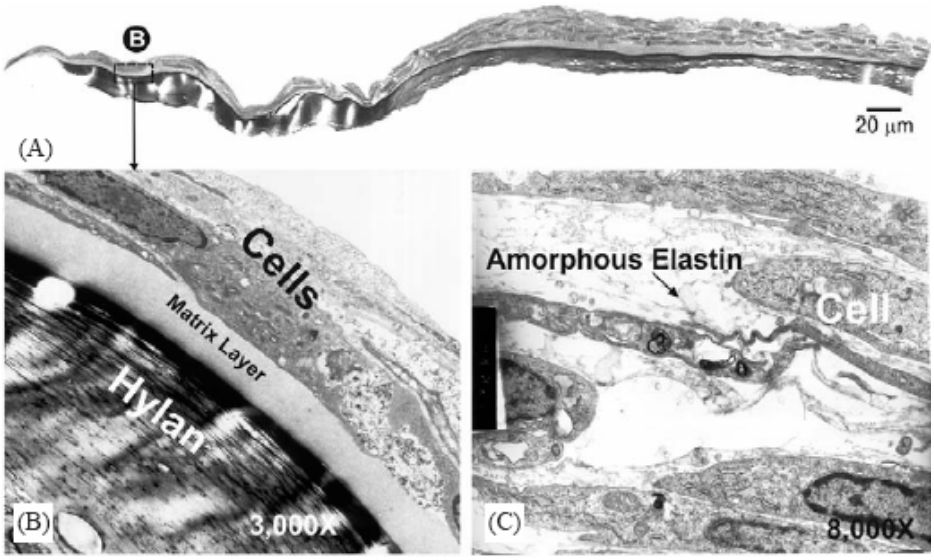

Figure 2.17. Light micrograph of elastin matrix at the cell-hylan interface. The sample was stained with Toluidine Blue dye to provide contrast (A; 100×). Representative TEM images show the presence of this layer in cell layers cultured atop hylans (B) but not on plastic (C). Images were obtained shown at 4 weeks of culture[110].

However, it should be noted that the cultured elastin constructs contained fewer, non-aligned elastic fibers, likely the result of culture on a 2-D surface, and not an ECM-like 3-D scaffold, and the failure to provide additional biologic cues important to elastic fiber formation and organization. Besides highlighting the need for such additional stimuli, these previous studies showed that (a) HA fragments induce greater biologic activity when incorporated within crosslinked gels composed of HMW HA and likely enhance elastin matrix deposition, and (b) elastin laid down atop hylans contain essential structural elements of native elastin matrices. Since the irradiation process is difficult to control, and can potentially cause material degradation by random ionizations, one

approach to creating cell-responsive HA scaffolds is to formulate gels based on mixtures of different HA fragment sizes, in quantity ratios optimized based on their individual and combined effects on desired (i.e., elastogenic) cell responses. However, the success of this approach is contingent on restricting the total content (wt.%) of HA fragments within the mixed gel to 10% or less (the balance composed of HMW HA), since this composition preserves gel handling properties and mechanics besides eliciting enhanced cell responses, and does not interfere with the inherent immunocompatibility of hylans.

Thus, encouraged by these previous studies which showed that HA gels are proactive in eliciting elastogenic responses by RASMCs[110, 267], recent *in vitro* studies by Joddar *et al.*, focused on elucidating the elastogenic effects of HA fragments (different molecular weights) and their dosages on adult RASMCs[243, 268]. In these studies, adult RASMCs were cultured with exogenous HA supplements (MW: 1500, 200, 20 and 0.75 kDa) at varying concentrations of 0-200 μg/mL over 3 weeks. At the end of 21 days, the effects of exogenous non-oligomeric HA on soluble tropoelastin and desmosine-crosslinked elastin matrix synthesis were nearly identical to each other (**Table 2.5**). Elastin synthesis was slightly stimulated by HMW HA and inhibited by exogenous non-oligo HA fragments in inverse correlation to fragment size, although in general, no dose-relationships were noted (**Table 2.5**). LMW and VLMW HA both inhibited tropo- and matrix elastin synthesis relative to controls, and to extents that correlated inversely to fragment size. Large exogenous HA fragments do not appear to increase elastin matrix deposition; on the contrary, a reverse trend is observed. However, the lack of any HA-mediated enhancement in per cell elastin output as previously determined for cells

cultured on HA gels suggests vital differences in cell response to HA, when delivered exogenously and or as a substrate. It is likely that the observed differences in elastin output are due to the combined influence of two possible factors namely, HA-mediated stabilization of elastin, and HA-induced differences in cellular elastin output.

TEM images of the cell layers concur with observed elastin deposition trends, and confirm normal fibrillin-mediated mechanisms of elastin matrix deposition. Most elastin in test and control (no HA) cell layers was deposited in the form of amorphous clumps. Within this group, many clumps appeared circular and measured roughly 100 nm across, supporting our assumption that these are transverse-sections of elastin fibers, several of which were seen in axial orientation. The presence of fibrillin microtubule networks surrounding elastin clumps, essential precursors to elastin fiber organization, suggests that elastic fiber organization in presence of HA proceeds via normal fibrillin-mediated mechanisms. The greater density of elastin fibers in cell layers cultured with HMW HA than smaller HA fragments, implicates HMW HA in the post-translational maturation of matrix elastin.

HA Size (Daltons)	Dosage (mg/ml)	Tropoelastin		Matrix Elastin (Soluble + Insoluble fractions)	
		Fastin Assay (10^4 ng/ng of DNA)	Band intensity relative to control	Fastin Assay (ng/ng of DNA)	Desmosine relative to control (ng/ng)
Control	0	40.0 ± 5.4	1.00 ± 0.04	389 ± 65	1.00
High (2×10^6)	200	47.5 ± 9.1 ↑↑	1.37 ± 0.54 ↑↑	494 ± 72 ↑	1.04 ↑
	2	55.3 ± 5.5 ↑	1.54± 0.52 ↑	389 ± 38	0.93
Low (2×10^5)	200	39.2 ± 6.3	1.00 ± 0.05	405 ± 51	0.66 ↓↓
	20	21.4 ± 10.3 ↓↓	0.59± 0.03 ↓↓	232 ± 11 ↓↓	0.71 ↓↓
	2	24.2 ± 3.3 ↓↓	0.62 ± 0.03 ↓↓	230 ± 22 ↓↓	0.61 ↓↓
	0.2	21.7 ± 6.0 ↓↓	0.49± 0.02 ↓↓	79 ± 25 ↓↓	0.52 ↓↓
Very Low (2×10^4)	200	14.2 ± 0.6 ↓↓↓	0.28 ± 0.15 ↓↓↓	178 ± 5 ↓↓↓	0.37 ↓↓↓
	2	18.2 ± 0.4 ↓↓↓	0.39 ± 0.25 ↓↓↓	186± 7 ↓↓↓	0.16 ↓↓↓

Table 2.5. Effects of exogenous HA/ HA fragments on elastin synthesis by adult RASMCs (select results only). Biochemical trends were confirmed semi-quantitatively by Western blot (tropoelastin only) and by quantifying desmosine crosslinks within the elastin matrix. Results represent mean ± SD of $n \geq 4$ repeat cultures for each case.

In-house synthesized HA oligomers (4-mers; 0.756 kDa; 0.2 μg/mL) however elicited different outcomes; oligomer presence did not influence cell proliferation after 3-weeks compared to non-additive controls, but increased DNA-normalized output of soluble tropoelastin by 1.6 fold and that of matrix elastin by 2.7 fold. The fraction of total synthesized elastin in the crosslinked matrix form as well as the desmosine crosslinks were also higher, relatively[58]. HA 4-mers also enhanced elastin resistance to enzymatic degradation (35% loss vs. 99% loss for non-HA control, 8 h study, 37 ^{o}C, 20 U/mL elastase) and halved elastin laminin receptor (ELR) activity, suggesting reduced elastin degradability. TEM images showed elastin deposits within oligomer-supplemented cultures to be distinct, longitudinally oriented, aggregating fibrils, and clumps, and to be less abundant and mostly amorphous in controls. HA oligomers preserved normal fibrillin-mediated elastin matrix deposition. Increase in fibrous elastin formation over an amorphous elastin deposition was also observed (**Figure 2.18**). Identical results were observed with rough enzymatic digests of HMW HA, containing 4-mer (75 ± 15% w/w) as the primary product[58]. SDS-PAGE/Western Blot and a desmosine assay semi-quantitatively confirmed the observed biochemical trends for tropoelastin and matrix elastin, respectively. In comparison to HMW HA supplementation studies, data suggest

that pure HA 4-mers or mixtures containing predominantly 4-mers enhance elastin matrix synthesis, stability and fiber formation, while HMW HA may only influence elastin crosslinking. Overall, results suggest that HA oligos are highly pro-elastogenic, promote elastin fibril formation, and stabilize elastin matrix and may thus be usefully incorporated into scaffolds containing HMW HA for guided elastin regeneration.

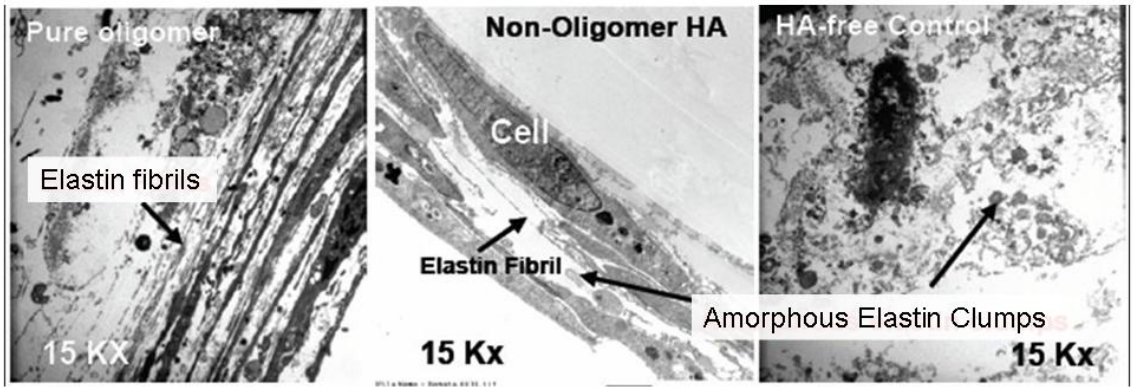

Figure 2.18. TEM images of elastin matrix produced by RASMCs cultured with or without HA oligomers[268]. Elastin fibrils formed when cultured with HA oligomers, unlike elastin deposited in the presence of HA-free controls and non-oligomer HA.

Studies conducted on valvular interstitial cells reported by Masters *et al.*[269], showed an up-regulation in elastin synthesis upon exposure to scaffold-derived HA fragments. Although the biological effects of HA are somewhat specific to cell type, these observations are in general agreement with previous reports that HA fragments, particularly the oligomers, interact more with cells. Since HA fragments can also potentially elicit inflammatory cell responses, they must be sparingly incorporated into

HA biomaterials after thorough investigation into their size-specific effects on desired (e.g., elastogenic)[270], and undesired (e.g., inflammatory) cell responses.

2.8. Role of Growth Factors on Elastin Sythesis

Crucial challenges to tissue engineering a mimic of native elastic tissue include the ability to regulate the amount, quality, ultrastructure and higher scale organization of the elastin matrix. Most of these challenges, however, can be overcome, by providing cells appropriate biomechanical and biochemical cues. Biomechanical regulators have been shown to both influence the cell phenotype, and dictate the pattern of matrix deposition. A primary source of biomechanical transductive signals is the cell scaffold itself. Thus, to faithfully regenerate elastin, the scaffold design must replicate micro-architectural facets of the ECM, such as circumferentially aligned, nano-sized fibers, and micron-sized pores to help mimic the attachment, migration, and circumferential orientation of SMCs within native vessels[271, 272].

Previous studies have shown that insulin-like growth factor-I (IGF-1) stimulates mitogenesis in SMCs, and upregulates elastin synthesis in embryonic aortic tissue[65]. Incubation of confluent cultures with various concentrations of IGF-I resulted in a dose-dependent stimulation of elastin synthesis, with a 2.4-fold increase over control levels at 1000 ng/mL of IGF-1[65]. Besides, this increase in elastin synthesis was reflected by a stimulation of the steady-state levels of tropoelastin mRNA. In a later study by Foster *et al*., it was observed that the effects of IGF-1 are age-dependent and tissue-specific[273]. For example, rats treated with IGF-1 (1.2 mg/kg/day) showed that administration of IGF-

1 elevated aortic tropoelastin mRNA steady-state levels, whereas lung tropoelastin mRNA levels were unaffected. The steady-state levels of tropoelastin mRNA decreased dramatically in both aorta and lung with increased rat-age, with the decrease greater in lung than aorta. Moreover, aortic tissue synthesized decreased amounts of insoluble elastin with increased age. In conclusion, these results establish a direct relationship between aortic tropoelastin mRNA levels and the synthesis of insoluble elastin in aging; and that administration of IGF-1 increased aortic elastin synthesis throughout the life span of the rat, although the proportionate increase diminished with age[273]. In a separate study, Noguchi *et al*. observed that when 500 ng/mL of IGF-1 was added, there was 86 ± 14 and 35 ± 5% increase in tropoelastin and total elastin protein synthesis, respectively, by rat neonatal pulmonary fibroblasts, relative to controls[67]. This was confirmed by a corresponding 95 ± 20% increase in the tropoelastin mRNA/beta-actin mRNA ratio[67] and a dosage dependence of tropoelastin synthesis on IGF-1 concentration. Wolfe et al. found in neonatal RASMC cultures, that addition of 50 ng/mL of IGF-1 to quiescent cells resulted in a 5-fold increase in the steady-state levels of tropoelastin mRNA beginning between 2 and 4 h and reaching maximal levels at 8 h[274]. Besides. transcription analyses of nuclei isolated from IGF-1 -treated cells showed increased synthesis of new tropoelastin transcripts indicating that transcriptional activation is a major component of IGF-1 up-regulation[274].

Other studies suggest that TGF-β family is involved in regulation of elastin deposition during fetal development and tissue repair, as well as in pathological conditions. McGowan *et al*. examined the influence of TGF-β on the production of

elastin by postconfluent cultures of neonatal rat lung fibroblasts[275]. They found that the tropoelastin was approximately 2-fold greater in the presence of 40 or 100 pM TGF-β than in its absence and that this increase in tropoelastin was accompanied by a smaller but significant increase in the steady-state level of elastin mRNA[275]. Kahari *et al*. examined the effects of TGF-β1 and TGF-β2 on human elastin mRNA abundance, promoter activity, and mRNA stability in cultured human skin fibroblasts and found that with varying concentrations of TGF-β1 or TGF-β2 for 24 h resulted in a dose-dependent increase in the elastin mRNA steady-state levels, with a maximum enhancement of approximately 30-fold being noted with 1 ng/mL[68]. These results demonstrate that TGF-β1 and TGF-β2 are potent enhancers of elastin gene expression and that this effect is mediated, at least in part, post-transcriptionally. In addition, TGF-β augments LOX-mediated crosslinking of soluble tropoelastin into a mature, insoluble matrix layer[69, 70].

The effects of human recombinant interleukin (IL-1β) on elastin gene expression were studied in human skin fibroblast cultures by Mauviel *et al.*, who found that incubation with IL-1β elevated the elastin mRNA steady-state levels by approximately 3-4 fold, with a similar increase at the protein level[276]. Their data conclusively indicates that IL-1β upregulates elastin gene expression in fibroblast cultures as well as in the skin *in vivo*, and that the activation occurs at the transcriptional level[276]. On the other hand, epidermal growth factor was found to inhibit elastin synthesis in chick aortic SMCs[277]. The inhibitory effect was dose-dependent with a 90% reduction at 100 ng/mL dosage, and the degree of inhibition in elastin synthesis was parallel to the decrease in the steady-state levels of elastin mRNA expression[277].

In conclusion, elastogenesis can be mediated by different receptors and by various growth factors and specific culture conditions as reviewed above[62, 278]. Besides growth factors, various biomolecules such as LOX helps to crosslink the tropoelastin to give elastic fibers. In the absence of LOX, tropoelastin tends to associate with GAGs due to the presence of amino groups in the elastin lysine residues, which offer positive charges for binding with negative charges of GAGs. Besides, in the absence of LOX, such electrostatic interaction could be important and prevent newly synthesized tropoelastin molecules from spontaneous random aggregation far from the cell surface[264, 279]. Other investigators showed calcitriol and retinoic acid as factors that promote elastogenesis[280-282].

In an effort to improve and control elastin generation and orientation in synthetic or natural scaffolds for an ideal tissue-engineered blood vessel substitute, many investigators have utilized mechanical stimulation to the constructs, contained within bioreactors. The primary purpose of a bioreactor is to provide, maintain and encourage tissue regeneration under permanently controlled culture parameters such as temperature, pH, biochemical gradients and mechanical stresses that mimic physiological conditions[283]. Different culture condition can be modified to study their influence on the growth of different tissues. The application of cyclic mechanical stretch simulating distension experienced by medial SMCs *in vivo*, may also significantly influence the phenotype[248, 284], alignment[285, 286], matrix deposition[287, 288], and growth factor release[289, 290] by both native and cultured SMCs. Pertinent to this discussion, pulsatile stretch has also been shown to up-regulate elastin synthesis and enhance circumferential alignment[85, 291].

Typical cyclic mechanical strains employed in bioreactors *in vitro* for the synthesis of elastin by SMCs seeded onto scaffolds range within a frequency of 0.05-1 Hz, an amplitude of 0-20%, pulsatile radial stress of 165 beats per minute, and 5% radial distention[85, 291, 292].

Bioreactors are particularly crucial for the regeneration of complex three-dimensional tissues in tissue engineering applications[248, 293], since culturing cells alone in a dish or in contact with materials in culture medium is not enough to obtain a functional tissue. In one of the most preliminary studies involving PGA scaffolds and collagen scaffolds seeded with RASMCs, Kim *et al*.[85, 213, 294] studied the effect of mechanical signals on elastin biosynthesis under dynamic stimulation and observed elastin biosynthesis on bonded PGA scaffold to be upregulated by dynamic stimulation, relative to static culture conditions. Elastin biosynthesis on collagen sponge scaffold, however, did not respond to the stimulation, which indicates that biomechanical stimulation alone was not sufficient for elastin biosynthesis but the nature of the scaffold also plays an important role. This finding is in agreement with the observation by Seliktar et al. who reported elastin mRNA expression to be independent of the dynamic stimulation on collagen gel scaffold[295]. In a recent study, Isenberg *et al*., applied sustained dynamic stimulation to vascular cell-seeded collagen gel scaffold in an attempt to promote elastogenesis, and the data suggested significant elastin biosynthesis on collagen scaffolds[291]. In another study, Opitz *et al.*, evaluated the effect of dynamic stimulation on elastin biosynthesis, wherein they seeded VSMCs on poly-4-hydroxybutyrate scaffold and dynamically pulsated the construct[218]. They found out that the elastin content in this

setup was significantly lower relative to the native aorta, though no elastin was detected in statically matured blood vessels. Though most of the studies employing mechanical stimuli succeeded in improving the general mechanical properties, such as burst strength, as a result of collagen biosynthesis, most of them failed to induce elastin biosynthesis[292, 296-298]. Nevertheless, the studies reviewed here are very promising, and future studies should be geared towards optimizing these conditions discussed above for specific tissues.

CHAPTER 3

SYNERGY BETWEEN ELASTOGENIC CUES: IMPACT OF TGF-β1 AND HA FRAGMENTS

3.1 Introduction

In chapter 2, we discussed in detail the role of elastin in facilitating elastic recoil and resilience necessary for cyclic distension and contraction in blood vessels[299]. Since compromised elasticity can contribute significantly to ageing of connective tissues and in the development of aortic aneurysms and emphysema, vascular elastin must be restored or regenerated as a priority. However, efforts to regenerate lost elastin structures *in vivo* and within tissue-engineered constructs are limited by the progressive destabilization of tropoelastin mRNA expression in adult vascular cells[24, 300], the current unavailability of appropriate cellular cues for upregulating elastin precursor production and its assembly into structural matrices, that are faithful mimics of native elastin networks[301]. Due to the frequently exaggerated and unnatural cell responses to cues such as those provided by synthetic biomaterial scaffolds, we seek to employ an alternate regenerative strategy based on ECM-derived biomolecular cues, which we expect would be more useful to faithfully regenerate matrices that replicate the functional architecture and mechanics of native elastin. A logical elastin regeneration approach is thus to select elastogenic cues from amongst a subset of ECM molecules that participate in or regulate elastic fiber deposition during development[302].

Among the ECM molecules involved with elastin synthesis and organization, HA apparently plays a key role in elastogenesis through its intimate binding of versican, which in turn interacts with other elastin protein-associated microfibrillar proteins (fibulin-1, 2) to form macromolecular structures responsible for elastic fiber assembly[48, 51]. Recently, our lab confirmed that elastin protein production by vascular SMCs is also influenced by HA fragment size[58, 60]; particularly, HA oligomers in the 4-6 mer range increased production of soluble elastin protein precursors (tropoelastin) and crosslinked elastin matrix, and enhanced formation of fibrillin-rich elastic fibers and of elastin matrix stability by increasing desmosine crosslink densities. Other studies have shown that elastin matrix synthesis can be modestly enhanced by stimulating vascular SMCs with growth factors such as TGF-β1[63, 66] at physiologically-relevant concentrations, typically in the order of 1 ng/mL [10^{-11} M][303]. Also at low doses [~1 picograms/cell; 1 pg = 10^{-12} g], TGF-β1 does not stimulate SMC proliferation[304] in a manner it does at higher doses.

Despite their standalone benefits, it is unknown if TGF-β1 and HA fragments cues together will synergistically improve elastin matrix synthesis and assembly, while retaining the benefits [e.g., suppressed cell proliferation, elastin-laminin receptor activity] of their standalone delivery. To assess these aspects, we presently investigate the pro-elastogenic effects of HA fragments supplemented exogenously to the cultured adult rat aortic SMCs (RASMCs) concurrent with an elastogenically-effective dose of TGF-β1.

3.2 Materials and Methods

3.2.1 HA Procurement and Oligomers Preparation

HA with molecular weights of 2000 kDa (Genzyme Biosurgery, Cambridge, MA), 200 kDa (Genzyme Biosurgery), 20 kDa (Lifecore Technologies, Minneapolis, MN), and 0.756 kDa, designated as HMW, LMW, VLMW and oligomers, respectively, were dissolved in sterile serum-free culture medium.

HA oligomer (4-mers) mixtures were prepared by testicular hyaluronidase digestion (Sigma Aldrich, MO; 37^{o}C, 16 h, 160 U/mg) of HMW HA as we previously optimized and reported[58]. HA 4-mers were prepared from long-chain HMW HA by digestion with hyaluronidase. The protocol used in our current study generates a mixture of oligomers containing primarily HA 4-mers (tetrasaccharides), and smaller fractions of HA 6-mers and 8-mers (hexa- and octa-saccharides respectively). Briefly, 20 mg of HMW HA (2000 kDa; Genzyme Biosurgery) was digested with bovine *testicular hyaluronidase* (3.6 mg; 451 U/ mg), in 4 mL of digest buffer (150 mM NaCl, 100 mM CH_3COONa, 1 mM Na_2EDTA, pH 5.0) at 37ºC for 18 h. Boiling the mixture in a water bath for 5 min following digestion terminated the enzyme activity. The mixture was centrifuged (500*g*, 7 min) to remove the phase-separated coagulated enzyme, dialyzed against water overnight, and stored at -20ºC. HA oligomers in the digestate were subsequently analyzed using a Polyacrylamide Gel Electrophoresis. The molecular weight of the generated series of oligosaccharide bands was calculated based upon their mobility in the electrophoresis gel, relative to a known ladder of standards.

3.2.2 Cell Isolation and Culture

RASMCs were isolated from adult male Sprague-Dawley rats (weighing 250-300 g) as per protocols approved by the Animal Research Committee at the Medical University of South Carolina and the Clemson University. Aortal segments were removed from euthanized rats from arch to the celiac axis under sterile conditions, and spliced lengthwise in petri dishes containing cold phosphate-buffered saline (PBS) containing 2 mM Ca^{2+}. These spliced sections were then transferred to a dish containing 1-2 mL of collagenase (2 mg/mL; Worthington, Lakewood, NJ) and incubated for 10 min at 37°C. DMEM: F12 media was then added to these collagenase treated samples and mixed well with gentle pipetting. Isolated aortal segments were further chopped crosswise into 0.5-mm long pieces and transferred using fine needles onto sterile petri dishes, pre-scratched to facilitate cell anchorage/ attachment. The explants were incubated in limited volumes of the above medium at 37°C for a week, to establish primary culture. At the end of one week, the explants were removed carefully and sufficient DMEM: F12 added to the dish to promote cell proliferation.

RASMCs from passages 1-5 were seeded onto 6-well tissue culture plates (Becton Dickinson, NJ; A = 10 cm^2) at 2×10^4 cells/ well. The total volume of medium added per well was 5 mL. A 1-mL bolus of HA/fragments/oligomers prepared in serum-rich DMEM (Invitrogen; 10% v/v FBS) was added to cell cultures at an ultimate dose of 0.2 μg/mL. In addition, TGF-β1 (Peprotech Inc., Rocky Hill, NJ) was supplemented at a final dose of 1 ng/mL. Thus, cells theoretically received an equivalent of 0.25 fg of TGF-β1/cell, which closely agrees with the dose supplied in prior published studies[305]. Other

cultures received either HA/ fragments/ oligomers or TGF-β1 alone, or no supplements (controls). Spent medium from each well was replaced twice weekly during the duration of culture, pooled, and frozen. At 21 days, these aliquots and their corresponding cell layers were biochemically analyzed. The cell layers cultured in the presence of HA fragments and TGF-β1 were imaged on an Axiovert 200 (Carl Zeiss, Thornwood, NY) at regular intervals.

3.2.3 DNA Assay for Cell Proliferation

The DNA content of cell layers was quantified at 1 and 21 days of culture using a fluorometric assay described earlier by Labarca and Paigen[306]. Briefly, cell layers at 1 and 21 days of culture were detached with 0.25% v/v trypsin-EDTA, pelleted by centrifugation, re-suspended in 1 mL of NaCl/Pi buffer (4 M NaCl, 50 mM Na_2HPO_4, 2 mM EDTA, 0.02% Na-Azide, pH 7.4), sonicated for 3 min over ice, and a 100 μL aliquot assayed. Actual cell counts were then calculated on the basis of 6 pg DNA/cell, assuming this amount remained unchanged through the period of culture[306].

3.2.4 Hydroxy-Proline Assay for Collagen

A Hydroxy-proline (OH-Pro) assay was used to estimate the collagen content within test and control cell layers, and in the supernatant medium fraction. Briefly, the cell layers were homogenized in distilled water after 21-days of culture, pelleted by centrifugation (10000 *g*, 10 min) and digested with 1 mL of 0.1 N NaOH (1 h, 98ºC). The digestate was then centrifuged to isolate a mass of insoluble, crosslinked elastin. The

supernatant containing solubilized collagen and uncrosslinked matrix elastin was neutralized with an equal volume of 12 N HCl, and divided into two equal volumetric halves. One half-volume was hydrolyzed at 110°C for 16 h, dried overnight, and 20 μL aliquots of the reconstituted residue assayed for hydroxy-proline content. The measured amounts of OH-Pro were corrected to account for the 4% w/w of OH-Pro contained in solubilized elastin. Total and matrix collagen amounts were then calculated on the basis of the 13.2% OH-Pro content of collagen, and normalized to DNA content of corresponding cell layers.

3.2.5 Fastin Assay for Elastin Protein

A Fastin assay (Accurate Scientific and Chemical Corporation, Westbury, NY) was used to quantify the total amount of matrix-elastin protein (present as alkali-soluble and insoluble fractions), and soluble tropoelastin in lyophilized pooled medium fractions from each well. Since the Fastin assay quantifies only soluble α-elastin, the insoluble elastin was first reduced to a soluble form by digesting with 0.25 N oxalic acid (1 h, 95°C), and filtering the pooled digestate in microcentrifuge tubes fitted with low molecular weight cut-off membranes (10 kDa). The insufficiently crosslinked, soluble elastin fraction retained in the oxalic acid-free fraction and in the water-reconstituted hydrolysate (from the collagen assay above) were also quantified using the Fastin assay. Spent fractions of media pooled at bi-weekly intervals over the 3-week culture period were lyophilized and processed for tropoelastin using the Fastin assay. The measured

elastin protein amounts were normalized to corresponding DNA amounts to provide a reliable basis of comparison between samples.

3.2.6 Desmosine Assay for Elastin Crosslinks

In select cases, desmosine crosslink densities within elastin matrices were quantified to determine if any of the provided cues enhanced efficiency of crosslinking of elastin molecules. The 21-day-old cell layers cultured with no additives (control), TGF-β1 alone, or TGF-β1 together with HMW HA or HA oligomers, were pooled and stored at -20^{o}C. Desmosine content was assayed using an ELISA method.

The cell layers were re-suspended in 1 mL of 5% v/v trichloroacetic acid and centrifuged (3000 *g*, 10 min, 4ºC). The pellet formed was digested with collagenase type VII (Sigma-Aldrich; 12 h, 37ºC) and re-centrifuged (3000*g*, 10 min, 4ºC) to obtain a supernatant (SI) and a pellet. The pellet was digested with pancreatic porcine elastase type III (Sigma-Aldrich; 12 h, 37ºC) to obtain soluble peptide fractions (SII). Fractions SI and SII were pooled together, hydrolyzed with 6 N HCl at 110ºC and dried to powder under inert nitrogen over 18 h. The dried samples were reconstituted in deionized water and diluted for assay. The wells in micro-titer plates to be used for assay were pre-blocked using desmosine-albumin conjugate (Elastin Products Company, Owensville, MO) in 0.05 M sodium carbonate buffer (pH 9.6, 4ºC), then washed with 0.05% v/v Tween-20 and phosphate-buffered saline (PBS) solution (1 h, 25ºC). Desmosine standards/ samples were incubated (12 h, 25ºC) with rabbit antiserum to desmosine-hemocyanin conjugate (Elastin Products Company). After removal of primary antibody

solution, the wells were successively incubated with peroxidase-conjugated anti-rabbit IgG 0.05% v/v Tween 20-PBS solution (2 h, 25ºC). Finally, the colorimetric compound 2,2′-Azino-bis (Sigma Aldrich; 3-ethylbenzothiazoline-6-sulfonic acid; 0.08 mg in 0.1 M citrate phosphate buffer containing 0.003% v/v H_2O_2; pH 4) was added to the wells and incubated (1 h, 25ºC). Absorbance were read in a UV-spectrophotometer at $\lambda = 405$ nm.

3.2.7 LOX Enzyme Activity

Spent culture medium pooled over 21 days of culture was assayed for LOX activity using a fluorometric assay based on measurement of H_2O_2 released when LOX oxidatively deaminates alkyl monoamines and diamines[307]. H_2O_2 was detected using an Amplex Red® kit (Molecular Probes)[308]. The fluorescence intensities were recorded with excitation and emission wavelengths at 560 and 590 nm, respectively.

3.2.8 Western Blot Analysis for Tropoelastin and LOX

Western blot analysis was performed to semi-quantitatively confirm observed biochemical trends in tropoelastin synthesis and to assess LOX protein synthesis. The spent medium from cultures, pooled at bi-weekly over 21-days of culture were lyophilized, and assayed for protein content using a DC protein assay kit (Biorad Corporation, Hercules, CA). Optimized sample amounts were mixed with a gel electrophoresis loading buffer (2% w/v SDS, 62 mM Tris, 10% v/v Glycerol, 600 mM dithiothreitol, 30 μg/mL of Bromophenol blue at pH 7.0, the mixture boiled (100ºC, 3 min), then cooled (5 min, 4ºC) and flash-centrifuged (500*g*, 2 min) to reduce

condensation prior to loading onto an electrophoresis gel. Samples were loaded onto 10% w/v polyacrylamide gels (Novex Tris-Glycine gels, Invitrogen), with prestained protein standards ranging from 10-190 kDa (Benchmark Pre-stained Protein Ladder, Invitrogen). Electrophoresis was carried out for 2 h at a constant voltage of 125 V, until the dye front touched the bottom of the gel. Proteins entrapped within the gel were transferred to a pre-wetted PVDF hydrophobic membrane (Immobilon-P membrane; Millipore Corporation, MA; 2 h, 25 V) immersed overnight in blocking buffer (5% w/v non-fat dry milk (Bio-Rad) solubilized in 0.05% v/v Tween 20-PBS) and developed using Western Breeze (Chromogenic western blot immunodetection kit, Invitrogen).

Protein bands detected with primary rabbit anti-rat polyclonal antibodies to elastin and fibrillin proteins (Elastin Products Company) and the 31 kDa active LOX protein (Santa Cruz Biotechnology, Santa Cruz, CA), and visualized in a Chemi-Imager IS 4400 system (Alpha Innotech, San Leandro, CA). The integrated density value of individual bands corresponds to the amount of tropoelastin in the loaded samples. The total amount of tropoelastin in the loaded samples was quantified on the basis of a total pixel intensity of 255 that was assigned to totally white and a pixel intensity of zero assigned to completely dark bands.

3.2.9 RT-PCR for Elastin mRNA Expression

RNA was extracted from RASMC cultures using an RNeasy kit (Qiagen, Valencia, CA) and samples were loaded onto RNeasy mini columns (Qiagen). After DNase treatment, total RNA was eluted with 30 μL of RNase-free water and its

concentration determined by absorbance measurement at 260 nm, and stored at −80°C. cDNA was transcribed with Omniscript Reverse Transcriptase (Qiagen) using 1 μg of DNase-treated total RNA and random hexamer primers (Roche). Samples (20 μL) were incubated (42°C, 50 min), then the RT inactivated (70°C, 15 min). Reverse transcriptase semi-quantitative PCR (RT-PCR) was performed in the ABI Prism 7700 sequence detection system (PE Applied Biosystems) using GoTaq DNA polymerase and PCR nucleotide mix (Promega). Reaction mixtures (20 μL) contained 1 μL cDNA, 18 μL of master mix (Promega) and 1 μL of appropriate primers. Optimal primer sets were designed for each target gene using Primer Express (PE Applied Biosystems) and concentration optimized. DNA sequences were obtained from GenBank (www.ncbi.nlm.nih.gov) and products <150bp with melting temperatures of 55-65°C were selected. For gene expression, we used the primer sequences for elastin rattus: 5′-CCTGGTGGTGTTACTGGTATTGG-3′ (forward) and 5′-CCGCCTTAGCAGCAGATTTGG-3′ (reverse). For each sample, gene expression was normalized to control samples (cells in medium alone) and the reaction success was compared to expression of the GAPDH housekeeping gene.

3.2.10 Amino Acid Analysis

OH-proline and amino acid content were evaluated in protein hydrolysates (18 h, 6 M HCl, 110ºC) of respective cell layers using liquid chromatography/mass spectrometry performed via methods described previously[309], but modified to detect desmosine in tandem MS mode.

3.2.11 Immunofluorescence Detection of Elastin, Fibrillin and LOX

Immunofluorescence techniques were used to confirm the presence of elastin protein within cell layers, and LOX expression for those treatments that appeared to upregulate elastin protein synthesis. Fibrillin presence within the cell layers was also verified to confirm whether the process of elastin matrix formation was mediated by pre-deposition of a fibrillin scaffold on which amorphous elastin protein was deposited to form a composite fiber. At 21 days, the cell layers were fixed with 4% w/v paraformaldehyde for 10 min, and labeled with Alexa 488 Phalloidin (Molecular Probes; 1:20 dilution; 20 min, 25°C), a marker for smooth muscle cell actin and then incubated with blocking serum (5% donkey serum, 0.3% Triton-100 in PBS; 20 min; 25°C). Elastin and fibrillin proteins detected with respective polyclonal antibodies (Elastin Products Company), as well as LOX (Santa Cruz Biotechnology) was visualized with a Rhodamine-conjugated donkey anti-rabbit IgG secondary antibody (Chemicon). Cell nuclei were visualized with the nuclear stain 4′, 6-diamino-2--phenylindole dihydrochloride (DAPI) contained in the mounting medium (Vectashield; Vector Labs, CA).

3.2.12 Matrix Ultrastructure

Transmission electron microscopy (TEM) was used to characterize the ultrastructure of the elastin matrix. Control and test cell layers were fixed with 2.5% v/v glutaraldehyde, post-fixed in 1% v/v osmium tetroxide (1 h), dehydrated in graded ethanol, embedded in Epon 812 resin, sectioned, placed on copper grids, stained with

uranyl acetate and lead citrate, and visualized on a Hitachi H7600T TEM. For immunogold labeling procedure to visualize fibrillin, the ultra-thin sections of cell layers (80-100 nm) were first blocked for 1 h in PBS containing 3% skim milk and 0.01% Tween-20, followed by washing (PBS, five changes, 5 min each). The sections were then incubated overnight at 4^{o}C with rabbit anti-VHb antibody (1:500 in PBS containing 0.3% skim milk and 0.001% Tween-20), followed by washing. The bound antibodies were visualized by incubating the sections for 1 h with goat anti-rabbit gold conjugate (10 nm; Sigma), diluted 1:20 in PBS (containing 0.3% skim milk and 0.001% Tween-20) at room temperature. The grids were finally washed on drops of water (five changes, 5 min each) before being stained with 2% aqueous uranyl acetate at room temperature.

3.2.13 Statistical Analysis

All biochemical data were obtained from nine independent repeat data per case, and were analyzed using Student's *t*-test and one-way ANOVA, assuming unequal variance and differences deemed significant for $p < 0.05$. The data was observed to follow a near Gaussian distribution in all the cases and the mean and standard deviation were calculated accordingly. For immunolabeling and TEM, test and control samples were analyzed at least in triplicate.

3.3 Results

3.3.1 Cell Proliferation

Figure 3.1 shows proliferation of RASMCs in the presence of TGF-β1 or HA/fragments, alone or together. Over 21 days of culture, non-additive control cells proliferated 3.4 ± 0.5 times the original seeded cell number, while addition of TGF-β1 suppressed this ratio to 0.5 ± 0.1 times (p = 0.005 vs. controls). When HA oligomers alone were present, the proliferation ratio was modestly lower than controls (p = 0.02 vs. control). Except in the presence of HMW HA, concurrent delivery of TGF-β1 and HA fragments inhibited cell proliferation to extents that inversely correlated to HA size.

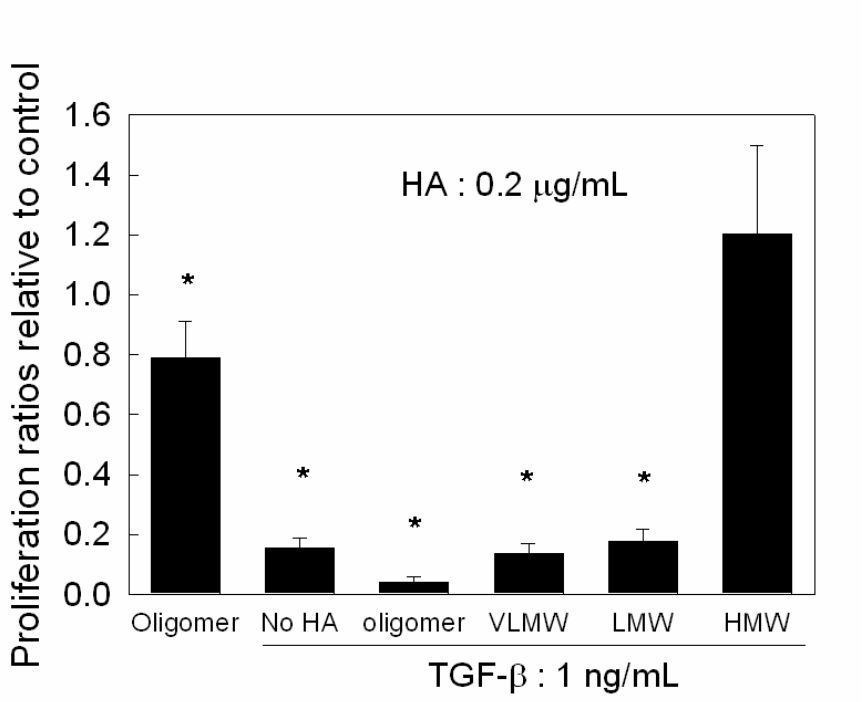

Figure 3.1. Effect of HA fragments and TGF-β1 on RASMCs. Proliferation ratios represent DNA content at 21-days to relative to day-1 of culture. Values shown represent mean ± SD of 3 repeat samples/ case. Differences vs. controls significant (*) for $p < 0.05$.

3.3.2 Matrix Synthesis

Relative to collagen matrix synthesis in control cultures (647 ± 21 ng/ng of DNA), TGF-β1 alone inhibited the same by 0.5 ± 0.2 –fold ($p = 0.009$ vs. control; **Figure 3.2A**), while HA oligomers alone induced a marginal 1.2 ± 0.2 -fold increase ($p = 0.12$ vs. controls). However, when TGF-β1 was provided together with HA oligomers, collagen matrix synthesis was upregulated drastically (14 ± 3 –fold). Concurrent delivery of TGF-β1 and non-oligomeric HA inhibited collagen synthesis in inverse correlation to HA fragment size (**Figure 3.2A**). The treatment-specific trends in synthesis of collagen matrix were identical to their differences in total collagen output (pooled medium and matrix fractions). **Figure 3.2B** shows fold-changes in total collagen production relative to non-additive control cultures (22059 ± 668 ng/ng of DNA).

TGF-β1 or HA oligomers alone stimulated tropoelastin production in controls (3.9 ± 0.9 μg/ng of DNA) by 1.2 ± 0.3 and 1.5 ± 0.2 –fold, respectively ($p = 0.12$ and 0.01 vs. controls; **Figure 3.3A**). When provided together with TGF-β1, HA oligomers stimulated an 8.0 ± 0.1 –fold increase in tropoelastin synthesis relative to controls ($p < 0.001$) while HMW HA inhibited the same to a 0.4 ± 0.05 -fraction of control values ($p = 0.001$ vs. controls); non-oligomeric HA had no significant effect on tropoelastin output. Western

blot analysis of tropoelastin in pooled spent medium confirmed these trends observed from biochemical assay (**Figure 3.3B**).

Elastin protein incorporated into the deposited matrix was measured as a sum of a highly cross-linked alkali-insoluble fraction, and an alkali-soluble fraction. The total DNA-normalized output of soluble matrix elastin protein (**Figure 3.3C**) broadly mirrored HA fragment size-specific trends reported for tropoelastin. While TGF-β1 alone or with HA/ fragments had no significant effect relative to controls (3403 ± 121 ng/ng of DNA), HA oligomers induced 8 ± 0.2 -fold increase in soluble matrix elastin protein synthesis ($p < 0.001$ vs. controls). Relative to controls, synthesis of alkali-insoluble, crosslinked elastin protein in the matrix was enhanced 4.4 ± 0.1 -fold by TGF-β1 alone (**Figure 3.3D**), and was further increased to 5.5 ± 0.4 and 4.5 ± 0.4 -fold on addition of HA oligomers and VLMW HA respectively ($p < 0.001$ vs. controls for all these cases); HMW HA however significantly inhibited deposition of crosslinked elastin protein relative to controls ($p < 0.01$).

As shown in **Figure 3.3E**, relative to non-additive control cell layers (28 ± 4 pg desmosine/ ng DNA), cells cultured with TGF-β1 alone showed modest, but significant increases in desmosine synthesis (1.07 ± 0.03 -fold; $p < 0.02$ vs. controls), while TGF-β1 together with HA oligomers (or HMW HA) significantly inhibited desmosine synthesis (0.71 ± 0.02 -fold; $p < 0.01$ vs. controls).

3.3.3 LOX Functional Activity and Protein Expression

Relative to control cultures, addition of TGF-β1 significantly inhibited cellular LOX activity ($p < 0.001$; **Figure 3.4A**), while HA oligomers with or without TGF-β1 had no significant effect ($p = 0.7$ and 0.42 vs. controls). Again, HMW HA had no effect on LOX activity ($p = 0.12$ vs. controls), though marginal inhibition was noted when TGF-β1 was also provided ($p = 0.025$ vs. controls). Western blot analysis of LOX protein exhibited trends similar to that for synthesis of matrix elastin protein (**Figure 3.4B**). TGF-β1 alone or together with HA oligomers stimulated 1.7 ± 0.1 and 2.2 ± 0.1 -fold increases respectively in LOX protein amounts compared to controls ($p < 0.001$ vs. controls in both the cases); larger HA fragments had no effect. HMW HA and TGF-β1 together inhibited control levels of LOX synthesis by 40 ± 7% ($p < 0.001$ vs. controls).

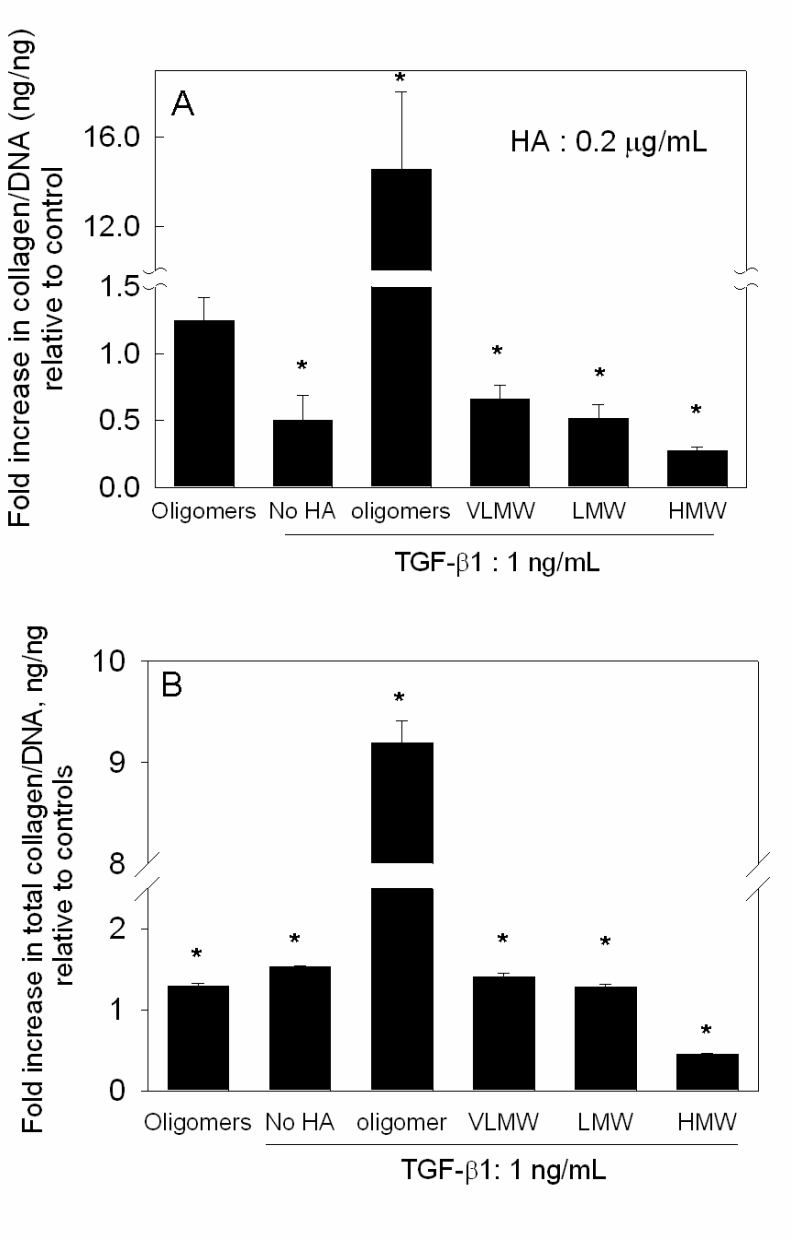

Figure 3.2. Impact of HA fragments and TGF-β1 on protein synthesis. (**A**) collagen matrix protein synthesis and (**B**) total collagen output (pooled medium and matrix fractions). Cells were cultured for 21 days. Data shown represent mean ± SD of 9 repeats/ case and are shown normalized to controls. Differences vs. controls were significant (*) for $p < 0.05$.

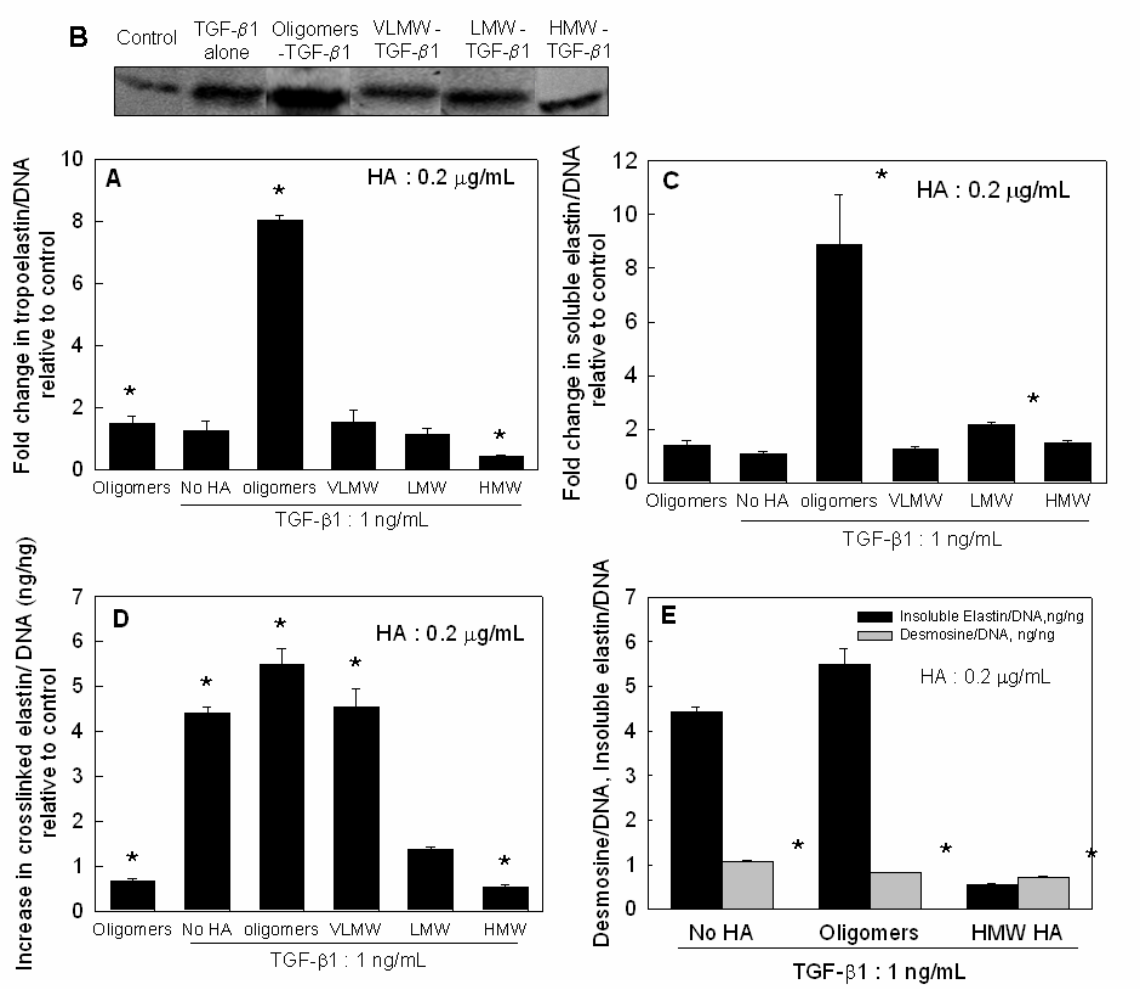

Figure 3.3. Effect of HA fragments and TGF-β1 alone and together on protein synthesis. Tropoelastin synthesis (**A**: Fastin assay; **B**: SDS-PAGE), alkali-soluble (**C**), and insoluble elastin matrix proteins (**D**). Case-wise trends for DNA-normalized amounts of desmosine mirrored that in insoluble matrix elastin protein (**E**). DNA normalized data represent mean ± SD of 3 repeats/ case, and are shown as fold change compared to controls. Differences vs. controls were significant (*) for $p < 0.05$.

3.3.4 Elastin mRNA Expression

RT-PCR studies showed TGF-β1 and HA oligomer cues to synergistically upregulate elastin mRNA expression by 1.52 ± 0.1 –fold versus control cultures (p = 0.001), more than that induced by TGF-β1 alone (1.14 ± 0.07 -fold; p = 0.03 vs. controls) or HA oligomers alone (1.05 ± 0.06 -fold; p = 0.07 vs. controls).

3.3.5 Amino Acid (AA) Analysis of Elastin

AA analysis was performed on insoluble crosslinked elastin protein isolated from control cell layers and those which received cues deemed to be most elastogenic (TGF-β1 and HA oligomers). The AA profile in cultured elastin protein closely matched that previously reported for aortic elastin protein isolated from rats of different strains. The AA content of elastin protein cultured in presence of elastogenic cues, and in their absence was dominated by the non-polar amino acids, glycine, alanine, proline and valine (65 % vs. 63.5 % respectively), similar to that described in literature (~ 71%)[310, 311]. Desmosine (Des) and isodesmosine (Ide), vital but minor constituents of crosslinked elastin protein[312], were barely resolved in the present analysis, while hydroxyproline (Hyp), which is present in elastin protein as a minor constituent (< 3 %), was sparingly detected (0.5 %) as expected.

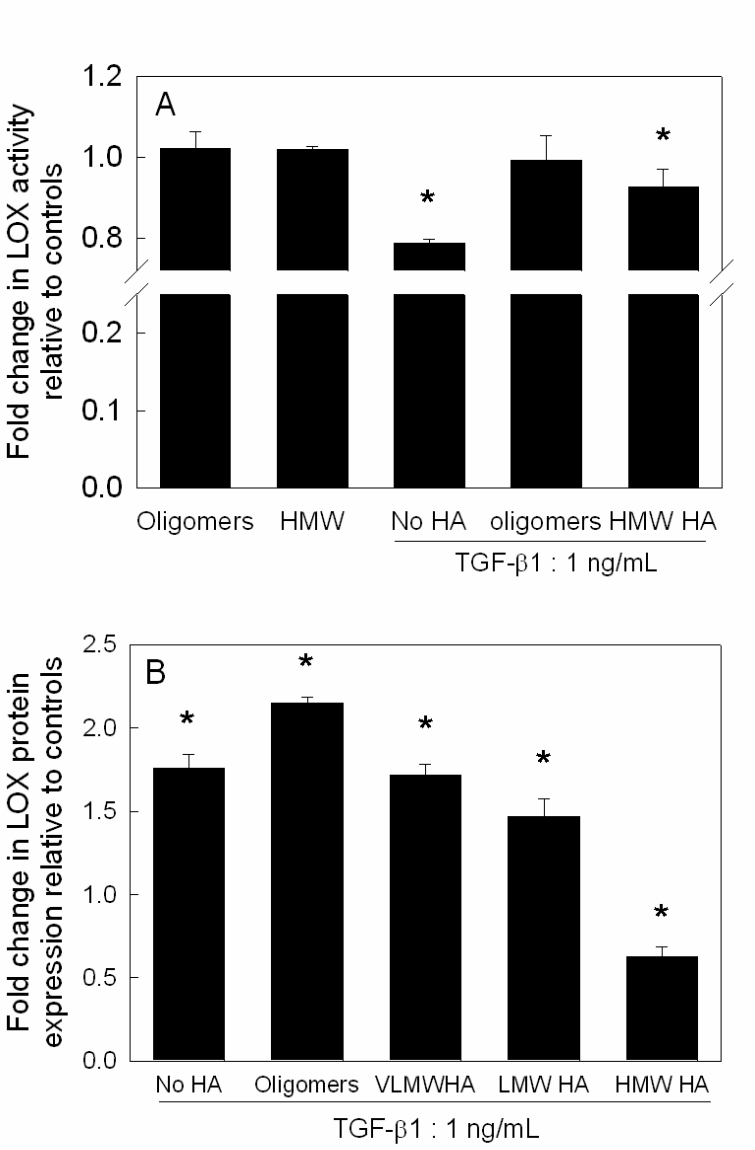

Figure 3.4. (**A**) LOX enzyme activities in test cultures at 21 day culture periods. (**B**) SDS-PAGE/ Western blots showed that TGF-β1 alone or together with HA oligomers/ fragments enhanced LOX protein synthesis. All the data are shown normalized to LOX activities in controls. Data shown represent mean ± SD of 9 repeats/case and are shown normalized to controls. Differences vs. controls were significant (*) for $p < 0.05$.

3.3.6 Immunofluorescence Studies

All cultures (Controls, TGF-β only, TGF-β + Oligomers) achieved confluence by day 21 of culture at which time they were immunolabeled. However cell densities in non-control cultures were visibly lower than in the control cultures (phase contrast images in **Figure 3.5A**). Immunofluorescence micrographs of 21-day old cell layers (**Figure 3.5B**) consistently showed significantly higher amounts of elastin protein and fibrillin (red fluorescence) in cultures that received either TGF-β1 alone or TGF-β1 and HA oligomers, than those that received HMW HA fragments and TGF-β1 (not shown), or no additives (control). Although elastin distribution within test and control cell layers was mostly uniform, occasional clumps of higher cell density were seen, which corresponded to much greater elastin localization at such sites (**Figure 3.5D, E**). However, LOX distribution within all test and control cell layers was fairly sparse. Cell layers untreated with primary antibodies (negative controls) exhibited no red fluorescence, confirming lack of non-specific binding of the fluorophore-conjugated secondary antibody (**Figure 3.5C**).

3.3.7 Ultrastructure of Matrix Elastin

Figure 3.6 shows representative transmission electron micrographs of elastin matrices from 21-day cultures. As did HA oligomers alone, TGF-β1 stimulated deposition of multiple layers of elongated, aggregating elastin fibrils uniformly sandwiched between alternating cell layers, different from the discrete clumps of amorphous elastin protein that were distributed within control cell layers. When both

TGF-β1 and HA oligomers were provided together, elastin fiber formation was likewise favored, though the matrix contained much greater number of fully-formed fibers (300-400 nm diameter) than in cultures provided with HA oligomers alone. Fibrillin (immunogold particle-stained), which appeared in transverse sections as darkly stained nodules, were located at the periphery of aggregating elastin fiber bundles, signifying normal elastic fiber assembly.

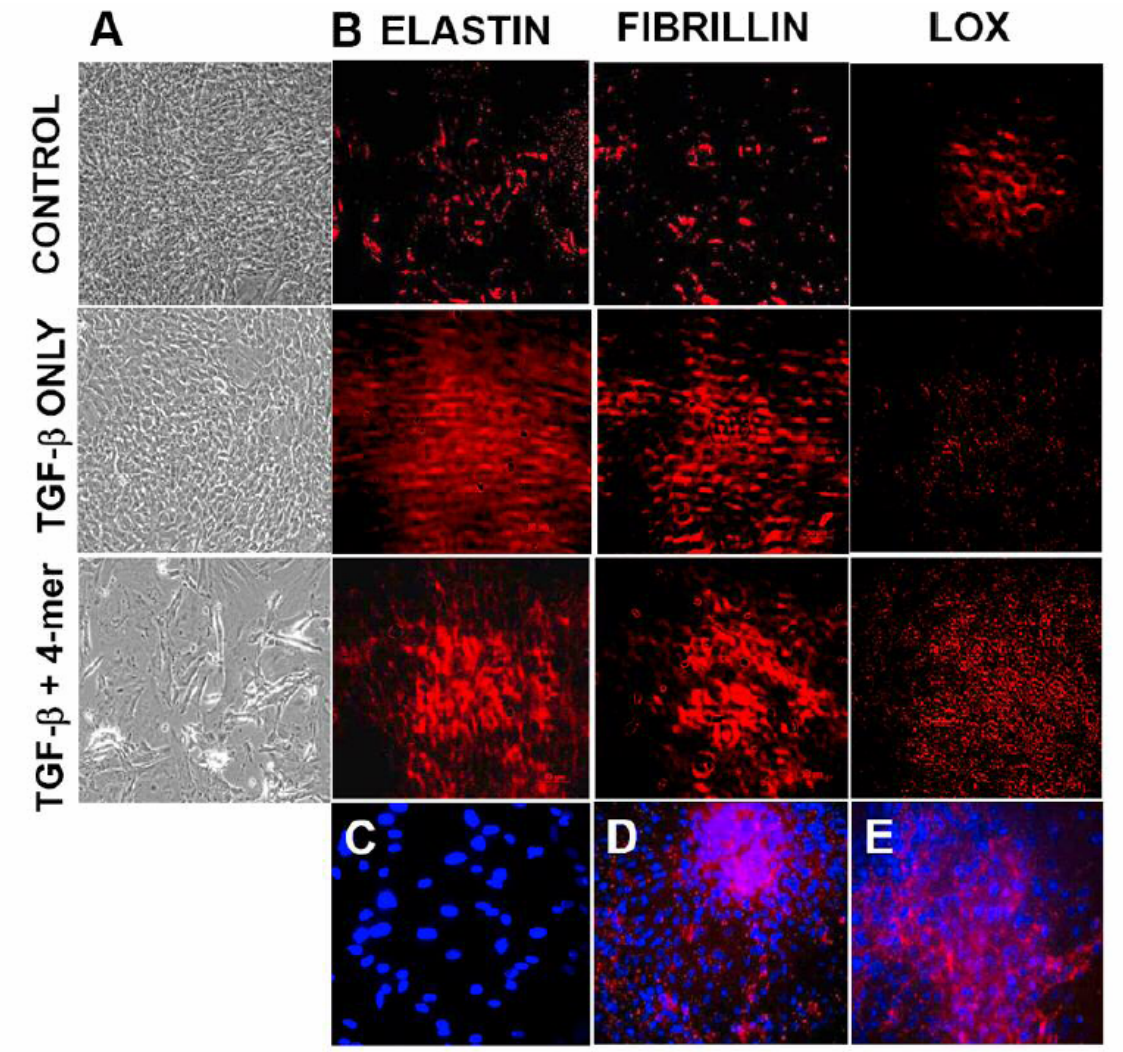

Figure 3.5. (**A**) Phase contrast images of 21-day cultures that did not receive additives (controls), or received TGF-β, or TGF-β and HA oligomers show that confluence was attained at the time of immunolabeleing, although cell density in the last-said culture was much lower. **(B)** TGF-β1 alone or together with HA oligomers, enhanced elastin, fibrillin, and LOX (red) production relative to non-additive control cultures; (**C**) Negative immunolabeling controls did not exhibit any red fluorescence confirming lack of non-specific binding of the fluorophore-conjugated secondary probe(s). Although distribution of the labeled proteins was mostly homogenous **(E)**, occasional clumps of high cell density were seen **(D)**, which co-localized with a higher density of elastin matrix. DAPI-stained cell nuclei fluoresce blue. Immunufluorescence images are typical of ≥3 cultures/case. All cultures were imaged under identical conditions. Magnification: 20× (panels A, D, E) and 40× (B, C).

3.4 Discussion

In a series of prior publications[58, 60, 313], we showed that HA upregulates elastin precursor (tropoelastin) and matrix synthesis by *adult* RASMCs. Specifically, HA oligomers enhanced elastin matrix assembly, maturation, and stability. Although larger HA fragments and long-chain (HMW) HA did not enhance tropoelastin synthesis, they enhanced elastin matrix deposition, possibly by coacervating soluble tropoelastin via opposite charge interactions[53], which supports our prior hypotheses that HA indirectly facilitates elastogenesis. Other studies have shown TGF-β1 to modestly enhance tropoelastin mRNA, suppresses production of elastin-degrading MMPs and elastases,

enhance mRNA expression for the tissue inhibitor of metalloproteinase (TIMP-1), and augments LOX mRNA expression and activity critical to elastin/collagen crosslinking and fiber assembly[314].

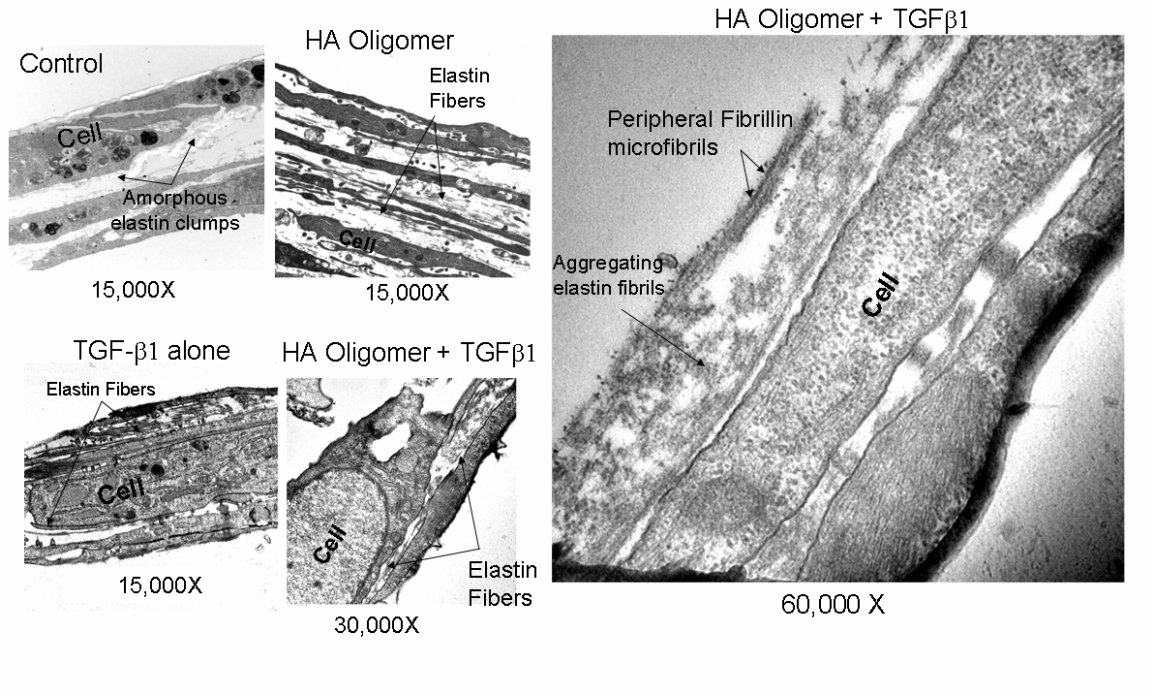

Figure 3.6. TGF-β1 and HA oligomers alone, or together, promote elastin fiber formation, as seen in transmission electron micrographs. Control cultures contained only amorphous clumps. Elastin was assembled as fibrils within a peripheral fibrillin scaffold (see black dots) and aggregated to form mature fibers ~ 400 nm in diameter, typical of fully-formed fibers.

Thus, we presently sought to investigate if concurrent delivery of HA fragments and TGF-β1 can synergistically enhance tropoelastin synthesis and matrix assembly, fiber formation, and stability beyond that possible with either of the cues alone, while

maintaining SMCs quiescent (non-proliferative) as in healthy vessels. Previously, we showed large HA fragments (20 and 200 kDa) to modestly increase cell proliferation in dose-independent manner[60], possibly as a downstream effect of phosphorylating the primary CD44 cell surface HA receptor[315], while HA oligomers (2 μg/mL) did not have any effect. Here we show 0.2 μg/mL-doses of HA oligomers to significantly inhibit SMC proliferation, indicating dose-specificity of cell responses to these oligomer cues. We have also determined that 0.2 μg/mL is the minimum dose of HA oligomers that induces a perceptible increase in tropo- and matrix elastin synthesis, though these effects are highly attenuated relative to a 2 μg/mL dose.

The stimulatory effect of TGF-β1 on elastin protein synthesis, both at the mRNA and protein levels, has been demonstrated in various *in vitro* models[316]. The predominant effect of TGF-β1 appears to be the stabilization of elastin mRNA[166], although a TGF-β1-responsive element has been identified in the human elastin promoter[317, 318]. Though our current findings that TGF-β1 (1 ng/mL, 0.25 fg/cell) inhibits cell proliferation confirm these prior observations, it is interesting that HA fragments/ oligomers when concurrently provided, maintain these trends. It is likely that the respective cellular-response initiating mechanisms of these cues operate differently, with HA fragments/ oligomers and TGF-β1 binding to different cell-surface receptors. In contrast, TGF-β1 has no effect on cell proliferation in the presence of long-chain HMW HA. We believe this might be due to long-chain HA forming a pericellular coat to isolate cells from each other and from signaling biomolecules[319]. Regardless, the utility of HA fragments/oligomers and TGF-β1 together to attenuation of SMC hyper-proliferation is clear.

Biochemical outcomes/ ng DNA	TGF-β1 addition				
	No HA	HA Oligomers	VLMW HA	LMW HA	HMW HA
Proliferation ratio	=	↓↓	=	=	↑
Total collagen	↑	↑↑	↑	↑	↓
Tropoelastin	=	↑↑	=	=	↓
Matrix Elastin	↑	↑↑	↑	↑	↓
Total elastin	↑	↑↑	↑	↑	↓

Table 3.1. Summary of treatment-specific trends in proliferation of adult RASMCs and in matrix protein synthesis. ↑ and ↑↑ indicates moderate but significant and dramatic (> 5-fold) increases respectively, = indicates no significant changes, while ↓ and ↓↓ indicates likewise decreases in the biochemical outcomes, all measured on a per ng of DNA basis.

Treatment-specific trends in cellular matrix protein synthesis are indicated in **Table 3.1**. Biochemical analyses showed that total cellular elastin protein output, as represented by the sum of tropoelastin and matrix elastin, was modestly enhanced by TGF-β1 and was indicated to be at least partly due to upregulation of elastin mRNA. HA oligomers (0.2 μg/mL) modestly enhanced tropoelastin synthesis (48 ± 23%) though these effects are likely elicited via post-translational mechanisms (no increase in elastin mRNA). HA oligomers (0.2 μg/mL) had no impact on synthesis of matrix elastin protein on a per cell basis, although we earlier showed doses of 2 μg/mL to double elastin matrix production[58]. Thus, elastin matrix synthesis by RASMCs positively correlates to HA oligomer dose, unlike HMW HA or larger HA fragments, as previously demonstrated[60]. We also showed that HA oligomers enhance LOX production but not activity, and enhance desmosine crosslinking relative to controls. Collectively, our data indicates that

at the tested dose, HA oligomers do not particularly increase recruitment of tropoelastin (i.e., yield of matrix from elastin precursors), as evidenced by lack of effect on elastin matrix amounts, but facilitate more robust crosslinking of generated matrices. In contrast, TGF-β1 appears to specifically facilitate tropoelastin recruitment for crosslinking and matrix assembly, as borne out by increases in the ratios of matrix to total (i.e., matrix + tropo) elastin over controls (**Figure 3.3**). Possibly, improved tropoelastin recruitment and crosslinking may be achieved by the observed TGF-β1-induced increases in LOX protein synthesis and activity. TGF-β1 does not appear to enhance the extent of crosslinking itself, since desmosine amounts on a per cell basis remained unchanged relative to controls. Possibly due to the exclusive nature of long-chain HA, concurrently provided TGF-β1 did not have any impact on desmosine crosslinking.

TGF-β1 and HA oligomers synergistically enhanced tropoelastin synthesis almost 9-fold. Since these cues only upregulated elastin mRNA expression by ~ 1.6 fold, not commensurate with total tropoelastin synthesis, it is possible that these cues also impact cells post-translationally, besides upregulating elastin mRNA expression. These cues together also greatly improved elastin precursor recruitment and crosslinking efficiency, as evidenced by multi-fold increases in both soluble and insoluble matrix elastin relative to controls, and of matrix to total elastin ratios (0.45 vs. 0.1 for controls). Further studies suggested that the improved crosslinking efficiency is possible, since a ~ 2.2-fold induction in LOX production was induced, though LOX activity itself remained unchanged. These upregulatory effects were not observed when TGF-β1 and long-chain HA or non-oligomeric HA fragments were concurrently delivered. While the lack of

effects observed with long-chain HA may be sourced to its ability to isolate cells from TGF-β1, differences in results obtained with large HA fragments and oligomers are likely due to differences in their interactive mechanisms with cells. HMW HA and non-oligomeric HA fragments primarily interact with CD44, to intracellularly regulate cell proliferation, motility[320], and other cell activities. Differently, HA oligomers likely interact via toll-like receptors 4 (TLR-4) and by CD44 clustering, to elicit responses quite different from those by larger HA fragments. Since our oligomer mixtures here contain mostly 4-mers (75% w/w) and 6-mers, likely, both CD44 and TLR-4 together elicit unique cell responses. Surprisingly, the ~ 6-fold increase in desmosine crosslinks per nanogram of DNA induced by HA oligomers (2-fold increase/ng of elastin matrix)[58] was restored to baseline control levels upon concurrent delivery of TGF-β1. Thus, TGF-β1 may competitively inhibit HA oligomer-induced effects by preferentially interacting with cell surface proteins that modulate intracellular mechanisms that lead to desmosine crosslink formation. A future challenge is to dramatically enhance LOX activity and production to enhance desmosine crosslinking efficiency and thus matrix formation.

Sustained over-expression of TGF-β1 can potentially induce matrix calcification[321]. However, Von-Kossa staining of 21 day-old cell layers (not shown), cultured with the elastogenic bolus of TGF-β1 and HA oligomers indicated no calcium accumulation. Thus, the 1 ng/mL dose (i.e., 10^{-11} M) of TGF-β1 delivered in this study is elastogenically useful and yet safe so as to not induce matrix calcification.

Imaging and ultrastructural analyses of synthesized elastin matrices qualitatively validated biochemical observations. Bundles of elastin fibrils distributed between cell

layers were seen in HA oligomer-supplemented cultures. In contrast, we previously showed cells cultured with large HA fragments and HMW HA to deposit amorphous elastin clumps, as did control cultures in the present study. The fibrillar elastin generated was continuous and associated laterally with surrounding fibrils to form larger, thickened, elastin fibers. The abundant presence of fibrillin microfibrils at the periphery of the amorphous clumps confirmed that elastin matrix assembly, involving pre-deposition of a fibrillin scaffold for deposition of amorphous elastin, was maintained. Similar to HA oligomers, TGF-β1 stimulated deposition of multiple layers of elongated, aggregating elastin fibrils and vastly different from the amorphous elastin clumps seen in controls. When both TGF-β1 and HA oligomers were provided concurrently, elastin fiber formation was likewise favored, though the matrix contained a visibly much greater number of fully-formed fibers than present in cell layers that received oligomers alone. As in oligomers- or TGF-β1-only cultures, here too, fibrillin microfibrils were localized at the periphery of aggregating elastin fiber bundles, signifying normal elastic fiber assembly.

3.5 Conclusions of the Study

1. The outcomes of this study demonstrate that TGF-β1 and HA oligomers (hereto referred as cues) synergistically and dramatically improve elastin matrix regeneration by adult vascular SMCs, a cell type otherwise capable of only minimal elastin turnover. These synergistic effects are particularly striking since

the HA oligomers cues themselves were of such low doses to impact elastin synthesis very modestly.

2. HA oligomers and TGF-β1 cues together inhibit cell proliferation and upregulate synthesis of tropo- and matrix elastin, improve tropoelastin recruitment for matrix assembly, and crosslinking efficiency, likely *via* increased LOX production.
3. In addition, these cues hasten maturation of elastin fibers relative to cultures receiving either of these cues alone. Importantly, sustained delivery of elastogenic doses of TGF-β1 (1 ng/mL) does not appear to induce matrix calcification.
4. **These cues might be of tremendous utility to restore elastin matrix homeostasis in de-elasticized vessels and tissue engineering constructs, and possibly even serve as an *in vitro* model to investigate elastogenesis during early morphogenesis and wound healing in adult tissues.**

CHAPTER 4

SYNERGY BETWEEN ELASTOGENIC CUES: IMPACT OF IGF-1 AND HA FRAGMENTS

4.1 Introduction

This study was conducted as part of our ongoing efforts to identify and optimize biomolecular cues which will upregulate elastin synthesis and organization by RASMCs. As explained in chapter 2, studies conducted by our group[58, 60] have shown HA fragments (MW < 1 MDa), especially HA oligomers (<10 kDa) provided to cells in a serum-rich environment, to be more cell-interactive and far more elastogenic than the relatively bioinert long-chain HA (MW > 2 MDa). Other studies with different cell types have shown that elastin synthesis and mRNA expression levels may be similarly enhanced by stimulating cells with growth factors such as IGF-1[64, 65, 67]. Noguchi *et al*. observed that a 500 ng/mL dosage of IGF-1 resulted in 1.8 ± 0.14 and 1.35 ± 0.05–fold increases in soluble tropoelastin precursors and total (*i.e.*, tropoelastin + matrix) elastin synthesis, respectively, by neonatal rat pulmonary cells, relative to controls[67]. In addition, IGF-1 has been shown to augment lysyl oxidase (LOX), a matrix crosslinking enzyme which mediates crosslinking of soluble tropoelastin into a mature, insoluble matrix layer[322].

Therefore, it is highly possible that HA/ fragments provided together with IGF-1 could provide greater benefits to tropoelastin synthesis, elastin matrix assembly/ stability, and simultaneously inhibit SMC over-proliferation, a common outcome in elastin-compromised vessels and other diseased vascular sites, where tissue engineered

constructs may be grafted. Since cell responses to HA/ fragment/ oligomers-based cues (in a physiologic serum-rich environment) could potentially be modulated by the presence of IGF-1, it is necessary to comprehensively evaluate the impact of different-sized HA fragments together with IGF-1, to identify that combination, which could be most usefully employed to faithfully regenerate elastin structural networks. Once identified, these cues could be presented to cells exogenously or incorporated within HA or non-HA based biomaterial scaffolds to elicit the desired elastogenic cell responses *in vivo* or *in vitro*.

Thus, in the current study, we first investigated the impact of 500 ng/mL of IGF-1 on elastogenesis by adult rat aortic smooth muscle cells (RASMCs) in a serum-rich culture environment. We then evaluated the benefits, if any, of concurrent delivery of HA/ fragments/ oligomers and IGF-1 on elastin synthesis, organization and maturation by adult RASMCs. We hypothesize that these results will not only help in designing biomaterial-based or other strategies to enable faithful elastin matrix regeneration, but also in understanding the role of HA and IGF-1 on regulation and maintenance of vascular matrix homeostasis.

4.2 Materials and Methods

4.2.1 Cell Culture

HA with different molecular weights were commercially obtained, and oligomers were prepared in the lab as per the protocols explained in section 3.2.1. Adult RASMCs from low passages (P3-5) were propagated in expansion medium (DMEM, Invitrogen,

USA) containing 10% v/v FBS and 1% v/v penstrep, and seeded onto 6-well tissue culture plates at a density of 3×10^4 cells/ well. A 1-mL bolus of HA/fragments/oligomers prepared in serum-rich medium was added to cell cultures at an ultimate dose of 0.2 μg/mL, except for control cultures which received serum-rich medium without HA. In a prior study, we deemed this to be the minimal dose of HA fragments (specifically, of HA 4mers) that induces a perceptible increase in both tropo- and matrix elastin synthesis. For the purpose of easy comparison with published literature in the field, we selected to study an IGF-1 dose (500 ng/mL) that was previously shown to cause maximal elastogenic upregulation of adult rat cells[67]. IGF-1 (Peprotech Inc., USA) was diluted in PBS to the above dose and supplemented exogenously to the culture wells, except in control cultures which received no supplements. The medium was changed twice weekly and all experimental conditions and controls were performed in triplicate. The spent medium over the 21-day culture period was pooled, frozen and biochemically analyzed along with their corresponding harvested cell layers.

4.2.2 Biochemical Assays

The DNA content in cell layers was measured at 1 and 21 days of culture to determine the proliferation of SMCs and to normalize the measured amounts of synthesized matrix, according to protocol explained in section 3.2.3.

The collagen content within the cell layers and in the pooled supernatant medium fractions was estimated using a hydroxy-proline assay, described in section 3.2.4. The amounts of matrix elastin (alkali-soluble and insoluble fractions) and soluble tropoelastin

(in pooled spent medium) were quantified using a Fastin assay (Accurate Scientific Corp), as detailed in section 3.2.5. The measured amounts of synthesized matrix were normalized to their respective DNA amounts to provide a reliable basis of comparison between samples, and to broadly assess if the observed changes in the amount of matrix synthesized could possibly be due to increases in elastin production on a per cell basis.

The desmosine crosslink densities within elastin matrices were quantified for selected cases using ELISA, as described in section 3.2.6. The desmosine amounts/ ng of DNA were compared to the DNA-normalized amounts of insoluble matrix elastin from corresponding cell layers. The LOX enzyme activity within the cell culture layers was determined using a flurometric assay based on generation of H_2O_2 when LOX acts on a synthetic substrate, described in detail in section 3.2.7. Western blot analysis of proteins within the pooled medium fractions at day 21 was performed using methods described in section 3.2.8, to semi-quantitatively confirm observed biochemical trends in tropoelastin synthesis and to assess LOX protein synthesis.

4.2.3 Immunofluorescence Studies and Matrix Structure

As explained in detail in section 3.2.11, immunofluorescence techniques were used to confirm the presence of elastin, fibrillin within selected cell layers, and LOX expression for those conditions that appeared to upregulate elastin synthesis. The ultrastructure of insoluble matrix elastin within control cell layers and those cultured in the presence of IGF-1 alone or together with HA fragments deemed most beneficial to

synthesis of structural matrix elastin (i.e., HMW HA) was characterized using high-resolution transmission electron microscopy (detailed procedure in section 3.2.12).

All experiments were performed in triplicate unless otherwise specified and the quantitative results are reported as mean ± SD. Statistical significance between and within groups was determined using one-way ANOVA, assuming unequal variance. Results were considered statistically significant compared to controls if $p < 0.05$.

4.3 Results

4.3.1 Cell Proliferation

All cultures were still sub-confluent (~80% confluent) at 3 weeks of culture. The proliferation ratios of RASMCs cultured in the presence of either IGF-1 alone or together with HA cues are shown in **Figure 4.1**; while that in the presence of HA/ fragments alone was determined in our earlier studies[58, 60]. Addition of IGF-1 alone suppressed the proliferation of cultures by 55 ± 5 % ($p = 0.005$ *vs.* control) at 21 days relative to control cell layers cultured without supplements in serum-rich medium. Concurrent delivery of IGF-1 and HA oligomers stimulated cell proliferation by 37 ± 15 % ($p = 0.03$ *vs.* control), while addition of other HA fragments in the presence of IGF-1 inhibited cell proliferation to extents that negatively correlated to HA fragment size (**Figure 4.1**).

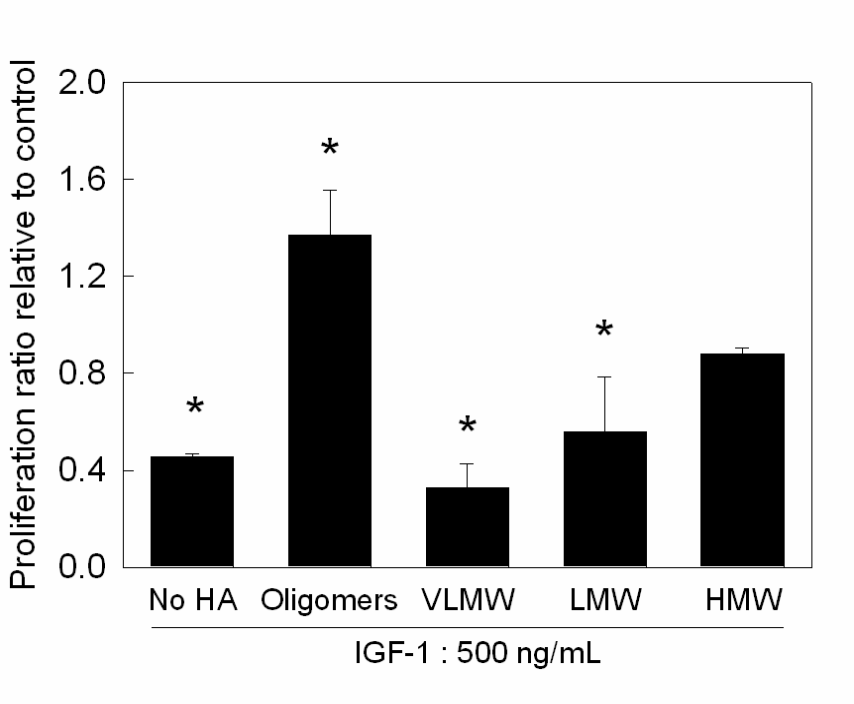

Figure 4.1. Proliferation ratios of RASMC cultures supplemented with IGF-1 (500 ng/mL) alone or together with HA cues (0.2 μg/mL). Data shown represent mean ± SD of DNA content of cell layers after 21 days of culture, normalized to initial seeding density and further normalized to control cultures that received no additives (n = 3/case). $P < 0.05$ represents significant differences from controls (*).

4.3.2 Matrix Synthesis

When IGF-1 alone was provided, synthesis of matrix collagen (i.e., within the cell layer; on a per ng DNA basis) increased by 1.85 ± 0.1 -fold over non-additive controls (2140 ± 104 ng/ng DNA) as shown in **Figure 4.2A**. While addition of IGF-1 to cultures also supplemented with HA oligomers did not significantly enhance collagen synthesis compared to controls ($p = 0.26$ vs. controls), concurrent delivery of IGF-1 and large HA

fragments (VLMW and LMW) enhanced collagen synthesis by 2.16 ± 0.12 and 1.54 ± 0.08-fold, respectively ($p < 0.001$ vs. controls in both the cases). In comparison, IGF-1 and HMW HA did not alter collagen production relative to controls. The treatment-specific trends in the synthesis of collagen matrix were identical to their differences in total collagen output (pooled medium and matrix fractions). **Figure 4.2B** shows fold-changes in total collagen production relative to non-additive control cultures (11628 ± 1011 ng/ng of DNA).

As shown in **Figure 4.3**, the trends in tropoelastin production by RASMCs closely mirrored those observed for collagen synthesis under identical conditions. In the absence of any HA, IGF-1 stimulated control levels (9630 ± 1963 ng/ng DNA) of tropoelastin production by 1.93 ± 0.35 fold ($p = 0.03$ *vs.* control). When provided together with IGF-1, HA oligomers suppressed tropoelastin production by 0.79 ± 0.02 fold relative to controls while HMW HA offered no additional benefit; HA fragments such as VLMW and LMW increased tropoelastin output by 2.27 ± 0.14 and 1.97 ± 0.49 fold, respectively ($p < 0.001$ vs. controls in both the cases), which however, induced no significant increase over IGF-1 alone ($p = 0.35$ and 0.77 *vs*. IGF-1 alone). Western blot analysis (**Figure 4.3A**) of tropoelastin in pooled spent medium collected over 21 days of culture period confirmed the observed biochemical trends in tropoelastin (**Figure 4.3B**).

As explained earlier, the elastin incorporated into the extracellular matrix was measured as a sum of two individual fractions, *i.e*., a highly cross-linked, alkali-insoluble elastin pellet (which represents structural elastin), and an alkali-soluble fraction. In the absence of HA cues, addition of 500 ng/mL of IGF-1 to cell cultures increased synthesis

of alkali-soluble matrix elastin by 1.75 ± 0.21-fold, relative to non-additive controls (5228 ± 487 ng/ng DNA; $p < 0.001$ vs. controls). The total DNA-normalized output of alkali-soluble matrix elastin (**Figure 4.3C**) broadly mirrored the HA fragment size-specific trends observed for collagen and tropoelastin. Though addition of IGF-1 along with HA oligomers or HMW HA exhibited no significant effect relative to controls, VLMW and LMW HA induced 2.22 ± 0.16 fold and 1.63 ± 0.17 fold increase in synthesis of alkali-soluble matrix elastin, respectively ($p < 0.001$ vs. controls in both the cases; $p < 0.001$ and $p = 0.07$ *vs*. IGF-1 only). The synthesis of alkali-insoluble, structural matrix elastin was not significantly affected by addition of IGF-1 alone, as shown in **Figure 4.3D**.

When both IGF-1 and oligomers were supplemented concurrently, significant inhibition was noted in synthesis of the alkali-insoluble structural matrix elastin relative to controls (397 ± 49 ng/ng DNA; $p < 0.03$ *vs*. controls). Relative to controls VLMW HA and IGF-1 together enhanced deposition of this form of matrix elastin by 2.14 ± 0.14 fold, while addition of LMW and HMW HA instead, increased the same by 3.6 ± 0.4 fold and 4.96 ± 0.77 fold, respectively ($p < 0.001$ vs. IGF-1 alone, in both the cases). Collectively, IGF-1 alone or together with HA oligomers, VLMW, LMW and HMW elicited synthesis of total matrix elastin (i.e., alkali-soluble plus alkali-insoluble matrix elastin) amounts that were 1.69 ± 0.22, 0.8 ± 0.17, 2.21 ± 0.16, 1.77 ± 0.19, 1.18 ± 0.12 fold respectively, relative to controls.

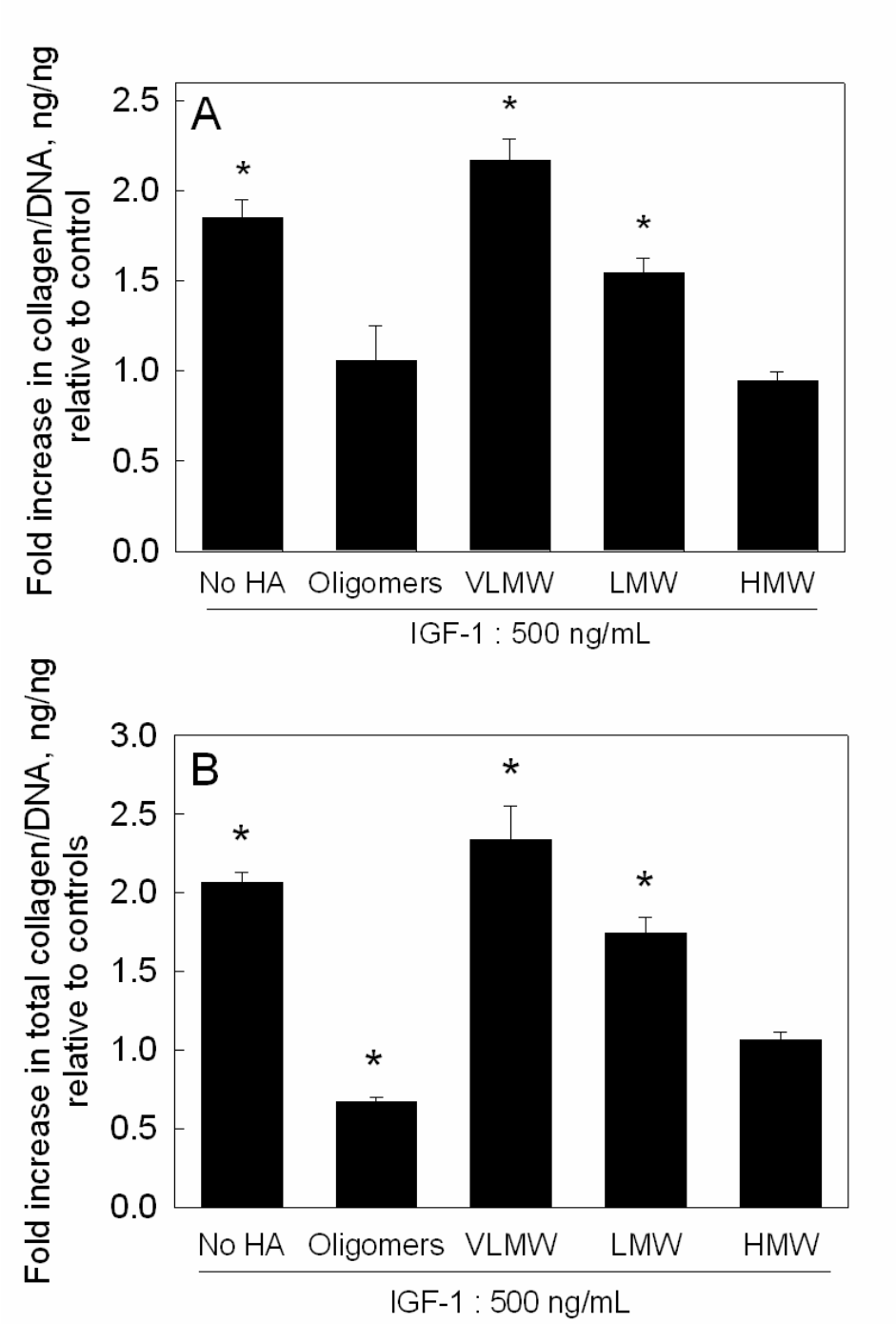

Figure 4.2. Effects of IGF-1 (500 ng/mL) with or without HA cues (0.2 μg/mL) on matrix collagen (A) and total collagen (B) synthesis by adult RASMCs. Values (mean ±

SD) are shown normalized to the DNA content of the respective cell layers at 21 days of culture (n = 3/case) relative to control cultures. (*) represents significant differences relative to control cultures, deemed for $p < 0.05$.

4.3.3 Desmosine Content in Crosslinked Elastin

Desmosine amounts measured in test cell layers were normalized to corresponding DNA amounts (ng/ng), and further normalized to a similar ratio obtained for the non-additive controls. Cells cultured with IGF-1 alone exhibited enhanced synthesis of desmosine (1.34 ± 0.06-fold *vs.* controls; **Figure 4.4**) while IGF-1 together with HA oligomers inhibited desmosine crosslinks by 0.74 ± 0.05 fold ($p = 0.026$ *vs.* control) mirroring their inhibition of the synthesis of crosslinked (insoluble) matrix elastin; HMW HA, which was earlier found to greatly enhance deposition of crosslinked matrix elastin also dramatically promoted desmosine synthesis by 3.12 ± 0.04 fold in the presence of IGF-1 ($p < 0.001$ vs. controls). As shown in **Figure 4.4**, trends in desmosine amounts/ng elastin correspond with that in amounts of crosslinked (insoluble) elastin synthesized in the respective cultures. Interestingly, IGF-1 alone or together with HA oligomers elicited desmosine crosslink densities (*i.e.*, desmosine amounts/ng of insoluble elastin ratios) that were ≤ 1, while HMW HA together with IGF-1 increased these ratios to values ~ 2, suggesting increased density of desmosine crosslinking per unit amounts of insoluble elastin.

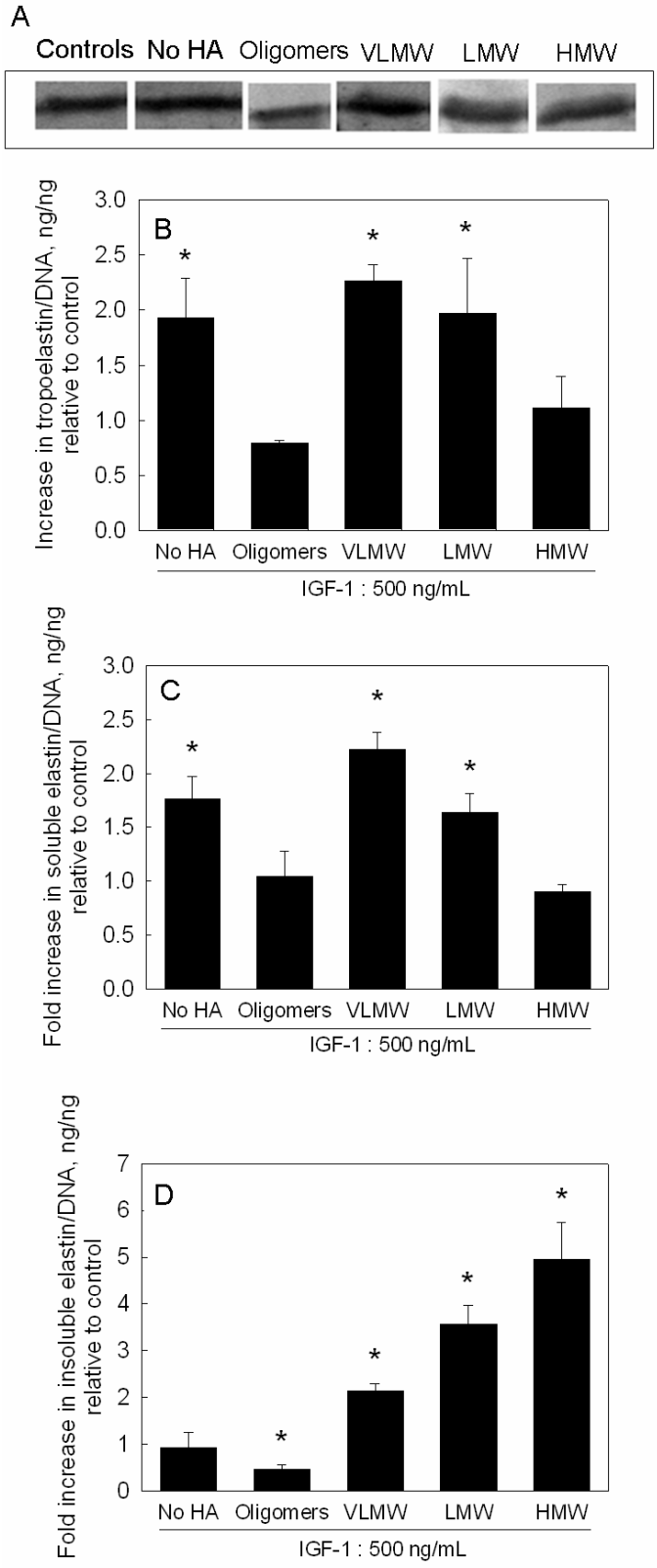
A
Controls
No HA
Oligomers
VLMW
LMW
HMW
B
Increase in tropoelastin/DNA, ng/ng relative to control
3.0
2.5
2.0
1.5
1.0
0.5
0.0
No HA
Oligomers
VLMW
LMW
HMW
IGF-1 : 500 ng/mL
C
Fold increase in soluble elastin/DNA, ng/ng relative to control
3.0
2.5
2.0
1.5
1.0
0.5
0.0
No HA
Oligomers
VLMW
LMW
HMW
IGF-1 : 500 ng/mL
D
Fold increase in insoluble elastin/DNA, ng/ng relative to control
7
6
5
4
3
2
1
0
No HA
Oligomers
VLMW
LMW
HMW
IGF-1 : 500 ng/mL

Figure 4.3. Elastin production by RASMCs cultured with IGF-1 alone (500 ng/mL) and together with HA fragments (0.2 μg/mL) for (B) tropoelastin (C) alkali-soluble matrix elastin, and (D) alkali-insoluble highly crosslinked matrix elastin. Data shown (mean ± SD) are normalized to cellular DNA content at 21 days of culture and represented as fold change in elastin production relative to controls (n = 3/case). Representative SDS-PAGE/ western blots containing bands corresponding to tropoelastin produced in the respective cases confirm biochemical trends in tropoelastin production as shown in panel 3A. $P < 0.05$ represents significant differences from controls (*).

4.3.4 LOX Functional Activity and Protein Expression

The change induced by addition of IGF-1 and HA fragments to LOX enzyme activity measured in spent culture medium on day 16 of culture was analyzed. LOX activities measured in IGF-1 supplemented cultures at 16 days were marginally but significantly higher to those measured in control cultures, except for HMW HA, where no significant decrease was noted after prolonged exposure. Western blot analysis showed that LOX protein amounts were enhanced by IGF-1 alone, or together with oligomers, VLMW, LMW and HMW HA by 26 ± 7, 40 ± 6, 38 ± 5, 39 ± 6 and 41 ± 6 % respectively, relative to controls ($p < 0.05$ *vs.* controls, in all cases).

4.3.5 Immunodetection of Elastin, Fibrillin and LOX

Immunofluorescence micrographs of 21-day old cell layers (**Figure 4.5**) confirmed the presence of elastin, fibrillin and LOX in cultures that received IGF-1 alone

or together with HA fragments. The intensities of fluorescence due to elastin were visibly greater in IGF-1 supplemented cultures, particularly those which also received HMW HA. Fluorescence intensity due to fibrillin was again greater in cultures supplemented with both IGF-1 and HA fragments, compared to controls, with the intensity most pronounced in cultures that received IGF-1 and HA oligomers. However, LOX, though present within all test and control cell layers, was rather sparse.

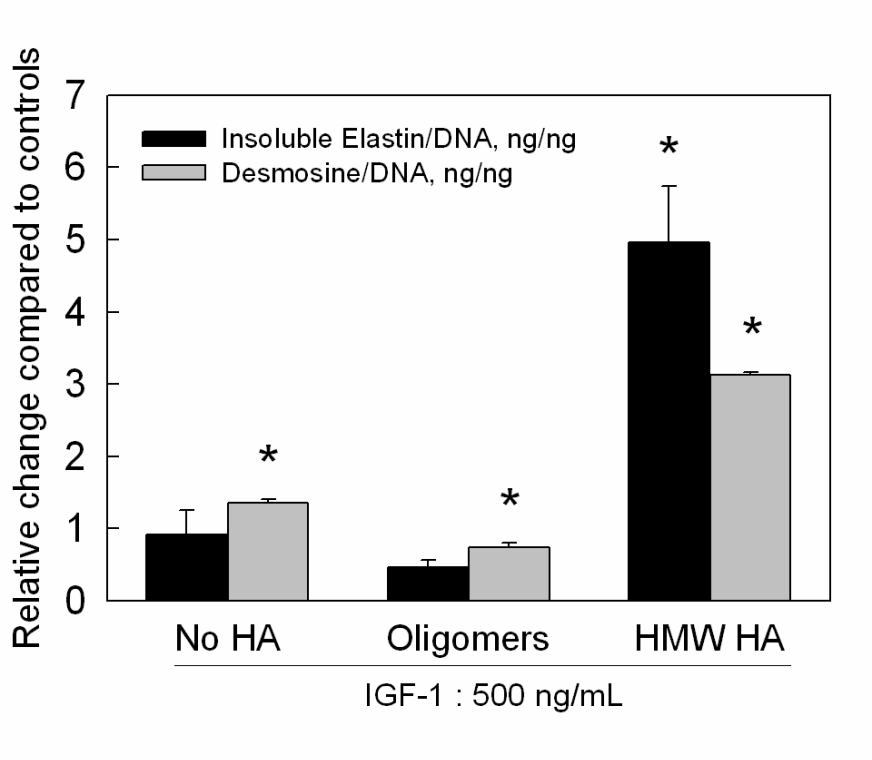

Figure 4.4. Desmosine amounts measured in selected test cell layers were normalized to corresponding DNA amounts (ng/ng), and further a similar ratio obtained for the non-HA controls. Comparable trends were observed for the desmosine/DNA density and respective insoluble matrix elastin/DNA for selected cases.

4.3.6 Ultrastructure of Matrix Elastin

Figure 4.6 shows transmission electron micrographs representative of elastin matrices within 21-day old cell layers cultured with no-additives (Figure 4.6A), IGF-1 alone (Figure 4.6B) and IGF-1 together with HMW HA (Figure 4.6C-D), the combination deemed most useful to enhance elastin matrix production, matrix yields and desmosine crosslinking. While only discrete amorphous elastin clumps and almost no fibers were distributed between stacks of cells within control cultures (Figure 4.6A), IGF-1 primarily induced deposition of multiple layers of elongated, aggregating elastin fibrils, often closely adjoining the cells (Figure 4.6B), significantly different from those observed in control cultures. Few elastin clumps were seen in these cultures (Figure 4.6B). When IGF-1 and HMW HA were provided together, elastin fiber formation and aggregation was likewise favored, though the matrix also contained a significantly greater density of amorphous elastin clumps similar to those present in control cell layers (Figure 4.6C-D). Indeed, the aggregating elastin fibers and amorphous elastin clumps (150-200 nm diameter, typical of young elastic fibers) in Figure 4.6D exhibited deep staining with microfibrils at their periphery, and thus signified normal mechanisms of elastin fiber formation observed at higher magnifications (100000 X) in additive-free control cultures, as shown in Figure 4.6E.

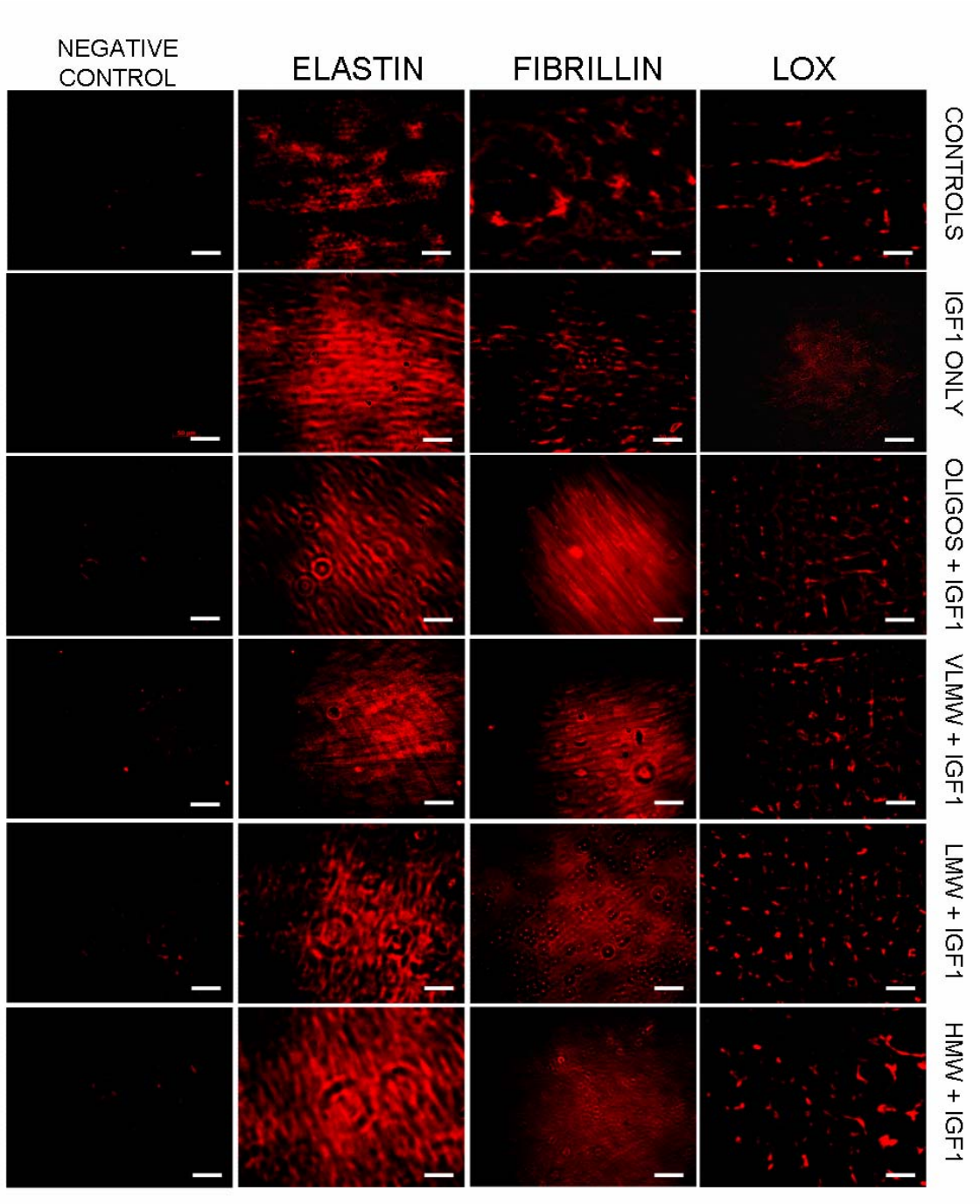

Figure 4.5. Immunodetection of elastin, fibrillin and LOX (red) within RASMC layers following 21 days of culture in the presence of IGF-1 alone (500 ng/mL) or together with HA fragments (0.2 μg/mL), respectively; control cultures received none. Coloration due

to respective proteins absent in cell layers not treated with the primary antibody (negative controls). Scale bar: 150 μm.

4.4 Discussion

The primary focus of our research is to develop tissue-engineering materials and methods to enable regeneration of ultrastructural and functional mimics of vascular elastin networks. Though several researchers have been able to tissue-engineer responsive, living conduits exhibiting properties similar to that of the native vessels[219, 323-325], key challenges such as progressive destabilization of tropoelastin mRNA expression[24, 300] leading to poor regeneration of elastin structures within, and unavailability of appropriate scaffolding materials and other biomolecular cues for upregulated elastin synthesis by cells, still remain. Recent studies by our group validated reports that HA-based biomaterials might be useful as elastogenic scaffolds, and demonstrated that HA plays vital[313] but possibly indirect roles in elastin synthesis by vascular SMCs, their structural organization to form higher-order macromolecules pertinent to elastic fiber assembly[50], and further subsequent stabilization of the assembled elastin matrix[58, 60].

Despite these favorable outcomes, from the standpoint of *in vivo* elastin matrix regeneration within elastin-compromised vessels and within tissue engineered vascular constructs applied therein, there is a critical need to simultaneously attenuate SMC hyper-proliferation, on which elastogenic HA oligomers do not appear to have any effect. There is also a need to further enhance elastin precursor synthesis and improve upon matrix yields, which we showed were limited to be 25% in the presence of HA oligomers

alone[58]. In other words, 75% of synthesized tropoelastin precursors remained unused towards building structurally useful matrix elastin. Moreover, a prior study by Evanko *et al.*, suggested that cell responses to HA may be modulated by other concomitantly present biomolecules[57]. Thus, in this study, we comprehensively evaluated cellular matrix synthesis response in the presence of IGF-1, not only to HA oligomers but also to larger sized HA fragments and long-chain HA.

	Total matrix elastin synthesized/ DNA, ng/ng (alkali soluble + insoluble elastin)	Matrix elastin/ Total elastin, %	Insoluble elastin/ Total matrix elastin, %
Controls	5624 ± 536	36.8	7.1 ± 0.8
IGF-1 alone	9533 ± 1282	33.9	3.8 ± 1.4
HA oligomers + IGF1	5432 ± 1190	46.6	24 ± 5.2
VLMW HA + IGF1	12477 ± 896	36.3	6.8 ± 0.4
LMW HA + IGF1	9953 ± 1089	34.3	14.2 ± 1.5
HMW HA + IGF1	6663 ± 677	38.3	29.5 ± 4.6

Table 4.1. The total matrix elastin, ratios of matrix elastin to the total elastin and ratios of insoluble elastin to total matrix elastin, synthesized by RASMCs supplemented with HA fragments and IGF-1.

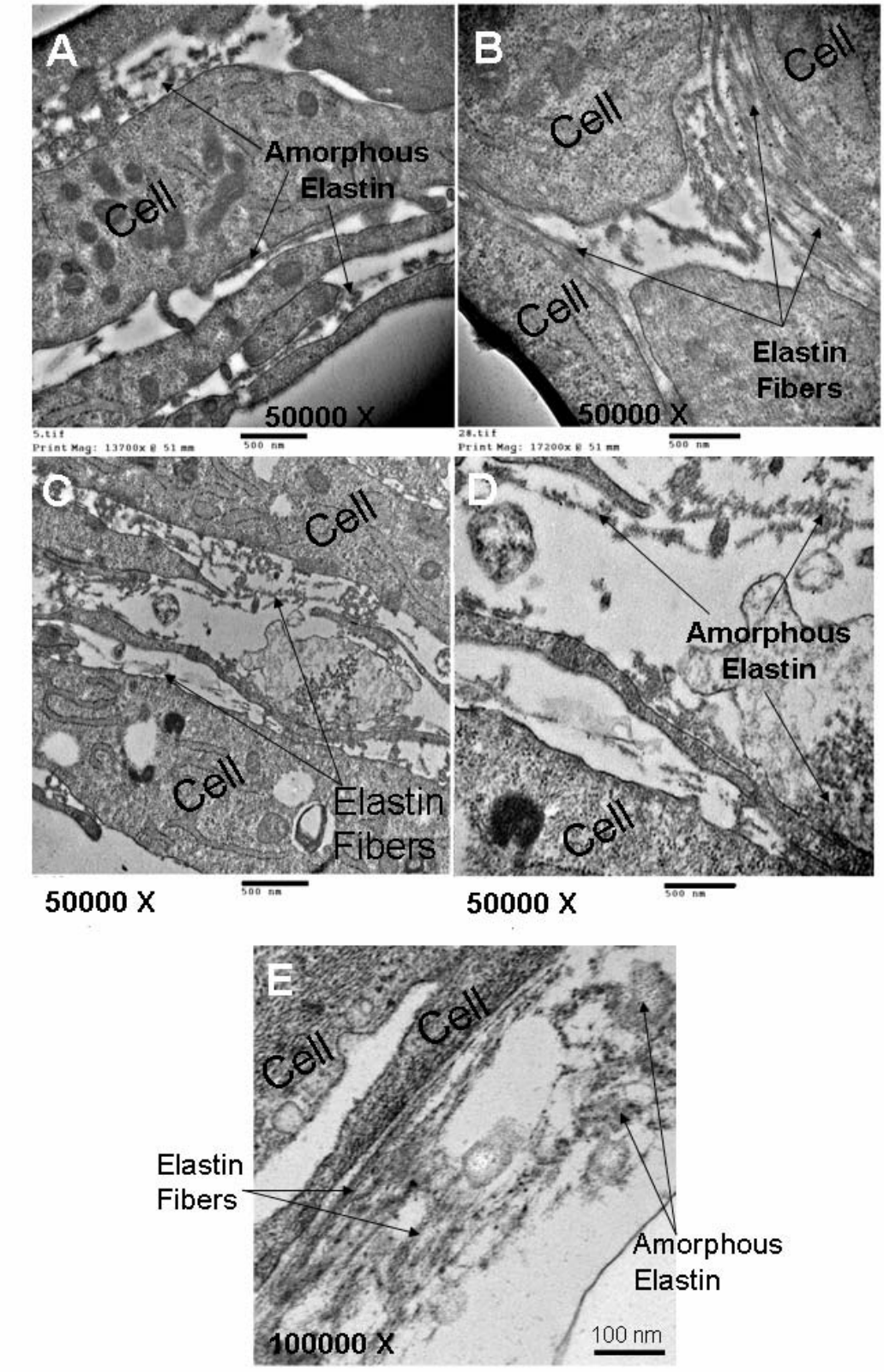
A
Amorphous
Elastin
Cell
50000 X
5.tif
Print Mag: 13700x @ 51 mm
500 nm
B
Cell
Cell
Cell
Elastin
Fibers
50000 X
28.tif
Print Mag: 17200x @ 51 mm
500 nm
C
Cell
Cell
Elastin
Fibers
500 nm
50000 X
D
Amorphous
Elastin
Cell
500 nm
50000 X
E
Cell
Cell
Elastin
Fibers
Amorphous
Elastin
100000 X
100 nm

Figure 4.6. Representative TEM images of 21-day old RASMC cell layers cultured additive-free (panel A), with IGF-1 alone (500 ng/mL; panel B) or together with HMW HA (0.2 μg/mL; panel C-D). Aggregating amorphous elastin clumps leading to the formation of elastin fibers can be clearly seen in this image (Figure 6D), which confirm the identity of elastin observed at higher magnifications (100000 X) in images obtained from additive-free control cultures (Figure 6E), also immunogold-labeled for fibrillin.

Studies conducted on both uncrosslinked[58, 60, 313] and crosslinked forms[326] of HA have shown that HA fragments (<1 MDa) and oligomers (<10 kDa) are more cell-interactive[55] than the relatively bio-inert HMW HA (>1 MDa). In our earlier studies, we showed large HA fragments (VLMW and LMW; 0.2 μg/mL) to marginally increase cell proliferation in dose-independent manner, likely by phosphorylating the primary cell surface HA receptor, CD44, to further activate a cytoplasmic cascade of events ultimately inducing mitosis[315]. HA oligomers (0.2 μg/mL) on the other hand, modestly inhibited cell proliferation[58]. In contrast to previous studies which have shown IGF-1 to stimulate cell proliferation[327], the current dose of IGF-1 (500 ng/mL) provided under serum-rich conditions, drastically inhibited SMC proliferation relative to non-additive control cultures. Moreover, when IGF-1 was added in conjunction with HA fragments, cell proliferation continued to be dramatically inhibited relative to controls, except when HA oligomers were present ($p < 0.04$ *vs*. control). These effects are in contrast to our prior findings on the effects of HA / fragments alone, as detailed above[58, 60]. Thus, we believe that the IGF-1-receptor mediated signaling pathway through which IGF-1 initiates and

promotes mitogenesis in RASMCs[328] may be negated by other upstream effects such as interaction of HA fragments with the primary HA receptor CD44, which can cause cells to become quiescent, although further study is needed to confirm this hypothesis. In indirect support of this hypothesis, we note in this study that in the presence of IGF-1, HA oligomers elicit responses different from larger-sized HA fragments, possibly due to their interaction with different HA receptors such as Toll-like 4 (TLR-4), unique to HA 4-mers. These experiments also showed that IGF-1 suppressed cell proliferation to an extent that inversely correlated to size of non-oligomeric HA fragments. We hypothesize that this might be due to the cell-shielding effect of larger HA fragments, due to which IGF-1 may be increasingly unable to interact with cell surface receptors and thus induce proliferative cell responses. This may possibly explain why cell proliferation remained unchanged relative to controls when HMW HA was provided. Nevertheless, our results suggest utility of combined HA/ fragments and IGF-1 cues to attenuation of SMC hyper-proliferation, a common outcome at sites of vascular aneurysms where in situ elastin regeneration may be desired.

Biochemical analysis showed that at the tested dose, IGF-1 almost doubled cellular output of tropoelastin precursors on a per cell basis (**Figure 4.3**). Contrary to our prior findings that HA oligomer supplements (0.2 μg/mL) upregulated tropoelastin synthesis, their delivery concurrent with IGF-1 suppressed tropoelastin synthesis. Such suppression perhaps occurs due to adverse cross-interactions of downstream elastin synthesis impacting pathways, initiated by interactions of IGF-1 and HA oligomers with their respective cell-surface receptors. Larger HA fragments likely interact with cells in a

different way from HA oligomers (through CD44 and not TLR-4 receptors), and thus possibly elicit enhanced elastin synthesis via convergent or independent downstream elastogenic cellular mechanisms. The lack of significant IGF-1 induced upregulation of tropoelastin synthesis (beyond controls) in the presence of HMW HA, might be as stated before, due to the formation of pericellular coats that isolate cells from IGF-1 cues.

Our results also showed that IGF-1 by itself increased total production of elastin matrix, *i.e.*, alkali-soluble and insoluble fractions, by nearly 1.7-fold relative to controls. Again, contrary to previous outcomes observed with HA cues alone, in the presence of IGF-1, HA oligomers marginally inhibited elastin matrix synthesis, while the greatest benefit was obtained with large HA fragments (VLMW, LMW); HMW HA however did not induce any increase in control levels of elastin matrix production. A comparison of the fold-increases in elastin matrix amounts in each case, and the corresponding fold-increases in tropoelastin production show remarkable similarities suggesting that elastin matrix deposition outcomes are a mere reflection of alterations to basal tropoelastin production. In other words, the results suggest that IGF-1 in the presence or absence of HA cues do not specifically benefit precursor recruitment for matrix assembly; this observation was supported by further results tabulated in **Table 4.1**, that indicated matrix yields (*i.e.*, matrix to total elastin ratios; total elastin = matrix elastin + tropoelastin) to remain unchanged at between 34-46%.

A more detailed analysis however indicated significant differences between these cases in the yields of highly crosslinked, alkali-insoluble structural elastin. Specifically, as shown in **Table 4.1**, our results showed that while IGF-1 together with oligomers or

HMW HA significantly enhanced the fractional yields of insoluble matrix elastin (*i.e.*, insoluble to total matrix elastin ratios) in controls, IGF-1 alone or together with other HA fragments marginally altered the same. These results suggest that while IGF-1 and HA fragments together do not upregulate tropoelastin recruitment beyond what can be achieved by providing IGF-1 alone, they influence the elastin crosslinking mechanism in manner whereby crosslinking efficiency and hence yields of insoluble matrix elastin correlate positively to HA fragment size. Likely, as our prior studies have suggested[58, 60], larger HA fragments and HMW HA coacervate tropoelastin precursors by an opposite-charge interaction mechanism, thereby facilitating more robust crosslinking, beyond that possible in the absence of HA. Since IGF-1 alone enhanced neither yield of insoluble matrix elastin, nor desmosine to insoluble elastin ratios, we believe that the nearly 26% increase in production of the elastin crosslinking enzyme, LOX, elicited by IGF-1, is not singularly capable of influencing desmosine crosslink formation. Similarly, crosslinking is improved only when increases in LOX production and localization of elastin precursors at cell layer due to coacervation by HA/ fragments simultaneously occur[329]. Thus, combinations of IGF-1 and HMW HA/ large HA fragment cues, most usefully promote elastin matrix synthesis and crosslinking.

Our ultrastructural characterization results showed that IGF-1 alone or together with HMW HA significantly promoted formation of mature elastic fibers via physiologic-like mechanisms that involve deposition of pre-scaffold of fibrillin microtubules. Fibrillin deposition appeared more pronounced in cultures that received IGF-1, which may explain the enhanced elastic fiber formation in those cultures. HMW HA along with

IGF-1 promoted deposition of significantly greater amounts of elastin, albeit less-structured. Thus, a possible future strategy to improve elastic fiber formation is to enhance doses of IGF-1 to render its effect more pronounced. Regardless, the utility of the mixtures of large HA fragments (> 20 kDa) as a scaffolding material to greatly enhance the yields of elastin matrix has been elucidated in this study.

4.5 Conclusions of this study

1. IGF-1 is not only effective in suppressing SMC proliferation in all the cases expect in the presence of HA oligomers, but also stimulated collagen, tropoelastin and soluble elastin production nearly 2-fold relative to non-additive controls.
2. IGF-1 and large HA fragments (> 200 kDa) together induce multi-fold increases in elastin precursor synthesis, elastin matrix yields and crosslink densities within adult vascular cell layers, relative to supplement-free cultures. In addition, these cues encourage elastic fiber formation. These outcomes are not all obtained when either of the cues is provided separately.
3. HA fragments upregulated crosslinked elastin matrix formation in inverse correlation to their fragment size, with HMW HA contributing for an almost 5-fold upregulation, though IGF-1 alone did not offer any additional advantage compared to control cultures. These results were confirmed by immunofluorescence and electron microscopy images of matrix elastin and by the quantification of LOX and desmosine activities in the cell cultures.

4. The results are of tremendous utility to our ongoing efforts to provide exogenous or scaffold-based elastogenic cues (IGF-1 + HMW HA/ large HA fragments) to enable robust and faithful regeneration of elastin matrix structures *in vivo* or *in vitro*. The present outcomes may be used to restore elastin matrix homeostasis in de-elasticized vessels and tissue engineered constructs that may be grafted as a substitute.

CHAPTER 5

BIOMIMETIC CUES FOR FIBROUS ELASTIN MATRIX ASSEMBLY AND MATURATION

5.1 Effect of Copper Sulfate and HA Fragments

5.1.1 Introduction

As already mentioned in chapters 1 and 2, elastic fibers are amongst the most difficult matrix structures to repair or regenerate because they contain other non-elastin protein components (e.g., fibrillin, elaunin), a highly regulated recruitment and deposition pattern, and a multi-step hierarchical assembly process[329]. Besides, the elastic fiber formation at the molecular level involves recruitment and patterned coacervation of cell-derived soluble tropoelastin precursors onto pre-formed templates of fibrillin-rich microfibrils[330], and their stabilization by lysyl oxidase (LOX)-catalyzed desmosine crosslinking[331]. Hence, cues for elastin regeneration must be able to mimic the spatio-temporal sequence of these events leading to elastin matrix assembly.

A key impediment to creating highly matured elastin matrices is the absence of cues to improve production and crosslinking efficiency of elastin precursors (tropoelastin) by vascular SMCs. Though our studies show that HA significantly increases tropoelastin and total elastin (matrix elastin + tropoelastin) amounts on a per cell basis, the net yield of crosslinked matrix elastin relative to the total elastin produced, remained quite low[58, 60]. This stresses the need to provide other exogenous cues that will facilitate and improve efficiency of tropoelastin recruitment and crosslinking into elastin

matrix structures. One possible strategy to achieve this is to enhance cellular production or activity of LOX enzyme that catalyzes elastin crosslinking[332-334]. Since extracellular LOX availability and activity are dependent on the presence of Cu^{2+} ions, we hypothesize that the simultaneous delivery of HA and Cu^{2+} cues may possibly enhance tropoelastin synthesis, recruitment and crosslinking into mature elastin matrix. Thus, the objective of the current study is to evaluate the benefits of Cu^{2+} ions delivery concurrent with elastogenic cues as represented by HA fragments/ oligomers, on elastin crosslinking in a culture model of adult rat aortic smooth muscle cells (RASMCs).

5.1.2 Materials and Methods

5.1.2.1 Cell Culture

Hyaluronic acid with molecular weights of 2000 kDa, 20 kDa (Lifecore Technologies, Minneapolis, MN), and 0.76 kDa, designated as high molecular weight (HMW), very low molecular weight (VLMW) and oligomers, respectively, were dissolved in sterile culture medium prior to addition to cell cultures. HA oligomer mixtures containing predominantly 4-mers were prepared in the lab using protocols reported in section 3.2.1.

Low passage (3-5) adult rat aortic SMCs (RASMCs) were selected for the current study due to their relatively lower levels of tropoelastin production compared to neonatal cells, and thus of greater relevance to regeneration of elastin in adult blood vessels. RASMCs were seeded onto 6-well tissue culture plates (Becton Dickinson Labware) at a density of 3×10^4 cells/ well and treated with DMEM (Invitrogen) containing 10% v/v

FBS and 1% v/v penstrep (VWR International). HA fragments prepared in serum-rich medium were added to cell cultures at an ultimate dose of 0.2 μg/mL. Copper sulfate ($CuSO_4$; Sigma Aldrich) was dissolved in distilled water and supplemented exogenously to the culture wells at final doses of either 0.1 M or 0.01 M, except in control cultures which received no supplements. The culture medium was replaced twice weekly, the spent medium from each well pooled over the 21 day culture period and frozen for further biochemical analysis. To isolate the observed effects on RASMCs as due to Cu^{2+} ions and not SO_4^{2-} ions, sodium sulfate (Na_2SO_4; Sigma Aldrich; 0.01 and 0.1 M) was supplemented instead of $CuSO_4$ to control cultures.

5.1.2.2 Biochemical Assays

The DNA content in cell layers was measured at 1 and 21 days of culture to determine the proliferation of SMCs and to normalize the measured amounts of synthesized matrix, according to protocol explained in section 3.2.3.

The collagen content within the cell layers and in the pooled supernatant medium fractions was estimated using a hydroxy-proline assay, described in section 3.2.4. The amounts of matrix elastin (alkali-soluble and insoluble fractions) and soluble tropoelastin (in pooled spent medium) were quantified using a Fastin assay (Accurate Scientific Corp), as detailed in section 3.2.5. The measured amounts of synthesized matrix were normalized to their respective DNA amounts to provide a reliable basis of comparison between samples, and to broadly assess if the observed changes in the amount of matrix synthesized could possibly be due to increases in elastin production on a per cell basis.

The desmosine crosslink densities within elastin matrices were quantified for selected cases using ELISA, as described in section 3.2.6. The desmosine amounts/ ng of DNA were compared to the DNA-normalized amounts of insoluble matrix elastin from corresponding cell layers. The LOX enzyme activity within the cell culture layers was determined using a flurometric assay based on generation of H_2O_2 when LOX acts on a synthetic substrate, described in detail in section 3.2.7. Western blot analysis of proteins within the pooled medium fractions at day 21 was performed using methods described in section 3.2.8, to semi-quantitatively confirm observed biochemical trends in tropoelastin synthesis and to assess LOX protein synthesis.

All experiments were performed in triplicate and quantitative results reported as mean ± SD. Statistical significance between and within groups was determined using 2-way ANOVA. Results are deemed significantly different from controls for $p < 0.05$.

5.1.2.3 Immunofluorescence Studies

As explained in detail in section 3.2.11, immunofluorescence techniques were used to confirm the presence of elastin, fibrillin within selected cell layers, and LOX expression for those conditions that appeared to upregulate elastin synthesis.

5.1.2.4 Matrix Ultrastructure

Scanning electron microscopy was used to discern the structural organization of matrix elastin within cell layers cultured with or without exogenous HA cues and various provided doses of copper ions. For sample preparation, medium-aspirated cell layers

were incubated in 1 N NaOH for 2 h at 60^{o}C to digest the cells and the non-elastogenous matrix, fixed with 2% w/v glutaraldehyde (4^{o}C, 1 h) and treated with increasing ethanol gradient series (60-100% v/v, each for 15 min). The dried matrix layers were sputter gold-coated at 30 mA for 1 min, and visualized in a Hitachi S4800 field emission scanning electron microscope.

5.1.3 Results

5.1.3.1 Cell Proliferation

Proliferation ratios of RASMCs cultured in the presence of either $CuSO_4$ alone or together with HA fragments/ oligomers are shown in **Figure 5.1**. The effects of Na_2SO_4 addition are also shown for comparison. Addition of Na_2SO_4 alone had no effect on RASMC morphology or proliferation (p = 0.4 vs. controls), irrespective of the added dose. $CuSO_4$ (0.1 M) induced significant rounding of RASMCs in the first 3 days that followed its addition, though the cells recovered sufficiently to exhibit normal morphology throughout the rest of the culture period. Differently, when 0.01 M $CuSO_4$ was added, the temporal change in cell morphology induced by the 0.1 M $CuSO_4$ was not observed. At 3-weeks of culture, cell proliferation ratios (ratio of cell number at day 21 to day 1) for 0.1 M $CuSO_4$ cultures was 5.6 ± 2.3 –fold, while those in cultures that received 0.01 M of $CuSO_4$ and in non-additive controls were 44.5 ± 6.7, and 22.9 ± 4.2 -fold respectively. Thus, in effect, the cell number in 0.1 M and 0.01 M $CuSO_4$ – supplemented cultures at 21 days were 0.24 ± 0.1 and 1.9 ± 0.3 -fold relative to non-additive controls (p = 0.005 and 0.001 vs. control). Cell proliferation ratios in the

presence of both HA fragments (all sizes) and $CuSO_4$ (0.1 M or 0.01M) were not different from those in cultures that received the respective doses of $CuSO_4$ alone.

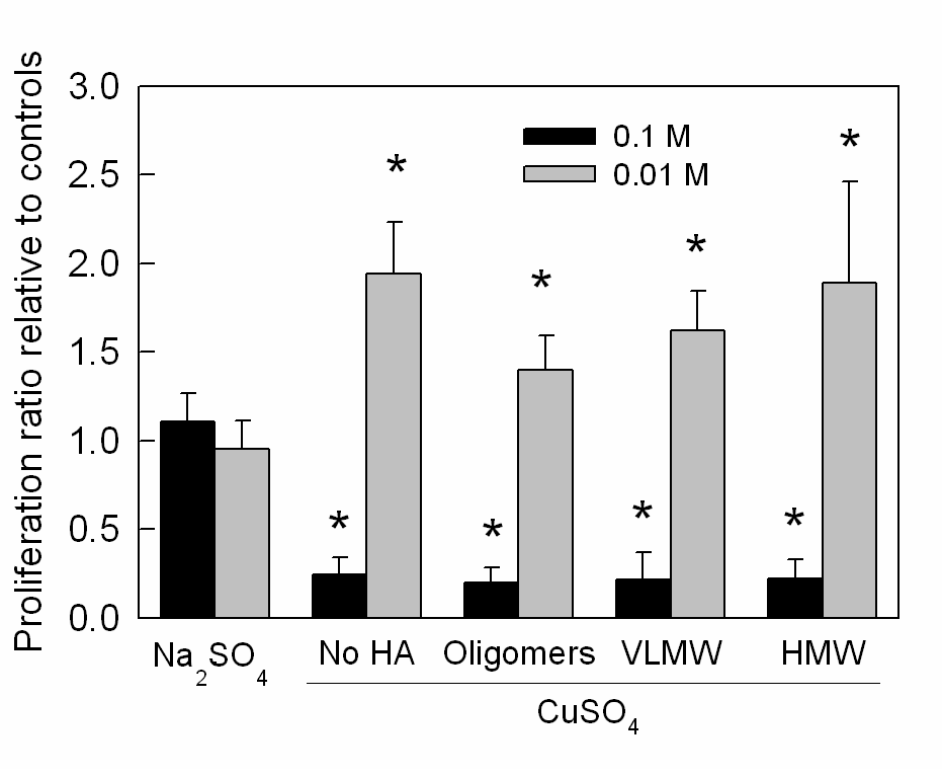

Figure 5.1. Proliferation ratios of RASMCs supplemented with Na_2SO_4 alone, $CuSO_4$ alone or together with HA fragments (0.2 μg/mL). Data shown represent mean ± SD of cell count after 21 days of culture, normalized to initial seeding density and further normalized to control cultures that received no additives (n = 3/case). $P < 0.05$ represents significant differences from controls (*).

5.1.3.2 Matrix Synthesis

The data shown in **Figure 5.2** represents mean ± SD of protein synthesized (n = 3/ case) in test groups, normalized initially to their respective cellular DNA contents at 21

days, and further normalized to the corresponding protein content in non-additive control cultures. The absolute (not normalized to DNA) amounts of total collagen, tropoelastin and matrix elastin produced in each case were shown in **Table 5.1**. As evident from **Figure 5.2A**, on a per cell basis, 0.1 and 0.01 M doses of Na_2SO_4 did not significantly impact total (matrix + soluble) collagen output by RASMCs (0.94 ± 0.15 and 1.1 ± 0.13 -fold vs. controls; $p = 0.2$ and 0.1, respectively). When 0.1 M $CuSO_4$ alone was provided, synthesis of collagen (on a per ng DNA basis) increased 4.1 ± 0.4 -fold over non-additive controls (1332 ± 140 ng/ ng DNA), while addition of 0.01 M $CuSO_4$ suppressed collagen production 0.5 ± 0.04 fold ($p < 0.001$ *vs.* controls). In the presence of oligomers, VLMW and HMW HA, 0.1 M $CuSO_4$ enhanced control-levels of collagen synthesis by 4.6 ± 0.4, 4.5 ± 0.8 and 4.5 ± 0.6 –fold respectively, while 0.01 M $CuSO_4$ consistently suppressed collagen synthesis in all the cases ($p < 0.001$ vs. controls). However, the absolute (not normalized to DNA content) collagen production levels in all the cases were not different from non-additive control cultures (see **Table 5.1**).

The trends in tropoelastin production by RASMCs (**Figure 5.2B**) closely mirrored those observed for collagen synthesis under identical conditions. Na_2SO_4 had no effect on control levels of tropoelastin production by RASMCs (20074 ± 1240 ng/ng DNA), irrespective of added dose ($p = 0.5$ vs. controls). In the absence of HA, 0.1 M $CuSO_4$ enhanced control levels of tropoelastin production on per ng of DNA basis by 4.1 ± 0.05 fold ($p < 0.001$ vs. control), while 0.01 M $CuSO_4$ inhibited the same by 0.5 ± 0.04 –fold ($p < 0.001$ vs. controls). When provided together with HA fragments, 0.1 M $CuSO_4$ likewise enhanced tropoelastin production, while 0.01 M $CuSO_4$ marginally decreased

the same ($p < 0.03$ in all the cases vs. controls). No HA fragment size dependent-effects were noted in either case, although in the presence of 0.1 M $CuSO_4$, HA oligomers stimulated a significantly greater increase in tropoelastin production (1.3 ± 0.01 -fold) over cultures that received $CuSO_4$ alone ($p < 0.001$). As apparent in **Table 5.1**, the absolute amounts of tropoelastin produced (not normalized to DNA amounts) in all cases, irrespective of $CuSO_4$ dose and HA fragment size, were almost identical to controls.

Elastin incorporated into the matrix was measured as a sum of two individual fractions, *i.e.*, a highly cross-linked, alkali-insoluble elastin pellet, and an alkali-soluble fraction. As shown in **Figure 5.2C**, irrespective of provided dose, Na_2SO_4 had no effect on control production levels of alkali-soluble and insoluble matrix elastin on a per ng of DNA basis ($p > 0.4$ vs. controls). Addition of 0.1 M $CuSO_4$ alone increased soluble elastin synthesis dramatically by 4.1 ± 0.1 -fold, while 0.01 M $CuSO_4$ inhibited the same by 0.5 ± 0.4 fold, relative to non-additive controls (5388 ± 363 ng/ ng DNA; $p = 0.001$ and 0.27 vs. controls, respectively). In the presence of HA fragments, 0.01 M $CuSO_4$ consistently suppressed production of alkali-soluble matrix elastin ($p < 0.01$ vs. controls; per ng of DNA basis), while addition of 0.1 M $CuSO_4$ dramatically increased the same by 4.47 ± 0.7, 5.02 ± 0.25 and 3.38 ± 0.6 -fold upon concurrent addition of HA oligomers, VLMW, and HMW HA, respectively ($p < 0.05$ vs. controls). Differences in outcomes between these cases were deemed to be statistically insignificant.

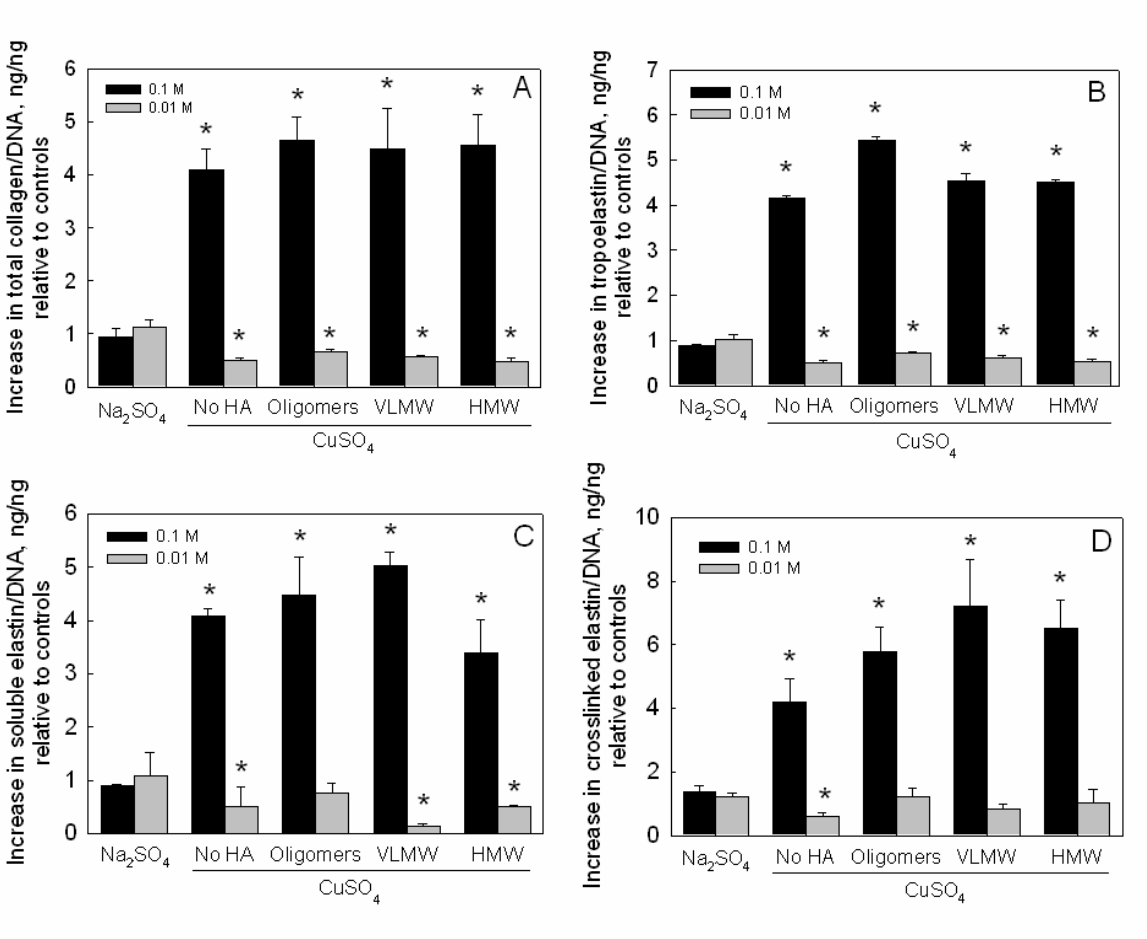

Figure 5.2. Effects of exogenous $CuSO_4$ with or without HA/ fragments (0.2 μg/mL) on collagen (A), tropoelastin (B), alkali-soluble matrix elastin (C) and crosslinked alkali-insoluble matrix elastin (D), synthesized by adult RASMCs. Values (mean ± SD) are shown normalized to the DNA content of the respective cell layers at 21 days of culture (n = 3/case) relative to control cultures. * represents significant differences relative to control cultures, deemed for $p < 0.05$.

On per ng of DNA basis, control production levels of alkali-insoluble, crosslinked matrix elastin (*i.e.*, structural elastin) were not influenced by addition of Na_2SO_4 (**Figure**

5.2D). When 0.1 M of $CuSO_4$ was delivered alone, crosslinked matrix elastin synthesis (122 ± 19 ng/ ng of DNA) was enhanced by 4.2 ± 0.7 –fold over control levels, while concurrent addition of oligomers, VLMW and HMW HA increased the same by 5.8 ± 0.7, 7.2 ± 1.4 and 6.5 ± 0.9 -fold, respectively ($p < 0.001$ vs. controls in all the cases). However, when 0.01 M $CuSO_4$ was supplemented alone or together with HA fragments, there was no benefit to crosslinked matrix elastin synthesis (on a per ng of DNA basis), over controls (0.6 ± 0.1, 1.2 ± 0.2, 0.8 ± 0.1 and 1.02 ± 0.4 –fold in the presence of 0.01 M $CuSO_4$ alone or together with oligomers, VLMW and HMW HA, respectively; $p > 0.05$ vs. controls in all the cases). However, irrespective of added HA fragment size and $CuSO_4$ dose, the absolute production levels (not normalized to DNA amounts) of alkali-soluble and –insoluble matrix elastin were not different from control cultures (see **Table 5.1**).

5.1.3.3 Western Blots for LOX Protein Synthesis

Spent medium fractions pooled over 21 days from test and control cultures were analyzed by western blot, and the DNA-normalized intensities of the LOX-protein bands within test cultures were further normalized to those in controls (**Figure 5.3**). Exogenous $CuSO_4$ (0.01 M) both alone and together with HA fragments did not enhance LOX protein synthesis relative to controls; there were no differences in LOX synthesis between cultures that received different-sized HA fragments either. LOX protein synthesis was however enhanced by 2.7 ± 0.3 –fold in the presence of 0.1 M $CuSO_4$ alone, and up to

3.5 –fold when HA fragments were additionally provided ($p < 0.01$ vs. controls, in all cases).

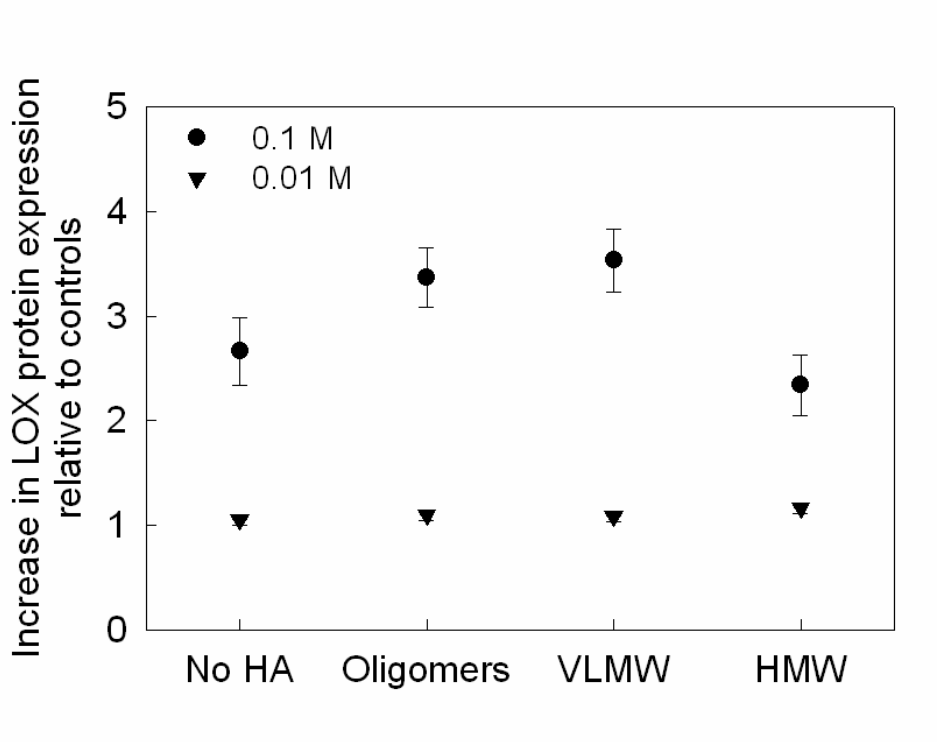

Figure 5.3. LOX protein amounts in pooled medium aliquots collected over 21 days of culture. Shown are mean ± SD of DNA-normalized intensities, measured from representative SDS-PAGE/ western blots containing bands corresponding to LOX produced in the respective cases.

5.1.3.4 LOX Functional Activity

Figure 5.4 describes the effect of addition of $CuSO_4$ alone or together with HA fragments on LOX enzyme activity. LOX activity was measured in the spent culture medium following 21 days of culture. Addition of 0.1 M $CuSO_4$ alone and concurrent

with HA fragments had no significant effect on basal LOX functional activity. LOX activities measured in cultures that received a 0.01 M dose of $CuSO_4$ were significantly higher than that in controls in most cases (1.4 ± 0.2, 1.12 ± 0.1, 1.4 ± 0.02 and 1.3 ± 0.17 for 0.01 M $CuSO_4$ alone and with oligomers, VLMW and HMW HA, respectively; $p < 0.05$ vs. control).

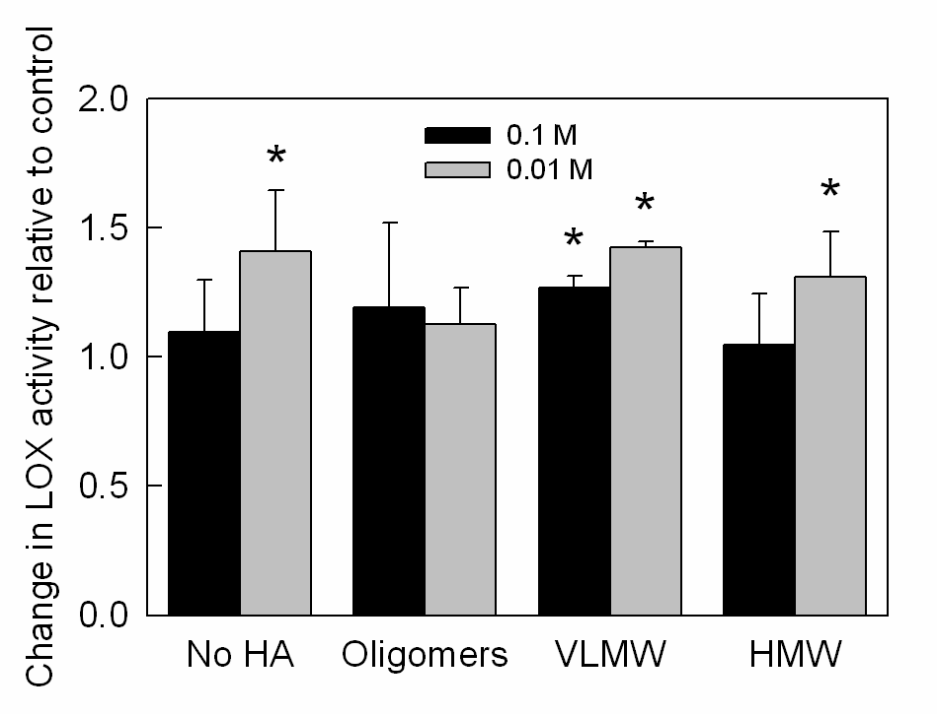

Figure 5.4. LOX enzyme activities in cultures treated with $CuSO_4$ and HA fragments. Values (mean ± SD) are shown normalized to the LOX activity measured in control cell layers at 21 days of culture (n = 3/case). * represents significance in differences relative to controls, for $p < 0.05$.

5.1.3.5 Immunodetection of Elastin, Fibrillin and LOX

Immunofluorescence micrographs of 21-day old cell layers (**Figure 5.5**) confirmed presence of elastin, fibrillin and LOX (red fluorescence) both in cultures that received 0.1 M $CuSO_4$ alone or together with HA fragments. Relative to control cultures, the fluorescence intensity due to elastin were visibly greater in cultures supplemented with $CuSO_4$, particularly those which also received HA fragments. Fluorescence intensity due to fibrillin was also greater in $CuSO_4$ -supplemented cultures than in controls, though it was most pronounced in cultures that also received VLMW and HMW HA. However, fluorescence due to LOX was relatively weak in all cultures.

5.1.3.6 Structural Analysis of Matrix Elastin

Figure 5.6 shows representative scanning electron micrographs of elastin matrices isolated from 21-day cultures. Compared to the non-additive control cultures where elastin was sparingly deposited as amorphous clumps (panel A), addition of $CuSO_4$ with or without other HA fragments appeared to greatly enhance matrix elastin amounts. However, addition of 0.01 M $CuSO_4$ alone or together with HMW HA resulted in featureless clump-like deposits, likely of amorphous elastin (panels B-C). $CuSO_4$ (0.1 M) and HA oligomers together promoted deposition of elongated, aggregating elastin fibrils (panel E), different from the discrete clumps of amorphous elastin that were uniformly distributed within cell layers when 0.1 M $CuSO_4$ was provided alone (panel D). When both 0.1 M of $CuSO_4$ and HMW HA were provided together, elastin fiber formation was likewise favored, with the matrix containing greater number of apparently

fully-formed fibers (~ 1 μm diameter; panel F) than in cultures provided with HA oligomers.

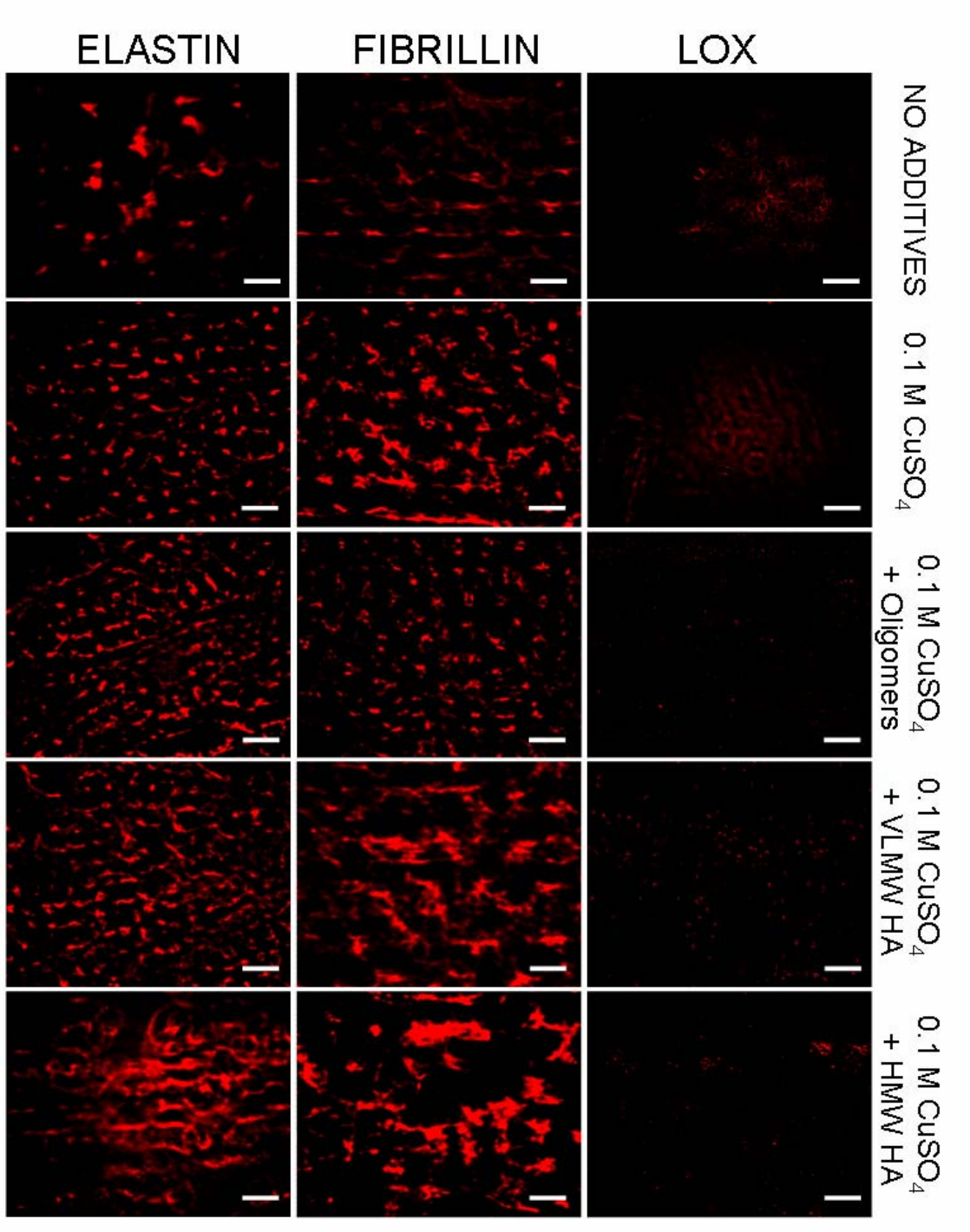

Figure 5.5. Immunodetection of elastin, fibrillin and LOX (red) within RASMC layers following 21 days of culture in the presence of $CuSO_4$ alone (0.1 M) or together with HA fragments (0.2 μg/mL); control cultures received no-additives. Immunolabeling controls received no primary antibodies and exhibited no background fluorescence when treated with the fluorophore-labeled secondary probe.

5.1.4 Discussion

Our long-term research goal is to develop exogenous or biomaterial-based cues to stimulate regeneration of structural and functional mimics of vascular elastin matrices on demand. Despite a variety of prior strategies to tissue engineer elastin-rich constructs[219, 323-325], positive outcomes have been severely limited by poor tropoelastin mRNA expression by adult cells[24, 300]. As we mentioned in our Introduction, our ongoing study of HA cues for elastin regeneration is driven by prior work that suggested several GAG types (HA, heparin sulfate) to have roles in elastin synthesis, maturation and organization *in vivo*[48]. For example, HA has been suggested to strongly bind versican[48], to likely facilitate its further interaction with elastin-associated microfibrils to form higher-order structures important for elastin fiber assembly[50, 51]. Also, it has been suggested that anionic HA chains coacervate soluble tropoelastin to locally facilitate its crosslinking into a stable matrix[52, 53]. Since the physico-chemical and biological properties of HA are often dependent on its size[54], we have sought to investigate these differences in the context of stimulating elastin matrix synthesis.

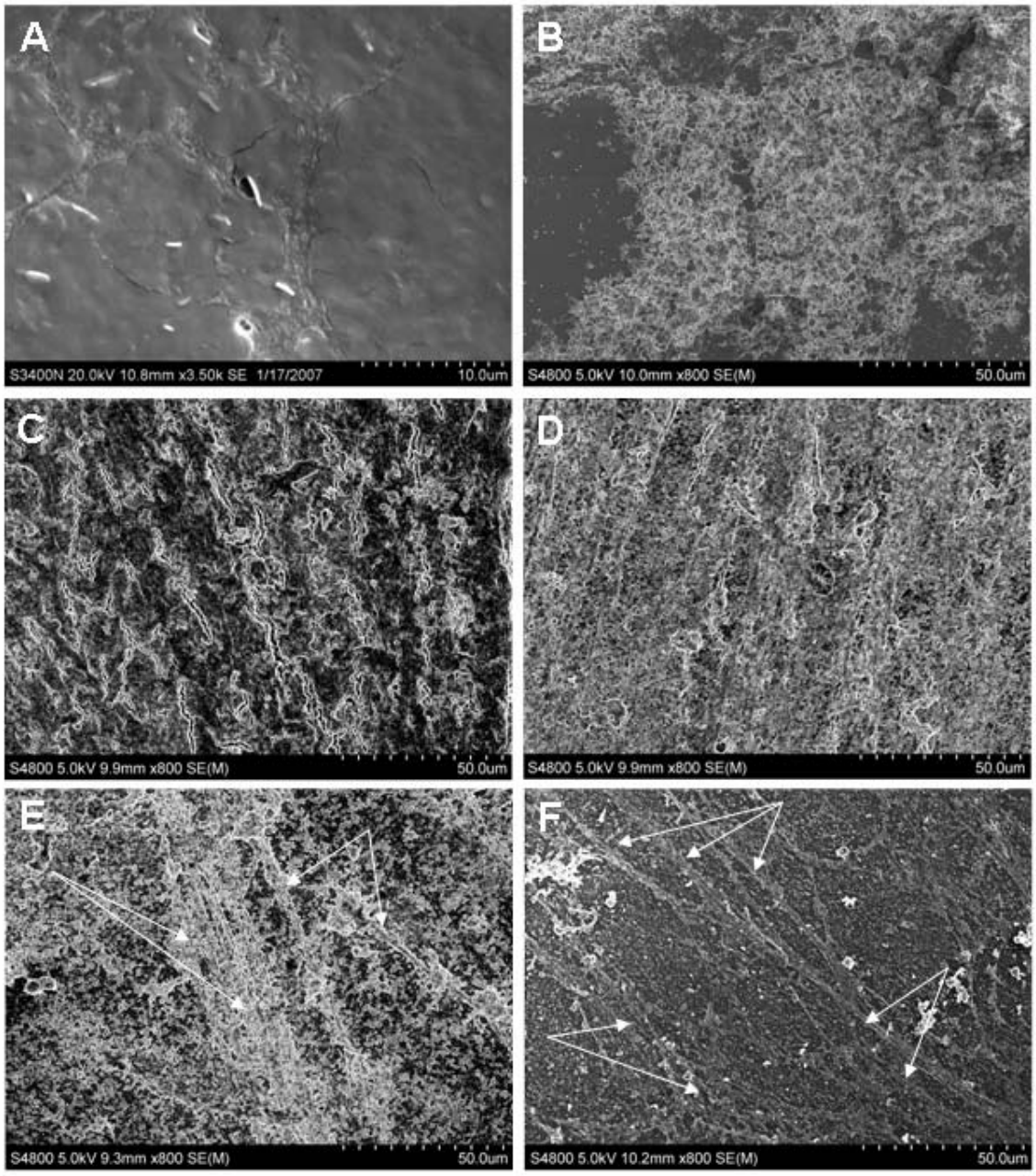

Figure 5.6. Representative SEM images of 21-day old RASMC cell layers for non-additive controls (panel A); cultured with $CuSO_4$ alone (0.01 M : panel B; 0.1 M : panel D), $CuSO_4$ (0.1 M) with oligomers (panel E) or together with HMW HA (0.01 M : panel C; 0.1 M : panel F). When compared to 0.1 M $CuSO_4$ supplemented cultures, additional

presence of oligomers or HMW HA enhanced formation of matrix elastin fibers with diameters ranging between 0.5-1 μm, indicated by arrows.

	Total collagen produced, mg		Tropoelastin produced, mg		Soluble matrix elastin, mg		Crosslinked matrix elastin, mg	
	0.1 M	0.01 M	0.1 M	0.01 M	0.1 M	0.01 M	0.1 M	0.01 M
Controls	5.4±0.5		82.6±1.4		22.2±1.5		0.51±0.08	
Na_2SO_4	5.7± 0.9	5.8± 0.8	81.7± 1.2	81.3± 0.7	22.2±0.8	23±0.5	0.77±0.1	0.6±0.05
$CuSO_4$	5.5± 0.5	5.4± 0.5	83.7± 1.4	82.5± 2.3	22.1±0.7	21.6±2.5	0.52±0.1	0.58±0.1
$CuSO_4$+ Oligos	5.1± 0.4	5.0± 0.3	89.3± 2.6	84.8± 0.3	19.7±3.2	23.6±0.8	0.58±0.1	0.87±0.2
$CuSO_4$+ VLMW	5.3± 0.9	4.9± 0.3	81.7± 0.9	83.4± 0.7	24.3±1.2	5.2±0.2	0.79±0.2	0.68±0.1
$CuSO_4$+ HMW	5.5± 0.7	5.0± 0.7	82.4± 0.7	82.6± 0.9	16.6±3	21.2±0.3	0.73±0.1	0.98±0.4

Table 5.1. The absolute amounts of total collagen, tropoelastin, soluble matrix elastin and crosslinked matrix elastin produced by RASMCs supplemented with either Na_2SO_4 alone, or $CuSO_4$ with and without HA fragments (oligomers, VLMW and HMW) over the 21 day culture period. The data shown here was not normalized to DNA content (i.e., cell number).

In other studies, copper ions (Cu^{2+}) have been shown to minimize vascular defects[71], promote angiogenesis[73] and enhance LOX enzyme activity[74]. Deficiency of nutritional copper has been linked to increased occurrence of vascular lesions and development of aneurysms[335-337]. One study showed that in the presence of HA, low doses (0.01 M) of $CuSO_4$ enhance tissue vascularization[338]. Dahl *et al*., investigated the

singular effects of increasing medium Cu^{2+} ion concentration on matrix crosslinking efficiency in an engineered vascular-like tissue, and showed increasing levels of crosslinks to form[339]. However, as yet, the synergistic benefits of HA and Cu^{2+} to elastin matrix regeneration by improving tropoelastin and matrix elastin synthesis and crosslinking, has not been elucidated. Thus, besides investigating this in an *in vitro* culture model, we have sought to identify the Cu^{2+} doses that provide greater benefits to elastin matrix synthesis.

In investigating the effects of exogenous Cu^{2+} ions on cell behavior and matrix synthesis, it is to be noted that all experiments were conducted in serum-rich medium. Although culture studies in a serum-free medium would be preferable to isolate the effects of Cu^{2+} ions on cell behavior, the need to stimulate matrix synthesis by cells necessitates that serum-rich conditions be provided. FBS has been shown to contain trace amounts of Cu^{2+} ions (~ 10-20 nM)[339], almost all of which is bound to ceruloplasmin and albumin. Estimations of free Cu^{2+} ions indicate that it is unlikely to exceed picomolar concentrations[340]. Thus, the background levels of Cu^{2+} ions are far lower than the lowest exogenous dose (0.01 M) used in this study, and may be deemed almost identical to Cu^{2+}-free control medium.

Our experiments indicated that Na_2SO_4 addition had no effect on cell proliferation ratios or matrix synthesis, signifying the absence of any counter ion (SO_4^{2-})-induced effects on cellular behavior, at least at the doses tested in this study. Previously, we showed large HA fragments (20-200 kDa) to modestly increase cell proliferation in a dose-independent manner, while HA oligomers (2 μg/mL) were ineffective[58, 60].

However, differently, in this study we found that in the presence of 0.01 M of $CuSO_4$, cell proliferation was not affected by HA fragment-size or dose, although Cu^{2+} itself enhanced cell proliferation relative to non-additive controls. On the other hand, 0.1 M $CuSO_4$ significantly inhibited cell proliferation, both in the presence and absence of HA fragments. These results suggest that (a) SMCs respond in a dose-dependent manner to Cu^{2+} ions in the context of cell proliferation, and (b) interaction of Cu^{2+} ions with SMCs appears to interrupt HA-induced intracellular signaling pathways influencing cell proliferation. Prior studies also showed much lower doses (0.5 mM) of Cu^{2+} ions do not influence SMC proliferation, though endothelial cells proliferated rapidly[341]. Here, we show that $CuSO_4$ in the range of 0.01 M induces SMC proliferation, results that suggest that Cu^{2+} ions impact on cells is specific to both cell type and dose. Interestingly, at the higher doses of $CuSO_4$ (0.1 M), though no cell death was observed, cells appeared rounded in the first 3 days after $CuSO_4$ addition, but gradually assumed a more spread morphology. Based on prior reports[342, 343], we hypothesize that at this higher tested dose, some degree of free-hydroxyl radical release occurs into the medium, which may suppress cell proliferation and influence cell spreading due to hitherto unknown intracellular signaling pathways. However, the lack of any consistent long-term hyper-trophic or hypo-trophic phenomena suggests that cellular metabolic pathways are not adversely affected at this tested Cu^{2+} dose, which can be safely applied in alternate tissue engineering approaches to improve matrix yields.

Though there were no significant differences between the absolute amounts of total elastin and matrix elastin produced in test groups and control cultures (as shown in

Table 5.1), 0.1 M $CuSO_4$ (with or without HA) improved elastin yield on a per cell basis by ~ 4-fold relative to control cultures. Qualitatively, cultures that received 0.1 M $CuSO_4$ (but not 0.01 M) and HA fragments also contained a far greater number of elastin fibers than in controls (amorphous clumps only); LOX protein production was also 2.5-fold greater and even more so (3.5-fold) in the presence of HA fragments. Literature suggests strong interplay between TGF-β availability and LOX[66, 344], which in turn may imply that the observed increases in LOX production may be mediated by Cu^{2+} ion-induced increases in endogenous TGF-β release. The increases in tropoelastin production in 0.1 M $CuSO_4$ –supplemented cultures could also possibly be due to the TGF-β-mediated effect of Cu^{2+} ions, though this hypothesis is subject to future validation. Regardless, these results strongly indicate that 0.1 M $CuSO_4$, provided with or without HA fragments, beneficially renders SMCs far more efficient in generating tropoelastin and matrix elastin, and enhances elastin fiber formation as well. However, cell proliferation though quite robust, is somewhat slower in such cultures, due to which absolute amounts of matrix generated over a defined culture period are similar to that generated by identically-seeded control cultures.

Typically, tissue engineering constructs for clinical and pre-clinical testing and use demands that they be of sufficient size. This necessitates seeding of scaffolds at higher cell densities and culturing these scaffolds over longer time periods to facilitate substantial elastin matrix accumulation[345], especially since the elastin yield by adult vascular cells is extremely limited. During these extended periods of culture, cells frequently proliferate rapidly (e.g., as in our control cultures here) to first super-saturate

the scaffold pores/ surface and may eventually die competing for essential gases and nutrients. In addition, studies have shown that post-confluence, density-arrested SMCs generate much less collagen matrix on a per cell basis[346], which negates the purpose of initial high cell seeding density and long-term culture; this logic likely also holds true for cellular elastin matrix production. Thus, robust production of elastin matrix by cells which remain viable and synthetic in long-term culture demands gradual proliferation, and high yields of elastin synthesis on per cell basis. In this context, supplying Cu^{2+} ions equivalent to the 0.1 M dose might enable these criteria to be met, while providing additional benefits of enhanced elastin fiber formation and crosslinking within these tissue engineered constructs.

Fluorescence imaging and ultrastructural analyses of synthesized elastin matrices qualitatively supported the biochemical observations. RASMCs cultured with 0.01 M of $CuSO_4$ alone or together with HA fragments were found to deposit amorphous elastin clumps, as in additive-free control cultures. When compared to 0.1 M $CuSO_4$-supplemented cultures, additional presence of HA fragments dramatically increased elastic fiber formation, with numerous elastic fibers measuring around 0.5-1 μm in diameter seen in abundance. Literature suggests that tropoelastin precursors are poorly capable of spontaneous self-assembly, and thus require helper proteins (e.g., microfibrils) to guide their alignment for further crosslinking and fiber assembly[347]. Once this initial alignment has been achieved, the structure is stabilized against proteolytic degradation by Cu^{2+} ion-dependent LOX, which oxidizes the lysine residues of the aligned elastin molecules and enables crosslinking. Thus, these stabilized and aligned elastin structures

act as nucleation sites for further coacervation and crosslinking of more tropoelastin resulting in organized elastic fiber growth. Moreover, highly anionic GAGs (HA in this case) also promote elastic fiber formation by electrostatically binding to the unoxidized lysine residues of newly synthesized tropoelastin during their association with microfibrils, thus preventing their random self-aggregation far away from the site of fiber formation[52]. The retention of the tropoelastin molecules by GAGs would thus indirectly facilitate their LOX-mediated crosslinking and encourage elastin fiber growth, as stated above. In direct support of this hypothesis, we believe that the simultaneous availability of HA fragments and increases in LOX synthesis (2.7 ± 0.3 –fold) on addition of 0.1 M of $CuSO_4$, along with significant presence of fibrillin in the cell layers (as shown in **Figure 5.5**), might have contributed to the observed increases in the structural quality of elastin fiber formation.

5.1.5 Conclusions of this study

1. The current study demonstrates the combined utility of a 0.1 M of $CuSO_4$ and HA, particularly HA oligomers (~ 756 Da) and HMW HA (~ 2000 kDa), to significantly increase tropoelastin release and improve elastin matrix synthesis, crosslinking and fiber formation by adult rat vascular SMCs.
2. On a per cell basis, 0.1 M of Cu^{2+} ions slowed cell proliferation (5.6 ± 2.3 –fold increase over 21 days vs. 22.9 ± 4.2 –fold for non-additive controls), stimulated synthesis of collagen (4.1 ± 0.4 -fold), tropoelastin (4.1 ± 0.05 -fold) and crosslinked matrix elastin (4.2 ± 0.7 -fold).

3. LOX protein synthesis increased 2.5–fold in the presence of 0.1 M of Cu^{2+} ions, and these trends were maintained even in the presence of HA fragments, although LOX functional activity remained unchanged in all cases.
4. The abundance of elastin and LOX in cell layers cultured with 0.1 M of Cu^{2+} ions and HA fragments was qualitatively confirmed by immunoflourescence. SEM images showed SMC cultures supplemented with 0.1 M of Cu^{2+} ions and HA oligomers/ large fragments to exhibit enhanced deposition of mature elastic fibers (~ 1 μm diameter).
5. The results obtained might be of tremendous utility to restore elastin matrix homeostasis in de-elasticized vessels and tissue engineering constructs both *in vivo* and *in vitro*, and possibly even serve as an accelerated *in vitro* model to investigate elastogenesis during wound healing in adult tissues.

5.2 Benefits of Copper Nanoparticles and HA Fragments

5.2.1 Introduction

Though our previous studies (chapters 3 and 4) demonstrated the utility of HA oligomers to increase tropoelastin and total elastin (matrix elastin + tropoelastin) amounts on a per cell basis, the net yield of crosslinked matrix elastin relative to the total elastin produced, remained low[58, 60, 348]. This stresses the need to provide other exogenous cues to enhance cellular production or LOX enzyme activity, that catalyzes enhanced elastin crosslinking[332, 334]. Since extracellular LOX availability and activity are dependent on the presence of copper ions[74], we hypothesize that the simultaneous delivery of HA oligomers and copper cues may possibly enhance tropoelastin recruitment and crosslinking into mature elastin matrix. Thus, the objective of the current study is to evaluate the benefits of copper ions delivery concurrent with elastogenic cues as represented by HA oligomers, on elastin crosslinking in a culture model of adult rat aortic smooth muscle cells (RASMCs). Since sudden exposure of vascular cells to copper ions provided at high doses, via exogenous supplementation, appears to induce some degree of cell injury and death[343, 349, 350], we now seek to determine if gradual release of copper ions from copper nanoparticles (CuNP) can improve crosslinking of soluble tropoelastin precursors, whose production is greatly enhanced by HA oligomeric cues.

5.2.2 Materials and Methods

5.2.2.1 Copper Ion Release from CuNP

To quantify concentration of copper ions in the culture medium, we measured release of copper ions (Cu^{2+}) from copper nanoparticles (CuNP; 80-100 nm size; Sigma Aldrich, St. Louis, MO) using atomic absorption spectrophotometry (PerkinElmer Model 3030, PerkinElmer, Norwalk, CT), fitted with copper lamp. Briefly, the nanoparticles were dispersed in distilled water at concentrations of 1 ng/mL, 10 ng/mL and 100 ng/mL, and Cu^{2+} ion content in 1-mL aliquots of these solutions were measured at regular intervals over a 30 day period. The spent aliquots were replaced with fresh distilled water (1-mL), and the concentration of Cu^{2+} ions in the removed aliquots was accounted for in calculating the cumulative release of Cu^{2+} ions. All measurements were done in triplicate and the Cu^{2+} ion concentrations expressed in moles. To estimate the CuNP amounts necessary to generate the equivalent of 0.1 M of Cu^{2+} ions, which in an earlier study[351], showed to be effective in promoting elastin crosslinking, but to be mildly cytotoxic, we fitted the Cu^{2+} ion release profiles to a mathematical model. The dependence of Cu^{2+} ion release on CuNP concentration and time was fit using a hierarchial regression analysis, wherein a new predictor is added to or dropped from those used in the previous analysis based on the statistical significance of a particular model. The quadratic regression model which can accommodate linear, curvature and interdependence of the time (x) and CuNP concentration (y) used in this study was

$$R = a + b*x + c*y + d*x*y + e*x^2 + f*y^2 \qquad (1)$$

where R represents the amount of copper ions released, and a-f are the estimated regression coefficients. After initialization with the full quadratic regression model given in eq.1, a backward elimination procedure was used to reduce the number of terms in the model until all the remaining terms were statistically significant ($p < 0.05$). Based on this modeling, it was estimated that 400 ng/mL of CuNP would generate around a cumulative release of 0.1 M of Cu^{2+} ions over the 21 day culture period.

5.2.2.2 Cell Culture

Hyaluronan oligomer mixtures containing predominantly 4-mers were prepared in the lab using protocols reported in section 3.2.1. Low passage (3-5) adult rat aortic SMCs (RASMCs; Cell Applications, San Diego, CA) were selected for the current study due to their relatively lower levels of tropoelastin production compared to neonatal cells, and thus of greater relevance to regeneration of elastin-rich constructs from adult cells. RASMCs were seeded onto 6-well tissue culture plates at a density of 3×10^4 cells/ well and cultured with DMEM-F12 (Invitrogen) containing 10% v/v fetal bovine serum and 1% v/v penstrep (VWR International). HA oligomers prepared in serum-rich medium were added to cell cultures at an ultimate dose of 0.2 μg/mL. CuNP dispersed in distilled water were supplemented exogenously to the culture wells at final doses of either 1, 10 or 400 ng/mL, except in control cultures which received no supplements. These concentrations were chosen based on the data obtained from section 2.1 procedure. The culture medium was replaced twice weekly, the spent medium from each well pooled over the 21 day culture period and frozen for further biochemical analysis.

5.2.2.3 Biochemical Assays

The DNA content in cell layers was measured at 1 and 21 days of culture to determine the proliferation of SMCs and to normalize the measured amounts of synthesized matrix, according to protocol explained in section 3.2.3. The collagen content within the cell layers and in the pooled supernatant medium fractions was estimated using a hydroxy-proline assay, described in section 3.2.4. The amounts of matrix elastin (alkali-soluble and insoluble fractions) and soluble tropoelastin (in pooled spent medium) were quantified using a Fastin assay (Accurate Scientific Corp), as detailed in section 3.2.5. The measured amounts of synthesized matrix were normalized to their respective DNA amounts to provide a reliable basis of comparison between samples, and to broadly assess if the observed changes in the amount of matrix synthesized could possibly be due to increases in elastin production on a per cell basis.

The desmosine crosslink densities within elastin matrices were quantified for selected cases using ELISA, as described in section 3.2.6. The desmosine amounts/ ng of DNA were compared to the DNA-normalized amounts of insoluble matrix elastin from corresponding cell layers. The LOX enzyme activity within the cell culture layers was determined using a flurometric assay based on generation of H_2O_2 when LOX acts on a synthetic substrate, described in detail in section 3.2.7. Western blot analysis of proteins within the pooled medium fractions at day 21 was performed using methods described in section 3.2.8, to semi-quantitatively confirm observed biochemical trends in tropoelastin synthesis and to assess LOX protein synthesis. All experiments were performed in triplicate and quantitative results reported as mean ± SD. Statistical significance between

and within groups was determined using 2-way ANOVA. Results are deemed significantly different from controls for $p < 0.05$.

5.2.2.4 Immunofluorescence and Matrix Ultrastructure Studies

As explained in detail in section 3.2.11, immunofluorescence techniques were used to confirm the presence of elastin, fibrillin within selected cell layers, and LOX expression for those conditions that appeared to upregulate elastin synthesis.

Scanning electron microscopy was used to discern the structural organization of matrix elastin within cell layers cultured with or without exogenous HA cues and various provided doses of copper ions, as explained in section 5.1.2.4. Transmission electron microscopy (TEM) was used to characterize the ultrastructure of the elastin matrix within test and control cultures using protocols described in section 3.2.12.

5.2.3 Results

5.2.3.1 Copper Ion Release from CuNP

Figure 5.7 shows the release profiles of Cu^{2+} ions for three different CuNP concentrations. While there were no significant differences in the release of Cu^{2+} ions between 1 and 10 ng/mL of CuNP, 100 ng/mL of CuNP generated significantly higher Cu^{2+} ions. It was observed that over the 30-day period, 1 and 10 ng/mL of CuNP resulted in cumulative release of ~ 0.03 M of Cu^{2+} ions, while 100 ng/mL CuNP resulted in cumulative release of ~ 0.05 M of Cu^{2+} ions. As seen from the modeling curves shown in Figure 5.7, the predictions quite closely fit the experimentally measured values ($p = 0.001$

for all the parameters and the overall fit; number of degrees of freedom for each fit = 29). Based on this mathematical analysis, we predict that a CuNP dose of 400 ng/mL will be required to generate Cu^{2+} ion release equivalent to 0.1 M over a 21 day period. The predicted Cu^{2+} ion release profile from 400 ng/mL of CuNP is also shown in Figure 5.7.

5.2.3.2 Cell Proliferation

Proliferation ratios (ratio of cell number at day 21 to day 1) of RASMCs cultured in the presence of either CuNP alone or together with HA oligomers are shown in **Figure 5.8**A. At 3-weeks, proliferation ratios within cell layers cultured with 1, 10 and 400 ng/mL of CuNP were 1.54 ± 0.15, 1.84 ± 0.23 and 1.32 ± 0.16–fold of that in controls, respectively (p = 0.002, 0.001 and 0.031 vs. controls). In cultures that received HA oligomers as well, the ratios were 1.35 ± 0.3, 1.28 ± 0.3, and 0.92 ± 0.2 –fold, respectively versus controls ($p > 0.2$, in all the cases). Moreover, cell proliferation ratios in the presence of CuNP alone were not significantly different from those that received HA oligomers also.

5.2.3.3 Elastin Protein Synthesis

Figure 5.8 shows mean ± SD of elastin protein synthesized (n = 3/ case) in the different test cultures, normalized initially to their respective cellular DNA contents at 21 days, and further normalized to the corresponding protein content in non-additive control cultures. CuNP alone and together with HA oligomers did not enhance tropoelastin synthesis (data not shown), relative to non-additive controls (28284 ± 5088 ng/ng DNA;

$p > 0.2$ in all the cases). Likewise, addition of CuNP alone or together with HA oligomers had no stimulatory effect on the collagen synthesis (soluble and matrix forms), compared to control cultures (826 ± 125 ng/ng DNA; $p > 0.4$ in all the cases).

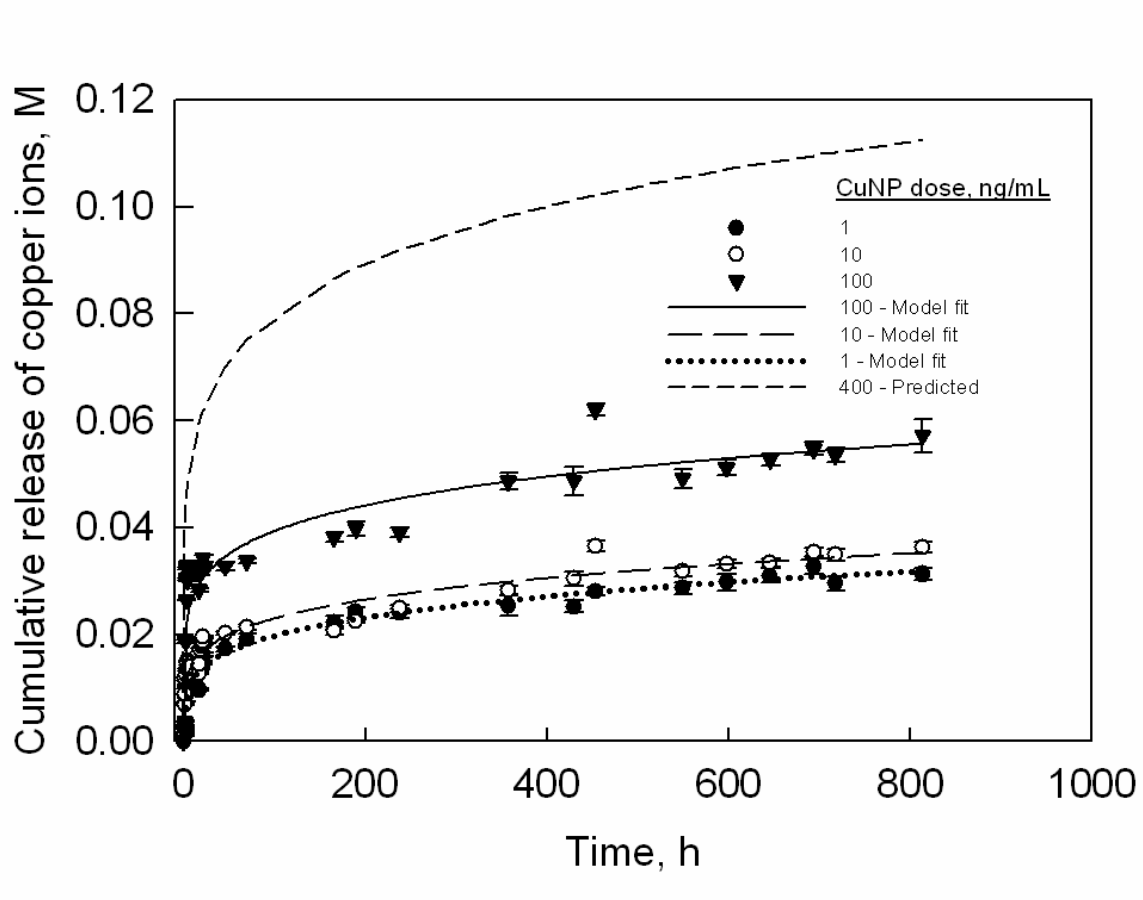

Figure 5.7. Copper ion release profiles from CuNP (1-100 ng/mL) in distilled water. The profiles were fitted with hierarchical regression analysis model described by equation 1. Based on this model, CuNP dosage equivalent to a cumulative release of 0.1 M of copper ions over a 21 day period was determined to be 400 ng/mL.

Elastin incorporated into the matrix was measured as the sum of two individual fractions, *i.e.*, a highly cross-linked, alkali-insoluble elastin pellet, and an alkali-soluble fraction. As shown in **Figure 5.8B**, of all the tested CuNP doses, only addition of 400 ng/mL of CuNP increased synthesis of alkali-soluble elastin by 1.54 ± 0.08-fold; concurrent supplementation of HA oligomers to these cultures furthered this increase to 2.16 ± 0.26-fold, relative to amounts in non-additive controls (6931 ± 1200 ng/ ng DNA; $p < 0.001$ vs. controls, in both the cases). Lower concentrations of CuNP (1 and 10 ng/mL) alone or together with HA oligomers, on the other hand, suppressed alkali-soluble matrix elastin production ($p < 0.01$ in all the cases vs. controls).

While culture with 1 ng/mL supplements of CuNP alone caused a 38 ± 4% decrease in production of alkali-insoluble, crosslinked matrix elastin relative to control cultures (183 ± 29 ng/ng DNA), concurrent delivery of HA oligomers enhanced the same by 2.7 ± 0.18 –fold over control levels ($p < 0.001$ vs. controls; **Figure 5.8C**). When 10 ng/mL and 400 ng/mL of CuNP were supplemented, alone or concurrent with HA oligomers, crosslinked elastin production increased by 1.26 ± 0.6 and 1.24 ± 0.09 -fold respectively ($p = 0.8$ and 0.001 vs. controls) and by 1.99 ± 0.18 and 3.14 ± 0.03 –fold ($p < 0.001$ vs. controls), respectively. The trends in total matrix elastin synthesis by RASMCs reflected those observed in soluble elastin synthesis (**Figure 5.8D**). When 400 ng/mL of CuNP were added, alone or together with HA oligomers, total matrix elastin synthesis increased by 1.6 ± 0.1-fold and 2.28 ± 0.23-fold ($p < 0.001$ vs. controls in both cases), respectively. Lower concentrations of CuNP (1 and 10 ng/mL) alone or together with HA oligomers, suppressed alkali-soluble matrix elastin production ($p < 0.01$ in all

the cases vs. controls). No significant increase in desmosine crosslink density was measured within test cultures compared to non-additive control cultures (0.92±0.05, 0.65±0.21 and 0.64±0.1-fold within 1, 10 and 400 ng/mL of CuNP alone cultures, respectively; 0.91±0.23, 0.9±0.05 and 0.94±0.2-fold within CuNP and HA oligomers supplemented cultures, respectively).

Figure 5.9A shows the elastin matrix yields [yield = matrix elastin/ (tropoelastin + matrix elastin)] calculated from the elastin amounts, presented in Figure 5.8. While only 20.1 ± 3.5 % of total elastin produced in non-additive control cultures was incorporated into the matrix, the elastin matrix yield was 61.3 ± 3.6% in those cultured with 400 ng/mL of CuNP alone and 58.8 ± 6.1% in those that received HA oligomers as well. Cultured that received 1 ng/mL of CuNP and HA oligomers exhibited elastin matrix yields of 35.5 ± 3.4% (Figure 3A). The matrix yield within the remaining test cultures was not significantly greater than that in control cultures.

5.2.3.4 LOX Protein Synthesis and Activity

Spent medium fractions pooled over 21 days from test and control cultures were analyzed by western blot, and the DNA-normalized intensities of the LOX-protein bands within test cultures were further normalized to those in controls (**Figure 5.9B**). Exogenous CuNP (1, 10, 400 ng/mL) either alone or together with HA oligomers (1 and 10 ng/mL only) did not enhance LOX protein synthesis relative to controls. LOX protein synthesis was however enhanced by 1.67 ± 0.13 –fold in the presence of both 400 ng/mL CuNP and HA oligomers ($p < 0.01$ vs. controls).

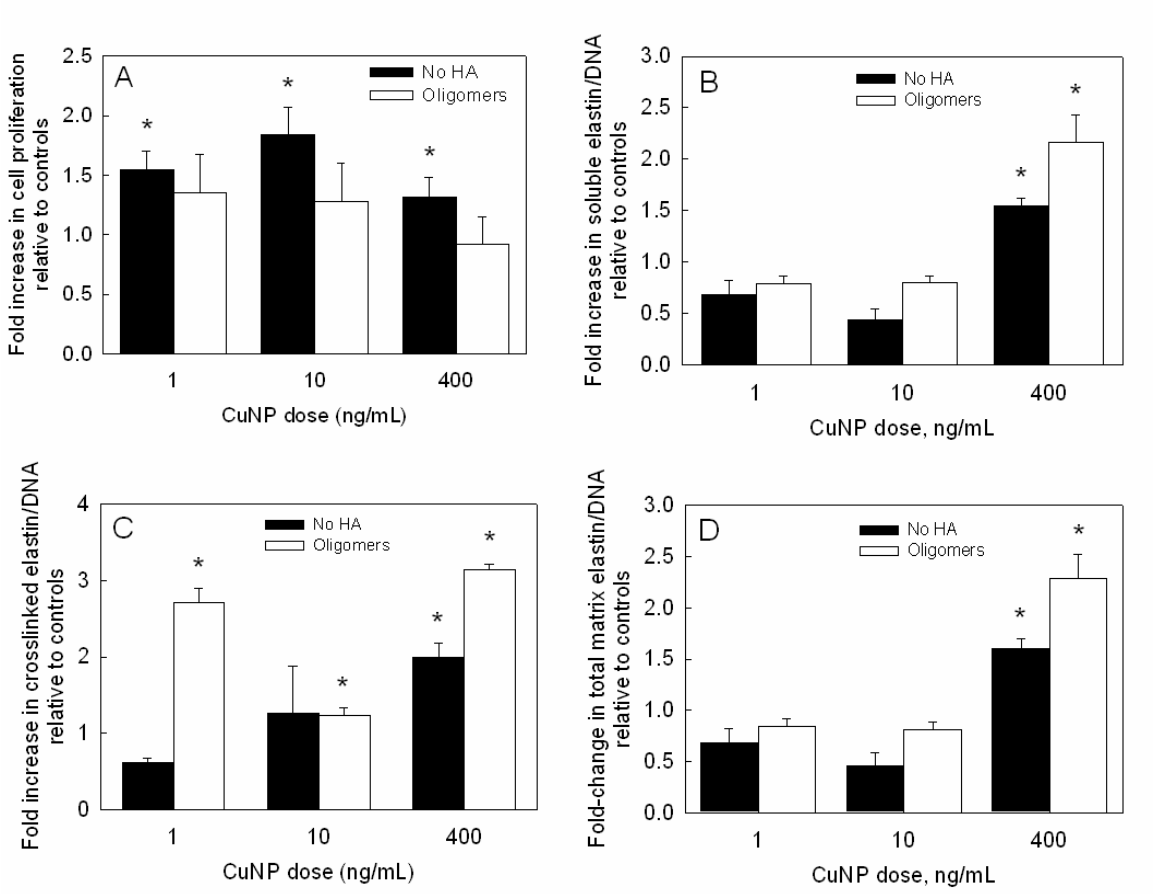

Figure 5.8. (A) Proliferation ratios of RASMCs supplemented with CuNP (1-400 ng/mL) alone or together with HA oligomers (0.2 μg/mL). Data shown represent mean ± SD of cell count after 21 days of culture, normalized to initial seeding density and further normalized to control cultures that received no additives (n = 3/case). Effects of exogenous CuNP with or without HA oligomers on alkali-soluble matrix elastin (B), crosslinked alkali-insoluble matrix elastin (C) and total matrix elastin (D), synthesized by adult RASMCs. Values (mean ± SD) are shown normalized to the DNA content of the respective cell layers at 21 days of culture (n = 3/case) relative to control cultures. * represents significant differences relative to control cultures, deemed for $p < 0.05$.

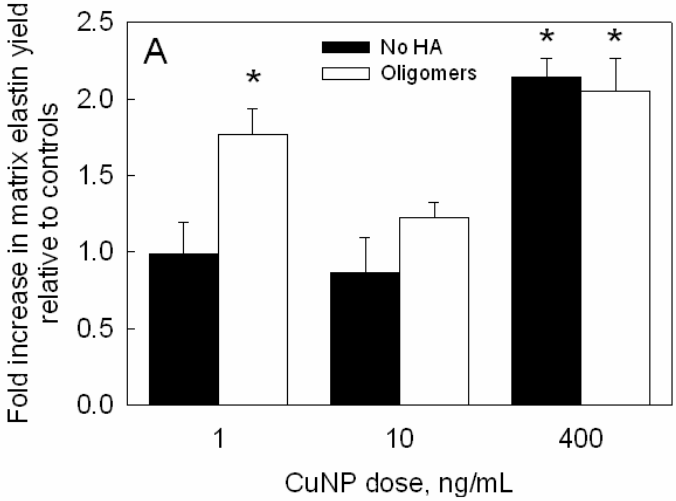
A
No HA
Oligomers
Fold increase in matrix elastin yield relative to controls
2.5
2.0
1.5
1.0
0.5
0.0
1
10
400
CuNP dose, ng/mL

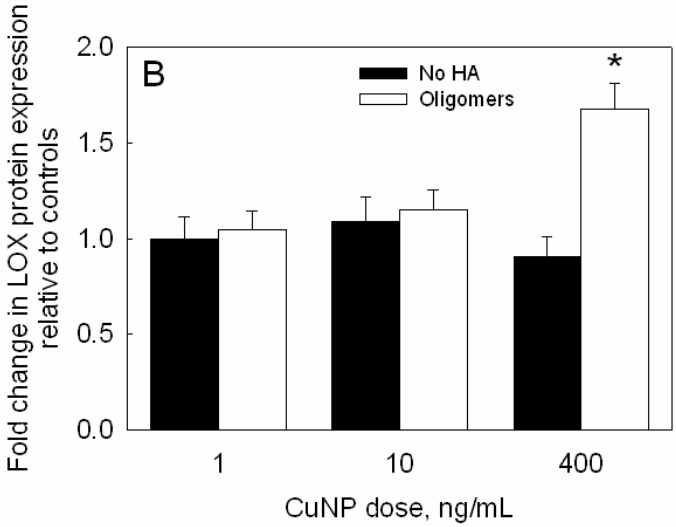
B
No HA
Oligomers
Fold change in LOX protein expression relative to controls
2.0
1.5
1.0
0.5
0.0
1
10
400
CuNP dose, ng/mL

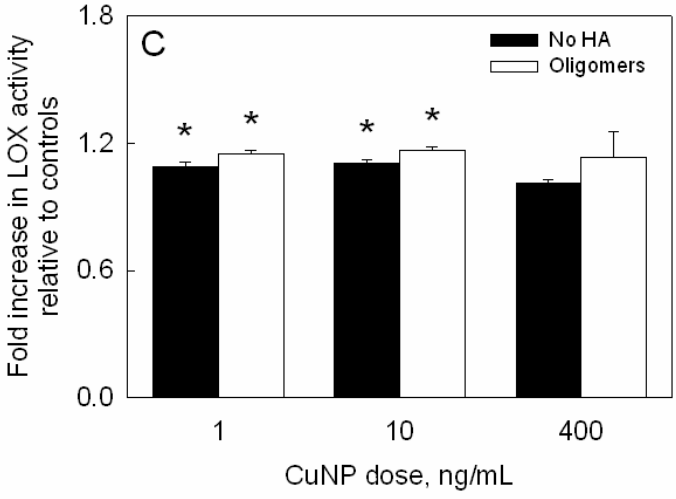
C
No HA
Oligomers
Fold increase in LOX activity relative to controls
1.8
1.2
0.6
0.0
1
10
400
CuNP dose, ng/mL

Figure 5.9. (A) Matrix elastin yield within RASMC cultures supplemented with CuNP and HA oligomers. The ratio of matrix elastin deposited to total elastin synthesized was calculated in each test case and further normalized to similar ratio in control cultures. (B) LOX protein amounts in pooled medium aliquots collected over 21 days of culture. Shown are mean ± SD of DNA-normalized intensities, measured from representative SDS-PAGE/ western blots containing bands corresponding to LOX produced in the respective cases. (C) LOX enzyme activities in cultures treated with CuNP and HA oligomers. Values (mean ± SD) are shown normalized to the LOX activity measured in control cell layers at 21 days of culture (n = 3/case). * represents significance in differences relative to controls, for $p < 0.05$.

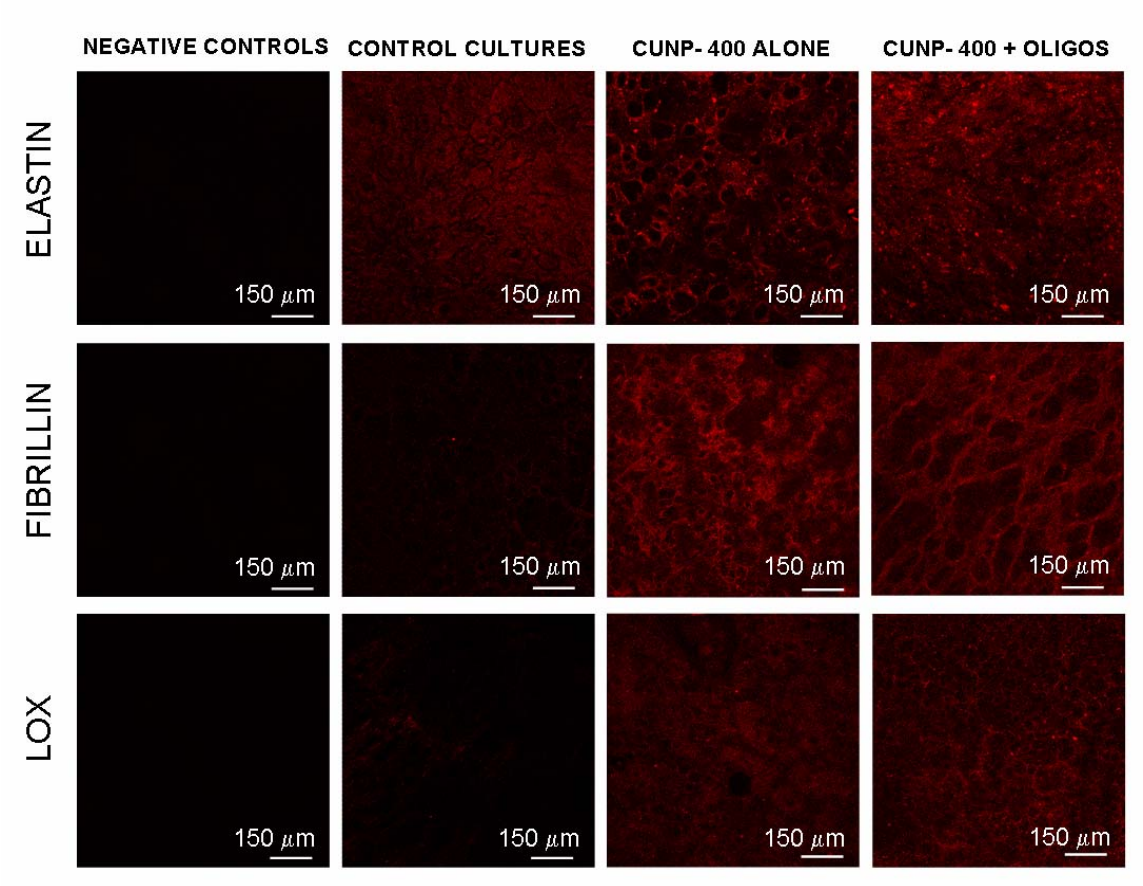

Figure 5.10. Immunodetection of elastin, fibrillin and LOX (red) within RASMC layers following 21 days of culture in the presence of 400 ng/mL of CuNP alone or together with HA oligomers (0.2 μg/mL); control cultures received no-additives. Immunolabeling controls received no primary antibodies and exhibited no background fluorescence when treated with the fluorophore-labeled secondary probe.

Figure 5.9C describes the effect of addition of CuNP alone or together with HA oligomers on LOX enzyme activity. Relative to controls, 1 ng/mL of CuNP alone or together with HA oligomers increased LOX activity by 1.09 ± 0.02 and 1.15 ± 0.02 –fold, respectively ($p < 0.01$ in both the cases); while 10 ng/mL of CuNP alone or together with HA oligomers increased the same by 1.1 ± 0.02 and 1.16 ± 0.01–fold, respectively ($p < 0.01$ in both the cases). However, surprisingly, no significant increases in LOX activity were detected on addition of 400 ng/mL of CuNP alone or together with HA oligomers ($p > 0.8$ in both the cases vs. controls).

5.2.3.5 Immunodetection of Elastin, Fibrillin and LOX

Immunofluorescence micrographs of selected 21-day old cell layers (**Figure 5.10**) confirmed the presence of elastin, fibrillin and LOX (red fluorescence) both in cultures that received 400 ng/mL of CuNP alone or together with HA oligomers. Relative to control cultures, the fluorescence intensity due to elastin were visibly greater in cultures supplemented with CuNP than in control cultures, and even more so within cultures which also received HA oligomers. In the latter cultures, fiber networks were visible,

while in control cultures, the elastin appeared as homogenous and amorphous masses. Fluorescence intensity due to fibrillin was much greater in CuNP-supplemented cultures than in non-additive controls, and is as pronounced in cultures that also received HA oligomers, thus confirming the fibrillin-mediated matrix elastin deposition process within these cultures. Interestingly, while fluorescence due to LOX was sparse in control cultures, abundant LOX staining was observed in CuNP added cultures, and more so in the presence of oligomers. Negative controls unstained for the primary antibody in each case are shown for comparison.

5.2.3.6 Structural Analysis of Matrix Elastin

Figure 5.11 shows representative scanning electron micrographs of isolated elastin matrices from 21-day cultures. Compared to the non-additive control cultures where elastin was sparingly deposited as amorphous clumps (panel A), addition of CuNP alone or together with HA oligomers resulted in enhanced fiber formation. Relative to the presence of nanoparticles alone (1 ng/mL in panel B; 10 ng/mL in panel C) where elongated elastin fibers with diameter ranging from 100-300 nm are clearly visible, concurrent presence of HA oligomers promoted deposition of bundles of aggregating elastin fibrils (1 ng/mL in panel E; 10 ng/mL in panel F). When 400 ng/mL of CuNP was added alone, elastin fiber formation was likewise favored, with a significantly higher density of elastin bundles observed (panel D). Concurrent presence of HA oligomers promoted dense elastin matrix (panel G) containing greater number of apparently fully-formed fibers (~ 300-500 nm diameter; panel H).

Figure 5.12 shows representative transmission electron micrographs of elastin matrices within 21-day cultures. Discrete amorphous clumps with relatively few fibers of elastin protein were observed in control cultures which received no-additives (panel A). The presence of Cu-400 ng stimulated deposition of aggregating elastin fibrils between the cells (panel B), higher in density compared to controls. However, when both Cu-400 ng and HA oligomers were provided to control cultures (panels C-D), mature elastin fiber formation was observed, with the matrix containing numerous fully-formed bundles of fibers (100-300 nm diameter), more than that observed in control and Cu-400 ng alone cultures. Fibrillin (immunogold particle-stained), which appeared in transverse sections as darkly stained nodules, were located at the periphery of aggregating elastin fiber bundles, signifying normal elastic fiber assembly under these conditions.

5.2.4 Discussion

An outstanding problem in the field of vascular tissue engineering is the insufficiency of conventional tissue engineering methods and materials to manufacture structurally- and functionally-faithful vascular elastic matrices on demand. This is because cardiovascular tissues are far more complex in their architecture and structural organization, and capacity of adult vascular cells for self-repair is less effective than what tissue-engineering principles demand. Though fully-developed mature elastic fibers are insoluble and inert to local changes in pH and chemical environment, various proteolytic enzymes secreted by SMCs, such as matrix metalloproteinases (MMPs-2, 9, 12) and elastases can degrade elastin fibers and its components[352-354]. Literature suggests that

these degradation products can modulate vascular remodeling via their interaction with SMCs[355], leading to structural and mechanical abnormalities in large arteries[356]. Thus, proper assembly and functioning of elastic fibers is critical for maintaining homeostasis in organs and tissues.

As mentioned above, elastic fibers are complex macromolecular structures which contain amorphous elastin and other non-elastin protein components (e.g., fibrillin, elaunin). They are difficult to repair because their deposition pattern requires the coordinated expression of all of the microfibrillar molecules as well as the cross-linking enzymes critical for elastin, so that the correct temporal sequence is followed[329]. The cell-secreted soluble elastin protein precursors, i.e., tropoelastin monomers[357], are recruited by coacervation onto pre-formed templates of fibrillin-rich microfibrils[330], and stabilized by LOX-catalyzed desmosine crosslinking[331]. Microfibrils, which appear first in the elastic fiber development and associates itself close to the cell surface, facilitates tropoelastin cross-linking to form the functional polymer[358]. Hence, approaches for elastin regeneration must be able to mimic the spatio-temporal sequence of these events leading to elastin matrix assembly. However, elastin-producing cells in adult tissues often synthesize elastin that does not polymerize or organize into a functional three-dimensional fiber, leading to organ or tissue failure in the long-term.

Current tissue engineering approaches to regenerate elastin-rich vascular constructs are limited by progressive destabilization of tropoelastin mRNA expression in adult vascular cells[24, 300] and the unavailability of cellular cues necessary to up-regulate elastin synthesis, maturation and organization[359]. Our recent studies strongly attest to the

utility of HA-based biomaterials and biomolecular cues for cellular-mediated elastin matrix regeneration[58, 60, 313, 348]. A key deduction from these studies is that though HA oligomers (< 1 kDa) are more biologically active than long-chain HA (> 1 MDa), and dramatically increase elastin synthesis and deposition, the elastin matrix crosslinking efficiency was not significantly upregulated[58, 60]. This suggests that an important aspect of tissue-engineering elastin rich vascular constructs is the ability to regulate the amount, quality, ultrastructure and hierarchical organization of the synthesized elastin precursors, so as to maximize their crosslinking efficiency and matrix formation.

Dahl et al. demonstrated the benefits of increasing medium copper ion concentration to elastin matrix crosslinking efficiency in an engineered vascular-like tissue[339]. Likewise, in our own prior studies[351], we investigated the effects of soluble copper salts, delivering steady state doses of 0.01 and 0.1 M of Cu^{2+} ions to elastin matrix deposition, assembly (i.e., fiber formation) and maturation (i.e., crosslinking) in RASMC cultures. Our results suggested that 0.1 M of $CuSO_4$ (but not 0.01 M) and HA oligomers (or HMW HA) significantly improved elastin matrix synthesis, crosslinking and fiber formation by adult rat vascular SMCs. However, cytotoxicity associated with long-term exposure of vascular cells to these effective doses of Cu^{2+} ions[350], delivered at steady-state levels from soluble copper salts, showed that more controlled modes of Cu^{2+} ion delivery, such as from copper nanoparticles (CuNP), may be important to deter the same. Thus, in this study, we have sought to deliver the equivalent of a 0.1 M dose of Cu^{2+} via controlled release from CuNP and investigate the impact of such delivery with or without HA oligomers on elastin matrix synthesis, assembly, and maturation.

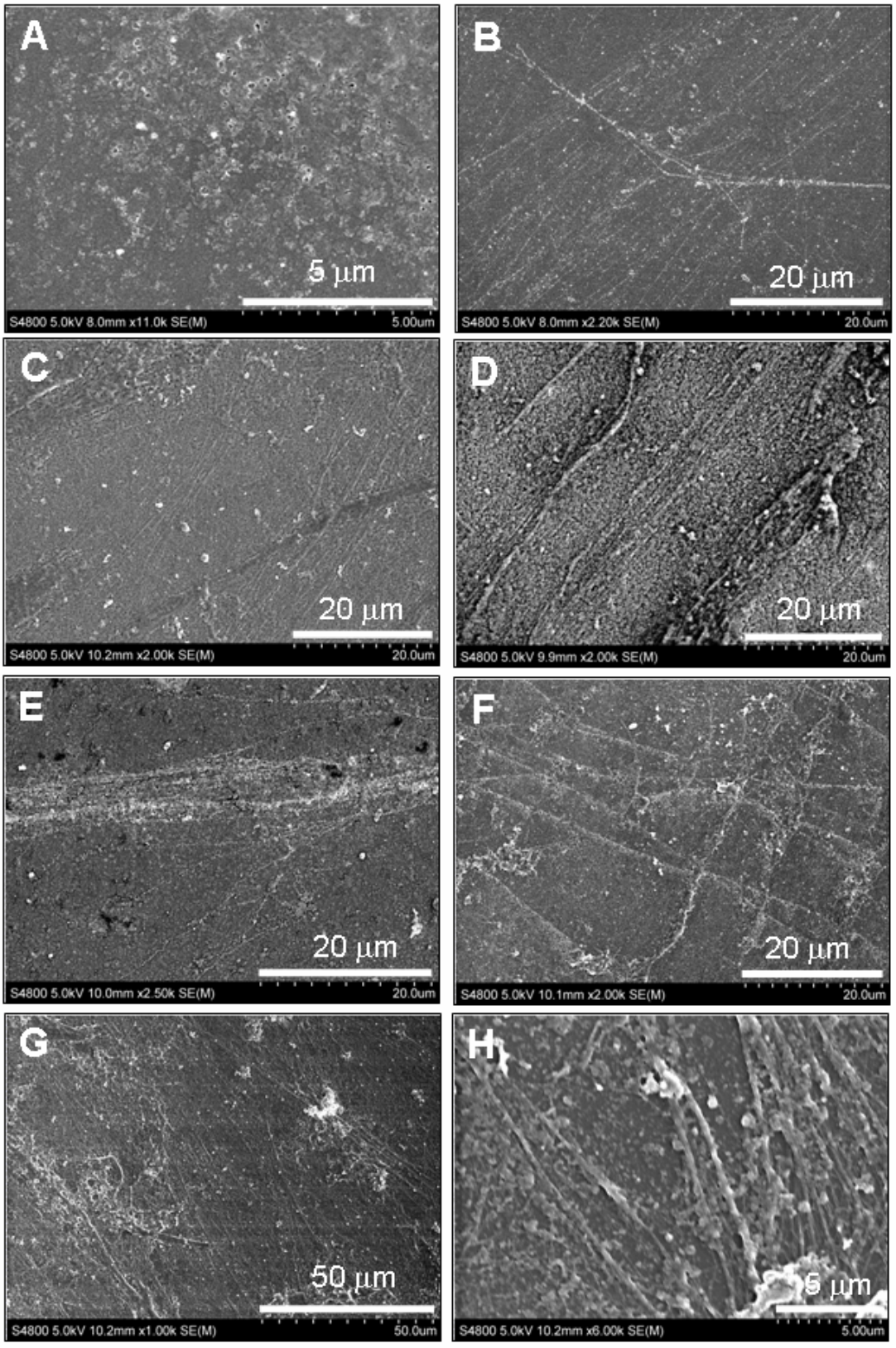
A
5 μm
S4800 5.0kV 8.0mm x11.0k SE(M)
5.00um
B
20 μm
S4800 5.0kV 8.0mm x2.20k SE(M)
20.0um
C
20 μm
S4800 5.0kV 10.2mm x2.00k SE(M)
20.0um
D
20 μm
S4800 5.0kV 9.9mm x2.00k SE(M)
20.0um
E
20 μm
S4800 5.0kV 10.0mm x2.50k SE(M)
20.0um
F
20 μm
S4800 5.0kV 10.1mm x2.00k SE(M)
20.0um
G
50 μm
S4800 5.0kV 10.2mm x1.00k SE(M)
50.0um
H
5 μm
S4800 5.0kV 10.2mm x6.00k SE(M)
5.00um

Figure 5.11. Representative SEM images of 21-day old RASMC cell layers for non-additive controls (panel A); cultured with CuNP alone (1 ng/mL : panel B; 10 ng/mL : panel C; 400 ng/mL : panel D); cultured with CuNP and HA oligomers (1 ng/mL : panel E; 10 ng/mL : panel F; 400 ng/mL : panel G, H). Compared to CuNP supplemented cultures, additional presence of oligomers enhanced formation of dense crosslinked matrix elastin fibers with diameters ranging between 0.2-0.5 μm.

Detectable amount of Cu^{2+} ions (~ 0.0012 M) were released even from 1 ng/mL of CuNP within the first 5 h, which shows that exogenous nanoparticles are effective vehicles for even short-term Cu^{2+} ion delivery. From the release profiles, it can be observed that irrespective of CuNP dose, Cu^{2+} ion release peaked within the first 30 h, after which sustained release of ions was maintained. Thus, in effect, Cu^{2+} release over the 21 day culture period can be deemed steady state. The concentration of released Cu^{2+} ions depended strongly on dose of CuNP, dissolution time, and also their interdependence, which is aptly described by eq.1, our model fit to experimental release profiles. Using this model, we predicted that addition of 400 ng/mL of CuNP to cell cultures would result in a cumulative release of ~ 0.1 M of Cu^{2+} ions over 21 days.

A significant observation was that 400 ng/mL of CuNP had no cytotoxic effects of SMCs, and thus no apparent change in morphology over the 21 day culture period. In contrast, our prior studies[351] showed that an equivalent dose of Cu^{2+}, released from soluble copper sulfate salt, induced mild cytotoxicity that was apparent within a day of addition, and caused visible initial cell rounding and some cell death. Previously, we

showed that in the presence and absence of HA oligomers, supplementation of 0.01 M of Cu^{2+} ions increased cell proliferation (1.5-2-fold relative to controls), while 0.1 M of Cu^{2+} ions suppressed the same (80% of controls)[351]. In this study, in the cases where CuNP delivered was less than 0.1 M of Cu^{2+} ions (i.e., 1 and 10 ng/mL of CuNP doses), a likewise 1.5-2-fold increase in cell proliferation over control cultures was observed. However, when ~ 0.1 M of Cu^{2+} ions was released by 400 ng/mL of CuNP, active promotion rather than suppression of cell proliferation was noted. Thus, our experiments show controlled release of Cu^{2+} ions from CuNP deters rapid increase in Cu^{2+} concentration in the initial period after cell seeding, and thus may not have long-term toxic effects. In accordance with our earlier observation that 0.2 μg/mL of HA oligomers inhibit SMC proliferation[360], in this study also, supplementation of HA oligomers to cultures together with CuNP, suppressed cell proliferation down to levels measured in control cultures. Thus, from a tissue engineering perspective, CuNP and HA oligomers do not promote cell proliferation, but simultaneously do not induce cell death to in turn adversely impact matrix synthesis and accumulation within the constructs.

In this study, exogenous CuNP had no effect on total elastin production, both in the presence and absence of HA oligomers. In general, lower doses of CuNP (1-10 ng/mL), delivering less than 0.1 M of Cu^{2+}, alone or together with HA oligomers, expectably offered no benefit to matrix elastin synthesis, except for a 2.7-fold increase in crosslinked elastin synthesis in the presence of 1 ng/mL of CuNP and HA oligomers. The lack of any benefits to elastin synthesis mimicked our prior observations when 0.01 M of $CuSO_4$ was supplemented to RASMC cultures[351]. However, production of matrix

elastin (both soluble and crosslinked forms) increased multi-fold with the addition of 400 ng/mL of CuNP, both alone and together with HA oligomers, suggesting the effectiveness of these cues in the recruitment and crosslinking of tropoelastin precursors into matrix structures. Since total cellular elastin production was unaffected by these cues, the net result of doubling in matrix deposition is a much higher matrix yield (400 ng/mL CuNP alone: 61.3 ± 3.6%; 400 ng/mL CuNP and HA oligomers: 58.8 ± 6.1%; control cultures: 20.1 ± 3.5%).

LOX protein synthesis was unchanged in cultures supplemented with CuNP only and those that received both CuNP (1 and 10 ng/mL) and HA oligomers. On the other hand, when 400 ng/mL of CuNP was added to cultures together with HA oligomers, a significant increase in LOX protein synthesis was observed. Collectively, these results suggest that (a) CuNP doses (1 and 10 ng/mL) that generate less than 0.1 M of Cu^{2+} ions do not induce LOX protein synthesis, (b) 0.1 M dose of Cu^{2+} ions generated by 400 ng/mL of CuNP may likely be able to stimulate LOX protein synthesis by cells, provided Cu^{2+} release occurs in close proximity to the cell layers where the ions can interact with cells and influence their behavior, and (c) HA oligomers which likely interact and bind to cell surface receptors (e.g., CD44, TLR-4) also likely immobilize Cu^{2+} ions via opposite charge interactions. Thus, when both CuNP and HA oligomers are present, it may certainly be possible that Cu^{2+} ions localize close to the cell layer where they may intimately influence cell behavior, including their induction of LOX production. Our results also show that LOX enzyme activity was enhanced at all provided doses of CuNP, though LOX activity did not increase as a function of CuNP dose. In all cases, addition

of HA oligomers induced a small but significant increase in LOX activity. Since we showed in an earlier publication that HA oligomers have no impact on LOX activity, the observed increases here may be solely due to opposite charge interactions of CuNP with HA oligomers and their resultant localization at the cell layer to more potently enhance activity of endogenous LOX enzyme.

Structural analysis (electron microscopy) of matrix elastin qualitatively supported the biochemical measurements within CuNP-stimulated cultures. While the control cultures contained only amorphous elastin deposits, aggregating elastin fibers were seen within cultures treated with CuNP (all doses) alone and together with HA oligomers, with multiple bundles of fully-formed elastin fibers with diameter ranging between 200-500 nm. Immunofluorescence images confirmed the amorphous and fibrillar nature of elastin matrix within control and test cell layers. Fluorescence (red) due to LOX expression was also much more intense in cell layers that received CuNP (400 ng/mL) alone or together with HA oligomers than in control cell layers. This confirms the outcomes of our biochemical measurements of LOX protein synthesis. The matrices also showed presence of fibrillin-1 microfibrils, which confirmed normal mechanisms of elastin fiber assembly. Literature indicates that the fibrillin microfibrils guide the alignment of tropoelastin molecules for crosslinking and fiber fomation[347]. This initial alignment is stabilized by copper ion-dependent LOX, which oxidizes the lysine residues of the aligned elastin molecules and enables crosslinking. Thus, these stabilized and aligned elastin structures act as nucleation sites for further coacervation and crosslinking of more tropoelastin resulting in organized elastic fiber growth. The presence of highly anionic

HA oligomers might also promote elastic fiber formation by electrostatically binding to the unoxidized lysine residues of newly synthesized tropoelastin during their association with microfibrils, thus preventing their random self-aggregation far away from the site of fiber formation[52]. However, these are only possibilities which remain to be investigated in future studies.

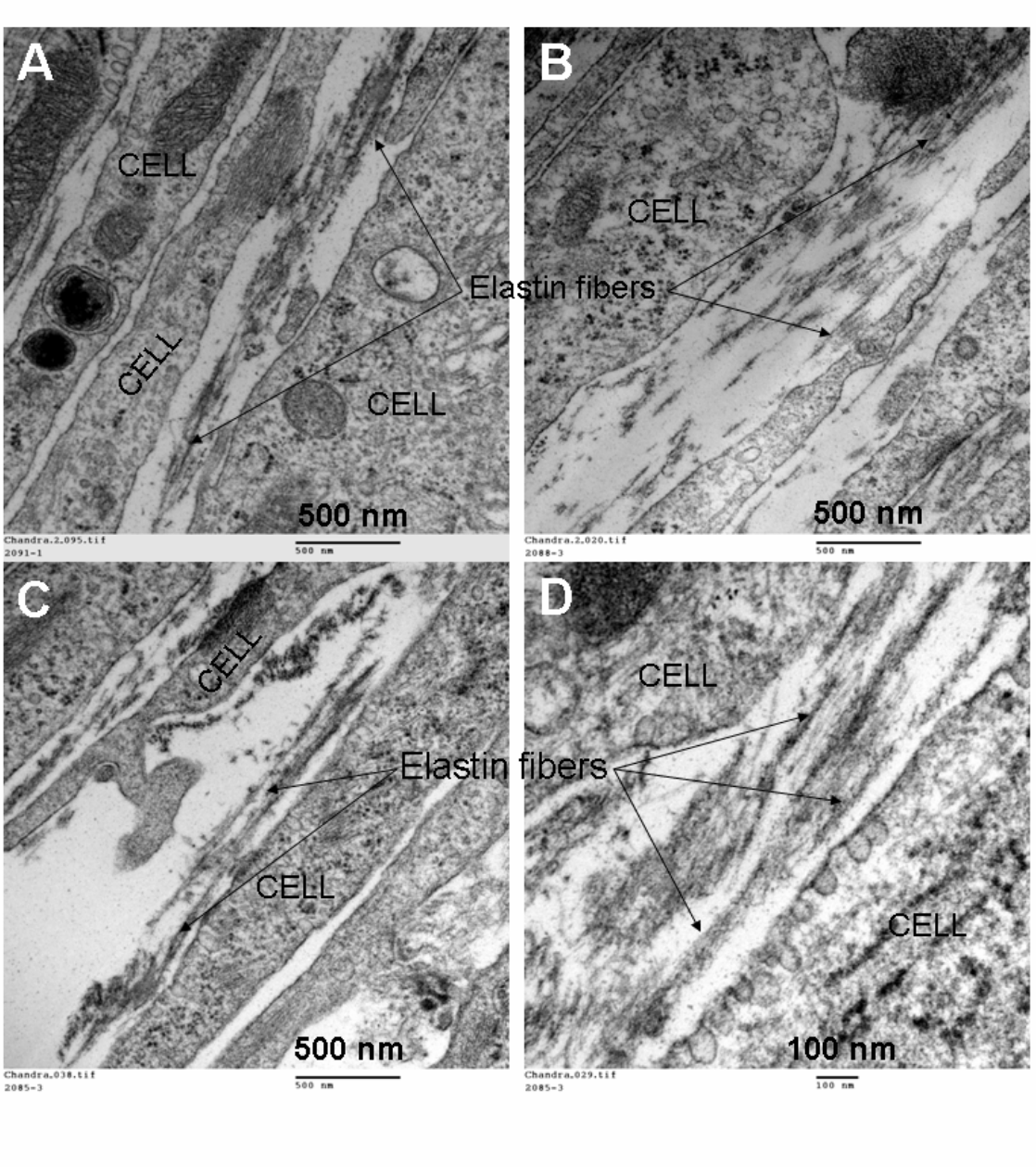

Figure 5.12. Representative TEM images of 21-day old RASMC cell layers cultured additive-free (panel A), with CuNP alone (400 ng/mL; panel B) or together with HA oligomers (panels C-D). Aggregating amorphous elastin clumps leading to the formation of elastin fibers can be clearly seen in these images (panel C), which confirm the identity of elastin observed at higher magnifications (100000 X; panel D).

5.2.5 Conclusions of this study

1. The utility of copper nanoparticles as an effective medium for copper ion delivery to *in vitro* cultures has been demonstrated.
2. Though the exogenous supplementation of CuNP did not upregulate tropoelastin production by RASMCs, they were highly effective in promoting crosslinked elastin matrix formation. Additional presence of HA oligomers within these CuNP-stimulated cultures furthered the crosslinked matrix elastin deposition process.
3. Structural analysis of the isolated matrix elastin revealed that within RASMC cultures treated with CuNP (1-10 ng/mL) alone or together with HA oligomers, an increase in the density of aggregating elastin fibers was evident, relative to amorphous elastin clumps observed within non-additive cultures.
4. The addition of 400 ng/mL of CuNP concurrent with HA oligomers resulted in the formation of multiple bundles of highly-crosslinked elastin fibers, with diameters ranging between 200-500 nm.

5. Immunofluorescence imaging and ultrastructural analysis of the elastin matrices within Cu-400 ng cultures suggested the fibrillin-mediated normal elastin deposition process with significant presence of LOX within these cultures.
6. Overall, the results attest to the elastogenic utility of copper nanoparticles and HA oligomers to highly crosslinked fibrillar elastin matrix generation within smooth muscle cell cultures, with potential applications in vascular tissue engineering.

5.3 Benefits of Bovine LOX to Elastin Synthesis

5.3.1 Introduction

In the previous sections 5.1 and 5.2, we have described the utility of exogenous delivery of copper ions (with or without HA fragments) via copper salts or copper nanoparticles, to elastogenesis by RASMCs in an *in vitro* culture model. The hypothesis for these studies was that the copper ions released from the copper sulfate/ CuNP will promote LOX protein synthesis and activity within these cultures, thereby influencing the crosslinking efficiency and matrix formation of elastin. Indeed, the results observed in both these cases (detailed and explained in sections 5.1 and 5.2) support our hypothesis, and attest to the utility of these cues to enhance matrix crosslinking efficiency and elastin fiber formation. This makes one wonder whether the observed elastogenic benefits of copper ion delivery via indirect increases in endogenous LOX production and activity, could also be achieved by direct delivery of purified LOX protein to the RASMC cultures. Thus, in this study, we explored the elastogenic benefits of delivering purified bovine LOX protein exogenously to RASMC cultures.

5.3.2 Materials and Methods

5.3.2.1 Purification of lysyl oxidase (LOX)

LOX was purified from bovine aorta according to the published methods by Kagan et al[308, 361]. Briefly, bovine aortae from 2-6 week old calves were cleaned, coarsely ground and extracted twice with buffer (0.4 M NaCl, 16 mM potassium phosphate, pH 7.8, 4^{o}C). The extracted pellets in 4 M urea (with 16 mM potassium

phosphate, pH 7.8) were mixed with hydroxyapatite, stirred for 10 min at 4°C, allowed to settle for 30 min, and decanted. The supernatant is centrifuged at 10,000*g* for 10 min, concentrated, and dialyzed against buffer containing 16 mM potassium phosphate, pH 7.8. The crude enzyme precipitated by adding equal volume of 1 M potassium phosphate, pH 7.8, is resolved by chromatography through a column eluting with 16 mM potassium phosphate, 6 M urea, pH 7.8. The enzymatically active fractions from the chromatography column were pooled and the urea concentration was adjusted from 6 to 2 M by dilution with 16 mM potassium phosphate, pH 7.8. The column was washed with buffer until optical density of the effluent < 0.002, and further washed with 16 mM potassium phosphate, pH 7.8, followed by 0.4 M NaCl, 16 mM potassium phosphate, pH 7.8. LOX was then eluted using a gradient of urea concentration (from 0 urea, 0.4 M NaCl, 16mM potassium phosphate, pH 7.8, to 6 M urea 0.4 M NaCl, 16 mM potassium phosphate, pH 7.8) at a flow rate of 1 ml/min. The enzymatically active fractions were pooled, concentrated, dialyzed against 16 mM potassium phosphate, pH 7.8, buffer and stored in aliquots at 280°C. SDS–PAGE revealed the presence of a 32-kDa (90%) and a low-molecular-weight (24-kDa) band (10%) in the purified sample. The yield of enzyme was 0.4 mg from 350 g of bovine aorta. These purified lysyl oxidase preparations have a specific activity of 0.5 nmol of H_2O_2 produced per mg LOX per minute at 37°C.

5.3.2.2 Cell Culture

Purified bovine aorta LOX was received from Dr. Herbert Kagan at Boston University. The enzyme which was sent in a 4 M urea, 16 mM potassium phosphate, pH

7.8, buffer was dialyzed with water overnight, lyophilized and reconstituted in 1 mL of distilled water. Two test doses were evaluated: 50 μL per well (LOX-1), or 100 μL per well (LOX-2).

Low passage (3-5) adult RASMCs were seeded onto 6-well tissue culture plates at a density of 4×10^4 cells/ well and treated with DMEM (Invitrogen) containing 10% v/v FBS and 1% v/v penstrep (VWR International). Each well contained 5 mL of medium. Bovine LOX reconstituted in distilled water was supplemented exogenously to the culture wells at final doses of either 50 μL/well (LOX-1) or 100 μL/well (LOX-2), except in control cultures which received no LOX. These concentrations were randomly chosen based on previous studies by Kagan et al. A 1-mL of culture medium was added weekly to the existing medium so as to not disturb the one-time delivery of LOX protein, and the final spent medium from each well pooled after the 21 day culture period and frozen for further biochemical analysis.

5.3.2.3 Biochemical Assays

The DNA content in cell layers was measured at 1 and 21 days of culture to determine the proliferation of SMCs and to normalize the measured amounts of synthesized matrix, according to protocol explained in section 3.2.3.

The collagen content within the cell layers and in the pooled supernatant medium fractions was estimated using a hydroxy-proline assay, described in section 3.2.4. The amounts of matrix elastin (alkali-soluble and insoluble fractions) and soluble tropoelastin (in pooled spent medium) were quantified using a Fastin assay (Accurate Scientific Corp),

as detailed in section 3.2.5. The measured amounts of synthesized matrix were normalized to their respective DNA amounts to provide a reliable basis of comparison between samples, and to broadly assess if the observed changes in the amount of matrix synthesized could possibly be due to increases in elastin production on a per cell basis.

The desmosine crosslink densities within elastin matrices were quantified for selected cases using ELISA, as described in section 3.2.6. The desmosine amounts/ ng of DNA were compared to the DNA-normalized amounts of insoluble matrix elastin from corresponding cell layers. The LOX enzyme activity within the cell culture layers was determined using a fluorometric assay based on generation of H_2O_2 when LOX acts on a synthetic substrate, described in detail in section 3.2.7. Western blot analysis of proteins within the pooled medium fractions at day 21 was performed using methods described in section 3.2.8, to semi-quantitatively confirm observed biochemical trends in tropoelastin synthesis and to assess LOX protein synthesis.

To evaluate whether the LOX supplementation might be activating RASMCs to release any inflammatory markers such as MMPs, we performed gel zymography to quantify MMPs-2 and 9 in these cultures, as per protocols described in section 6.2.5.

All experiments were performed in triplicate and quantitative results reported as mean ± SD. Statistical significance between and within groups was determined using 2-way ANOVA. Results are deemed significantly different from controls for $p < 0.05$.

5.3.3 Results and Discussion

5.3.3.1 Cell Proliferation

Figure 5.13A shows the cell proliferation ratios of RASMCs cultured with bovine LOX; cell proliferation in non-additive control cultures are also shown for comparison. It was observed that RASMCs in control cultures proliferated 11.7 ± 2.35 –fold over the 21 day period compared to their initial seeding density of 40,000 cells/well. However, LOX exogenous supplementation promoted cell proliferation at both the doses studied by 1.45 ± 0.34 and 1.23 ± 0.23 –fold, respectively, relative to controls (p = 0.031 and 0.8, respectively).

5.3.3.2 Matrix Protein Synthesis

Addition of bovine LOX suppressed collagen protein synthesis in RASMC cultures, relative to controls (2226 ± 144 ng/ng of DNA). The collagen synthesis was suppressed by 62 ± 9% in both the cases, relative to controls ($p < 0.001$ vs. controls).

Similarly, the tropoelastin synthesis was also suppressed in the LOX-supplemented cases, relative to controls (**Figure 5.13C**). While 14990 ± 1618 ng/ng of DNA of tropoelastin protein was synthesized in control cultures, the addition of LOX-1 suppressed the same to 6441 ± 1834 ng/ng DNA ($p < 0.001$) and the addition of LOX-2 suppressed the same to 13235 ± 225 ng/ng DNA (p = 0.11 vs. controls). These results suggest that exogenous LOX protein do not interfere with the endogenous tropoelastin or collagen protein synthesis process.

Elastin incorporated into the matrix was measured as the sum of two individual fractions, *i.e.*, a highly cross-linked, alkali-insoluble elastin pellet, and an alkali-soluble fraction. As shown in **Figure 5.13D**, addition of LOX-1 increased soluble elastin synthesis by 1.37 ± 0.2 -fold, while LOX-2 addition furthered this increase by 1.7 ± 0.02 –fold, relative to non-additive controls (5268 ± 719 ng/ ng DNA; $p < 0.01$, in both the cases). Similarly, as shown in **Figure 5.14A**, the addition of LOX-1 promoted crosslinked alkali-insoluble matrix elastin production by 1.71 ± 0.04-fold ($p < 0.001$ vs. controls), while LOX-2 promoted the same by 2.46 ± 0.08 –fold, compared to that within control cultures (758 ± 106 ng/ng DNA).

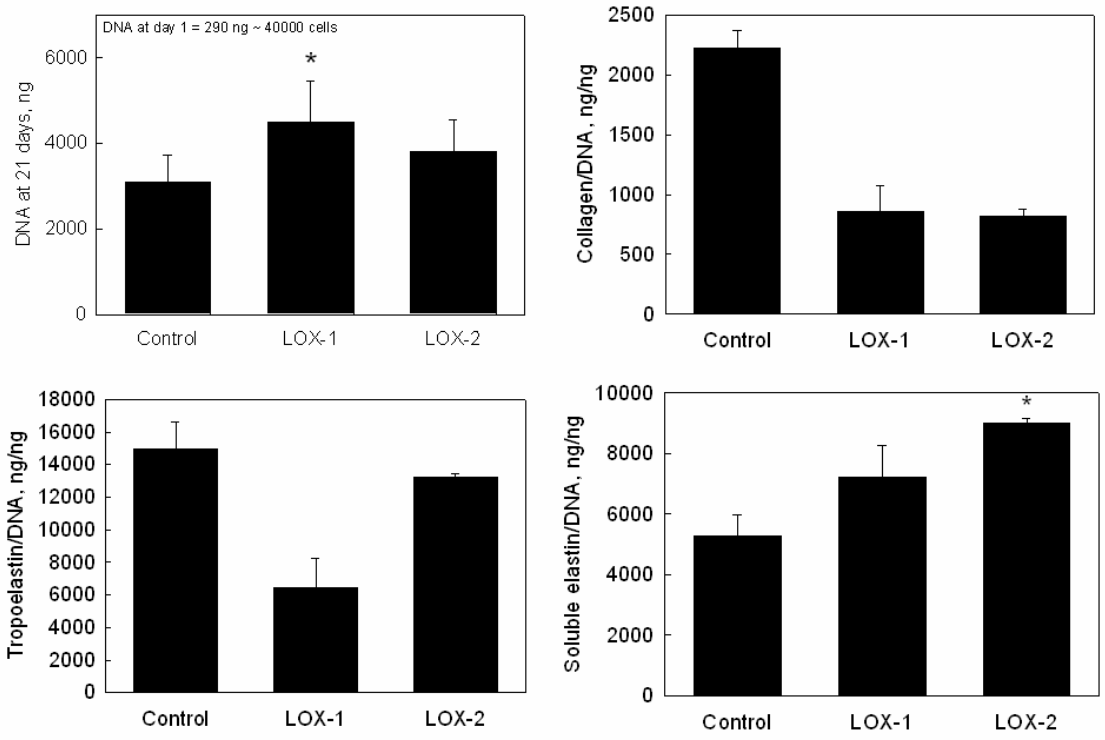

Figure 5.13. (A) Proliferation ratios of RASMCs supplemented with LOX (50-100 μL/mL). Data shown represent mean ± SD of DNA count after 21 days of culture (n = 3/case). Effects of exogenous LOX on collagen (B), tropoelastin (C) and alkali-soluble matrix elastin (D), synthesized by adult RASMCs. Values (mean ± SD) are shown normalized to the DNA content of the respective cell layers at 21 days of culture (n = 3/case). * represents significant differences relative to control cultures, deemed for $p < 0.05$.

As shown in **Figure 5.14B,** the trends in total matrix elastin synthesis were similar to that observed for insoluble matrix elastin synthesis within these cultures. Addition of LOX-1 and LOX-2 increased the total matrix elastin synthesis by 1.4 ± 0.17 –fold and 1.8 ± 0.03 –fold, respectively, relative to controls (6027 ± 826 ng/ng DNA). The elastin matrix yields [matrix yield = matrix elastin/ (tropoelastin + matrix elastin)] calculated from the elastin synthesis data is presented in **Figure 5.14C**. The matrix yield within test cases was normalized to that observed in non-additive controls. While only 28.6 ± 3.9% of total elastin produced in non-additive control cultures was deposited as a matrix, the elastin matrix yield increased to 57 ± 7.1% by addition of LOX-1, and to 45.1 ± 1 % with addition of LOX-2. Thus, the matrix yield within the test cases was significantly higher compared to that in non-additive controls. However, the desmosine amounts (ng/ng of insoluble matrix elastin) in LOX-additive cultures were not significantly higher than those in control cultures (**Figure 5.14D**). These results suggest

that though LOX addition may not increase basal levels of RASMC tropoelastin synthesis, it definitely enhances matrix elastin formation and crosslinking.

5.3.3.3 LOX Protein Synthesis and Activity

Figure 5.15A describes the effect of addition of exogenous bovine LOX protein on LOX enzyme activity within the RASMC cultures. LOX activity was measured in the spent culture medium following 21 days of culture. Interestingly, addition of LOX-1 and LOX-2 had significant effect on basal LOX functional activity. Relative to controls, they increased LOX activity by 1.14 ± 0.06 and 1.132 ± 0.017 –fold, respectively ($p < 0.01$ in both the cases).

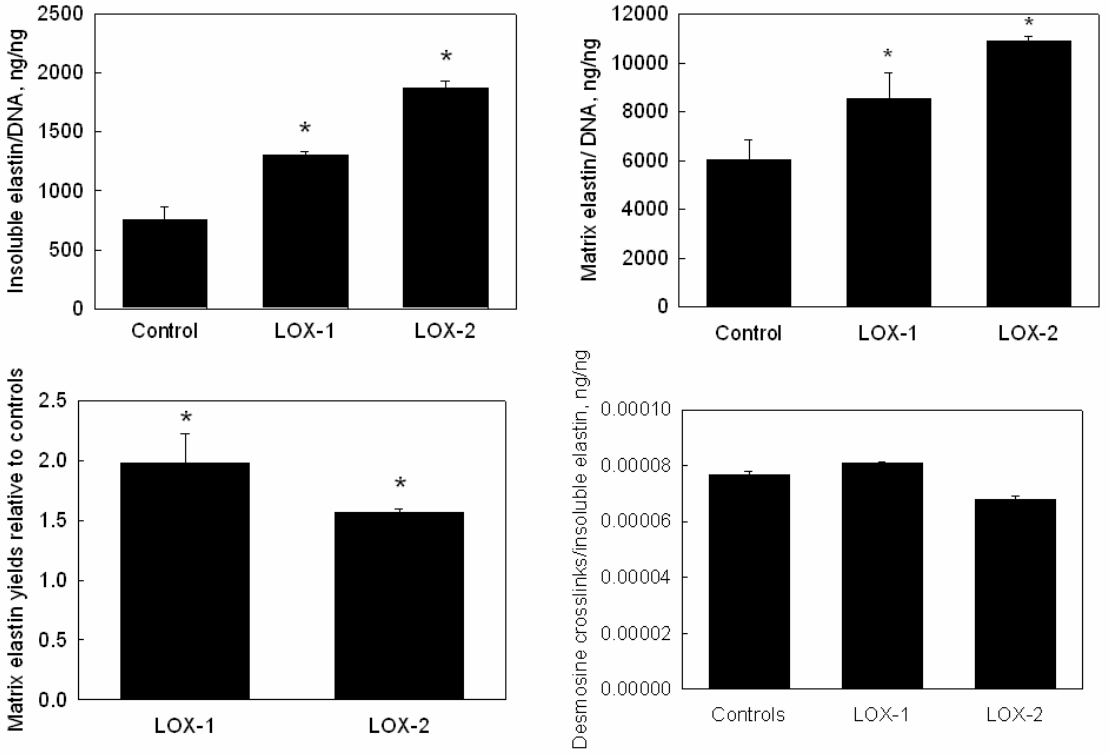

Figure 5.14. (A) Crosslinked insoluble matrix elastin synthesized by RASMCs over the 21 day period. Values are shown as mean ± SD of n=3/case normalized to the DNA content in the cultures. (B) Total matrix elastin (sum of alkali-soluble and insoluble matrix elastin fractions) within the LOX supplemented cultures. (C) Matrix elastin yield within RASMC cultures supplemented with LOX. The ratio of matrix elastin deposited to total elastin synthesized was calculated in each test case and further normalized to similar ratio in control cultures. (D) Desmosine amounts were assayed and normalized to the insoluble matrix elastin protein observed within the respective cultures (n=3/case).

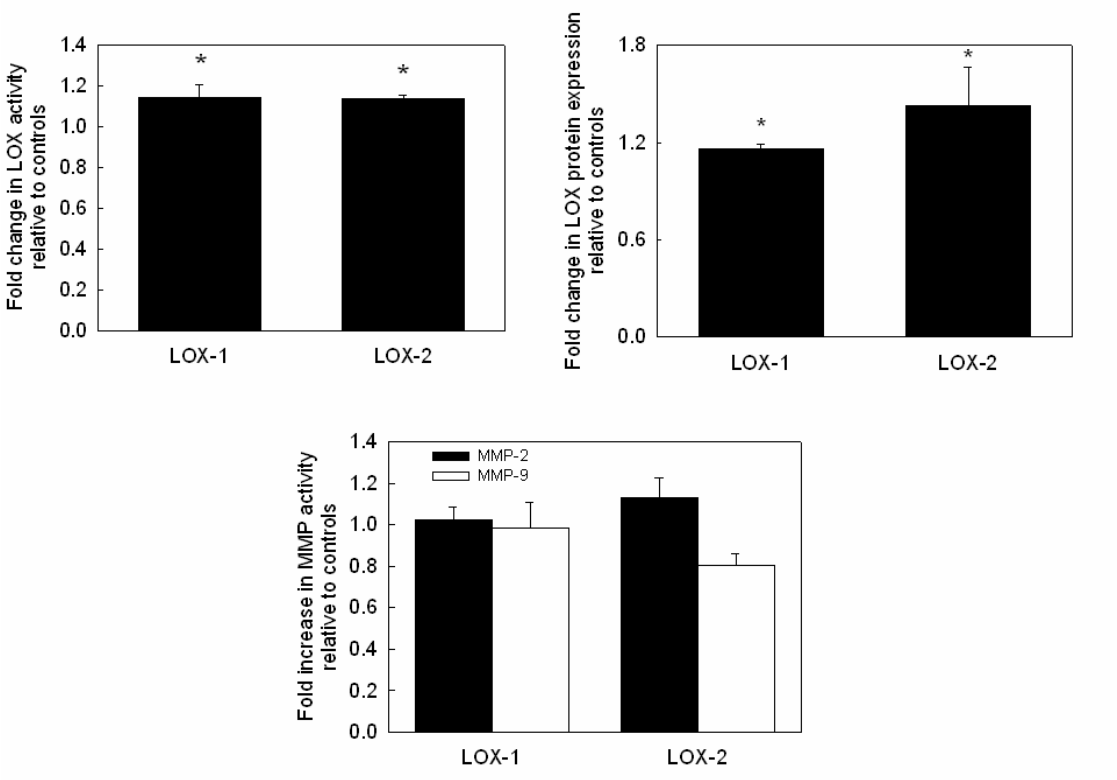

Figure 5.15. (A) LOX enzyme activities in cultures treated with bovine LOX. Values (mean ± SD) are shown normalized to the LOX activity measured in control cell layers at

21 days of culture (n = 3/case). (B) LOX protein amounts in pooled medium aliquots collected over 21 days of culture. Shown are mean ± SD of DNA-normalized intensities, measured from representative SDS-PAGE/ western blots containing bands corresponding to LOX produced in the respective cases. (C) The release of MMPs-2 and 9 within the RASMC cultures receiving LOX were quantified using gel zymography procedures. The values are shown as mean ± SD of n =3/case for each test case, and further normalized to the respective amounts in control cultures. * represents significance in differences relative to controls, for $p < 0.05$.

Spent medium fractions pooled over 21 days from test and control cultures were analyzed by western blot, and the DNA-normalized intensities of the LOX-protein bands within test cultures were further normalized to those in controls (**Figure 5.15B**). Exogenous LOX-1 and LOX-2 enhanced LOX protein synthesis relative to controls by 1.16 ± 0.03 and 1.42 ± 0.24 –fold, respectively ($p = 0.008$ and 0.01, vs. controls). Gel zymography analysis showed that the production of the MMPs-2, 9 were not enhanced by LOX addition versus those that received no additives (**Figure 5.15C**; $p = 0.71$).

Overall, the data suggests that the observed increases in elastin matrix synthesis and deposition were an indirect outcome of exogenous bovine LOX-induced increases in endogenous LOX activity and protein synthesis. Though no differences in desmosine crosslink density were noted, significant increases in crosslinked elastin matrix production and yield – despite the absence of similar increases in tropoelastin synthesis within these cultures – suggests that exogenously provided LOX protein to cell cultures is

a viable and safe method and can be applied in other tissue engineering applications as well.

5.3.4 Conclusions of this study

1. Exogenously provided bovine LOX (50-100 μL/well) promotes RASMC proliferation relative to control cultures, without significantly increasing MMPs-2, 9 activity.
2. Bovine LOX enhanced total elastin production, elastin matrix deposition, and elastin crosslinking efficiency (yield) in a dose-dependent manner. This was achieved via significant increases in endogenous LOX protein production and activity within these cultures.
3. The concept of exogenous LOX addition to enhance matrix elastin synthesis and deposition is a viable and safe approach and has great potential in vascular tissue engineering applications.

CHAPTER 6

EFFICACY OF ELASTOGENIC CUES IN CHRONICALLY-STIMULATED VASCULAR SMOOTH MUSCLE CELL CULTURES

6.1 Introduction

In chapter 2, we explained in detail the role of various cytokines and chemokines, in regulating SMC-activation and healthy elastin destruction, thereby contributing to the aggravation of diseased state. The pathogenesis of aortic aneurysms (AAs) is characterized by injury, infiltration of extracellular inflammatory cells (e.g., monocytes, lymphocytes, plasma cells), and their secretion of matrix metalloproteinases (MMPs) and inflammatory cytokines (e.g., TNF-α, IL-1β), which in turn can induce a change in SMC phenotype and their mediation of vascular wall matrix remodeling[362, 363]. Since elastin is a major component of the extracellular matrix in vascular connective tissues, the released MMPs degrade crosslinked fiber structures of elastin (and collagen) to generate soluble peptides[11]. Prior studies have shown that macrophages migrate into the developing AA[364], likely attracted by these elastin peptides[365], and further exacerbate matrix breakdown by secreting cytokines, chemokines, interleukins, elastase, and collagenases[12]. These peptide fragments can activate the elastin-laminin receptors present on the surface of vascular cells[366] to trigger diverse responses including further production of elastases, increased Ca^{2+} influx into cells, switch of SMCs from healthy contractile to synthetic phenotype, and their further proliferation and disorganized matrix deposition[367]. Thus, in summary, this cascade of events is typically associated with elastin breakdown[368], and

concomitant loss of vessel elasticity[369], and ultimately leads to vascular calcification and aneurysm progression.

Among the various cytokines secreted by macrophages within aneurysmal lesions, tumor necrosis factor (TNF-α) has been found to be particularly dominant within the calcified aortic wall[370]. TNF-α is a vital mediator of inflammation and has been implicated to play a major role in inciting SMC proliferation[371] and MMP release[372]. Under inflammatory conditions, elastin gene expression by SMCs has been shown to be down-regulated by TNF-α[373], and existing elastin degraded by MMPs and macrophage-derived elastases[374], to subsequently interrupt intact elastin-SMC signaling pathways. Despite this clinical relevance and significance, the chronic-stimulatory effects of TNF-α on SMCs and their resultant effects on the quality and quantity of basal elastin matrix repair and regeneration by SMCs are not clearly understood and worth investigating.

As explained in chapter 3, we observed that HA oligomers (4-6 mer; MW ~ 756-1221 Da; 0.2 μg/mL) and TGF-β1 (1 ng/mL), henceforth referred to as *elastogenic cues*, attenuated proliferation of *healthy* vascular SMCs and dramatically increased cellular elastin production, matrix yield, maturation, and stability[360]. We hypothesize that delivery of TGF-β and HA oligomeric *cues* may likewise be useful to coax elastin matrix regeneration and minimize inflammation within aneurysm sites.

Despite their benefits to elastin production by healthy cells, it is yet unknown if the elastogenic *cues* will suppress pro-calcific and elastolytic activities of chronically-stimulated cells within vascular aneurysms, such as those incited by TNF-α, and simultaneously upregulate their ability to synthesize and assemble matrix elastin. To

investigate these aspects, we assessed the elastogenic effects of these cues, in TNF-α stimulated rat aortic SMC cultures. Since the numerous influencing parameters *in vivo* (e.g., source and nature of injury stimulus and heterogeneity in matrix composition as a function of proximity to site of aneurysmal rupture) can make initial assessment of the efficacy of these cues very difficult, the above culture model of TNF-α stimulated cells will enable assessment under tightly regulated conditions as other such studies have also found useful[375, 376].

6.2 Materials and Methods

6.2.1 SMCS Isolation and Culture

HA oligomer mixtures used in this study contained 75 ± 15% w/w of HA 4-mers (henceforth referred to oligomers), with 6-mers and 8-mers forming the balance, and were prepared in the lab as per the protocols explained in section 3.2.1.

The RASMCs were isolated from rat aorta as explained in section 3.2.2, and SMCs from passages 3-5 were seeded onto 6-well tissue culture plates (A = 10 cm^2) at a seeding density of 4.0×10^4 cells/ cm^2 and cultured in DMEM-F12 media with 10% FBS and 1% Penstrep. A total volume of medium was added per well was 5 mL. The cultures were divided into the following experimental groups: no-additives treatment (controls), TNF-α alone, TGF-β and HA oligomeric *cues* with or without TNF-α. TNF-α (Sigma Aldrich) was supplemented at a concentration of 10 ng/mL, HA oligomers were added at a dose of 0.2 μg/mL, and TGF-β1 (Peprotech Inc.) at a dose of 1 ng/mL. Fresh medium was added to cultures twice weekly, and the spent medium aliquots collected from each

well at different time points, pooled and stored at -20 ^{o}C. These pooled aliquots and the corresponding harvested cell layers were biochemically analyzed at 21 days of culture.

6.2.2 Biochemical Assays

The DNA content in cell layers was measured at 1 and 21 days of culture to determine the proliferation of SMCs and to normalize the measured amounts of synthesized matrix, according to protocol explained in section 3.2.3.

The collagen content within the cell layers and in the pooled supernatant medium fractions was estimated using a hydroxy-proline assay, described in section 3.2.4. The amounts of matrix elastin (alkali-soluble and insoluble fractions) and soluble tropoelastin (in pooled spent medium) were quantified using a Fastin assay (Accurate Scientific Corp), as detailed in section 3.2.5. The measured amounts of synthesized matrix were normalized to their respective DNA amounts to provide a reliable basis of comparison between samples, and to broadly assess if the observed changes in the amount of matrix synthesized could possibly be due to increases in elastin production on a per cell basis.

The desmosine crosslink densities within elastin matrices were quantified for selected cases using ELISA, as described in section 3.2.6. The desmosine amounts/ ng of DNA were compared to the DNA-normalized amounts of insoluble matrix elastin from corresponding cell layers. The LOX enzyme activity within the cell culture layers was determined using a flurometric assay based on generation of H_2O_2 when LOX acts on a synthetic substrate, described in detail in section 3.2.7. Western blot analysis of proteins within the pooled medium fractions at day 21 was performed using methods described in

section 3.2.8, to semi-quantitatively confirm observed biochemical trends in tropoelastin synthesis and to assess LOX protein synthesis.

6.2.3 Immunofluorescence Studies and Matrix Structure

As explained in detail in section 3.2.11, immunofluorescence techniques were used to confirm the presence of elastin, fibrillin within selected cell layers, and LOX expression for those conditions that appeared to upregulate elastin synthesis. The ultrastructure of insoluble matrix elastin within control cell layers and test layers was characterized using high-resolution transmission electron microscopy (detailed procedure in section 3.2.12).

6.2.4 Cytokine Array

The type and amount of cytokines produced by RASMCs in response to exogenous TNF-α, or together with *elastogenic cues* was compared using an ELISA-based cytokine array to deduce the cell-activation potential of TNF-α. RASMCs were cultured to semi-confluence and then subjected to exogenous TNF-α (10 ng/mL) for 48 h, in the presence or absence of HA oligomers (0.2 μg/mL) and TGF-β (1 ng/mL). The release of different cytokines and chemokines from cultured SMCs into the media were detected by a ChemiArray™ rat cytokine array I (Millipore), consisting of the corresponding antibodies spotted in duplicate onto a membrane. The membranes were processed in accordance with the manufacturer's protocol and imaged under chemiluminescence in a FluorChem 8900 gel imaging station (Alpha Innotech) to

quantify relative spot intensities. Intensities due to each cytokine were normalized according to the positive signal of each membrane, and the results were averaged from the outcomes of three replicate runs.

6.2.5 Gel Zymography

MMPs-2, 9 were detected in the culture medium by gelatin zymography methods described elsewhere[321]. Briefly, aliquots of culture medium were assayed for protein content using the BCA assay, and all lanes were loaded in triplicate with 15 μg of protein from each extract alongside with pre-stained molecular weight standards (Bio Rad). After development and staining, densities of MMP-2 and 9 bands on a dark background of stained gelatin were measured using Gel Pro Analysis software (Media Cybernetics), and reported as relative density units (RDU).

6.2.6 Elastase Assay

Elastase activity in the cell cultures was assayed using an *EnzChek*® Elastase Assay kit for elastin hydrolytic activity (Molecular Probes). Briefly, 50-μL of spent culture medium at 21 days of culture was mixed with 50 μL of diluted bovine neck ligament elastin, incubated for 30 min incubation at 37 ºC, and the fluorescence intensity measured at 485 nm excitation and 510 nm emission wavelengths. One unit of elastase was defined as the amount of porcine pancreatic elastase required to solubilize 1 mg of elastin at pH 8.8 and 37 ºC.

6.2.7 Von Kossa Staining for Calcific Deposits

After 21 days of culture, the respective cell cultures were incubated with 1% silver nitrate solution and placed under UV light for 20 min. After several changes of distilled water, the unreacted silver was removed with 5% sodium thiosulfate for 5 min, and the cells were rinsed and kept in distilled water. The slides were counterstained with hematoxylin. The presence of black stain confirmed the presence of calcium phosphate deposits.

Data were measured in triplicate from experiments that were also performed in triplicate (n = 3 samples/case). Since the data followed nearly Gaussian distribution, we statistically analyzed the data using Student's *t*-test, assuming unequal variance. Asterisks in figures denote statistically significant differences between test cultures and non-additive control cultures, deemed for $p < 0.05$.

6.3 Results

6.3.1 TNF-α Stimulation of SMCs

Figure 6.1A shows release of inflammatory cytokines, interleukins and chemokines by RASMCs when stimulated with TNF-α, relative to non-stimulated control RASMCs. TNF-α prompted ~30-70% increases in production of interleukins (IL-1, 4, 6, 10), ~20% increase in that of chemokines (FNK, LIX, MCP-1, MIP-3a), and increases between 30-50% in production of cytokines (TNF-α) and tissue inhibitor of matrix mealloproteinases (TIMP-1), compared to non-additive controls ($p < 0.05$ in all the cases). Von kossa staining also indicated a significantly greater number of calcific deposits

(stained black) within TNF-α –treated cell layers (**Figure 6.1B**) compared to controls. Gel zymography showed that production of the elastolytic MMPs-2, 9 were enhanced by 43 ± 14% and 51 ± 17% respectively in cultures that received TNF-α versus those that received no additives (**Figure 6.1C**; $p < 0.001$). These results suggest that the provided dose of TNF-α (10 ng/mL) is capable of stimulating cells to release more MMPs and cytokines, and that this *in vitro* system might serve as a suitable model of chronically-activated SMCs to ascertain their elastogenic upregulation by provided *cues*. Also, as shown in **Figure 6.1D**, TNF-α supplements enhanced elastase production within non-additive control cultures by 39 ± 4 % ($p < 0.01$).

6.3.2 Effect of TNF-α and *Cues* on SMC Proliferation and Matrix Synthesis

Control cultures proliferated 14.9 ± 2.1 –fold over 21 days. TNF-α supplementation to RASMC cultures had no effect on their basal proliferation rate (0.94 ± 0.22 –fold increase relative to controls; $p = 0.58$). As shown in **Figure 6.2A**, in the presence of the *cues*, TNF-α significantly suppressed cell proliferation relative to controls (0.74 ± 0.23 –fold; $p = 0.03$), although this decrease was less relative to cultures that received the *cues* alone (0.54 ± 0.1 –fold increase compared to controls, $p < 0.001$).

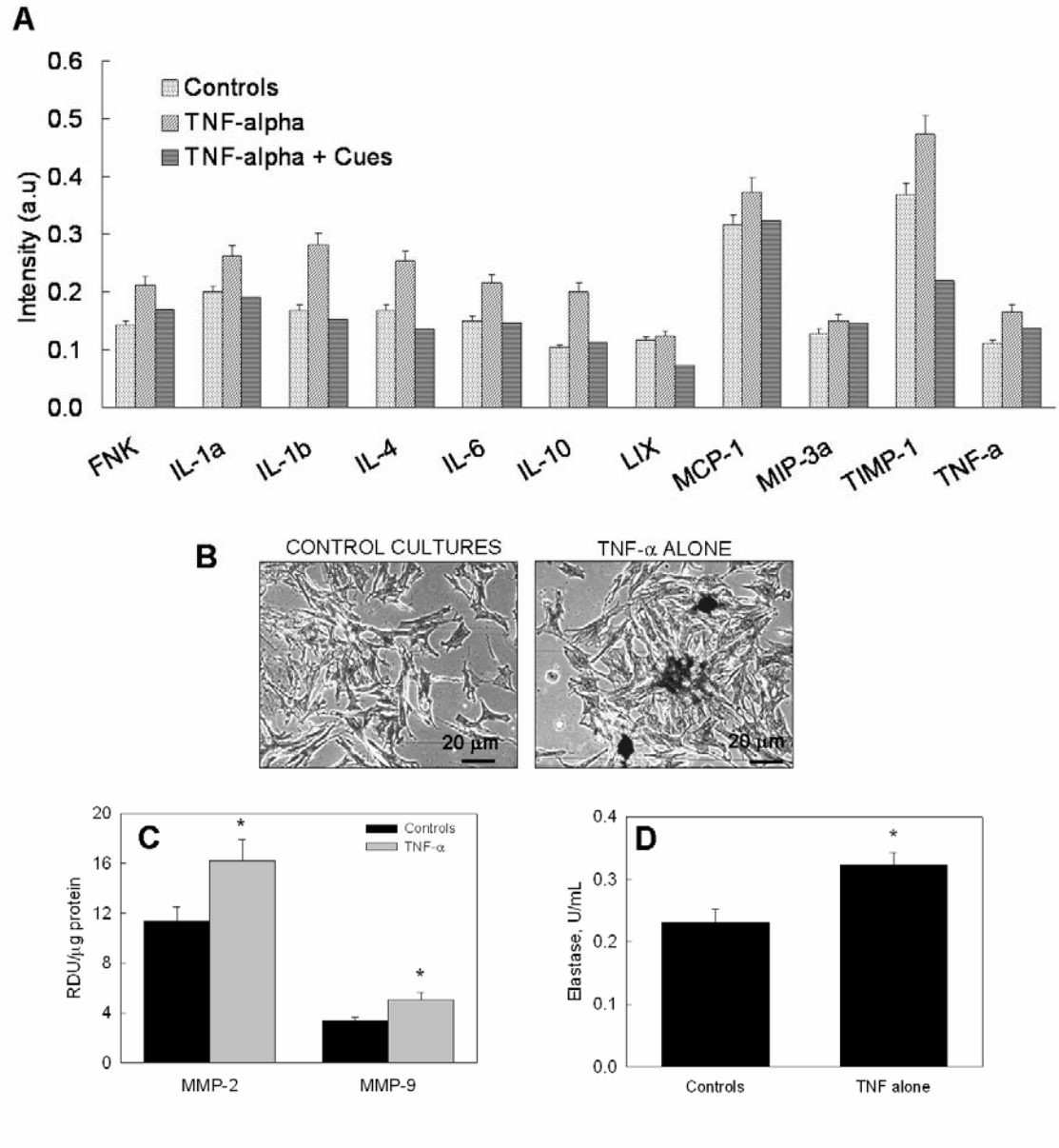

Figure 6.1. (A) Cytokine array analysis revealed the type and amount of inflammatory markers released within non-additive RASMC cultures, and cultures treated with TNF-α in the absence or presence of *cues*. (B) Von kossa staining of RASMC cultures stimulated with TNF-α shows significant calcific deposits formation, while control cultures showed none. (C) Gel zymography analysis revealed significant increases in

MMPs-2 and 9 release from RASMC cultures over the 21 day period, upon exposure to 10 ng/mL of TNF-α. (D) Elastase enzyme activity was also significantly higher within TNF-α stimulated cultures relative to control RASMC cultures.

Over 21 days of culture, non-additive RASMC cultures generated 35774 ± 4662 ng and 18931 ± 1966 ng of collagen and tropoelastin precursors per ng of DNA. TNF-α addition had no effect on collagen synthesis (0.97 ± 0.07 -fold) and tropoelastin synthesis (1.06 ± 0.08 -fold), relative to control cultures. Collagen synthesis was however increased by 1.16 ± 0.1 –fold and 1.84 ± 0.1 -fold relative to controls, when *cues* were supplemented in the presence and absence of TNF-α, respectively (p = 0.04 and p = 0.005 respectively vs. controls; **Figure 6.2B**). As shown in **Figure 6.2C**, addition of *cues* also enhanced tropoelastin synthesis by 2.01 ± 0.19 –fold ($p < 0.001$ vs. controls) when no TNF-α was added, and by 2.06 ± 0.12 –fold, when TNF-α was also supplemented ($p < 0.001$ vs. controls in both cases).

Elastin laid down as matrix within cell layers was measured as the sum of a highly crosslinked alkali-insoluble fraction, and an alkali-soluble fraction. **Figure 6.2D** shows the relative proportions of these elastin fractions in each of the tested cases. Synthesis of soluble and insoluble matrix elastin increased by 20 ± 3.5 -fold and 3.23 ± 0.2 -fold in TNF-α –treated cultures, relative to their production levels in controls (1026 ± 269 ng/ng and 1186 ± 546 ng/ng respectively, $p < 0.001$ in both cases). HA oligomer and TGF-β *cues* together stimulated production of soluble and insoluble matrix elastin by 12.3 ± 4.6 and 5.9 ± 1.9 –fold, respectively, relative to controls ($p < 0.001$ in both cases).

The addition of *cues* to the TNF-α stimulated cultures furthered these increases to 27.3 ± 1.7 and 4.9 ± 1.1 –fold versus controls, respectively (**Figure 6.2D**; $p < 0.001$ in both cases). Overall, relative to controls, the total matrix elastin (sum of alkali-soluble and insoluble elastin fractions) synthesis increased by 11 ± 1.8, 8.8 ± 3.1 and 15.3 ± 1.4 –fold, respectively, on addition of TNF-α alone, *cues* alone or the *cues* together with TNF-α, respectively.

Figure 6.2E shows the elastin matrix yields [matrix yield = matrix elastin/ (tropoelastin + matrix elastin)] calculated from the elastin synthesis data presented in **Figures 6.2C-D**. While only 10.5 ± 3.9 % of total elastin produced in non-additive control cultures was deposited as a matrix, this yield was increased to 54 ± 9% by addition of TNF-α alone, 34 ± 12 % with the addition of *cues* alone, and 46.5 ± 4.3% upon supplementation of both the *cues* and TNF-α.

6.3.3 Effects of TNF-α and *Cues* on Elastin Matrix Crosslinking

As shown in **Figure 6.3A**, relative to control cell layers (12.8 ± 1.7 pg desmosine/ ng DNA), cells cultured with TNF-α alone did not show any significant increase in desmosine synthesis (1.06 ± 0.17 -fold; $p = 0.31$ vs. controls), while *cues* significantly enhanced desmosine synthesis by 1.91 ± 0.42 –fold and 1.42 ± 0.3 –fold respectively in the absence and presence of TNF-α ($p < 0.01$ and $p < 0.02$ vs. controls).

Western blot analysis of tropoelastin protein expression (**Figure 6.3B**) showed trends similar to that observed from biochemical analysis. TNF-α alone had no significant effect on the tropoelastin protein amounts (1.16 ± 0.16 –fold relative to

controls), while *cues* alone and in the presence of TNF-α promoted tropoelastin protein expression by 1.51 ± 0.16 and 1.48 ± 0.17 –fold, respectively. Western blot analysis showed LOX protein expression to be enhanced in cultures supplemented with TNF-α or *cues* alone by 1.27 ± 0.05 and 1.31 ± 0.03 –fold, relative to controls ($p < 0.005$; **Figure 6.3B**) but less so in cultures that received both the *cues* and TNF-α (1.17 ± 0.09 –fold increase vs. controls; $p = 0.03$). However, there were no significant differences in cellular LOX activities between control cultures and those supplemented with TNF-α, either alone or together with *cues*.

6.3.4 *Cues* Repress TNF-α –Induced Activation of RASMCs

Gel zymography analysis revealed that MMP-2 production was increased by addition of *cues*, alone and together with TNF-α (1.78 ± 0.05 and 1.73 ± 0.05 –fold vs. controls, respectively; $p < 0.05$ vs. controls). However, these increases were not very different from that measured in cultures supplemented with TNF-α alone (**Figure 6.3C**). Again, though MMP-9 production levels, both in the presence of *cues* alone and together with TNF-α were similar, they were only marginally higher than in control or TNF-α treated cultures (**Figure 6.3C**; $p < 0.05$ vs. controls). However, as shown in **Figure 6.3D**, assays for elastase activity in the presence of *cues* alone was comparable to that in control cultures (0.24 ± 0.01 U/mL), while addition of *cues* to TNF-α stimulated cultures decreased elastase activity from 0.32 ± 0.01 U/mL down to activity levels slightly higher than in control cultures (0.28 ± 0.009 U/mL; $p < 0.01$ for TNF-α + *cues* vs. TNF-α alone).

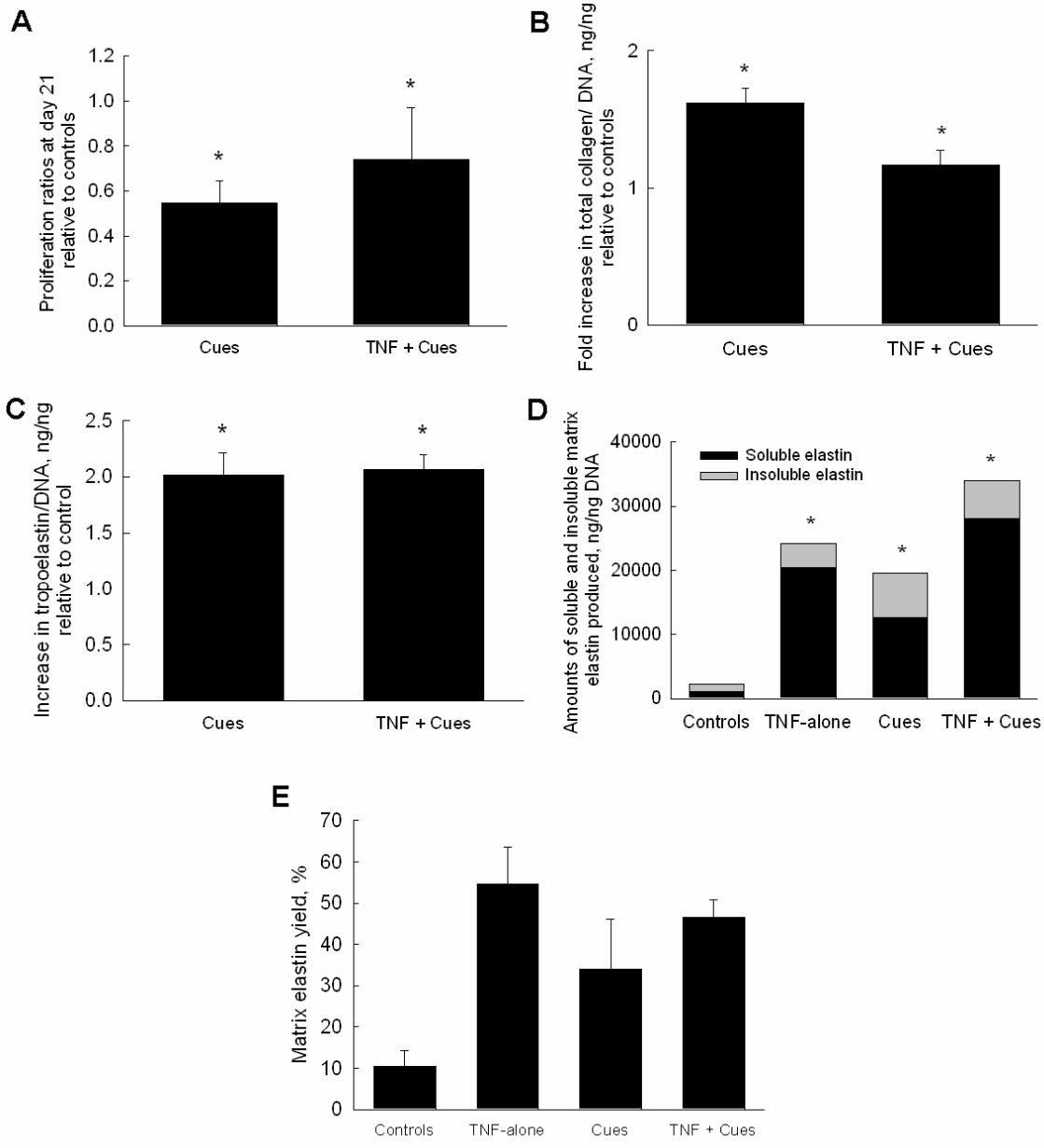

Figure 6.2. (A) Proliferation ratios of RASMC cultures supplemented with *cues* alone or together with TNF-α (10 ng/mL). Data shown represent mean ± SD of DNA content of cell layers after 21 days of culture, normalized to initial seeding density and further normalized to control cultures that received no additives (n = 3/case). Effects of *cues*

alone or together with TNF-α on total collagen (B) and tropoelastin (C) synthesis by adult RASMCs. Data shown (mean ± SD) are normalized to cellular DNA content at 21 days of culture and represented as fold change in protein production relative to controls (n = 3/case). (D) Relative amounts of alkali-soluble and crosslinked matrix elastin produced by RASMCs in all the cases. (E) Matrix elastin yields (i.e., ratio of matrix elastin to total elastin) were significantly higher in cultures that received TNF-α alone, *cues* alone or together with TNF-α. $P < 0.05$ represents significant differences from controls (*).

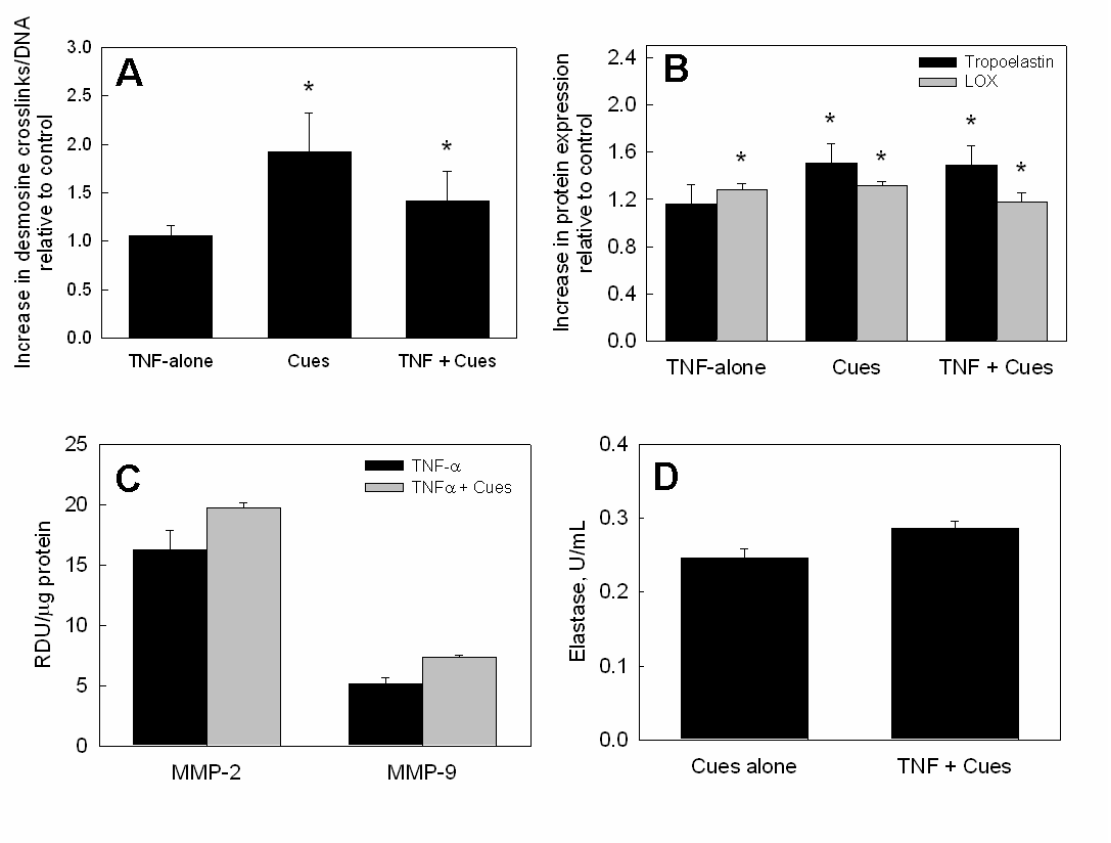

Figure 6.3. (A) Desmosine amounts measured in test cell layers were normalized to corresponding DNA amounts (ng/ng), and further a similar ratio obtained for the non-additive controls. Comparable trends were observed for the desmosine/DNA density and respective insoluble matrix elastin/DNA for selected cases. (B) SDS-PAGE/ Western blot analysis of tropoelastin and LOX proteins within the pooled medium cultures at the end of 21 days. Data shown represent mean ± SD of 3 repeats/ case and are shown normalized to controls. (C) Gel zymography analysis revealed the presence of MMPs-2 and 9 within TNF-α cultures even upon addition of *cues*. However the relative amounts were not significantly higher compared to TNF-α alone stimulated cultures. (D) Elastase enzyme activity within RASMC cultures treated with cues alone or together with TNF-α was not significantly different from that observed with non-additive cultures.

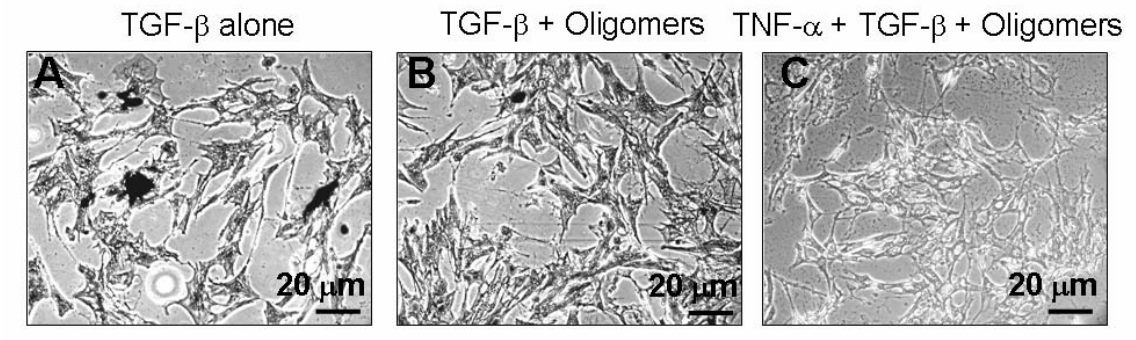

Figure 6.4. Von kossa staining images of cell layers treated with TGF-β alone, *cues* alone and *cues* together with TNF-α. Significant calcific deposits were evident in cultures treated with TGF-β alone, while cultures which received *cues* alone or together with TNF-α showed none.

As seen in **Figure 6.1A**, the release of inflammatory cytokines and interleukins by TNF-α stimulated RASMCs decreased significantly when *cues* were added to these cultures. It was observed that on average, addition of the *cues* contributed to ~ 28-46% decrease in the production of interleukins (IL-1, 4, 6, 10), ~ 12-40% decrease in production of chemokines (FNK, LIX, MCP-1, MIP-3a), and ~ 19-53% decrease in release of cytokines (TNF-α) and TIMP-1 by TNF-α treated cell cultures, compared to those conditioned with TNF-α alone ($p < 0.05$ vs. TNF-α alone, in all the cases).

Von kossa staining of cultures treated with TGF-β alone (panel A), TGF-β and HA oligomeric *cues* alone or together with TNF-α (panels B-C) are shown in **Figure 6.4**. It was observed that cultures treated with TGF-β (1 ng/mL) alone contained large black calcific deposits, while further addition of HA oligomers in the presence and absence of TNF-α completely inhibited calcific deposits.

6.3.5 Structural Analysis of Matrix Elastin

Immunofluorescence imaging showed that compared to non-additive controls (**Figure 6.5A**) or cultures that received only TNF-α (Figure 6.5B), elastin (red) was more abundant in cultures that received TGF-β and HA oligomeric cues alone (Figure 6.5C) or together with TNF-α (Figure 6.5D). However, elastin-containing cultures that were not treated with the anti-elastin primary antibody did not exhibit any florescence confirming lack of non-specific binding of the fluorophore.

Figure 6.6 shows representative transmission electron micrographs of elastin matrices from 21-day cultures. Similar to those observed in control cultures which

received no-additives (Figure 6.6A), TNF-α alone stimulated deposition of discrete clumps of amorphous elastin protein distributed, with sparse amounts of aggregating elastin fibrils (Figure 6.6B). When both TGF-β1 and HA oligomers were provided to control cultures (Figure 6.6C), mature elastin fiber formation was favored, with the matrix containing numerous fully-formed bundles of fibers (100-200 nm diameter), than in control and TNF-α alone cultures. Fibrillin (immunogold particle-stained), which appeared in transverse sections as darkly stained nodules, were located at the periphery of aggregating elastin fiber bundles, signifying normal elastic fiber assembly. The elastogenic *cues* also promoted fiber formation within TNF-α stimulated cultures (Figure 6.6D), with less amorphous elastin and more fibrilliar elastin observed when compared to TNF-α alone cultures.

6.4 Discussion

Literature attests to the significant contribution of inflammatory mechanisms in the pathogenesis of cardiovascular disease. Pro-inflammatory cytokines such as TNF-α, IL-1, IL-β1, and IL-6, produced by a variety of cell types, act as essential mediators of many biological signaling mechanisms[377], and play an important role in primary host responses and tissue repair[378]. Elastolytic activity and generation of elastin peptides are also enhanced within these tissues and have been implicated to induce SMC migration and neointima formation[379]. The importance of TNF-α to initiation of aneurysm development thus justifies the adoption of *in vitro* culture models of TNF-α -stimulated vascular cells to study activated cell responses and to assess the efficacy of drugs aimed

at suppressing these responses. Although pharmacological approaches to attenuate MMP production and activity, and chemical approaches to stabilize elastin against breakdown appear to proffer some promise in halting aneurysm progression, regression of aneurysms via active regeneration of elastin matrices within has not been possible to date. This is primarily due to poor elastin regenerative capacity of adult vascular cells. In this context, in a series of earlier studies, we showed for the first time, that TGF-β and HA oligomeric *cues* together synergistically enhance elastin matrix synthesis and fiber formation by healthy adult vascular SMCs[58, 360]. To gauge their similar utility for regeneration of elastin matrices by chronically-activated vascular cells in an aneurysmal environment, in this study we have sought to evaluate the benefits of these elastogenic *cues* to upregulating elastin matrix regeneration by TNF-α -activated RASMCs in culture, and possibly simultaneously suppressing adverse responses to their activation.

In contrast to some prior studies where significant apoptotic cell death was observed upon their exposure to TNF-α[380], we observed active cell proliferation over the 21 days of culture. One explanation might be proffered on the basis of studies by Wang et al.[381], who showed that the response of vascular smooth muscle cells to TNF-α is not generic, but instead only sub-populations apoptose in response to TNF-α. It is certainly possible that the cell layers in this study might represent the sub-population of RASMCs which do not apoptose. Regardless, TNF-α -induced activation of these cell layers was confirmed by (a) increased cellular release of MMPs-2, 9 and other elastases relative to non-additive controls, (b) enhanced endogenous production of interleukins and other cytokines – including TNF-α itself, and (c) enhanced *in vitro* calcification of cell layers

relative to controls, quite likely due to TNF-α -mediated increases in intracellular cAMP and osteoblastic differentiation[155].

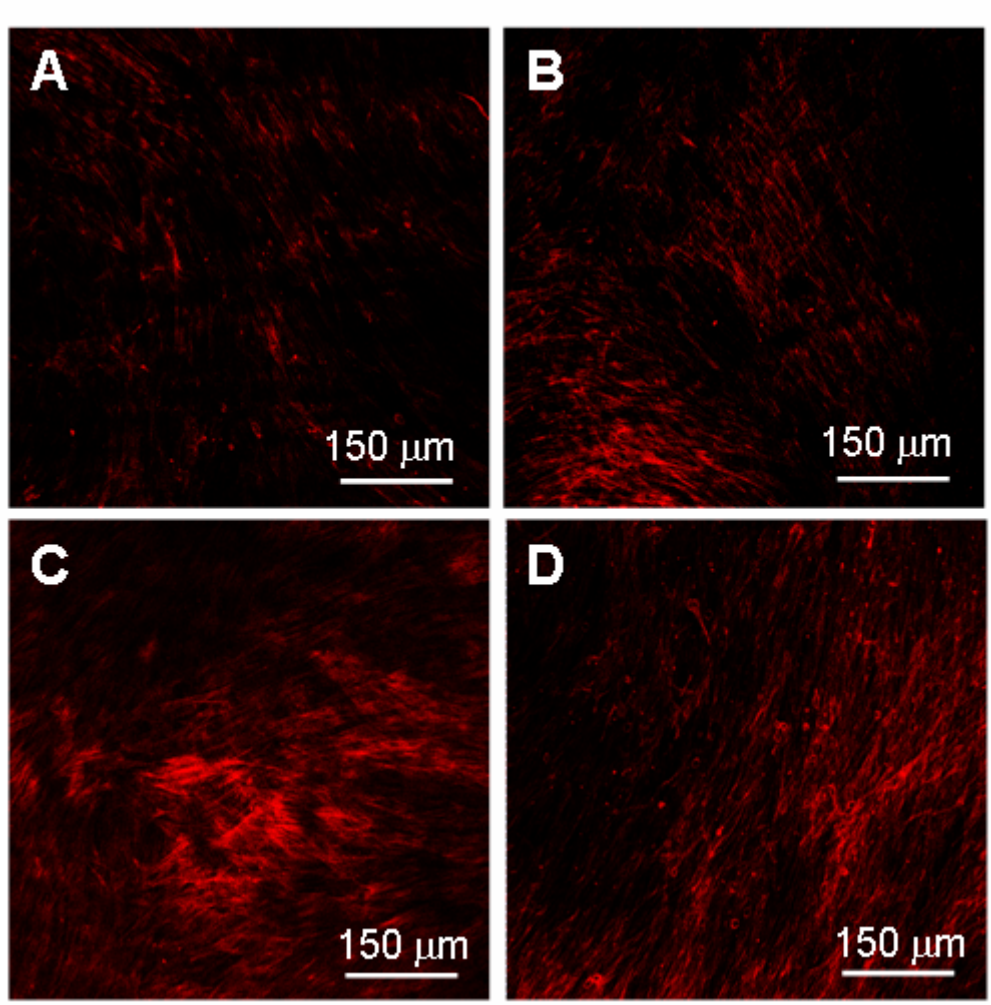

Figure 6.5. Immunodetection of elastin protein within control and test cell layers after 21 days of culture. An increase in matrix elastin protein is evident in cultures which received *cues* alone or together with TNF-α (panels C-D), while cultures which received no-additives (panel A) or TNF-α alone (panel B) showed relatively less coloration. Scale bar: 150 μm.

Further, we noted that collagen and tropoelastin production in TNF-α supplemented cultures was not significantly different from control cultures. Some prior studies have also shown TNF-α to suppress collagen gene expression and protein synthesis by fibroblasts[382, 383], fat-storing cells[384], vascular SMCs and endothelial cells[375]. Specifically, a prior study[375] showed that 10 ng/mL TNF-α, dosage identical to that used in this study, suppressed collagen production by ~ 20% relative to control cultures, only when the treated cultures were confluent. However, 10 ng/mL TNF-α did not have any impact on collagen production within sub-confluent SMC cultures[375], which agrees well with our present findings since the SMCs reached only ~60% confluence within the 3 weeks. Besides, our culture system closely mimics chronic, long-term TNF-α –induced signaling in aneurysms than a 24-h study. We also note in our study that TNF-α induces multi-fold increases in total matrix elastin synthesis relative to controls, which we hypothesize to be an indirect outcome of TNF-α –induced increase in LOX production (Figure 6.3B), an enzyme critical for normal biosynthesis and assembly/maturation of elastin matrix. Moreover, our analysis shows that tropoelastin was not more efficiently crosslinked by desmosine, as the crosslink density (i.e., desmosine content/ insoluble elastin matrix ratio) remained unaffected relative to controls. Taken together, these results suggest that TNF-α induces release of many cytokines and other factors (e.g., LOX) by SMCs that may in turn modulate cellular matrix synthesis.

When TGF-β (1 ng/mL) and HA oligomers (0.2 μg/mL) were provided to healthy SMCs in the absence of TNF-α, the cellular responses were in agreement with those observed earlier[360]. The increases in collagen and tropoelastin may as well be due to the

interaction of TGF-β and HA oligomers with their respective cell-surface receptors[318], which may have downstream intracellular-signaling effects that are anti-mitotic, as others have also demonstrated to occur upon cellular interaction with HA fragments[385]. The enhanced elastin matrix yield in the presence of *cues* may also be due to the observed increase in production of elastin crosslinking enzyme LOX (Figure 6.3B). In addition, the *cues* also improved the quality of matrix elastin relative to controls. As others have previously suggested[47], this may occur via physical coacervation of tropoelastin precursors by HA oligomers to result in more efficient crosslinking by LOX into matrix structures. However the observation that *cues* did not enhance basal elastase activity of the SMCs or their release of MMPs, and that they suppress calcification of the cell layers as induced by TGF-β alone, reinforce our prior-observed benefits of TGF-β and HA oligomeric *cues* to tropoelastin synthesis and elastin matrix assembly and maturation.

Relative to cultures which received TNF-α alone, production of cytokines/ chemokines/ interleukins was significantly attenuated and TIMP-1 production elevated within cultures that received both TNF-α and elastogenic *cues*. We hypothesize that such attenuation may be due to the contradictory downstream effects of simultaneous cellular interactions with TNF-α and TGF-β[88]. Regardless, this outcome is of immense significance to treatment of vascular aneurysms *in vivo*. A very important determinant of vascular patency following injury/ disease initiation *in vivo* is the interaction between recruited leukocytes and endothelial cells. Enhanced production and release of chemokines (e.g., IL-8) and acute inflammatory cytokines (e.g., TNF-α, IL-1) by ECs/ SMCs can attract polymorphonuclear neutrophils (PMNs) and T-cells to the injury site

(i.e., aneurysms) to incite acute inflammation[386], while chemokines such as MCP-1, MIP-3a also summon monocytes/ macrophages/ eosinophils/ basophils that cause chronic inflammation, matrix degradation and remodeling[387]. Thus, under these enhanced inflammatory conditions, an attenuated release of leukocyte-recruiting cytokines/ chemokines, as affected by TGF-β/ HA oligomers cues in the presence of TNF-α – is likely to provide a micro-environment that is more conducive to maintaining matrix stability.

Vascular calcification is a complex process that frequently involves differentiation of SMCs to an osteoblastic phenotype, which can be induced by both TNF-α and TGF-β[155, 321]. In agreement with this, we observed calcific deposits in SMC layers exposed to either of these factors alone (Figures 6.1B and 6.4A). While TNF-α induces matrix calcification via increases in intracellular cAMP[155], TGF-β appears to influence calcification by enhancing bone protein production via increased expression of the elastin-laminin receptor (ELR)[321]; other studies have shown that TGF-α promotes matrix calcification by upregulating cGMP[388]. An interesting finding in this study was that HA oligomers and TGF-β, when provided together to healthy SMC cultures, inhibited calcific deposits formation. In a previous study[58], we showed that HA oligomers suppress ELR activity, which might explain the absence of calcific deposits even when TGF-β is supplemented. Another finding was that these elastogenic *cues* together also inhibit TNF-α -induced calcification. The mechanisms underlying the anti-calcific effects of HA and TGF-β on TNF-α –activated SMCs, is beyond the scope of this study. However, we believe that our results strongly point to the involvement of these

factors via two different mechanisms of calcification that exhibit some downstream opposition, resulting in a net decrease in matrix calcification.

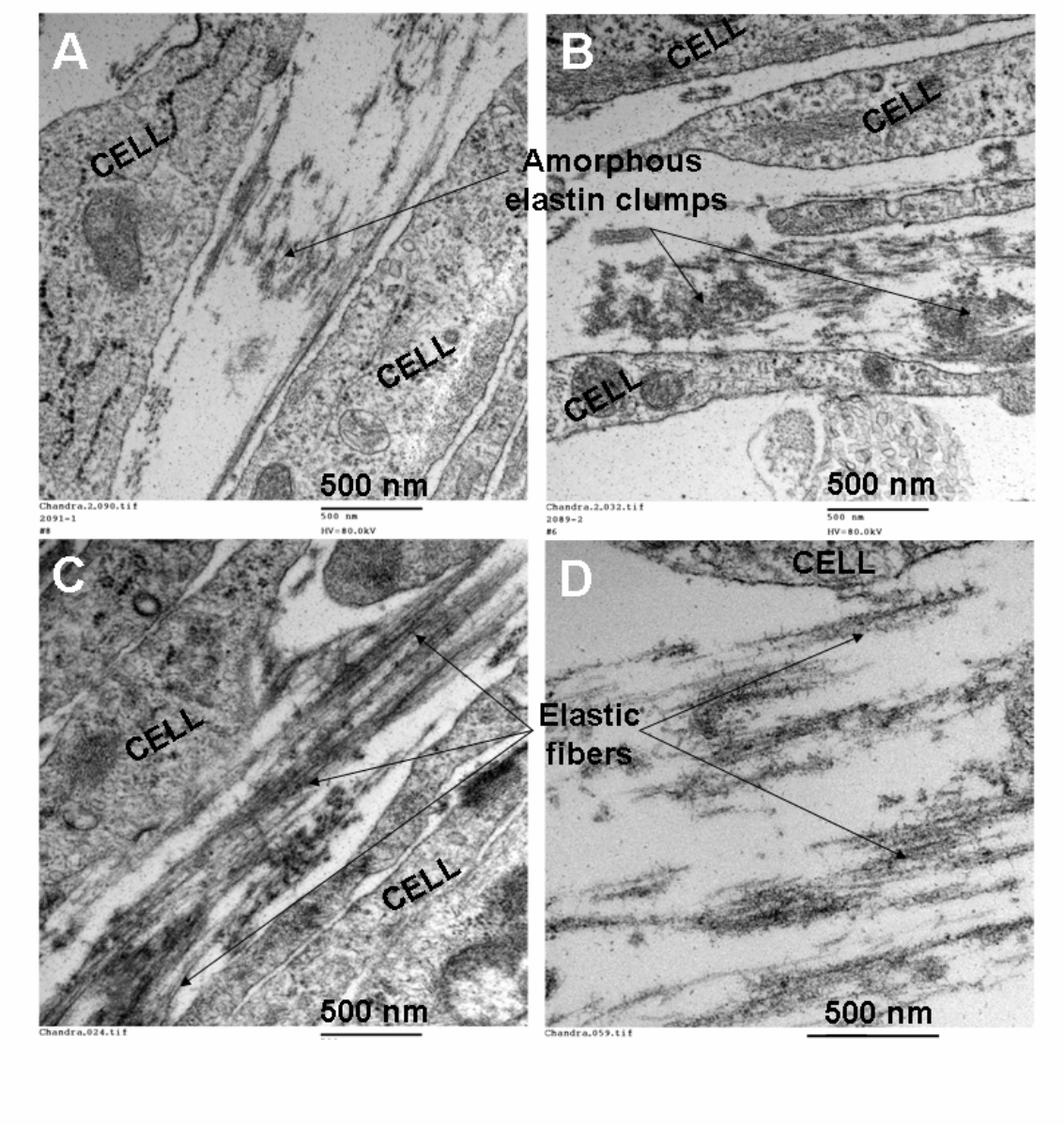

Figure 6.6. Representative TEM images of 21-day old RASMC cell layers cultured additive-free (panel A), with TNF-α alone (10 ng/mL; panel B), *cues* alone (panel C) or

together with TNF-α (panel D). Aggregating amorphous elastin clumps leading to the formation of elastin fibers can be clearly seen in TNF-α –activated cultures treated with *cues* (panel D), while cultures which received no-additives (panel A) or TNF-α alone (panel B) showed amorphous elastin deposits with sparse fiber formation. However, in the presence of *cues* alone, fibrillin-mediated elastin fiber formation is clearly evident (panel C).

Upregulated collagen matrix production by elastogenic cues was attenuated down to control levels on addition of TNF-α. This might be due to our observed decrease in LOX production in the latter cultures, relative to TNF-α alone or *cues* alone supplemented cultures (Figure 6.3B). On the other hand, tropoelastin and matrix elastin production continued to be enhanced by elastogenic *cues*, more so in the presence of TNF-α than its absence, indicating some synergy in elastin synthesis signaling pathways. Though matrix elastin production was enhanced by TNF-α alone or together with *cues*, dramatic differences in the quality of elastin matrix was observed between these cases. While elastin was deposited as amorphous, non-fibrillar clumps in TNF-α alone cultures, the *cues* provided in the presence of TNF-α promoted mature elastin fiber formation with fibrillar microfibrils bordering their periphery, as explained in our earlier study[360]. We believe that the observed increase in elastic fiber quality in the latter case (Figure 6.6D) might be due to the presence of HA oligomers, which can physically coacervate amorphous elastin protein onto their surface, facilitating mature fiber formation[47].

6.5 Conclusions of this study

1. TNF-α activates cultured vascular SMCs to release cytokines/ chemokines/ interleukins, elastolytic MMPs-2, 9 and other elastases, to promote calcific deposition in a manner that simulates events within inflammation-ridden vascular aneurysms *in vivo.*
2. Though TNF-α did not influence collagen and tropoelastin synthesis, further addition of *cues* (1 ng/mL TGF-β and 0.2 μg/mL HA oligomers) to these activated cultures not only doubled basal levels of tropoelastin and collagen production, but also significantly upregulated matrix elastin and total elastin production, in a manner mimicking their effects on healthy unactivated SMCs.
3. The elastogenic *cues* promoted deposition of a fibrillar elastin matrix and improved desmosine crosslinking and elastin matrix yield, while suppressing elastase activity, MMPs/ cytokines/ chemokines release, as well as inhibited TNF-α -induced matrix calcification.
4. The data provides preliminary evidence as to the efficacy of elastogenic *cues* in upregulating elastin matrix production by activated vascular SMCs, organizing elastin protein into fibers, and simultaneously stabilizing this matrix by attenuating production of elastolytic enzymes.
5. These results could form a basis for future elastin regenerative therapies for regression/ repair of vascular aneurysms.

CHAPTER 7

THERAPEUTIC CUES FOR ELASTIN MATRIX REPAIR BY AORTIC ANEURYSMAL SMOOTH MUSCLE CELLS

7.1 Introduction

In previous chapters 1 and 2, we have detailed the underlying mechanims of of AAs formation, and the role of elastin in initiating and participating in this process. Since the pathogenesis of AAAs could also arise from enzymatic degradation of healthy elastic fibers and excessive accumulation of proteoglycans[14], leading to loss of elasticity and strength of the aortic wall, and progressive dilation to form a rupture-prone sac of weakened tissue[1], we hypothesize restoration of elastin in these segments will likely stabilize and restore homeostasis in these tissues. We believe that active cellular-mediated regeneration of lost elastin within the aneurysmal sites could potentially revolutionize AAA treatment via standalone application or by integration with other surgical and non-surgical approaches. However, this is challenging since adult vascular cells do not generate much elastin on their own and mature elastic fibers rarely undergo active remodeling.

In chapters 3-5, we evaluated and optimized the effects of various biomolecules to elastin synthesis and crosslinking by RASMCs. In chapter 4, we explored the utility of these optimized elastogenic cues, namely HA oligomers and TGF-β, to elastin repair and regeneration within chronically-stimulated RASMCs. Despite their benefits to elastin synthesis by healthy adult SMCs, it is yet unknown if these *cues* will suppress pro-

calcific and elastolytic activities of diseased vascular cells, such as those within aneurysmal segments, and improve elastin matrix synthesis and assembly potential.

To ascertain this, in this study, we adopted an established abdominal aorta injury protocol involving application of calcium chloride to induce an aneurysm within, in rats, over 4-weeks[154]. We then investigated the standalone and combined elastogenic benefits of TGF-β and HA oligomer cues on SMCs isolated and cultured from these aneurysmal aortae, in an *in vitro* culture model. Based on the outcomes, we believe that this approach may be employed stand-alone or in consort with existing surgical or pharmacological approaches to regenerate elastin matrices within aneurysmal aortic vessels.

7.2 Materials and Methods

7.2.1 Calcium Chloride–Induced Aortic Aneurysm

Adult Sprague-Dawley rats (300-350 g in weight) were procured and acclimatized for one-week before surgery. The rats were placed under general anesthesia (2% to 3% isoflurane) and the infrarenal abdominal aorta was exposed surgically. The aorta were treated using a protocol adopted by various groups[154, 389, 390] (**Figure 7.1**), wherein sterile cotton gauze presoaked with 0.15 mol/L $CaCl_2$ was rubbed on the aorta for 15 min. Sufficient care was taken not to expose other organs to this caustic treatment. Following treatment, the abdominal cavity was thoroughly washed with sterile silane to remove the residual $CaCl_2$. The cavity was then closed, subcutaneously sutured and stapled, and the rats were allowed to recover. After 28 days in rehabilitation, the animals were humanely

euthanized by CO_2 asphyxiation, the abdominal aorta was excised from the arch to the celial axis and processed for SMCs isolation. The abdominal aortae were photographed before surgery and after 28 days to compare the changes in aortic diameter. All protocols regarding animal surgery were approved by Clemson University animal facility center.

7.2.2 SMC Isolation and Culture

The isolated aortae (n = 3) were opened lengthwise and the intima was scraped gently with a scalpel blade. The medial layer dissected from the underlying adventitia was chopped into ~ 0.5 mm-long sections, and washed twice with warm silane. The resulting tissue slices were pooled, enzymatically degraded in DMEM-F12 (125 U/mg collagenase and 3 U/mg elastase) for 30 min at 37 °C, centrifuged at 400 *g* for 5 min; washed and seeded in T-75 flasks containing DMEM-F12 (10% fetal bovine serum) for 15 days. Rat aortic SMCs (RASMCs) derived by outgrowth from these tissue explants were monitored over this 2-week period, and the cells were finally pooled and stored. SMCs from passage 2 were seeded onto 6-well tissue culture plates (A = 10 cm^2) at a seeding density of 2×10^5 cells/well and cultured in DMEM-F12 media with 10% FBS and 1% Penstrep. The total volume of medium added per well was 5 mL.

HA oligomer mixtures used in this study contained around 75 ± 15% w/w of HA 4-mers (henceforth referred to oligomers), and were prepared in the lab using protocols reported in section 3.2.1. The experimental groups were: aneurysmal cells with no-additives (controls), aneurysmal cells treated with HA oligomers alone, TGF-β alone, or TGF-β and HA oligomers together. TGF-β (Peprotech Inc.) was added at a final

concentration of 1 ng/mL, while oligomers were added at a final dose of 0.2 μg/mL. Media was replaced twice weekly and the spent media was collected and stored at -20^{o}C. At 21 days, these pooled aliquots and their corresponding cell layers were biochemically analyzed.

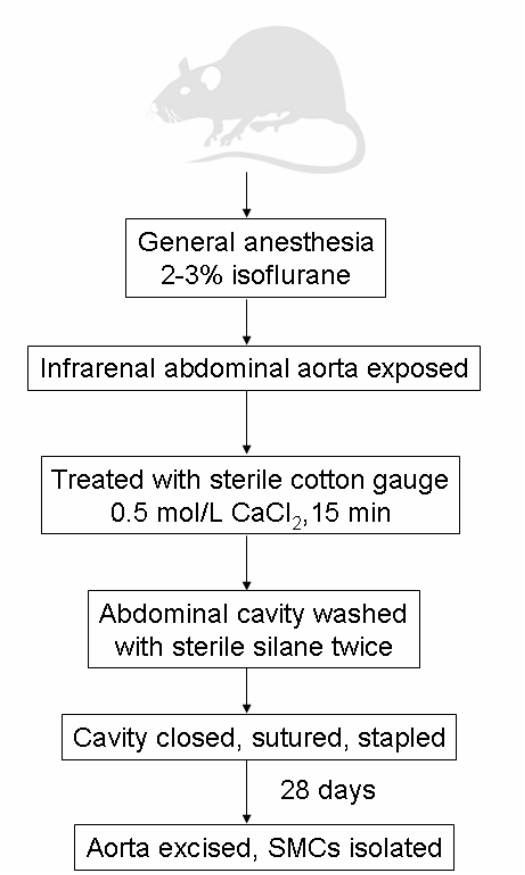

Figure 7.1. Schematic of aneurysm induction in rat aorta using $CaCl_2$-treatment protocol.

7.2.3 Biochemical Assays

The DNA content in cell layers was measured at 1 and 21 days of culture to determine the proliferation of SMCs and to normalize the measured amounts of synthesized matrix, according to protocol explained in section 3.2.3.

The collagen content within the cell layers and in the pooled supernatant medium fractions was estimated using a hydroxy-proline assay, described in section 3.2.4. The amounts of matrix elastin (alkali-soluble and insoluble fractions) and soluble tropoelastin (in pooled spent medium) were quantified using a Fastin assay (Accurate Scientific Corp), as detailed in section 3.2.5. The measured amounts of synthesized matrix were normalized to their respective DNA amounts to provide a reliable basis of comparison between samples, and to broadly assess if the observed changes in the amount of matrix synthesized could possibly be due to increases in elastin production on a per cell basis.

The desmosine crosslink densities within elastin matrices were quantified for selected cases using ELISA, as described in section 3.2.6. The desmosine amounts/ ng of DNA were compared to the DNA-normalized amounts of insoluble matrix elastin from corresponding cell layers. The LOX enzyme activity within the cell culture layers was determined using a flurometric assay based on generation of H_2O_2 when LOX acts on a synthetic substrate, described in detail in section 3.2.7. Western blot analysis of proteins within the pooled medium fractions at day 21 was performed using methods described in section 3.2.8, to semi-quantitatively confirm observed biochemical trends in tropoelastin synthesis and to assess LOX protein synthesis.

Von Kossa staining was performed on cell layers at the end of 21 days, as per protocols detailed in section 6.2.7. Elastase assay was performed to evaluate the activity of elastases in the cell cultures, as per the protocol detailed in section 6.2.6. Gel zymography analysis of MMPs-2, 9 release was performed as per protocol detailed in section 6.2.5.

All experiments were performed in triplicate and quantitative results reported as mean ± SD. Statistical significance between and within groups was determined using 2-way ANOVA. Results are deemed significantly different from controls for $p < 0.05$.

7.2.4 Immunofluorescence Detection and Matrix Structure

As explained in detail in section 3.2.11, immunofluorescence techniques were used to confirm the presence of elastin within the cultured cell layers. The ultrastructure of insoluble matrix elastin within control cell layers and test layers was characterized using high-resolution transmission electron microscopy (detailed procedure in section 3.2.12).

7.3 Results

7.3.1 Aneurysm Progression and SMC Phenotype

Figures 7.2A and B show a representative rat abdominal aortae before and 28-days post-injury with $CaCl_2$. It was observed that ~ 45% local increase in aortic diameter was attained over this period, agreeing with prior observations[390]. As shown in Figures 1C and D, SMCs outgrowing from aneurysmal aortal explants initially appeared rounded, then more spindle-shaped, and thereafter somewhat more spread attaining 50% confluence by 15 days. In contrast, SMCs isolated from healthy rat aortae exhibited more spread morphology on day 7 after seeding (panel E). The SMC phenotype was confirmed by staining for SMC α-actin (panel F).

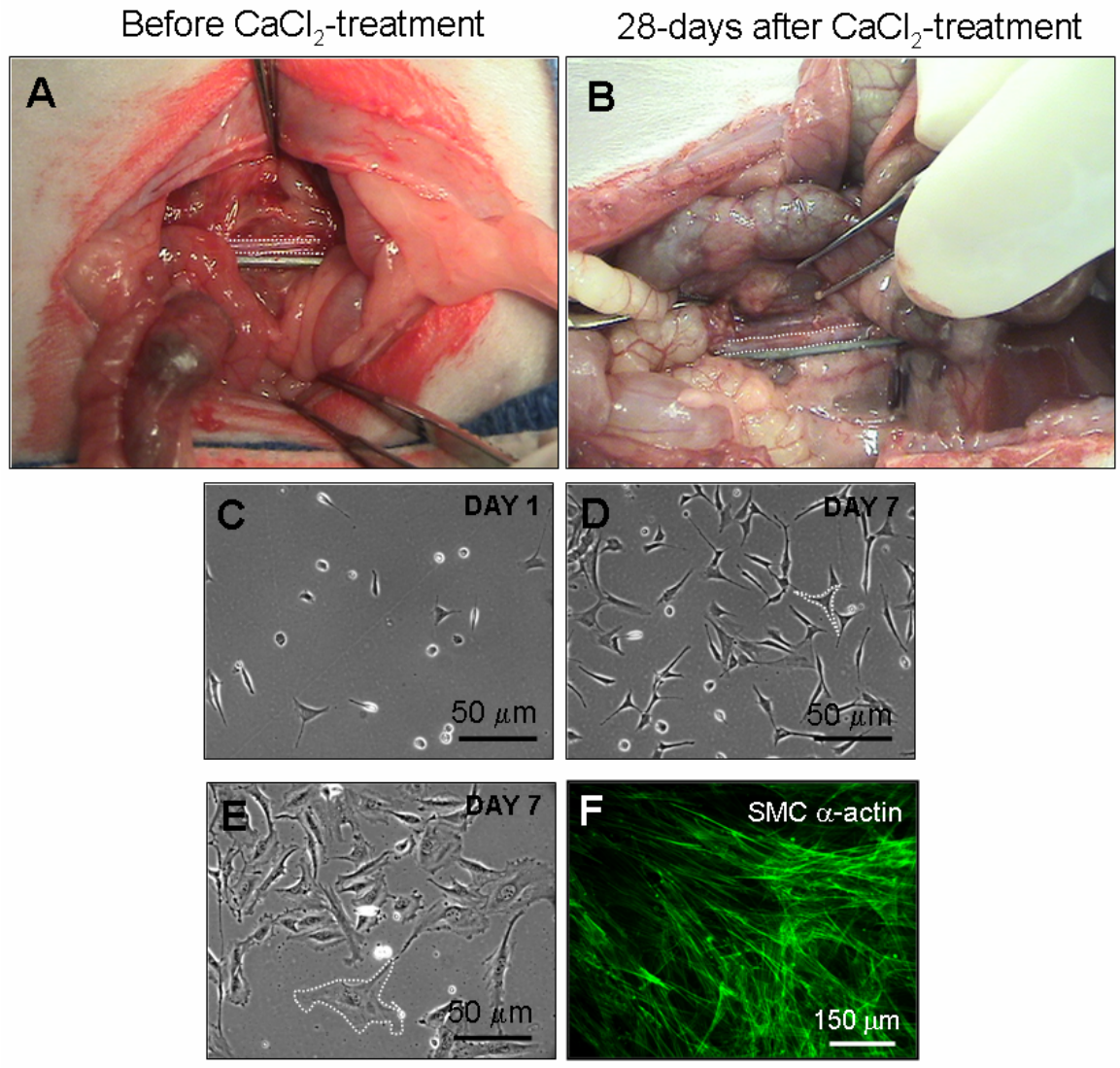

Figure 7.2. Representative images of abdominal rat aorta before calcium-chloride treatment (A), and after 28 days of aneurysm progression (B). Significant rounding of the SMCs isolated from the aneurysmal segment was observed on day 1 (C) and more spindle-shaped by day-7 (D). SMCs isolated from healthy aortae showed more spread morphology on day 7 of seeding (E). The cells were stained with SMC-α actin to confirm the smooth muscle cell phenotype (F).

7.3.2 Aneurysmal SMC Proliferation and Matrix Synthesis

Figure 7.3A shows the proliferation ratios of passage-2 aneurysmal SMCs cultured in the presence of TGF-β alone, oligomers alone, or both. Non-additive control aneurysmal SMCs proliferated 2.5 ± 0.32–fold over the 21 days. Addition of TGF-β to SMC cultures had no effect on proliferation ratios exhibited by non-additive controls (0.97 ± 0.08 –fold at 21 days vs. controls; p = 0.56). However, HA oligomers supplemented alone or together with TGF-β, suppressed cell proliferation ratios significantly relative to non-additive controls (0.81 ± 0.1 and 0.66 ± 0.15 –fold respectively; p = 0.002 and 0.0001).

When HA oligomers or TGF-β alone were provided to SMCs, significant increase in collagen synthesis (1.4 ± 0.07 and 1.33 ± 0.05–fold, respectively; **Figure 7.3B**) was observed, relative to untreated-cultures (p = 0.008 and 0.005, respectively). Addition of both the cues furthered collagen synthesis by 1.78 ± 0.18–fold, relative to controls (p = 0.008).

As shown in **Figure 7.4A**, addition of HA oligomers alone or together with TGF-β promoted tropoelastin synthesis by 1.17 ± 0.02–fold and 1.47 ± 0.05–fold, respectively, relative to non-additive cultures (p = 0.007 and 0.0001 vs. controls, respectively). However, addition of TGF-β alone had no effect on tropoelastin synthesis (0.94 ± 0.02-fold; p = 0.13). Interestingly, collagen and tropoelastin synthesis (779 ± 62 ng/ng DNA and 3516 ± 149 ng/ng DNA, respectively) observed within additive-free aneurysmal SMC cultures were much lower than we measured within healthy SMC cultures (22509 ± 668 ng/ng of DNA and 39070 ± 8707 ng/ng DNA)[360].

As explained earlier, elastin protein incorporated into the extracellular matrix was measured as a sum of two individual fractions, *i.e.*, a highly cross-linked, alkali-insoluble elastin (which represents structural elastin), and an alkali-soluble fraction. As shown in **Figure 7.4B** and C, the trends in matrix elastin protein production mirrored those observed for tropoelastin synthesis under identical conditions. Addition of 0.2 μg/mL of HA oligomers to aneurysmal cell cultures increased soluble and insoluble matrix elastin synthesis by 1.5 ± 0.11 and 1.23 ± 0.09–fold respectively, relative to non-additive controls (157 ± 26 ng/ng DNA and 216 ± 54 ng/ng DNA; p = 0.017 and 0.031, respectively). However, addition of TGF-β (1 ng/mL) alone had no effect on basal matrix elastin synthesis levels (soluble elastin: p = 0.56, insoluble elastin: p = 0.54). On the other hand, HA oligomers and TGF-β cues together stimulated the soluble and insoluble elastin fractions by 1.78 ± 0.29 and 1.56 ± 0.34–fold, respectively, relative to controls (p = 0.014 and 0.026, respectively). Overall, relative to controls, the total elastin output (sum of tropoelastin and matrix elastin fractions) increased by 1.19 ± 0.03, 0.96 ± 0.03 and 1.49 ± 0.06–fold, respectively, upon addition of oligomers alone, TGF-β alone, or both the cues together, respectively (**Figure 7.4D**).

7.3.3 LOX Protein Expression and Functional Activity

Figure 7.5A compared outcomes of western blot analysis of LOX protein expression with trends in biochemical quantification of matrix elastin. LOX protein expression increased significantly in cultures supplemented with TGF-β alone or together with HA oligomers (1.59 ± 0.05 and 1.72 ± 0.04–fold, relative to controls; $p < 0.001$ in

both the cases). However, addition of HA oligomers alone promoted only 1.03 ± 0.14–fold increase in LOX protein expression relative to controls (p = 0.73). In all the cases, no significant differences in the cellular LOX activities were observed though, relative to non-additive controls (data not shown). As shown in **Figure 7.5B**, relative to healthy control cell layers (11.85 ± 0.37 pg desmosine/ ng DNA), aneurysmal cells alone or in the presence of oligomers did not show any significant increase in desmosine synthesis (0.78 ± 0.01 and 0.92 ± 0.08-fold), while TGF-β alone or together with HA oligomers enhanced the desmosine synthesis by 1.07 ± 0.07–fold and 1.21 ± 0.03–fold, respectively (p = 0.06 and $p < 0.001$ vs. healthy controls).

7.3.4 Detection of Proteolytic Enzymes

As shown in **Figure 7.6A-B**, gel zymography analysis revealed that the MMPs-2 and 9 release was significantly higher within non-additive aneurysmal cell cultures relative to healthy control cultures (1.67 ± 0.16 and 2.07 ± 0.35–fold, respectively; p = 0.03 and 0.01), confirming their activated/ diseased phenotype. Addition of either oligomers or TGF-β alone to aneurysmal SMCs did not alter their basal MMP production levels. However, in the presence of both HA oligomers and TGF-β, production of MMPs-2 and 9 was marginally lower than those in aneurysmal control cultures (p = 0.08 and 0.03), and not different than those in healthy SMC cultures (p = 0.67 and 0.71). Similarly, as shown in **Figure 7.6C**, elastase activity within additive-free aneurysmal cell cultures was 1.19 ± 0.09–fold higher than those in healthy SMC cultures (0.23 ± 0.02 U/mL; p = 0.04). Addition of HA oligomer- or TGF-β-supplements to aneurysmal cell

cultures further increased elastase activity by 1.29 ± 0.08 and 1.39 ± 0.18–fold, respectively, (p = 0.015 and 0.03), relative to healthy SMC cultures, though these values are not significantly different from those in aneurysmal control cultures. In the presence of both the cues, elastase activity however remained unchanged relative to that in control aneurysmal cell cultures (1.01 ± 0.06–fold vs. 1.19 ± 0.09-fold higher than in healthy SMC cultures; p = 0.85).

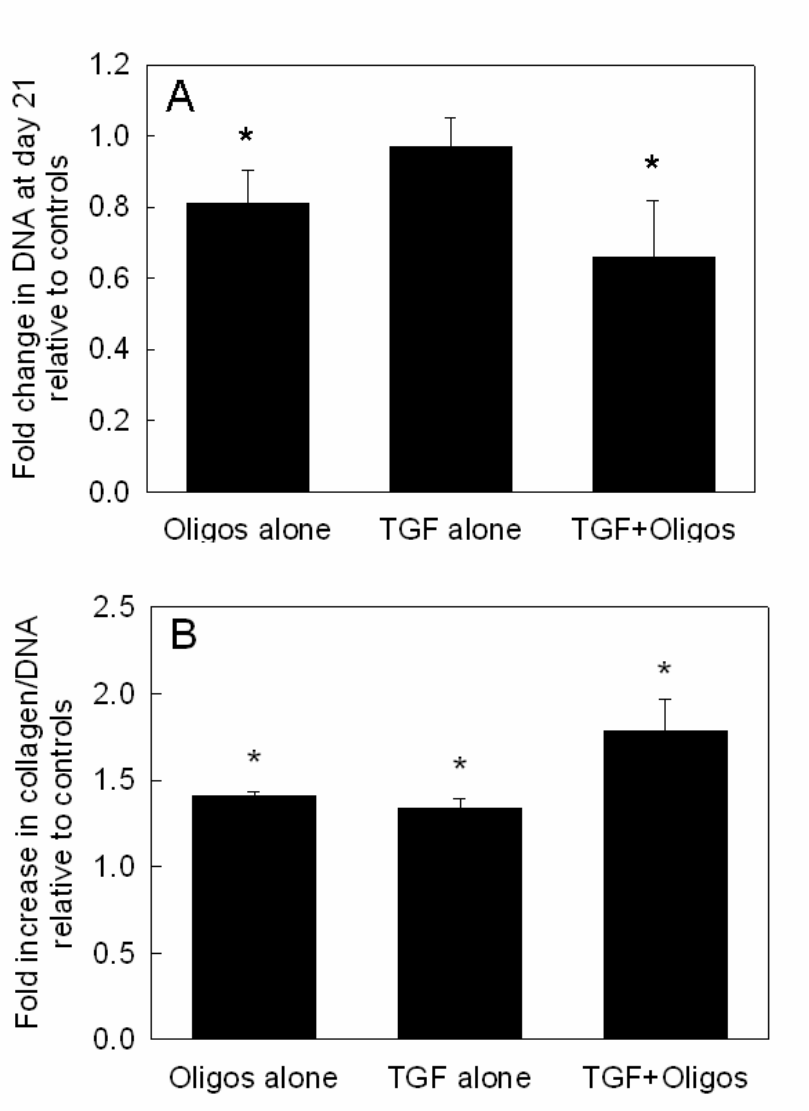

Figure 7.3. (A) Proliferation ratios of aneurysmal SMC cultures supplemented with oligomers alone, TGF-β alone, or cues together. Data shown represent mean ± SD of DNA content of cell layers after 21 days of culture, normalized to initial seeding density and further normalized to aneurysmal control cultures that received no additives (n = 3/case). (B) Effects of oligomers alone, TGF-β alone, and cues together, on total collagen synthesis by aneurysmal SMCs. Data shown (mean ± SD) are normalized to cellular DNA content at 21 days of culture and represented as fold change in protein production relative to aneurysmal controls (n = 3/case). $P < 0.05$ represents significant differences from controls (*).

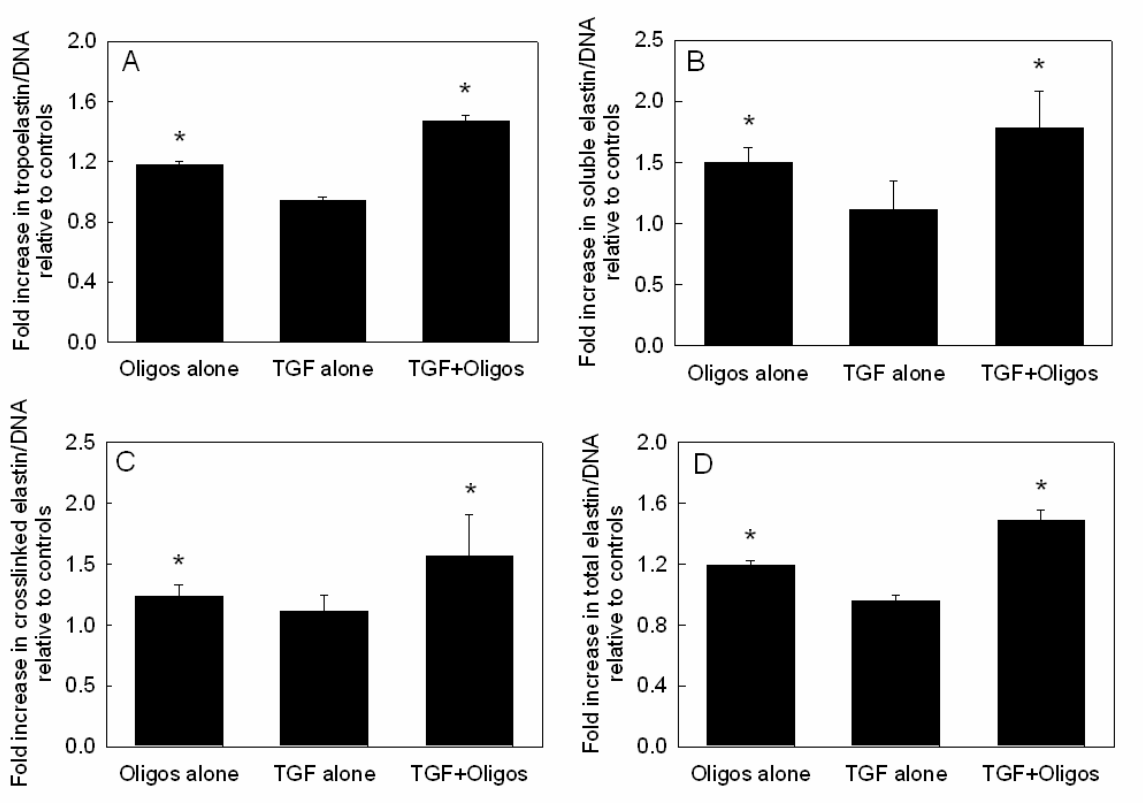

Figure 7.4. Effects of oligomers alone, TGF-β alone, and cues together, on tropoelastin (A), alkali-soluble (B), crosslinked matrix elastin (C), and total elastin (D) produced by aneurysmal SMCs. Data shown (mean ± SD) are normalized to cellular DNA content at 21 days of culture and represented as fold change in protein production relative to aneurysmal controls (n = 3/case). $P < 0.05$ represents significant differences from controls (*).

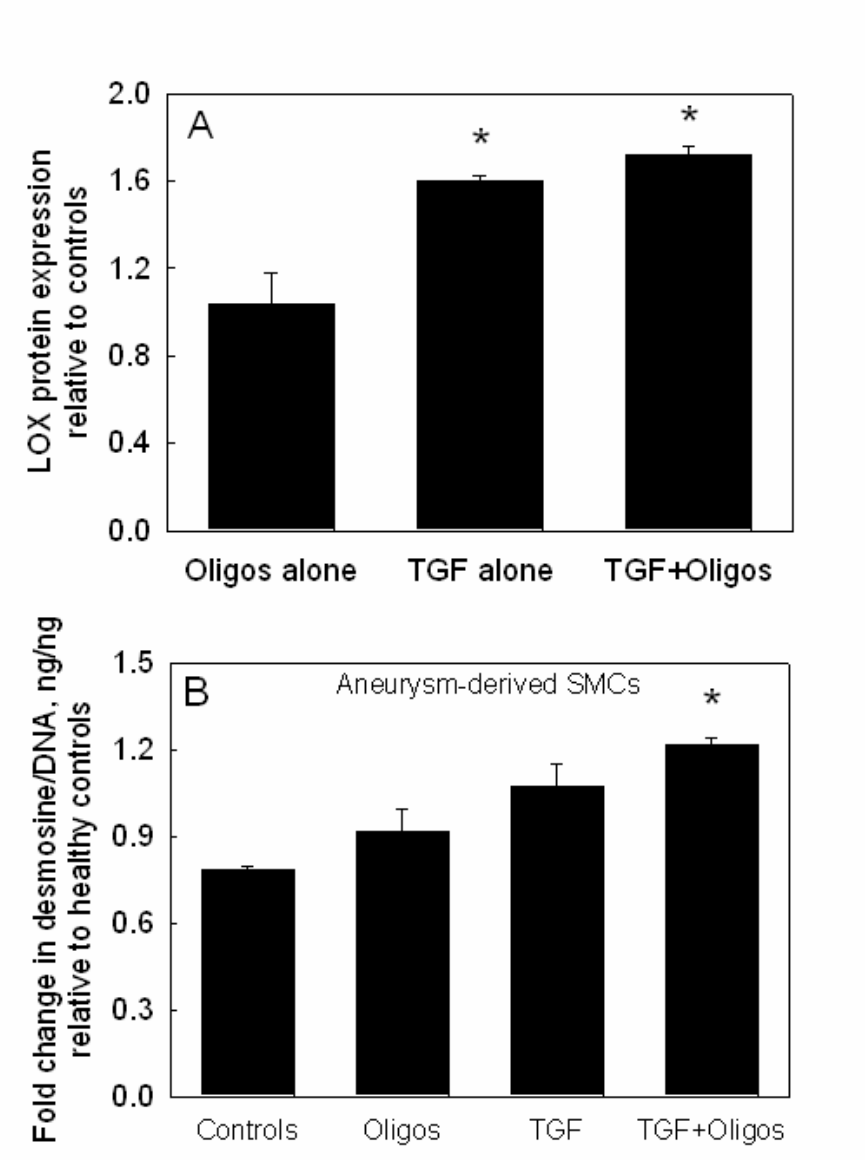

Figure 7.5. (A) SDS-PAGE/ Western blot analysis of tropoelastin and LOX proteins within the pooled medium of aneurysmal cultures at the end of 21 days. Data shown represent mean ± SD of 3 repeats/ case and are shown normalized to controls. (B) Desmosine amounts measured in test cell layers were normalized to corresponding DNA amounts (ng/ng), and further a similar ratio obtained for the healthy non-additive controls. Comparable trends were observed for the desmosine/DNA density and respective insoluble matrix elastin/DNA for selected cases.

Figure 7.6C shows the images of von kossa stained aneurysmal cell cultures treated with no-additives (panel D), oligomers alone (panel E), TGF-β alone (panel F), TGF-β and HA oligomers together (panel G). Untreated aneurysmal SMC cultures exhibited multiple calcific deposits (black); supplementing cultures with TGF-β alone did not alter patterns of matrix calcification, while addition of HA oligomers appeared to decrease the density of these deposits. However, the presence of both the cues significantly suppressed calcified deposits formation, though complete inhibition was not observed.

7.3.5 Immunodetection of Elastin, Fibrillin and LOX

Figure 7.7 shows immunofluorescence micrographs of 21-day old cell layers stained for elastin, fibrillin and LOX (red fluorescence) in cultures treated with oligomers alone, TGF-β alone or cues together. Non-additive aneurysmal cultures and negative controls (not-stained for primary antibodies) are also shown for comparison. While

featureless amorphous elastin deposits are seen in non-additive control cultures and TGF-β alone -treated cultures, more organized fibrous elastin was visible in cultures supplemented with HA oligomers alone or together with TGF-β. Fluorescence intensity of elastin matrices within cultures supplemented with both TGF-β and oligomers was much greater than in the absence of the cues, or either of the cues alone. Fluorescence intensity due to microfibrillin was similarly greater in cultures supplemented with HA oligomers alone or together with TGF-β, compared to non-additive controls or TGF-β alone treated cultures. The fibrillin appeared organized into honey-comb-like structures in cultures treated with cues alone or together, than in non-additive control cultures. However, in all cases, LOX was rather faintly expressed and was sparsely distributed.

7.3.6 Ultrastructure of Matrix Elastin

Figure 7.8 shows representative transmission electron micrographs of elastin matrices from 21-day aneurysmal cell cultures. Non-additive aneurysmal SMCs deposited discrete clumps of amorphous elastin protein between the cell layers (panel A – 50000x; panel B – 100000x). When TGF-β1 and HA oligomers were provided to aneurysmal SMC cultures (panel C – 50000x; panel D – 100000x), mature elastin fiber formation was favored, with the matrix containing numerous fully-formed bundles of fibers (100-200 nm diameter). Fibrillin (immunogold particle-stained) appeared in transverse sections as darkly stained nodules, and was located at the periphery of aggregating elastin fiber bundles, signifying normal elastic fiber assembly.

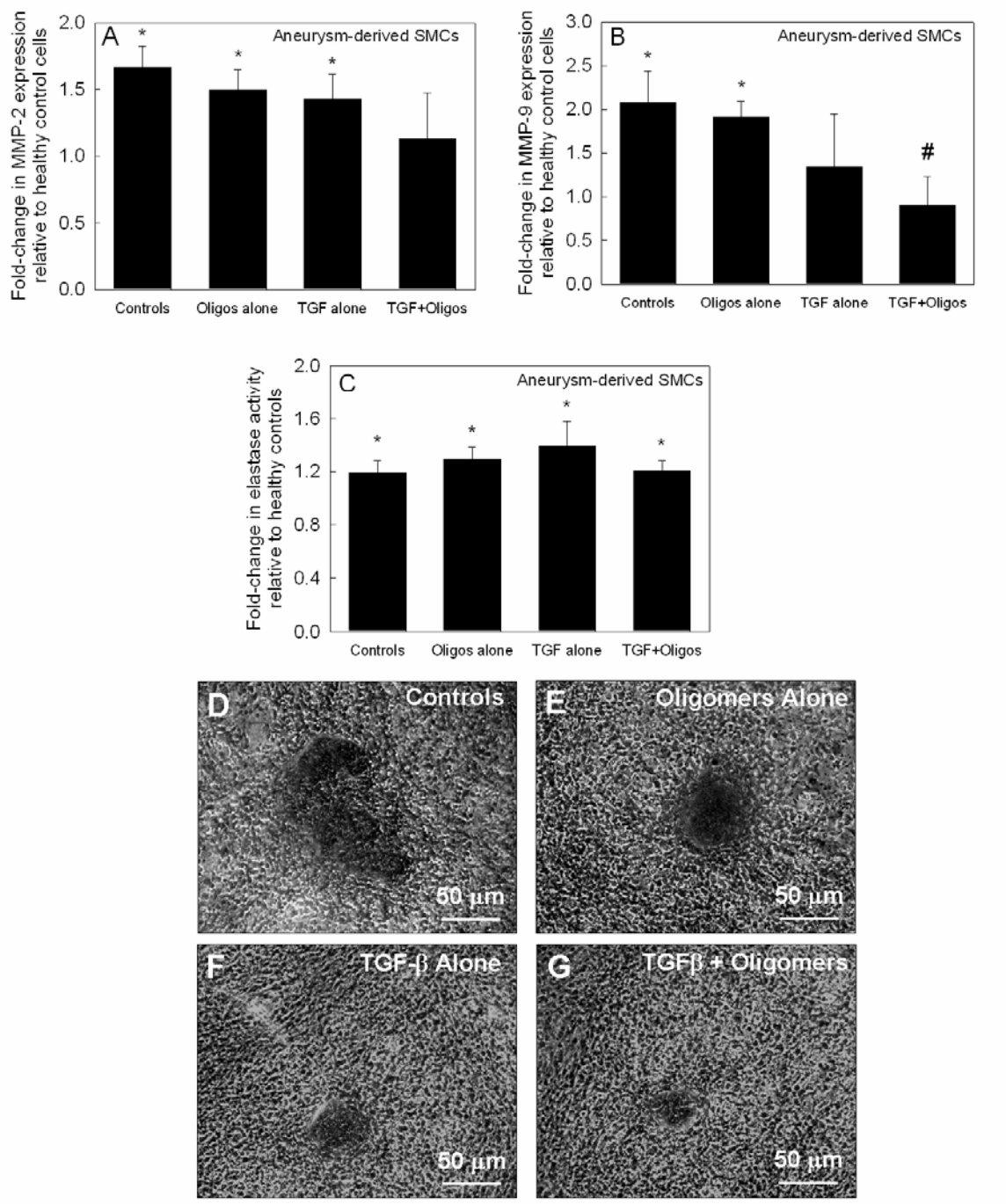

Figure 7.6. Gel zymography analysis revealed the presence of MMP-2 (A) and MMP-9 (B) within aneurysmal cultures treated with or without cues. Data were shown normalized to the respective values observed in healthy non-additive controls (n = 3/case).

(C) Elastase enzyme activity within aneurysmal SMC cultures treated with oligomers alone, TGF-β alone or together with HA oligomers. Data was shown normalized to the corresponding values in healthy non-additive cultures (n = 3/case). Von kossa staining images of aneurysmal cell layers treated with TGF-β alone, oligomers alone, or cues together. Significant calcific deposits were evident in control cultures and those treated with TGF-β alone or oligomers alone, while cultures which received cues together showed a decrease in the calcification.

7.4 Discussion

Our long-term goal is to enable elastin matrix regeneration on demand within elastin-degraded vessels such as within AAs, so as to stabilize and possibly even regress growing aneurysms and thus eliminate need for surgical intervention. Under normal physiological conditions, elastin turnover is very slow, and very little remodeling of elastin fibers occurs in adults[108]. This implies that active elastin matrix synthesis is almost a one-time phenomenon occurring pre- and post-natally, and that elastin repair/ regeneration is highly limited in adult tissues. Thus, regenerating elastin matrices following their enzymatic breakdown in certain inflammatory pathologies (e.g., atherosclerosis, aneurysms), or due to inherited (genetic) abnormalities in matrix assembly is not currently possible. Recent studies on aneurysm development and progression[156] reveal upregulated synthesis of elastolytic MMPs in inflamed vascular tissues, which rapidly degrade the elastin matrix to result in loss of tensile strength and elasticity of the vessel wall, and in progressive increases in vessel diameter[157]. Currently,

surgical excision of aneurysmal vessel segments at near-rupture stages of development, and their replacement with vascular grafts is the major mode of AA treatment. Recently, therapeutic approaches aimed at pharmacologically inhibiting MMP activity[157] or at chemically stabilizing existing aortic elastin against enzymatic degradation have been attempted. While these approaches are useful to stabilize aneurysms, their active regression is not possible, since healthy elastin architecture can not be regenerated. Thus, alternate tools to stimulate elastin regeneration and repair are required.

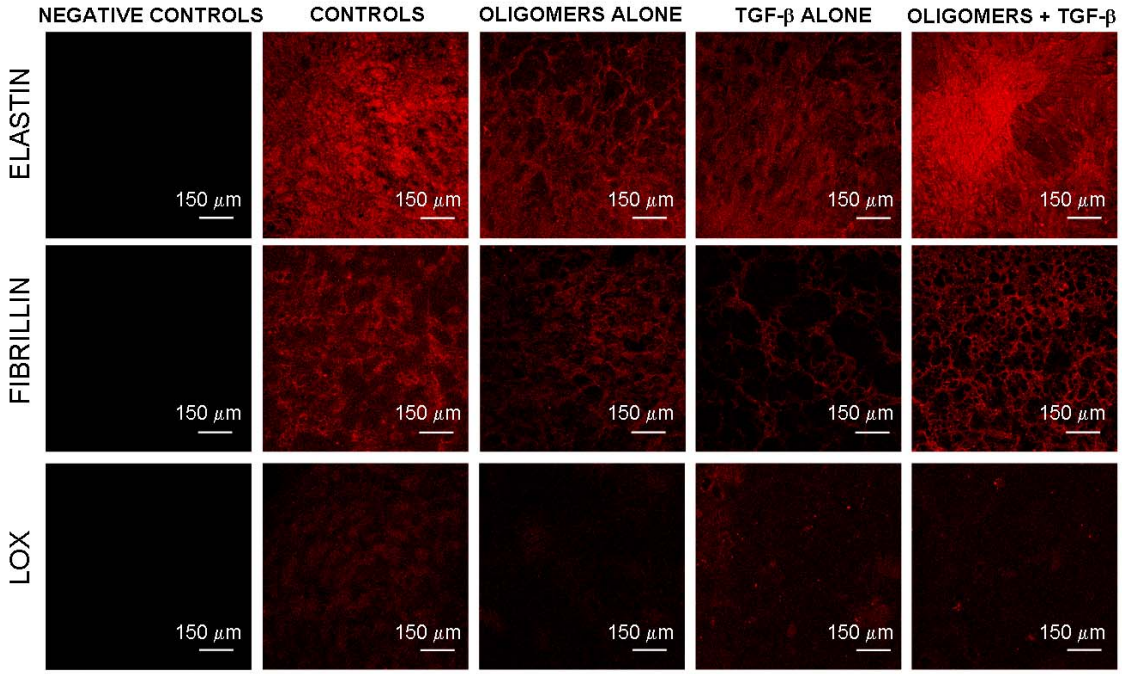

Figure 7.7. Immunodetection of elastin, fibrillin and LOX within control and test cell layers after 21 days of culture. An increase in matrix elastin, fibrillin and LOX is evident in aneurysmal cultures which received cues together, while cultures which received TGF-β alone or oligomers alone showed relatively less coloration. Scale bar: 150 μm.

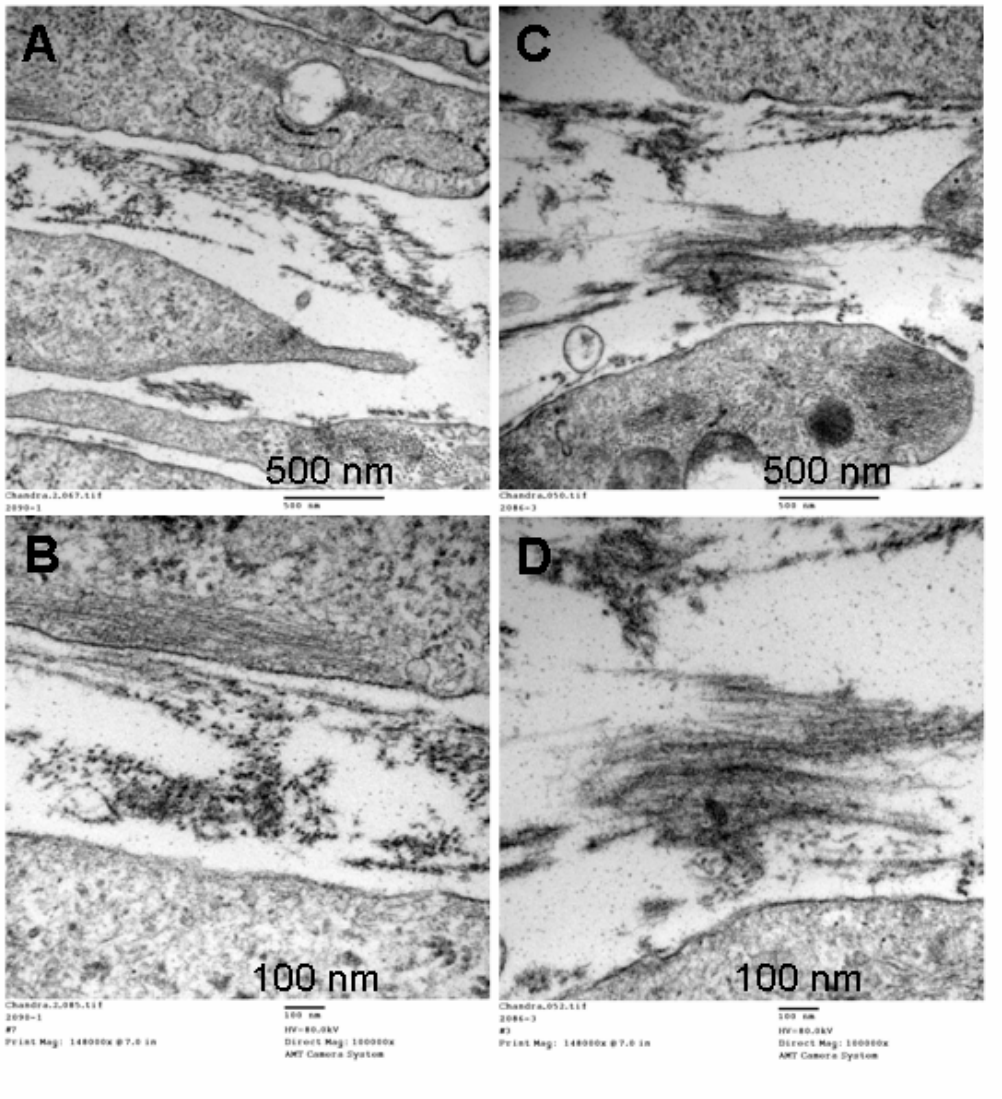

Figure 7.8. Representative TEM images of 21-day old aneurysmal SMC layers cultured additive-free (panel A - 50000x; panel B – 100000x) and aneurysmal cell layers cultured with elastogenic cues (panel C – 50000x; panel D – 100000x). Aggregating amorphous elastin clumps leading to the formation of elastin fibers can be clearly seen in aneurysmal cell cultures treated with cues (panels C, D), while aneurysmal SMC cultures which received no-additives (panels A, B) showed amorphous elastin deposits with sparse fiber formation.

Rodents have in recent years been popular as animal models to study AAs[391, 392]. These AAs have been induced either by genetic manipulation (deficiencies in LOX, TIMP-1, LDL-receptor, etc) or by chemical induction (intraluminal elastase infusion, peri-adventitial aortic injury with $CaCl_2$). These rodent models have exhibited several key facets of human aneurysms, such as medial layer disruption, inflammation, thrombus formation and rupture[3]. Of these, elastase infusion into infrarenal segment of aorta[393] and peri-aortic application of $CaCl_2$[390, 394], were shown to induce significant and progressive aortic dilation, and localized inflammation at the site of application within 4 weeks[389]. In a prior publication, Vyavahare et al. showed elevated MMP production at $CaCl_2$ aortic injury sites in rats, and extensive destruction of the elastic lamellae within[154, 395]. In the current study, $CaCl_2$-treated rat abdominal aortae developed aneurysms within 4 weeks post-injury, with an ~ 45% increase in aortic diameter, which is within the range reported by others as well[389, 390]. However, isolation of individual factors influencing cell behavior, e.g., changes in matrix composition and architecture, activation of inflammatory cells, is difficult in animal models. In this context, *in vitro* cell culture models of aneurysms may help to circumvent these problems, though such models have never been studied to date in the context of matrix regenerative therapies. Since cells can be propagated in culture, limitations to tissue procurement do not restrict rigorous evaluation of parameters that influence cell phenotype and matrix regenerative potential. Though a 2D cell culture model may not replicate the physiologic 3D matrix microenvironment, it is nevertheless invaluable to study biochemical regulation of cell phenotype by supplemented biomolecules.

Though the cells isolated from the rat aneurysmal aorta explants expressed smooth muscle α-actin confirming a SMC-phenotype, a significant number amongst them exhibited decreased volume/spreading especially in the first 10-days after seeding, in contrast to the spread morphology typically observed in healthy aortic SMC cultures. Such differences in phenotype between healthy and aneurysmal vascular SMCs have also been reported by others[396]. In general, these aneurysmal SMCs generated greater amounts of MMPs and elastases than did healthy control SMCs, and promoted deposition of a greater number of calcific deposits than in healthy SMC cultures, suggesting an activated phenotype. Interestingly, the aneurysmal SMCs proliferated more slowly than healthy SMCs[360] over the 21 day period (33 ± 4 % of healthy SMCs; $p < 0.001$), produced far less tropoelastin (9 ± 0.3 % of healthy SMCs; $p < 0.001$), collagen (3.4 ± 0.5 % of healthy SMCs; $p < 0.001$) and matrix elastin (11 ± 2 % of healthy SMCs; $p < 0.001$) than did by healthy control SMCs[360]. These results were supported by a significant decrease in the production of elastin crosslinking proteins (LOX and desmosine), as gauged from our biochemical analysis, and a visible decrease in elastin matrix density within these cultures relative to healthy cell controls[360]. Overall, these results point to the activated state of these isolated 'aneurysmal' SMCs when cultured *in vitro*.

To date, very few studies have investigated the effects of HA oligomers on RASMCs[58, 348], and none in the context of elastin matrix synthesis by aneurysmal cells. In our recent studies exploring the elastogenic benefits of HA oligomers (0.2 μg/mL) to elastin synthesis by *healthy* RASMCs[360], we found tropoelastin synthesis to be modestly

enhanced (48 ± 23%), though matrix elastin synthesis on a per cell basis remained unchanged. In this study, addition of HA oligomers alone (0.2 μg/mL) to aneurysmal RASMCs suppressed aneurysmal cell proliferation, promoted tropoelastin and insoluble matrix elastin synthesis (~ 1.2–fold), and increased collagen and soluble matrix elastin synthesis (~ 1.5-fold). However, the elastin matrix yield remained similar to that in non-additive aneurysmal cell cultures (10.8 ± 0.8 vs. 9.6 ± 2.1 %), which might be due to the lack of any significant, parallel increase in desmosine and LOX protein content within these cultures. Interestingly, the production of the MMPs-2 and 9 and the levels of elastase activity and matrix calcification in these cultures remained almost similar to that within additive-free (control) aneurysmal cell cultures, and significantly higher than that within additive-free healthy cell cultures. In contrast to their benefits to deposition of a fibrillar rather than amorphous elastin matrix deposition by healthy SMCs[58], HA oligomers alone provided no particular advantage to the quality of elastin matrix deposited by aneurysmal SMCs, since the elastin matrix was still largely non-fibrillar. These results lead us to speculate that much higher doses of HA oligomers may be necessary to stimulate aneurysmal RASMCs to enhance elastogenesis and elastin fiber deposition, in a manner that healthy RASMCs respond to when these oligomers are provided at low doses (0.2 μg/mL).

Though in a previous study[360], we found TGF-β1 (1 ng/mL) to significantly suppress healthy SMC proliferation and increase synthesis of matrix elastin (~2.5-fold) and collagen (~1.3-fold), the same dose of TGF-β had no effect on aneurysmal cell cultures, except for collagen synthesis (~ 1.3-fold). Also, TGF-β had no impact on

elastin yield within aneurysmal SMC cultures (11.2 ± 1.8% vs. 9.6 ± 2.1% in additive-free aneurysmal cultures; $p = 0.72$), although the same dose of TGF-β enhanced elastin matrix yield in healthy SMC cultures. The lack of elastogenic impact of TGF-β on rat aneurysmal SMCs when provided at doses optimized for healthy rat SMCs, similar to that with HA oligomers, suggests attenuated sensitivity of aneurysmal SMCs to these cues and thus the necessity to likely increase and re-optimize doses of these cues to upregulate elastogenesis by these diseased cell types. Nevertheless, attenuated TGF-β-induced effects on aneurysmal cell cultures also appear to directly correlate with increases in production of MMPs-2 and 9 and elastase activity, and greater distribution of non-fibrillar elastin, suggesting higher elastolytic activity within these cultures. Thus, the presence of either oligomers or TGF-β alone could be inciting increased elastolytic activity within aneurysmal cell cultures to rapidly generate soluble elastin peptides, and thereby discouraging accumulation of crosslinked elastin matrix.

When aneurysmal SMCs were exposed to both TGF-β1 and HA oligomeric cues, their impact on aneurysmal SMCs differed from that on healthy SMCs. The cues suppressed proliferation of aneurysmal SMCs, though not as severely as they did healthy SMCs[360]. The suppression in proliferation of aneurysmal SMCs has vital implications in deterring hyper-proliferation of these activated cell types when cues are delivered to an intact aneurysm site. Again, in both aneurysmal and healthy cell cultures, the cues enhanced tropo- and matrix elastin synthesis and that of collagen matrix, although the level of increase in aneurysmal cell cultures was far less compared to the healthy cell cultures. Besides, the cues improved elastin matrix yields in healthy SMC cultures, quite

possibly by increasing LOX protein synthesis and desmosine content[360]. Based on these outcomes, we logically expected similar improvements in elastin matrix yields within aneurysmal SMC cultures that received these cues, which however was not the case (10.7 ± 2.1% yield with cues vs. 9.6 ± 2.1% for additive-free aneurysmal cultures), despite measured increases in production of the elastin crosslinking enzyme, LOX. Perhaps due to increased LOX production, desmosine content per nanogram of insoluble elastin within these cultures was higher. Relative to healthy SMC cultures, the lack of net increase in matrix yield however may not be due to cues-derived benefits to recruitment and crosslinking of tropoelastin precursors, rather due to innately enhanced elastolytic activity within aneurysmal SMC cultures. Regardless, on a positive note, these elastogenic cues reduced matrix calcification and MMP production by aneurysmal SMCs, results that were not observed when either of these cues was provided to the same cultures.

7.5 Conclusions of this study

1. Calcium chloride-treatment was successfully used to induce aneurysm in a rat aorta within 4 weeks. Though the cells isolated from the medial portion of aneurysmal segments of aorta had SMC phenotype, they exhibited significant rounding within the first few days of culture.
2. Compared to healthy control RASMC cultures, aneurysmal SMCs proliferated less and produced less amounts of collagen, tropoelastin and matrix elastin. The

protein synthesis within these aneurysmal cell cultures could not be upregulated by adding either HA oligomers or TGF-β alone.

3. Relative to control aneurysmal cultures, addition of both the cues together resulted in significant increases of matrix elastin production by aneurysmal cells, which was not achieved by the presence of either of them.
4. The cues also significantly promoted crosslinking and deposition of matrix elastin, as evident from immunofluorescence and structural analysis images.
5. The cues might be of tremendous utility to enhance elastin matrix synthesis and organization into a mature form within aneurysmal or diseased vessels *in vivo*.

CHAPTER 8

CONCLUSIONS AND FUTURE OUTLOOK

8.1 Conclusions

The broad goal of this project was to develop biomolecular tools for enabling robust and faithful regeneration of elastin matrix networks within tissue engineered constructs, a severe problem at present. Extending upon this theme, an additional goal is to develop alternate therapies based on matrix engineering, for elastin repair and regeneration within aortic aneurysmal vessels. Drawing cues from pre-elastogenic microenvironments in developing embryos and within developing vascular plaques, we identified and evaluated a set of cues based on hyaluronic acid, growth factors, and other biomolecules, which we hypothesized would stimulate adult vascular SMCs to regenerate biologically and ultrastructurally faithful mimics of native vascular elastin networks in injured and diseased vessels. To achieve this goal, the project was divided into two modules. In the first module, the elastogenic effects of HA fragments (0.756-2000 kDa), growth factors (TGF-β1, IGF-1) and biomolecules (Cu^{2+} ions, LOX peptide), either alone or in combination, on healthy adult vascular SMCs was evaluated. Based on optimization of these cues in the first module, their utility for elastin synthesis, crosslinking and maturation by chronically-stimulated (TNF-α, aneurysmal) vascular SMCs was evaluated in the second module. These latter studies are expected to lay guidelines for further investigation into elastogenic stimulation of these diseased cell

types, and further delivery of these cues for effecting in situ elastin matrix regeneration within induced aneurysms.

Studies from module 1 demonstrated that the elastogenic responses of healthy adult SMCs can be influenced by the presence of growth factors and HA fragments. In general, HA oligomers (< 2 kDa) enhanced elastin synthesis and fibrillar organization by healthy adult SMCs, relative to other HA fragment-sizes (20-200 kDa), while HMW HA (> 2 MDa) appeared to influence elastin matrix deposition via purely physical means. Together, HA oligomers and TGF-β1, termed elastogenic cues, synergistically enhanced elastin synthesis, crosslinking and organization into mature elastin fibers within healthy adult SMC cultures. Interestingly, these cues also suppressed RASMC proliferation, which is advantageous from the standpoint of not inciting SMC hyperplasia if and when such cues are incorporated into HA biomaterials deployed within diseased vessels. These dramatic increases were achieved by significantly upregulating LOX production and activity, desmosine crosslink density and fibrillin deposition, thus signifying the normal elastin deposition process. The amino acid content of matrix elastin generated by the SMCs in the presence of these cues resembled that in native rat aortic elastin. This suggests a strong interplay between the TGF-β1 and HA oligomer signaling pathways for elastin synthesis, assembly and maturation by SMCs.

Further studies in module 1 investigated the standalone and combined benefits of Cu^{2+} ions and HA fragments on elastin synthesis, assembly and maturation. Higher tested doses (0.1 M) of copper ions delivered directly from soluble copper sulfate salt, increased matrix elastin yield and promoted deposition of fully-formed, highly-

crosslinked matrix elastin fibers (200-500 μm diameter). Interestingly, additional presence of HA oligomers or HMW HA furthered these increases. Despite these benefits of 0.1 M copper sulfate to elastin synthesis and maturation, an initial step increase in Cu^{2+} ion concentration (0.1 M) was mildly cytotoxic, causing temporary cell rounding and partial cell death in the initial days after cell seeding. Accordingly, an alternate strategy based on continuous release of Cu^{2+} ions from copper nanoparticles (CuNP) over the culture period was tested. Supplementation of cell cultures with CuNP (400 ng/mL) resulted in a cumulative release of Cu^{2+} ions equivalent to 0.1 M, with no cytotoxic effects on SMCs. The yields of matrix elastin tripled to ~ 60% in the presence of CuNP and HA oligomers, while the prevalence of mature elastin fibers in the ECM increased dramatically. These results are highly encouraging, because it validates our central hypothesis that (a) upregulation of LOX protein and activity within healthy adult SMC cultures by Cu^{2+} ions enhance crosslinking of elastin, and (b) highly-anionic HA fragments coacervate tropoelastin molecules on their surface to facilitate localized-crosslinking into elastin fibers. Similarly, in separate studies, we found that direct supplementation of exogenous LOX peptides (18.6 - 37.3 fg per cell) to RASMC cultures promoted yields of matrix elastin by 1.6-2-fold, via increases in endogenous LOX activity and production.

Taken together, the results from module 1 suggest that, a combination of cues comprising HA oligomers (0.2 μg/mL), TGF-β1 (1 ng/mL) and Cu^{2+} ions (0.1 M), might be highly effective in upregulating elastin synthesis, crosslinking, matrix deposition, and mature fiber formation, within healthy adult SMC cultures. These elastogenic cues might

be of tremendous utility to restore elastin matrix homeostasis in de-elasticized vessels and tissue engineering constructs, and possibly even serve as an *in vitro* model to investigate elastogenesis during early morphogenesis and wound healing in adult tissues.

Results from module 2 attest to the utility of elastogenic cues, HA oligomers and TGF-β1, identified and optimized in module 1, to elastin repair and regeneration by chronically-stimulated SMCs. As expected, TNF-α-activated vascular SMCs and aneurysmal SMCs released cytokines/ chemokines/ interleukins, elastolytic MMPs-2, 9 and other elastases, to promote calcific deposition and matrix destruction in a manner that simulates events within inflammation-ridden vascular aneurysms *in vivo*. Encouragingly, addition of cues suppressed release of inflammatory markers within these cultures, encouraged elastin synthesis, crosslinking, and matrix formation. These increases were facilitated by simultaneously promoting LOX protein synthesis and activity within these cultures. Finally, these cues were also instrumental in suppressing elastolytic activity within these cultures. Overall, these results attest to the elastogenic utility of the cues in (a) upregulating elastin matrix production by activated vascular SMCs, (b) organizing elastin protein into fibers, and (c) simultaneously stabilizing this matrix by attenuating production of elastolytic enzymes. Unfortunately, despite elastogenic upregulation by provided cues, tropoelastin/ matrix elastin production by aneurysmal SMCs remains one order of magnitude lower than that produced by healthy SMCs seeded at identical density and passage. Thus, though indications are that our elastogenic cues could potentially be useful, either by themselves or together with other treatment options to repair and regenerate elastin matrices within diseased and aneurysmal blood vessels, delivery doses

need to be re-optimized separately for these diseases cell types *in vitro*. Further, the concentration of these cues refined based on pharmaco-kinetics *in vivo*, i.e., systemic transport, diffusion and consumption by cells.

8.2 Future Outlook

Despite the numerous positive outcomes listed above, the long-term realization of the project objectives is contingent on elucidating several unknowns, which have not yet been explored in this project and will be addressed by others in our group. For example, the cellular-signaling pathways mediating the observed increases in elastin synthesis and maturation, on addition of cues is not yet clear. Similarly, the mechanisms by which Cu^{2+} ions promote endogenous LOX production and activity in SMC cultures, thereby enhancing elastin crosslinking mechanism is still elusive. Thus, future studies can investigate:

1. Benefits of culturing SMCs in 3-D scaffolds or gels (made of HA fragments) over the current 2-D cultures to elastin synthesis and matrix quality
2. Effects of dynamic-conditioning, i.e., mechanical stimuli (such as shear force, pulsatile-stretch) of cell-seeded HA scaffolds to elastin synthesis, matrix formation and organization into fibrillar networks
3. Design and fabrication of a customized bioreactor for long-term (6-8 week), high-density SMC cultures, with or without cues, and/or mechanical stimuli
4. Benefits of LOX gene-transfected cells to recruitment and crosslinking of tropoelastin into a structural matrix elastin

5. Identification and quantification of specific genes and cell surface-receptors involved in elastogenesis, modulated by the addition of HA oligomers and/or TGF-β1
6. Re-optimizing the concentrations of cues which will upregulate elastin synthesis and matrix deposition in chronically-stimulated cell cultures to levels observed in healthy SMC cultures
7. Controlled localized-delivery of these re-optimized elastogenic cues to aneurysm sites in a rat aorta *in vivo*, using an osmotic pump fitted with a catheter
8. Impact of diverse pre-existing matrix microenvironments (such as within aneurysms) on cell phenotype and response to elastogenic cues, in the presence or absence of leukocyte-mediated matrix debridements.
9. Utility of these cues in other relevant areas of tissue engineering, such as in wound healing, and cosmetic/ dermal tissue regeneration.

APPENDIX

1. Study Limitations

Despite the perceived potential advantages of HA fragments, growth factors and biomolecules to elastin biosynthesis by adult RASMCs, limitations pertaining to this study must be addressed prior to their application to tissue engineering systems. These limitations are outlined below.

1. The elastogenic utility of these optimized cues was demonstrated only in *healthy* and not *diseased/activated* rat aortic smooth muscle cell cultures.
2. While protein synthesis by lower passage (1-8) cells was upregulated by the provided elastogenic cues, it is possible that higher passage cells will be capable of diminished basal elastin synthesis and less responsive to the cues.
3. The HA oligomers used in this study were obtained by enzymatic digestion of HMW HA, using optimized protocols developed in our lab. These oligomeric mixtures contained predominantly 4-mers, with 6-mers and 8-mers forming the balance. However, any changes in digestion conditions (time, concentrations, temperature, source of HMW HA, etc) can alter the composition of the HA oligomer mixtures, which might significantly alter the cellular response to these mixtures. Thus, high level of quality control in the preparation of these oligomer mixtures is warranted.
4. In general, the source and gender of rats from which healthy cells were sourced for our study, are not expected to significantly affect elastin protein synthesis.

However, since elastin gene transcription, mRNA stability, secretion and deposition is development stage-specific, the utility of these cues need to be optimized separately for stimulating elastin expression in neonatal, post-natal and adult stages. Similarly, irrespective of the cell seeding density, the concentrations of TGF-β1, HA oligomers and Cu^{2+} ions must be similar on a per cell basis, to achieve identical results.

5. While our experiments indicate that adult RASMCs respond well to exogenous cues, similar outcomes may not be guaranteed with other elastin-producing cell types such as fibroblasts (dermal, valvular, pulmonary), smooth muscle cells (lung, intestines, bladder), endothelial cells, etc. Characterization of the elastogenic potential of these cells under basal and induced conditions is therefore necessary.
6. Since we observed that elastin synthesis, matrix yield and deposition within aneurysmal and TNF-α stimulated cultures was much lower than that observed within healthy SMC cultures, when exposed to similar concentrations of elastogenic cues, we believe that the doses of these cues must be increased incrementally and re-optimized to obtain the level of elastin/elastin matrix synthesis exhibited by healthy, neonatal SMCs.
7. The *in vitro* cultures of aneurysmal cells in this study were performed under tightly-regulated conditions, i.e., absence of localized inflammatory-, and degraded matrix-microenvironment in which these cells typically exist *in vivo*. Thus, for these cues to be successfully delivered *in vivo* within diseased/ injured

rat aorta for elastin regeneration by SMCs, the doses of these cues have to be appropriately re-optimized. Re-optimized doses of these cues in the context of aneurysmal cell cultures and elastin/matrix-compromised vessels maintained in organ culture, might serve as a starting point for their *in vivo* delivery to sites of induced rat aneurysms.

8. SMC density *in vivo* within blood vessels will be much higher than that within cultures *in vitro*. Thus, it would seem logical to deliver scaled-up concentrations so that cells *in vivo* receive similar dose of cues on a per cell basis. In addition, detailed pharmacokinetic analysis of the fate of delivered biomolecular cues in rats will be necessary to account for unavailability of cues at the targeted site of delivery (i.e., induced aortic aneurysm) via reaction, excretion, systemic distribution etc.

2. Analysis of Elastin Protein Synthesis within RASMC Cultures

In chapters 3-5, we have detailed the benefits of growth factors (TGF-β1, IGF-1) or copper ions ($CuSO_4$, CuNP), in the presence or absence of HA fragments, to RASMC proliferation and protein (collagen, elastin) synthesis. The elastin protein synthesis data was shown normalized to DNA amounts in respective cultures, and then normalized to similar ratios observed in non-additive control cultures. From the data, it might appear that the observed increase/decrease in elastin synthesis (e.g., in the presence of HA oligomers and TGF-β1) may be due to the corresponding decrease/increase in cell proliferation over the three weeks, in the respective cases. In other words, one might

wonder whether the cues really affected elastin synthesis on a per cell basis, and if so, what reliable comparison models can be applied to verify the same. To check these ambiguities, here we will detail two alternative ways to represent the elastin synthesis data shown in chapters 3-5. In Table A-1, we present absolute amounts of total elastin protein synthesized and the total elastin protein amounts normalized to total collagen synthesized in the respective cases. Since collagen is also a predominant protein synthesized by SMCs, we choose to normalize the elastin protein synthesis to collagen protein amounts within respective cell cultures. We believe that similar arguments can be extended for individual protein components such as tropoelastin, collagen and matrix elastin synthesized in the respective cases. A few salient points which merit detailed discussion are presented here.

As shown in Figure 3.1, even though RASMC proliferation was inhibited in the presence of TGF-β relative to controls, the cell density still increased 1.7 ± 0.1-fold within the 21 days of culture. Over 21 days of culture, while cells proliferated from an initial seeding density of 20,000 cells/well to 68000 ± 10000 cells/well in non-additive control cultures, these 20,000 cells/well proliferated to 34000 ± 6800 cells/well within TGF-β additive cultures. Similarly, in the presence of both TGF-β and HA oligomers, the initial cell seeding density increased by 1.9 ± 0.06–fold over the 21 day culture period. Thus, RASMCs did not undergo apoptosis or necrosis in the presence of external cues, but rather proliferated slowly compared to those in non-additive cultures. Similar logic can be evoked even with the RASMC proliferation in cultures treated with IGF-1 or Cu^{2+} ions.

As shown in Table A-1, the absolute total elastin protein amounts synthesized by SMCs significantly depend on the culture conditions, i.e., varying HA fragment sizes and growth factors. These amounts were not normalized to the respective DNA content in these cultures at the end of 21 days. When TGF-β alone or together with HA oligomers (or VLMW HA) were provided to SMCs, the total elastin protein synthesis increased relative to that in non-additive controls. These trends also broadly represent the DNA normalized values of tropoelastin and matrix elastin within these cultures. Similarly, when the absolute elastin protein amounts were normalized to the respective collagen amounts in those cultures, significant differences were observed between experimental groups and controls. These observations were supported by similar differences in elastin mRNA expression, western blots of tropoelastin and LOX proteins and LOX activity in these cultures, and mature elastin fiber formation as clearly evident from electron microscopy images. Thus, in conclusion, we believe that the significant fold-changes in elastin protein expression (normalized to DNA content) achieved by provision of elastogenic cues, is not a mere reflection of corresponding fold-changes in cell density, but due to altered changes at transcription and translation levels.

	Experimental condition	Total elastin protein synthesized (avg), mg	Total elastin/total collagen, mg/mg
TGF-β study	Controls	189.3	1.88±0.02
	TGF-β alone	203.1	1.97±0.04
	Oligomers+TGF-β	329.6	0.55±0.05
	VLMW HA+TGF-β	219.3	2.16±0.04
	LMW HA+TGF-β	183.5	1.8±0.002
	HMW HA+TGF-β	190.5	1.84±0.04
IGF-1 study	Controls	64.9	1.31±0.21
	IGF-1 alone	66.1	1.17±0.2
	Oligomers+ IGF-1	59.3	1.49±0.18
	VLMW HA+IGF-1	70.8	1.26±0.08
	LMW HA+IGF-1	78.9	1.42±0.28
	HMW HA+IGF-1	82.8	1.4±0.27

Table A-1. Representative data of total elastin protein synthesized and elastin protein synthesized relative to collagen in respective cultures, for selected cases in this study.

REFERENCES

1. Selle JG, Robicsek F, Daugherty HK, Cook JW. Thoracoabdominal aortic aneurysms. A review and current status. Ann Surg. 1979;189(2):158-164.

2. Milewicz DM, Dietz HC, Miller DC. Treatment of aortic disease in patients with Marfan syndrome. Circulation. 2005;111(11):e150-157.

3. Daugherty A, Cassis LA. Mouse Models of Abdominal Aortic Aneurysms. Arterioscler Thromb Vasc Biol. 2004;24:429-434.

4. Rentschler M, Baxter BT. Pharmacological approaches to prevent abdominal aortic aneurysm enlargement and rupture. Ann N Y Acad Sci. 2006; 1085:39-46.

5. Thompson RW. Basic science of abdominal aortic aneurysms: emerging therapeutic strategies for an unresolved clinical problem. Curr Opin Cardiol. 1996;11:504–518.

6. Huffman MD, Curci JA, Moore G, Kerns DB, Starcher BC, Thompson RW. Functional importance of connective tissue repair during the development of experimental abdominal aortic aneurysms. Surgery. 2000;128:429–438.

7. Campa JS, Greenhalgh RM, Powell JT. Elastin degradation in abdominal aortic aneurysms. Atherosclerosis. 1987;65:13–21.

8. Sinha S, Frishman WH. Matrix metalloproteinases and abdominal aortic aneurysms: a potential therapeutic target. J Clin Pharmacol. 1998;38:1077–1088.

9. Freestone T, Turner RJ, Coady A, Higman DJ, Greenhalgh RM, Powell JT. Inflammation and matrix metalloproteinases in the enlarging abdominal aortic aneurysm. Arterioscler Thromb Vasc Biol. 1995;15:1145–1151.

10. Adam DJ, Mohan IV, Stuart WP, Bain M, Bradbury AW. Community and hospital outcome from ruptured abdominal aortic aneurysm within the catchment area of a regional vascular surgical service. J Vasc Surg. 1999;30:922-8.

11. Mecham RP, Broekelmann TJ, Fliszar CJ, Shapiro SD, Welgus HG, Senior RM. Elastin degradation by matrix metalloproteinases. Cleavage site specificity and mechanisms of elastolysis. J Biol Chem. 1997;272:18071–18076.

12. Petersen E, Gineitis A, Wagberg F, Angquist KA. Activity of matrix metalloproteinase-2 and -9 in abdominal aortic aneurysms. Eur J Vasc Endovasc Surg 2000;20:457-461.

13. Lindholt JS, Jorgensen B, Klitgaard NA, Hennererg EW. Systemic levels of cotinine and elastase, but not pulmonary function, are associated with the progression of small abdominal aortic aneurysms. Eur J Vasc Endovasc Surg. 2003;26:418-422.

14. Guo DC, Papke CL, He R, Milewicz DM. Pathogenesis of thoracic and abdominal aortic aneurysms. Ann N Y Acad Sci. 2006; 1085:339-52.

15. Ernst CB. Abdominal aortic aneurysms. N Engl J Med. 1993;328:1167-1172.

16. Nowygrod R, Egorova N, Greco G, Anderson P, Gelijns A, Moskowitz A, et al. Trends, complications, and mortality in peripheral vascular surgery. J Vasc Surg. 2006;43:205-16.

17. Isselbacher EM. Thoracic and abdominal aortic aneurysms. Circulation 2005; 111:816-28.

18. Dawson J, Choke E, Sayed S, Cockerill G, Loftus I, Thompson MM. Pharmacotherapy of abdominal aortic aneurysms. Curr Vasc Pharmacol. 2006;4:129–149.

19. Miralles M, Wester W, Sicard GA, Thompson R, Reilly JM. Indomethacin inhibits expansion of experimental aortic aneurysms via inhibition of the cox2 isoform of cyclooxygenase. J Vasc Surg. 1999;29:884–892.

20. Baxter BT, Pearce WH, Waltke EA, Littooy FN, Hallett JW Jr, Kent KC, Upchurch GR Jr, Chaikof EL, Mills JL, Fleckten B, Longo GM, Lee JK, Thompson RW. Prolonged administration of doxycycline in patients with small asymptomatic abdominal aortic aneurysms: report of a prospective (phase II) multicenter study. J Vasc Surg. 2002;36:1–12.

21. Isenburg JC, Simionescu DT, Starcher BC, Vyavahare NR. Elastin stabilization for treatment of abdominal aortic aneurysms. Circulation. 2007, 3;115(13):1729-37.

22. Kim BS, Nikolovski J, Bonadio J, Smiley E, Mooney DJ. Engineered smooth muscle tissues: regulating cell phenotype with the scaffold. Exp Cell Res. 1999;251(2):318-328.

23. Mitchell SL, Niklason LE. Requirements for growing tissue-engineered vascular grafts. Cardiovasc Pathol. 2003;12(2):59-64.

24. Johnson DJ, Robson P, Hew Y, Keeley FW. Decreased elastin synthesis in normal development and in long-term aortic organ and cell cultures is related to rapid and selective destabilization of mRNA for elastin. Circ Res. 1995;77(6):1107-1113.

25. Butler DL, Goldstein SA, Guilak F. Functional tissue engineering: the role of biomechanics. J Biomech Eng. 2000;12(6):570-575.

26. Hoffman AS. Hydrogels for biomedical applications. Ann N Y Acad Sci. 2001;944:62-73.

27. Wang Y, Ameer GA, Sheppard BJ, Langer R. A tough biodegradable elastomer. Nat Biotechnol. 2002;20(6):602-606.

28. Langerak SE, Groenink M, van der Wall EE, Wassenaar C, Vanbavel E, van Baal MC, Spaan JA. Impact of current cryopreservation procedures on mechanical and functional properties of human aortic homografts. Transpl Int. 2001;14(4):248-255.

29. Allaire E, Guettier C, Bruneval P, Plissonnier D, Michel JB. Cell-free arterial grafts: morphologic characteristics of aortic isografts, allografts, and xenografts in rats. J Vasc Surg. 1994;19(3):446-456.

30. Allaire E, Bruneval P, Mandet C, Becquemin JP, Michel JB. The immunogenicity of the extracellular matrix in arterial xenografts. Surgery. 1997;122(1):73-81.

31. Daamen WF, Hafmans T, Veerkamp JH, Van Kuppevelt TH. Comparison of five procedures for the purifi-cation of insoluble elastin. Biomaterials. 2001;22(14):1997-2005.

32. Bailey MT, Pillarisetti S, Xiao H, Vyavahare NR. Role of elastin in pathologic calcification of xenograft heart valves. J Biomed Mater Res A. 2003;66(1):93-102.

33. Schenke-Layland K, Vasilevski O, Opitz F, Konig K, Riemann I, Halbhuber KJ, Wahlers T, Stock UA. Impact of decellularization of xenogeneic tissue on extracellular matrix integrity for tissue engineering of heart valves. J Struct Biol. 2003;143(3):201-208.

34. Grauss RW, Hazekamp MG, Oppenhuizen F, van Munsteren CJ, Gittenberger-de Groot AC, DeRuiter MC. Histological evaluation of decellularised porcine aortic valves: matrix changes due to different decellularisation methods. Eur J Cardiothorac Surg. 2005;27(4):566-571.

35. Wright ER, Conticello VP. Self-assembly of block copolymers derived from elastin-mimetic polypeptide sequences. Adv Drug Deliv Rev. 2002;54(8):1057-1073.

36. Bellingham CM, Lillie MA, Gosline JM, Wright GM, Starcher BC, Bailey AJ, Woodhouse KA, Keeley FW. Recombinant human elastin polypeptides self-assemble into biomaterials with elastin-like properties. Biopolymers. 2003;70(4):445-455.

37. Mithieux SM, Rasko JE, Weiss AS. Synthetic elastin hydrogels derived from massive elastic assemblies of self-organized human protein monomers. Biomaterials. 2004;25(20):4921-4927.

38. Lee SH, Kim BS, Kim SH, Choi SW, Jeong SI, Kwon IK, Kang SW, Nikolovski J, Mooney DJ, Han YK, Kim YH. Elastic biodegradable poly(glycolide-co-caprolactone) scaffold for tissue engineering. J Biomed Mater Res A. 2003;66(1):29-37.

39. Stankus JJ, Guan J, Wagner WR. . Fabrication of biodegradable elastomeric scaffolds with sub-micron morphologies. J Biomed Mater Res A. 2004;70(4):603-614.

40. Jeong SI, Kwon JH, Lim JI, Cho SW, Jung Y, Sung WJ, Kim SH, Kim YH, Lee YM, Kim BS, Choi CY, Kim SJ. Mechano-active tissue engineering of vascular smooth muscle using pulsatile perfusion bioreactors and elastic PLCL scaffolds. Biomaterials. 2005;26(12):1405-1411.

41. Trask TM, Trask BC, Ritty TM, Abrams WR, Rosenbloom J, Mecham RP. Interaction of tropoelastin with the amino-terminal domains of fibrillin-1 and fibrillin-2 suggests a role for the fibrillins in elastic fiber assembly. J Biol Chem. 2000;275(32):24400-24406.

42. Werth VP, Shi X, Kalathil E, Jaworsky C. Elastic fiber-associated proteins of skin in development and photoaging. Photochem Photobiol. 1996;63(3):308-313.

43. Long JL, Tranquillo RT. Elastic fiber production in cardiovascular tissue-equivalents. Matrix Biol. 2003;22(4):339-350.

44. Opas M. Substratum mechanics and cell differentiation. Int Rev Cytol. 1994;150:119-137.

45. Radhakrishnamurthy B, Ruiz H, Berenson GS. Interactions of glycosaminglycans with collagen and elastin in bovine aorta. Adv Exp Med Biol. 1977;82:160-163.

46. Bartholomew JS, Anderson JC. Investigation of relationships between collagens, elastin and proteoglycans in bovine thoracic aorta by immunofluorescence techniques. Histochem J. 1983;15(12):1177-1190.

47. Baccarani-Contri M, Vincenzi D, Cicchetti F, Mori G, Pasquali-Ronchetti I. Immunocytochemical localization of proteoglycans within normal elastin fibers. Eur J Cell Biol. 1990;53(2):305-312.

48. Wight TN. Versican: a versatile extracellular matrix proteoglycan in cell biology. Curr Opin Cell Biol. 2002;14(5):617-623.

49. Aspberg A, Adam S, Kostka G, Timpl R, Heinegard D. Fibulin-1 is a ligand for the C-type lectin domains of aggrecan and versican. J Biol Chem. 1999;274(29):20444-20449.

50. Isogai Z, Aspberg A, Keene DR, Ono RN, Reinhardt DP, Sakai LY. Versican interacts with fibrillin-1 and links extracellular microfibrils to other connective tissue networks. J Biol Chem. 2002;277(6):4565-4572.

51. Zimmermann DR, Dours-Zimmermann MT, Schubert M, Bruckner-Tuderman L. Versican is expressed in the proliferating zone in the epidermis and in association with the elastic network of the dermis. J Cell Biol. 1994;124(5):817-825.

52. Fornieri C, Baccarani-Contri M, Quaglino D Jr, Pasquali-Ronchetti I. Lysyl oxidase activity and elastin/glycosaminoglycan interactions in growing chick and rat aortas. J Cell Biol. 1987;105(3):1463-1469.

53. Bressan GM, Pasquali-Ronchetti I, Fornieri C, Mattioli F, Castellani I, Volpin D. Relevance of aggregation properties of tropoelastin to the assembly and structure of elastic fibers. J Ultrastruct Mol Struct Res. 1986;94(3):209-216.

54. Lapcik L. Jr, Lapcik L, De Smedt S, Demeester J, Chabrecek P. Hyaluronan: Preparation, structure, properties, and applications. Chem Rev. 1998;98(8):2663-2684.

55. Toole BP. Hyaluronan: from extracellular glue to pericellular cue. Nat Rev Cancer. 2004;4(7):528–539.

56. Rockey DC, Chung JJ, McKee CM, Noble PW. Stimulation of inducible nitric oxide synthase in rat liver by hyaluronan fragments. Hepatology. 1998;27(1):86-92.

57. Evanko SP, Johnson PY, Braun KR, Underhill CB, Dudhia J, Wight TN. Platelet-derived growth factor stimulates the formation of versican-hyaluronan aggregates and pericellular matrix expansion in arterial smooth muscle cells. Arch. Biochem. Biophys. 2001;394(1):29–38.

58. Joddar B, Ramamurthi A. Elastogenic effects of exogenous hyaluronan oligosaccharides on vascular smooth muscle cells. Biomaterials. 2006;27(33):5698-5707.

59. Noble PW. Hyaluronan and its catabolic products in tissue injury and repair. Matrix Biol. 2002;21(1):25-29.

60. Joddar B, Ramamurthi A. Fragment size- and dose-specific effects of hyaluronan on matrix synthesis by vascular smooth muscle cells. Biomaterials. 2006;27(15):2994-3004.

61. Robert L, Jacob MP, Fulop T. Cell– elastin interaction and signaling. Pathol Biol. 2005;53:399-404.

62. Rodgers UR, Weiss AS. Cellular interactions with elastin. Pathol Biol. 2005;53:390-398.

63. Davidson JM, Zoia O, Liu JM. Modulation of transforming growth factor-beta 1 stimulated elastin and collagen production and proliferation in porcine vascular smooth muscle cells and skin fibroblasts by basic fibroblast growth factor, transforming growth factor-alpha, and insulin-like growth factor-I. J Cell Physiol. 1993;155(1):149-156.

64. Wolfe BL, Rich CB, Goud HD, Terpstra AJ, Bashir M, Rosenbloom J, Sonenshein GE, Foster JA. Insulin-like growth factor-I regulates transcription of the elastin gene. J Biol Chem. 1993;268(17):12418-12426.

65. Badesch DB, Lee PD, Parks WC, Stenmark KR. Insulin-like growth factor I stimulates elastin synthesis by bovine pulmonary arterial smooth muscle cells. Biochem. Biophys. Res. Commun. 1989;160(1):382-387.

66. Shanley CJ, Gharaee-Kermani M, Sarkar R, Welling TH, Kriegel A, Ford JW, Stanley JC, Phan SH. Transforming growth factor-beta 1 increases lysyl oxidase enzyme activity and mRNA in rat aortic smooth muscle cells. J Vasc Surg. 1997;25(3):446-452.

67. Noguchi A, Nelson T. IGF-I stimulates tropoelastin synthesis in neonatal rat pulmonary fibroblasts. Pediatr Res. 1991;30(3):248-251.

68. Kahari VM, Olsen DR, Rhudy RW, Carrillo P, Chen YQ, Uitto J. Transforming growth factor-beta up-regulates elastin gene expression in human skin fibroblasts. Evidence for post-transcriptional modulation. Lab Invest. 1992 May;66(5):580-8.

69. Smith-Mungo LI, Kagan HM. 1998. Lysyl oxidase: Properties, regulation and multiple functions in biology. Matrix Biol 16: 387-398.

70. Shanley CJ, Gharaee-Kermani M, Sarkar R, Welling TH, Kriegel A, Ford JW, Stanley JC, Phan SH. Transforming growth factor-beta 1 increases lysyl oxidase enzyme activity and mRNA in rat aortic smooth muscle cells. J Vasc Surg. 1997; 25(3):446-52.

71. Reiser K, McCormick R, Rucker R. Enzymatic and nonenzymatic cross-linking of collagen and elastin. FASEB J. 1992;6:2439-2449.

72. Badet J, Soncin F, N'Guyen T, Barritault D. Blood Coagul. Fibrinolysis 1990;1:721-724.

73. Sen CK, Khanna S, Venojarvi M, Trikha P, Ellison EC, Hunt TK, Roy S. Copper-induced vascular endothelial growth factor expression and wound healing. Am J Physiol Heart Circ Physiol. 2002;282:1821-1827.

74. Rucker R, Kosonen T, Clegg MS, Mitchell AE, Rucker RB, Uriu-Hare JY, CL Keen. Copper, lysyl oxidase, and extracellular matrix protein crosslinking. Am J Clin Nutr. 1998;67:996S-1000S.

75. Ross MH. Histology, A text and atlas. Fourth edition. Lippincott Williams and Wilkins.:326-327.

76. http://herkules.oulu.fi/isbn951426973X/html/equation2222.png.

77. Ju H, Dixon IM. Extracellular matrix and cardiovascular diseases, Can J Cardiol 12 (1996), pp. 1259–1267.

78. Madri JA, Dreyer B, Pitlick FA, Furthmayr H. The collagenous components of the subendothelium. Correlation of structure and function. Lab Invest. 1980;43(4):303-315.

79. Terranova VP, DiFlorio R, Lyall RM, Hic S, Friesel R, Maciag T. Human endothelial cells are chemotactic to endothelial cell growth factor and heparin. J Cell Biol. Dec 1985;101(6):2330-2334.

80. Macarak EJ, Howard PS. Adhesion of endothelial cells to extracellular matrix proteins. J Cell Physiol. Jul 1983;116(1):76-86.

81. Hasson JE., Wiebe DH, Sharefkin JB, Abbott WM. Migration of adult human vascular endothelial cells: effect of extracellular matrix proteins. Surgery. Aug 1986;100(2):384-391.

82. Buonassisi V. Sulfated mucopolysaccharide synthesis and secretion in endothelial cell cultures. Exp Cell Res. 1973;76(2):363-368.

83. Oohira A, Wight TN, Bornstein P. Sulfated proteoglycans synthesized by vascular endothelial cells in culture. J Biol Chem. 1983;258(3):2014-2021.

84. Davies PF. Flow-mediated endothelial mechanotransduction, Physiol Rev 1995; 75:519–560.

85. Kim BS, Nikolovski J, Bonadio J, Mooney DJ. Cyclic mechanical strain regulates the development of engineered smooth muscle tissue. Nat Biotechnol 1999; 17: 979-983.

86. Leung DY, Glagov S, Mathews MB. Cyclic stretching stimulates synthesis of matrix components by arterial smooth muscle cells in vitro, Science 1976;191:475–477.

87. Nilsson J. Growth factors and the pathogenesis of atherosclerosis. Atherosclerosis 1986; 62:185-9.

88. Thyberg J. Differentiated properties and proliferation of arterial smooth muscle cells in culture. Int Rev Cytol. 1996;169:183-265.

89. Chamley-Campbell J, Campbell GR, Ross R. The smooth muscle cell in culture. Physiol Rev 1979; 59:1–61.

90. Huxley-Jones J, Robertson DL, Boot-Handford RP. On the origins of the extracellular matrix in vertebrates. Matrix Biol. 2007; 26: 2–11.

91. Balazs EA. Chemistry and molecular biology of the intercellular matrix. Vol Chapter I, II, IV: Academic press.; 1970.

92. Uitto J, Hoffman H, Prockop DJ. Synthesis of elastin and procollagen by cells from embryonic aorta. Arch. Biochem. Biophys. 1976;173:187-200.

93. Marneros AG, Olsen BR. The role of collagenderived proteolytic fragments in angiogenesis. Matrix Biol. 2001; 20: 337–45.

94. Uitto J, Chung-Honet LC, Christiano AM. Molecular biology and pathology of type VII collagen. Exp Dermatol. 1992; 1: 2–11.

95. Kuhn K, Wiedemann H, Timpl R, Risteli J, Dieringer H, Voss T, Glanville RW. Macromolecular structure of basement membrane collagens. FEBS Lett. 1981; 125: 123–8.

96. Iozzo RV. Basement membrane proteoglycans: from cellar to ceiling. Nat Rev Mol Cell Biol. 2005; 6: 646–56..

97. Varki A, Cummings R, Esko J, Freeze H, Hart G, Marth M. (Editors) Essentials of glycobiology. Cold Spring Harbor, NY : Cold Spring Harbor Press; 1999.

98. Ruoslahti E. Fibronectin and its receptors. Annu Rev Biochem. 1988; 57:375–413.

99. Wierzbicka-Patynowski I, Schwarzbauer JE. The ins and outs of fibronectin matrix assembly. J Cell Sci. 2003; 116: 3269–76.

100. Lindahl U, Roden, L. In Glycoproteins (Gottschalk, A. ed) 1972. pp. 491-517, Elsevier, New York.

101. Wolinski H, Glagov S. Lamellar unit of aortic medial structure and function in mammals. Circ Res. 1967; 20: 99–111.

102. Brooke BS, Bayes-Genis A, Li DY. New insights into elastin and vascular disease. Trends Cardiovasc Med. 2003; 13: 176–81.

103. Hay ED. Cell biology of extracellular matrix. 1991 Plenum press, New York. Chapter III.

104. Parry DAD, Squire JM. Fibrous proteins: New structural and functional aspects revealed. Adv Protein Chem 2005 70:1-10.

105. Pasquali-Ronchetti I, Baccarani-Contri M. Elastic fiber during development and aging. Microsc Res Tech. 1997;38(4):428-35. .

106. Osborne-Pellegrin MJ, Farjanel J, Hornebeck W. Role of elastase and lysyl oxidase activity in spontaneous rupture of internal elastic lamina in rats. Arterioscler Thromb Vasc Biol 1990;10(6):1136-1146.

107. Debelle L, Tamburro AM. Elastin: molecular description and function. Int J Biochem Cell Biol. 1999;31:261-272.

108. Robert AM, Robert L. Biology and Pathology of elastic tissues. S.Karger. 1980 Chapter II, III, IV.

109. Kielty CM, Sherratt MJ, Shuttleworth CA. Elastic fibres. Cell Sci. 2002;115 14:2817-28.

110. Ramamurthi A, Vesely I. Evaluation of the matrix-synthesis potential of crosslinked hyaluronan gels for tissue engineering of aortic heart valves. Biomaterials. 2005; 26(9): 999-1010.

111. Gosline JM, French CJ. Dynamic mechanical properties of elastin. Biopolymers. 1979;18(8):2091–2103.

112. Lillie MA, Gosline JM. The effects of hydration on the dynamic mechanical properties of elastin. Biopolymers. 29(8-9):1147–1160.

113. Dobrin PB. Mechanical properties of arteries. Physiol Rev 1978, 58 397–460.

114. Parks WC, Pierce RA, Lee KA, Mecham RP. Elastin. Adv Mol Cellular Biol 1990 6,133–182.

115. Gundiah N, Ratcliffe MB, Pruitt LA. Determination of strain energy function for arterial elastin: Experiments using histology and mechanical tests. J Biomech. 2007;40(3):586-594.

116. Bashir M, Indik Z,Yeh H, Ornstein-Goldstein N, Rosenbloom J. Characterization of the complete human elastin gene. Delineation of unusual features in the 58-flanking region. J Biol Chem, 1989, 264:8887–8891.

117. Gosline JM. Hydrophobic interaction and a model for the elasticity of elastin. Biopolymers, 1978, 17:677–695.

118. Hoeve CAJ, Flory PJ. The elastic properties of elastin. Biopolymers, 1974, 13:677–686.

119. Foster JA, Bruenger E, Gray WR, Sandberg LB. Isolation and amino acid sequences of tropoelastin peptides. J Biol Chem, 1973, 248:2876–2879.

120. Hinek A. Elastin receptor and tropoelastin chaperone. In Tamburro AM (Ed.) Elastin and elastic tissue. Armento Potenza, Italy, 1997, 75-81.

121. Fazio MJ, Mattei MG, Passage E, Chu ML, Black D, Solomon E, Davidson JM, Uitto J. Human elastin gene: New evidence for localization to the long arm of chromosome 7. Am J Hum Genet, 1991, 48:696–703.

122. Indik Z, Yeh H, Ornstein-Goldstein N, Sheppard P, Anderson N, Rosenbloom JC, Peltonen L, Rosenbloom J. Alternative splicing of human elastin mRNAindicated by sequence analysis of cloned genomic and complementary DNA. Proc Natl Acad Sci USA, 1987, 84:5680–5684.

123. Hinek A, Mecham RP, Keeley F, Rabinovitch M. Impaired elastin fiber assembly related to reduced 67-kD elastin-binding protein in fetal lamb ductus arteriosus and in cultured aortic smooth muscle cells treated with chondroitin sulfate. J Clin Invest. 1991; 88(6): 2083–2094.

124. Uitto J, Hoffmann HP, Prockop DJ. Synthesis of elastin and procollagen by cells from embryonic aorta. Differences in the role of hydroxyproline and the effects of proline analogs on the secretion of the two proteins. Arch Biochem Biophys, 1976, 173:187–200.

125. Grosso LE, Mecham RP. In vitro processing of tropoelastin: Investigation of a possible transport function associated with the carboxy-terminal domain. Biochem Biophys Res Commun,1988, 153:545–551.

126. Brown PL, Mecham L, Tisdale C, Mecham RP. The cysteine residues in the carboxy terminal domain of tropoelastin form an intrachain disulfide bond that stabilizes a loop structure and positively charged pocket. Biochem Biophys Res Commun, 1992, 186:549–555.

127. Hinek A, Wrenn DS, Mecham RP, Barondes SH. The elastin receptor is a galactoside binding protein. Science, 1988, 239:1539–1541.

128. Jaques A, Serafini-Fracassini A. Morphogenesis of the elastic fibers:An immunoelectron microscopy investigation. J Ultrastruct Res. 1985;92(201-210).

129. Parks WC, Pierce RA, Lee KA, Mecham RP. The extracellular matrix. Adv Mol Cell Biol. 1993;6:133-182.

130. Mecham RP, Hinek A, Griffin GL, Senior RM, Liotta LR. 67 kD elastin binding protein is homologous to the tumor cell 67 kD laminin receptor. J. Biol. Chem. 1989, 264:16652-16657.

131. Hinek A, Mecham RP. Characterization and functional properties, Tamburro of elastin receptor. In Elastin: Chemical and Biological Aspects. A. M., and J. Davidson editors. Gelatina Congedo, Padova, Italy. 1990, pp., 369-381.

132. Kagan HM, Vaccaro CA, Bronson RE, Tang SS, Brody JS. Ultrastructural immunolocalization of lysyl oxidase in vascular connective tissue. J Cell Biol., 1986, 103:1121–1128.

133. Csiszar K. Lysyl oxidases: A novel multifunctional amine oxidase family. Prog Nucleic Acid Res Mol Biol., 2001, 70:1-32.

134. Borel A, Eichenberger D, Farjanel J, Kessler E, Gleyzal C, Hulmes DJ, Sommer P, Font B. Lysyl oxidase-like protein from bovine arota. Isolation and maturation to an active form by bone morphogenetic protein I. J Biol Chem 2001, 276: 48944-48949.

135. Kagan HM, Li W. Lysyl oxidase: properties, specificity, and biological roles inside and outside of the cell. J Cell Biochem. 2003;88(4):660-72.

136. Ross R, Fialkow PJ, Altman LK. The morphogenesis of the elastic fibers. Adv Exp Biol Med, 1977; 79:7–16.

137. Pasquali-Ronchetti I, Fornieri C, Baccarani-Contri M, Volpin D. The ultrastructure of elastin revealed by freeze-fracture electron microscopy. Micron, 1979;10:89–99.

138. Baccarani-Contri M, Vincenzi D, Cicchetti F, Mori G, Pasquali-Ronchetti I. Immunochemical localization of proteoglycans within normal elastin fibre. Eur J Cell Biol., 1990; 53:305–312.

139. Kagan HM, Vaccaro CA, Bronson RE, Tang SS, Brody JS. Ultrastructural immunolocalization of lysyl oxidase in vascular connective tissue. J Cell Biol, 1986;103:1121–1128.

140. Hodgkin DD, Gilbert RD, Roos PJ, Sandberg LB, Boucek RJ. Dietary lipid modulation of connective tissue matrix in rat abdominal aorta. Am J Physiol, 1992;262:R389–394.

141. Lee KA, Pierce RA, Mecham RP, Parks WC. Increased mesenchymal cell density accompanies induction of tropoelastin expression in developing elastic tissue. Dev Dyn, 1994;200:53–67.

142. Durmowicz AG, Parks WC, Hyde DM, Mecham RP, Stenmark KR. Persistence, re-expression, and induction of pulmonary arterial fibronectin, tropoelastin, and type I procollagen mRNA expression in neonatal hypoxic pulmonary hypertension. Am J Pathol, 1994;145:1411–1420.

143. Foster J, Rich CB, Florini JR. Insulin-like Growth Factor I, Somatomedin C, induces the synthesis of tropoelastin in aortic tissue. Collagen Rel Res, 1987;7:161–169.

144. Liu J, Davidson JM. The elastogenic effect of recombinant transforming growth factor-b on porcine aortic smooth muscle cells. Biochem Biophys Res Commun, 1989;154:895–899.

145. Katchman SD, Hsuwong S, Ledo I, Wu M, Uitto J. Transforming growth factor beta up-regulates human elastin promoter activity in transgenic mice. Biochem Biophys Res Commun,1994;201:485–490.

146. Quaglino D. Jr, Nanney LB, Kennedy R, Davidson JM. Localized effect of transforming growth factor beta on extracellular matrix gene expression during wound healing. Lab Invest,1990;63:307–319.

147. Galis ZS, Khatri JJ. Matrix metalloproteinases in vascular remodeling and atherogenesis: the good, the bad, and the ugly. Circ Res 2002;90:251–262. .

148. Raines EW, Ross R. Smooth muscle cells and the pathogenesis of the lesions of atherosclerosis. Br Heart J 1993;69:S30–S37. .

149. Thyberg J. Phenotypic modulation of smooth muscle cells during formation of neointimal thickenings following vascular injury. Histol Histopathol 1998;13 :871–891.

150. Ito S, Ishimaru S, Wilson SE. Inhibitory effect of type 1 collagen gel containing alpha-elastin on proliferation and migration of vascular smooth muscle and endothelial cells. Cardiovasc Surg 1997;5:176–183.

151. Yamamoto M, Yamamoto K, Noumura T. Type I collagen promotes modulation of cultured arterial smooth muscle cells from a contractile to a synthetic phenotype. Exp Cell Res 1993;204:121–129.

152. Urban Z, Riazi S, Seidl TL, et al., Connections between elastin haploinsufficiency and cell proliferation in patients with supravalvular aortic stenosis and Williams-Beuren syndrome. Am J Hum Genet 2002;71:30–44.

153. Hashimoto S, Seyama Y, Yokokura T, Mutai M. Effects of chlorella phospholipid on the aortic collagen and elastin metabolism and on the serum lipid content in rats with experimental arteriosclerosis. Exp Mol Pathol, 1982;37: 150-155.

154. Basalyga DM, Simionescu DT, Xiong W, Baxter BT, Starcher BC, Vyavahare NR. Elastin degradation and calcification in an abdominal aorta injury model: role of matrix metalloproteinases. Circulation. 2004;110:3480-3487.

155. Tintut Y, Patel J, Parhami F, Demer LL. Tumor Necrosis Factor-a Promotes In Vitro Calcification of Vascular Cells via the cAMP Pathway. Circulation. 2000;102:2636-2642.

156. Swee MH, Parks WC, Pierce RA. Developmental regulation of elastin production. Expression of tropoelastin pre-mRNA persists after down-regulation of steady-state mRNA levels. J Biol Chem. 1995; 270(25):14899-906.

157. Keeling WB, Armstrong PA, Stone PA, Bandyk DF, Shames ML. An overview of matrix metalloproteinases in the pathogenesis and treatment of abdominal aortic aneurysms. Vasc Endovascular Surg. 2005;39(6):457-464.

158. Fulop T, Jacob MP, Wallach J, Hauck M, Seres I, Varga Z, Robert L. The elastin-laminin receptor. J Soc Biol. 2001;195(2):157-64.

159. Laurent S, Boutouyrie P, Lacolley P. Structural and genetic bases of arterial stiffness. Hypertension. 2005;45(6):1050-5.

160. Ewart AK, Morris CA, Ensing GJ, Loker J, Moore C, Leppert M, Keating M. A human vascular disorder, supravalvular aortic stenosis, maps to chromosome 7. Proc Natl Acad Sci USA 1993;90:3226–3230.

161. Stone PJ, Morris SM, Griffin S, Mithieux S, Weiss AS. Building Elastin. Incorporation of recombinant human tropoelastin into extracellular matrices using nonelastogenic rat-1 fibroblasts as a source for lysyl oxidase. Am J Respir Cell Mol Biol. 2001;24(6):733-739.

162. O'Connor WN, Davis JB Jr, Geissler R, Cottrill CM, Noonan JA, Todd EP. Supravalvular aortic stenosis: clinical and pathologic observations in six patients. Arch Path Lab Med, 1985;109:179–185.

163. Curran ME, Atkinson DL, Ewart AK, Morris CA, Leppert MF, Keating MT. The elastin gene is disrupted by a translocation associated with supravalvular aortic stenosis. Cell, 1993;73:159–168.

164. Kerl H, Burg G, Hashimoto K. Fatal, penicillin-induced, generalized, postinflammatory elastolysis (cutis laxa). Am J Dermatopathol 1983;5:267–276.

165. Weir EK, Joffe HS, Blaufuss AH, Beighton P. Cardiovascular abnormalities in cutis laxa. Eur J Cardiol 1977;5:255–261.

166. Kähäri VM, Olsen DR, Rhudy RW, Carrillo P, Chen YQ, Uitto J. Transforming growth factor-b up-regulates elastin gene expression in human skin fibroblasts. Evidence for post-transcriptional modulation. Lab Invest. 1992;66:580-588.

167. Brown-Augsburger P, Broekelmann T, Rosenbloom J, Mecham RP. Functional domains on elastin and microfibril-associated glycoprotein involved in elastic fibre assembly. Biochem J. 1996;318:149–155.

168. Ewart AK, Morris CA, Atkinson D, et al., Hemizygosity at the elastin locus in a developmental disorder, Williams syndrome. Nat Genet. 1993;5:11–16. .

169. Francke U. Williams-Beuren syndrome: genes and mechanisms. Hum. Mol Genet. 1999;8:1947–1954.

170. Urban Z, Riazi S, Seidl TL, Katahira J, Smoot LB, Chitayat D, Boyd CD, Hinek A. Connection between elastin haploinsufficiency and increased cell proliferation in patients with supravalvular aortic stenosis and Williams-Beuren syndrome. Am J Hum Genet. 2002;71(1):30-44.

171. Pyeritz RE, McKusick VA. The Marfan syndrome: diagnosis and management. New Engl J Med, 1979;300:772–777.

172. Segura AM, Luna RE, Horiba K, Stetler-Stevenson WG, McAllister HA, Willerson JT, Ferrans VJ. Immunohistochemistry of matrix metalloproteinase and their inhibitors in thoracic aortic aneurysms and aortic valves of patients with Marfan's syndrome. Circulation, 1998;98:331–338.

173. Sims FH. The initiation of intimal thickening in human arteries. Pathology 2000;32:171–175.

174. Lusis AJ. Atherosclerosis. Nature 2000; 233–241. .

175. Ernst CB. Abdominal aortic aneurysm. N Engl J Med. 1993; 328(16): 1167-72.

176. Gorham TJ, Taylor J, Raptis S. Endovascular treatment of abdominal aortic aneurysm. Br J Surg. 2004 ; 91(7):815-27.

177. Murphy G. Matrix metalloproteinases and their inhibitors. Acta Orthop Scand Suppl 1995 266:55-60.

178. Chew DKW, Conte MS, Khalil RA. Matrix metalloproteinase-specific inhibition of Ca2+ entry mechanisms of vascular contraction. J Vasc Surg, 2004;40(5):1001-1010.

179. Newman KM, Malon AM, Shin RD, Scholes JV, Ramey WG, Tilson MD. Matrix metalloproteinases in abdominal aortic aneurysm: characterization, purification, and their possible sources. Connect Tissue Res 1994;30:265–276.

180. Patel MI, Melrose J, Ghosh P, Appleberg M. Increase synthesis of matrix metalloproteinases by aortic smooth muscle cells is implicated in the etiopathogenesis of abdominal arotic aneurysms. J Vasc Surg 1996; 24: 82-92.

181. Bendeck MP, Conte M, Zhang M, Nili N, Strauss BH, Farwell SM. Doxycycline modulates smooth muscle cell growth, migration, and matrix remodeling after arterial injury. Am J Pathol. 2002; 160: 1089–1095.

182. Teckman JH, Lindblad D. Alpha-1-antitrypsin deficiency: diagnosis, pathophysiology, and management. Curr Gastroenterol Rep. 2006;8(1):14-20.

183. Sodian R, Lueders C, Kraemer L, Kuebler W, Shakibaei M, Reichart B, Daebritz S, Hetzer R. Tissue engineering of autologous human heart valves using cryopreserved vascular umbilical cord cells. Ann Thorac Surg. 2006; 81(6):2207-16.

184. Hogan P, Duplock L, Green M, et al., Human aortic valve allografts elicit a donor-specific immune response. J Thorac Cardiovasc Surg 1996;112:1260–1266.

185. Hoekstra FME, Knoop CJ, Vaessen LMB, et al., Donor-specific cellular immune response against human cardiac valve allografts. J Thorac Cardiovasc Surg 1996;112: 281–286. .

186. Wilson GJ, Courtman DW, Klement P, Lee JM, Yeger H, Acellular matrix: a biomaterials approach for coronary artery bypass and heart valve replacement. Ann Thorac Surg 1995; 60:S353–358.

187. Bader A, Schilling T, Teebken OE, et al., Tissue engineering of heart valves—human endothelial cell seeding of detergent acellularized porcine valves. Eur J Cardiothorac Surg 1998;14:279–284. .

188. Steinhoff G, Stock U, Karim N, et al., Tissue engineering of pulmonary heart valves on allogenic acellular matrix conduits: in vivo restoration of valve tissue. Circulation 2000;102:50–55.

189. Booth C, Korossis SA, Wilcox HE, et al., Tissue engineering of cardiac valve prostheses I: development and histological characterization of an acellular porcine scaffold. J Heart Valve Dis 2002;11:457–462.

190. Ross DN. Evolution of the homograft valve. Ann Thorac Surg 1995; 59:565–567.

191. Tzanakakis ES, Hess DJ, Sielaff TD, Hu WS. Extracorporeal tissue engineered liver-assist devices. Annu Rev Biomed Eng. 2000;2:607-32.

192. Schlitt HJ, Brunkhorst R, Haverich A, Raab R. Attitude of patients toward transplantation of xenogeneic organs. Langenbecks Arch Surg 1999;384(4):384-91.

193. Johnson LF, deSerres S, Herzog SR, Peterson HD, Meyer AA. Antigenic cross-reactivity between media supplements for cultured keratinocyte grafts. J Burn Care Rehabil. 1991;12(4):306-12.

194. Bucher P, Morel P, Buhler LH. Xenotransplantation: an update on recent progress and future perspectives. Transpl Int. 2005;18(8):894-901.

195. Schuurman H, Cheng J, Lam T. Pathology of xenograft rejection: a commentary. Xenotransplantation 2003; 10: 293.

196. Robson S, Schulte AM, Esch J, Bach F. Factor in xenograft rejection. Ann N Y Acad Sci 1999; 875: 261.

197. Peppas NA, Langer R. New Challenges in Biomaterials. Science, 1994;263, 1715-1720.

198. Kennedy JP. Designed rubbery biomaterials. Makromol. Chem., Macromol. Symp. 2001;175:127-132.

199. Sodian R, Sperling JS, Martin DP, Egozy A, Stock U, Mayer JE Jr, Vacanti JP. Fabrication of a trileaflet heart valve scaffold from a polyhydroxyalkanoate biopolyester for use in tissue engineering. Tissue Eng. 2000;6(2):183-8.

200. Zdrahala RJ. Small caliber vascular grafts. Part II: Polyurethanes revisited. J Biomater Appl. 1996;11:37-61.

201. Caeuana CM. Chem Eng Prog. 1999, 9.

202. Salacinski HJ, Goldner S, Giudiceandrea A, Hamilton G, Seifalian AM, Edwards A, Carson RJ. The mechanical behavior of vascular grafts: a review. J Biomater Appl. 2001;15(3), 241-278.

203. Chinn JA, Sauter JA, Philipsa RE. Jr, Kao WJ, Anderson JM, Hanson SR, Ashton TR. Blood and tissue compatibility of modified polyester: thrombosis, inflammation, and healing. J Biomed Mater Res 1998, 39(1), 130-140.

204. Rhee K, Tarbell JM. A study of the wall shear rate distribution near the end-to-end anastomosis of a rigid graft and a compliant artery. J Biomech. 1994; 27(3): 329-338.

205. Zhuang YJ, Singh TM, Zarins CK, Masuda H. Sequential increases and decreases in blood flow stimulates progressive intimal thickening. Eur J Vasc Surg 1998; 16(4):301-310.

206. Vrhovski B, Jensen S, Weiss A. Coacervation characteristics of recombinant human tropoelastin. Eur J Biochem 1997; 250:92-98.

207. Urry DW, Pattanaik A, Xu J, Woods TC, McPherson DT, Parker TM. Elastic protein-based polymers in soft tissue augmentation and generation. J Biomater Sci Polym Ed. 1998;9(10):1015-1048.

208. Reiersen H, Clarke A, Rees AR. Short elastin-like peptides exhibit the same temperature-induced structural transitions as elastin polymers: implications for protein engineering. J Mol Biol 1998; 283:255-264.

209. Bressan G, Pasquali-Ronchetti I, Fornieri C, Mattioli F, Castellani I, Volpin D. Relevance of aggregation properties of tropoelastin to the assembly and structure of elastic fibers. J Ultrastruct Res 1986; 94:209-216. .

210. Narayanan AS, Page RC, Kuzan F, Cooper CG. Elastin cross-linking in vitro. Studies on factors influencing the formation of desmosines by lysyl oxidase action on tropoelastin. Biochem J 1978; 173:857-862.

211. Stitzel J, Liu J, Lee SJ, Komura M, Berry J, Soker S, Lim G, Van Dyke M, Czerw R, Yoo JJ, Atala A. Controlled fabrication of a biological vascular substitute. Biomaterials. 2006;27(7):1088-94.

212. Rabkin E, Schoen FJ. Cardiovascular tissue engineering. Cardiovasc Pathol Biol. 2002;11:305-317.

213. Kim BS, Mooney DJ. Engineering smooth muscle tissue with a predefined structure. J Biomed Mater Res 1998;41:322– 32.

214. Patel A, Fine B, Sandig M, Mequanint K. Elastin biosynthesis: The missing link in tissue-engineered blood vessels. Cardiovasc Res. 2006;71(1):40-49.

215. Higgins SP, Solan AK, Niklason LE. Effects of polyglycolic acid on porcine smooth muscle cell growth and differentiation. J Biomed Mater Res 2003;67A:295–302.

216. Stock UA, Wiederschain D, Kilroy SM, Shum-Tim D, Khalil PN, Vacanti JP, Mayer JE Jr, Moses MA. Dynamics of extracellular matrix production and turnover in tissue engineered cardiovascular structures. J Cell Biochem. 2001;81(2):220-228.

217. Stock UA, Wiederschain D, Kilroy SM, Shum-Tim D, Khalil PN, Vacanti JP, Mayer JE Jr, Moses MA. Dynamics of extracellular matrix production and turnover in tissue engineered cardiovascular structures. J Cell Biochem. 2001;81(2):220-8.

218. Opitz F, Schenke-Layland K, Cohnert TU, Starcher B, Halbhuber KJ, Martin DP, et al. tissue engineering of aortic tissue: dire consequence of suboptimal elastic fiber synthesis in vivo. Cardiovasc Res 2004;63:719–30.

219. Weinberg CB, Bell E. A blood vessel constructed from collagen and cultured vascular cells. Science. 1986;231:397-400.

220. L'Heureux N, Paquet S, Labbe R, Germain L, Auger FA. A completely biological tissue-engineered human blood vessel. FASEB J. 1998;12:47-56.

221. Imberty A, Lortat-Jacob H, Pérez S. Structural view of glycosaminoglycan–protein interactions. Carbohydrate Research 2007; 342(3-4):430-439.

222. Kjellen L, Lindahl U. Proteoglycans: structures and interactions. Annu Rev Biochem. 1991;60:443–475.

223. Schneider-Brachert W, Tchikov V, Neumeyer J, Jakob M, Winoto-Morbach S, Held-Feindt J, Heinrich M, Merkel O, Ehrenschwender M, Adam D, Mentlein R, Kabelitz D, Schutze S. Compartmentalization of TNF receptor 1 signaling: internalized TNF receptosomes as death signaling vesicles. Immunity. 2004;21:415–428.

224. Rapport M, Weismann B, Linker A, Meyer K. Isolation of a crystalline disaccharide, hyalobiuronic acid, from hyaluronic acid. Nature 1951;168:996-7.

225. Weigel PH, Hascall VC, Tammi M. Hyaluronan synthases. J Biol Chem 1997;272:13997-4000.

226. Toole BP. Hyaluronan and its binding proteins, the hyaladherins. Curr Opin Cell Biol. 1990;2:839-44.

227. Aruffo A, Stamenkovic I, Melnick M, Underhill CB, Seed B. CD44 is the principal cell surface receptor for hyaluronate. Cell 1990;61:1303-13.

228. Aruffo A, Stamenkovic I, Melnick M, Underhill CB, Seed B. CD44 is the principal cell surface receptor for hyaluronate. Cell 1990;61:1303-13.

229. Miyake K, Underhill CB, Lesley J, Kincade PW. Hyaluronate can function as a cell adhesion molecule and CD44 participates in hyaluronate recognition. J Exp Med. 1990;172:69-75.

230. Turley EA, Austen L, Vandeligt K, Clary C. Hyaluronan and a cell-associated hyaluronan binding protein regulate the locomotion of ras-transformed cells. J Cell Biol. 1991;112:1041-7.

231. Hardwick C, Hoare K, Owens R, Holn HP, Hook M, Moore D, Cripps V, Austen L, Nance DM, Turley EA. Molecular cloning of a novel hyaluronan receptor that mediates tumor cell motility. J Cell Biol. 1992;117:1343-50.

232. Laurent TC, Fraser JRE. Hyaluronan. FASEB J 1992; 6: 2397-2404.

233. Day BS. Structural and functional diversity of hyaluronan binding protiens. In: Garg H, Hales C, editors. Chemistry and biology of hyaluronan. Amsterdam: Elsevier Press, 2004. p. 184-204.

234. Wight T, Tammi. Hyaluronan-cell interactions in cancer and vascular disease. J Biol Chem 2002;277:4593-6.

235. Xu H, Ito T, Tawada A, Maeda H, Yamanokuchi H, Isahara K, Yoshida K, Uchiyama Y, Asari A. Effect of hyaluronan oligosaccharides on the expression of heat shock protein 72. J Biol Chem. 2002; 277(19): 17308-14.

236. West DC, Kumar S. The effect of hyaluronate and its oligosaccharides on endothelial cell proliferation and monolayer integrity. Exp Cell Res 1989;183:179-96.

237. West DC. Is hyaluronan degradation an angiogenic/metastatic switch? In: Kennedy JF Phillips G. O., Williams P. A., Hascall V., editor. Hyaluronan. Cambridge, U.K.: Woodhead Publishing Ltd, 2002. p. 165-72.

238. Sugahara KN, Hirata T, Hayasaka H, Stern R, Murai T, Miyasaka M. Tumor cells enhance their own CD44 cleavage and motility by generating hyaluronan fragments. J Biol Chem. 2006;281(9):5861-5868.

239. Rossler A, Hinghofer-Szalkay H. Hyaluronan fragments: an information-carrying system? Horm Metab Res 2003;35:67-8.

240. Chen WY, Abatangelo G. Functions of hyaluronan in wound repair. Wound Repair Regen 1999;7:79-89.

241. Misra S, Ghatak S, Zoltan-Jones A, Toole BP. Regulation of multidrug resistance in cancer cells by hyaluronan. J Biol Chem. 2003; 278(28): 25285-8.

242. Toole BP. Hyaluronan: from extracellular glue to pericellular cue. Nat Rev Cancer. 2004; 4(7):528-39.

243. Joddar B, Ramamurthi A. Fragment size- and dose-specific effects of hyaluronan on matrix synthesis by vascular smooth muscle cells. Biomaterials. 2006;27(15):2994-3004.

244. Gabelt BT, Kaufman PL. Changes in aqueous humor dynamics with age and glaucoma. Prog Retin Eye Res. 2005;24(5):612-37.

245. Lee JY, Spicer AP. Hyaluronan: A multifunctional, megaDalton, stealth molecule. Curr Opin Cell Biol. 2000, 12 (5), 581–586.

246. Modawal A, Ferrer M, Choi HK, Castle JA. Hyaluronic acid injections relieve knee pain. J Fam Pract. 2005;54(9):758-67.

247. Pavesio A, Renier D, Cassinelli C, Morra M. Antiadhesive surfaces through hyaluronan coatings. Med Device Technol. 1997 8 (7), 20–21, 24–27.

248. Kanda K, Matsuda T, Oka T. Mechanical stress induced cellular orientation and phenotypic modulation of 3-D cultured smooth muscle cells. ASAIO J. 1993;39(3):M686-690.

249. Horch RE, Kopp J, Kneser U, Beier J, Bach AD. Tissue engineering of cultured skin substitutes. J Cell Mol Med. 2005;9(3):592-608.

250. Knudson CB, Knudson W. Hyaluronan and CD44: modulators of chondrocyte metabolism. Clin Orthop Relat Res. 2004;(427 Suppl):S152-62.

251. Leach JB, Bivens KA, Patrick CW. Jr, Schmidt CE. Photocrosslinked hyaluronic acid hydrogels: Natural, biodegradable tissue engineering scaffolds. Biotechnol. Bioeng. 2003, 82, 578–589.

252. Peer D, Margalit R. Tumor-Targeted Hyaluronan Nanoliposomes Increase the Antitumor Activity of Liposomal Doxorubicin in Syngeneic and Human Xenograft Mouse Tumor Models. Neoplasia. 2004; 6(4): 343-53.

253. Price RD, Myers S, Leigh IM, Navsaria HA. The role of hyaluronic acid in wound healing: assessment of clinical evidence. Am J Clin Dermatol. 2005;6(6):393-402.

254. Duranti F, Salti G, Bovani B, Calandra M, Rosati ML. Injectable hyaluronic acid gel for soft tissue, augmentation. A clinical and histological study. Dermatol. Surg. 1998 24 (12), 1317–1325.

255. Kirker KR, Luo Y, Nielson JH, Shelby J, Prestwich GD. Glycosaminogylcan hydrogel films as bio-interactive dressings for wound healing. Biomaterials 2002, 23 (17), 3661–3671.

256. Balazs EA, Bland PA, Denlinger JL, Goldman AI, Larsen NE, Leshchiner EA, Leshchiner A, Morales B. Matrix engineering. Blood Coagul Fibrinolysis 1991, 2 (1), 173–178.

257. Chen G, Ito Y, Imanishi Y, Magnani A, Lamponi S, Barbucci R. Photoimmobilization of sulfated hyaluronic acid for antithrombogenicity. Bioconjug Chem. 1997, 8 (5), 730–734.

258. Kito H, Matsuda T. Biocompatible coatings for luminal and outer surfaces of small-caliber artificial grafts. J Biomed Mater Res. 1996; 30(3):321–330.

259. Wight TN. Versican: a versatile extracellular matrix proteoglycan in cell biology. Curr Opin Cell Biol. 2002; 14(5): 617-23.

260. Olin AI, Morgelin M, Sasaki T, Timpl R, Heinegard D, Aspberg A. The proteoglycans aggrecan and versican form networks with fibulin-2 through their lectin domain binding. J Biol Chem.2001; 276(2): 1253-61

261. Hinek A, Wilson SE. Impaired elastogenesis in Hurler disease: dermatan sulfate accumulation linked to deficiency in elastin-binding protein and elastic fiber assembly. Am J Pathol. 2000;156(3):925-38.

262. Merrilees MJ, Lemire JM, Fischer JW, Kinsella MG, Braun KR, Clowes AW, Wight TN. Retrovirally mediated overexpression of versican v3 by arterial smooth muscle cells induces tropoelastin synthesis and elastic fiber formation in vitro and in neointima after vascular injury. Circ Res. 2002;90(4):481-487.

263. Baccarani-Contri M, Vincenzi D, Cicchetti F, Mori G, Pasquali-Ronchetti I. Immunocytochemical localiza-tion of proteoglycans within normal elastin fibers. Eur J Cell Biol. 1990; 53(2):305-12.

264. Fornieri C, Baccarani-Contri M, Quaglino D Jr, Pasquali-Ronchetti I. Lysyl oxidase activity and elastin/ glycosaminoglycan interactions in growing chick and rat aortas. J Cell Biol.1987; 105(3): 1463-9

265. Wu WJ, Vrhovski B, Weiss AS. Glycosaminoglycans mediate the coacervation of human tropoelastin through dominant charge interactions involving lysine side chains. J Biol Chem 1999;274(31):21719–24.

266. Fornieri C, Baccarani-Contri M, Quaglino D. Jr, Pasquali-Ronchetti I. Lysyl oxidase activity and elastin-glycosaminoglycans interactions in growing chick and rat aortas. J Cell Biol.1987;105:1463–1469.

267. Ramamurthi A, Vesely I. Ultraviolet light-induced modification of crosslinked hyaluronan gels. J Biomed Mater Res 2003; 66A:317–329.

268. Joddar B, Ramamurthi A. Elastogenic effects of exogenous hyaluronan oligosaccharides on vascular smooth muscle cells. Biomaterials 2006;27:5698–5707.

269. Masters KS, Shah DN, Leinwand LA, Anseth KS. Crosslinked hyaluronan scaffolds as a biologically ac-tive carrier for valvular interstitial cells. Biomaterials. 2005; 26(15): 2517-25.

270. Zeng C, Toole BP, Kinney SD, Kuo JW, Stamenkovic I. Inhibition of tumor growth in vivo by hyaluronan oligomers. Int J Cancer. 1998; 77(3): 396-401.

271. Desai TA. Micro- and nanoscale structures for tissue engineering constructs. Med Eng Phys. 2000; 22(9):595-606.

272. Flemming RG, Murphy CJ, Abrams GA, Goodman SL, Nealey PF. Effects of synthetic micro- and nano-structured surfaces on cell behavior. Biomaterials. 1999;20(6):573-588.

273. Foster JA, Rich CB, Miller M, Benedict MR, Richman RA, Florini JR. Effect of age and IGF-I administration on elastin gene expression in rat aorta. J Gerontol. 1990;45(4):B113-8.

274. Wolfe BL, Rich CB, Goud HD, Terpstra AJ, Bashir M, Rosenbloom J, Sonenshein GE, Foster JA. Insulin-like growth factor-I regulates transcription of the elastin gene. J Biol Chem. 1993; 268(17):12418-26. .

275. McGowan SE, McNamer R. Transforming growth factor-beta increases elastin production by neonatal rat lung fibroblasts. Am J Respir Cell Mol Biol. 1990;3(4):369-76.

276. Mauviel A, Chen YQ, Kahari VM, Ledo I, Wu M, Rudnicka L, Uitto J. Human recombinant interleukin-1 beta up-regulates elastin gene expression in dermal fibroblasts. Evidence for transcriptional regulation in vitro and in vivo. J Biol Chem. 1993; 268(9):6520-4. .

277. Ichiro T, Tajima S, Nishikawa T. Preferential inhibition of elastin synthesis by epidermal growth factor in chick aortic smooth muscle cells. Biochem Biophys Res Commun.1990;168(2):850-6. .

278. Robert L. Cell– elastin interaction and signaling. Pathol Biol 2005;53:399–404.

279. Narayanan AS, Sandberg LB, Ross R, Layman DL. The smooth muscle cell: III. Elastin synthesis in arterial smooth muscle cell culture. J Cell Biol 1976;68:411–9.

280. Tukaj C, Kubasik-Juraniec J, Kraszpulski M. Morphological changes of aortal smooth muscle cells exposed to calcitriol in culture. Med Sci Monit 2000;6:668–74.

281. Hayashi A, Suzuki T, Tajima S. Modulations of elastin expression and cell proliferation by retinoids in cultured vascular smooth muscle cells. J Biochem 1995;117:132–6.

282. Tajima S, Hayashi A, Suzuki T. Elastin expression is upregulated by retinoic acid but not by retinol in chick embryonic skin fibroblasts. J Dermatol Sci 1997;15:166–72.

283. Griffith LG, Naughton G. Tissue engineering--current challenges and expanding opportunities. Science. 2002;295(5557):1009-14

284. Birukov KG, Shirinsky VP, Stepanova OV, Tkachuk VA, Hahn AW, Resink TJ, Smirnov VN. Stretch affects phenotype and proliferation of vascular smooth muscle cells. Mol Cell Biochem. 1995;144(2):131-139.

285. Dartsch PC, Hammerle H, Betz E. Orientation of cultured arterial smooth muscle cells growing on cyclically stretched substrates. Acta Anat (Basel). 1986; 125(2):108-13.

286. Liu SQ. Influence of tensile strain on smooth muscle cell orientation in rat blood vessels. J Biomech Eng. 1998; 120(3):313-20.

287. O'Callaghan CJ, Williams B. Mechanical strain-induced extracellular matrix production by human vascu-lar smooth muscle cells: role of TGF-beta (1). Hypertension. 2000;36(3):319-324.

288. Stanley AG, Patel H, Knight AL, Williams B. Mechanical strain-induced human vascular matrix synthesis: the role of angiotensin II. J Renin Angiotensin Aldosterone Syst. 2000; 1(1):32-5.

289. Cheng GC, Briggs WH, Gerson DS, Libby P, Grodzinsky AJ, Gray ML, Lee RT. Mechanical strain tightly controls fibroblast growth factor-2 release from cultured human vascular smooth muscle cells. Circ Res. 1997; 80(1):28-36.

290. Sudhir K, Hashimura K, Bobik A, Dilley RJ, Jennings GL, Little PJ. Mechanical strain stimulates a mito-genic response in coronary vascular smooth muscle cells via release of basic fibroblast growth factor. Am J Hypertens. 2001;14(11):1128-1134.

291. Isenberg BC, Tranquillo RT. Long-term cyclic distention enhances the mechanical properties of collagen-based media-equivalents. Ann Biomed Eng. 2003;31(8):937-949.

292. Niklason LE, Gao J, Abbott WM, Houser S, Marini R, Langer R. Functional arterial grown in vitro. Science 1999;284:489–93.

293. Kolpakov V, Rekhter MD, Gordon D, Wang WH, Kulik TJ. Effect of mechanical forces on growth and matrix protein synthesis in the in vitro pulmonary artery. Circ Res. 1995;77:823-831.

294. Kim BS, Mooney DJ. Scaffolds for engineering smooth muscle under cyclic mechanical strain conditions. J Biomech Eng 2000;122:210– 5.

295. Seliktar D, Nerem RM, Galis ZS. Mechanical strain-stimulated remodeling of tissue-engineered blood vessel constructs. Tissue Eng 2003;9:657 –66.

296. Niklason L, Langer RS. Advances in tissue engineering of blood vessels and other tissues. Transpl Immunol 1997;5:303 – 6.

297. Ye Q, Zu¨nd G, Jockenhoevel S, Hoerstrup SP, Schoeberlein A, Grunenfelder J, Turina M. Tissue engineering in cardiovascular surgery: new approach to develop completely human autologous tissue. Eur J Cardio-thorac 2000;17:449–54.

298. Niklason LE, Abbott W, Gao G, Klagges B, Hirschi KK, Ulubayram K, et al. Morphologic and mechanical characteristics of engineered bovine arteries. J Vasc Surg 2001;33:628–38.

299. Davidson JM, Giro M G. Regulation of matrix accumulation. New York: Academic Press; 1986.

300. McMahon MP, Faris B, Wolfe BL, Brown KE, Pratt CA, Toselli P, Franzblau C. Aging effects on the elastin composition in the extracellular matrix of cultured rat aortic smooth muscle cells. In Vitro Cell Dev Biol. 1985;21(12):674-680.

301. Taylor PM. Biological matrices and bionanotechnology. Phil Trans R Soc B. 2007;362:1313-1320.

302. Kielty CM, Stephan S, Sherratt MJ, Williamson M, Shuttleworth CA. Applying elastic fibre biology in vascular tissue engineering. Phil Trans R Soc B. 2007;362:1293-1312.

303. Walker GA, Masters KS, Shah DN, Anseth KS, Leinwand LA. Valvular Myofibroblast Activation by Transforming Growth Factor-ß: Implications for Pathological Extracellular Matrix Remodeling in Heart Valve Disease. Circ Res. 2004;95:253 - 260.

304. Owens GK, Geisterfer AA, Yang YW, Komoriya A. Transforming growth factor-β induced growth inhibition and cellular hypertrophy in cultured vascular smooth muscle cells. J Cell Biol. 1988;107:771-779.

305. Moses KL, Yang EY, Pietenpol JA. TGF-β stimulation and inhibition of cell proliferation: new mechanistic insights. Cell. 1990;63:245-247.

306. Labarca C, Paigen K. A simple, rapid, and sensitive DNA assay. Anal Biochem. 1980;102(2):344-352.

307. Trackman PC, Kagan HM. Nonpeptidyl amine inhibitors are substrates of lysyl oxidase. J Biol Chem. 1979;254:7831-7836.

308. Palamakumbura AH, Trackman PC. A Fluorometric Assay for Detection of Lysyl Oxidase Enzyme Activity in Biological Samples. Anal Biochem. 2002;300:245-251.

309. Slominska EM, Adamski P, Lipinski M, Swierczynski J, Smolenski RT. Liquid chromatographic/mass spectrometric procedure for measurement of NAD catabolites in human and rat plasma and urine. Nucleosides Nucleotides Nucleic Acids. 2006;25(9-11):1245-1249.

310. Starcher BC, Galione MJ. Purification and comparison of elastins from different animal species. Anal. Biochem. 1976;74:441–447.

311. Labella FS, Vivian S. Amino acid composition of elastin in the developing human aorta. Biochim Biophys Acta 1967;133:189-194.

312. John R, Thomas J. Chemical compositions of elastins isolated from aortas and pulmonary tissues of humans of different ages. Biochem J. 1972;127:261-269.

313. Ramamurthi A, Vesely I. Evaluation of the matrix-synthesis potential of crosslinked hyaluronan gels for tissue engineering of aortic heart valves. Biomaterials. 2005;26(9):999-1010.

314. Draude G, Lorenz RL. TGF-beta1 downregulates CD36 and scavenger receptor A but upregulates LOX-1 in human macrophages. Am J Physiol Heart Circ Physiol. 2000;278(4):H1042-1048.

315. Slevin M, Krupinski J, Kumar S, Gaffney J. Angiogenic oligosaccharides of hyaluronan induce protein tyrosine kinase activity in endothelial cells and activate a cytoplasmic signal transduction pathway resulting in proliferation. Lab Invest. 1998;78(8):987–1003.

316. Liu JM, Davidson JM. The elastogenic effect of recombinant transforming growth factor-beta on porcine aortic smooth muscle cells. Biochem Biophys Res Commun. 1988;154:895-901.

317. Marigo V, Volpin D, Bressan GM. Regulation of the human elastin promoter in chick embryo cells. Tissue specific effect of TGF-b. Biochem Biophys Acta. 1993;1172:31-36.

318. Marigo V, Voplin D, Vitale G, Bressan GM. Identification of a TGF-b responsive element in the human elastin promoter. Biochem Biophys Res Commun. 1994;99:1049-1056.

319. Goldberg RL, Toole BP. Hyaluronate inhibition of cell proliferation. Arthritis Rheum. 1987;30(7):769-778.

320. Turley E, Noble P, Bourguignon L. Signaling properties of hyaluronan receptors. J Biol Chem. 2002;277:4589-4592.

321. Simionescu A, Philips K, Vyavahare N. Elastin-derived peptides and TGF-beta1 induce osteogenic responses in smooth muscle cells. Biochem Biophys Res Commun. 2005;334:524-532.

322. Smith-Mungo LI, Kagan HM. Lysyl oxidase: properties, regulation and multiple functions in biology. Matrix Biol. 1998;16(7):387-398.

323. Niklason L, Langer RS. Advances in tissue engineering of blood vessels and other tissues. Transpl Immunol. 1997;5:303-306.

324. Mann BK, West JL. Tissue engineering in the cardiovascular system: progress towards a tissue engineered heart. Anat Rec. 2001;263:367-371.

325. Alsberg E, Anderson KW, Albeiruti A, Rowley JA, Mooney DJ. Engineering growing tissues. Proc Natl Acad Sci U S A. 2002;99:12025-12030.

326. Masters KS, Shah DN, Leinwand LA, Anseth KS. Crosslinked hyaluronan scaffolds as a biologically active carrier for valvular interstitial cells. Biomaterials. 2005;26(15):2517-2525.

327. Bornfeldt KE, Raines EW, Nakano T, Graves LM, Krebs EG, Ross R. Insulin-like growth factor-I and platelet-derived growth factor-BB induce directed migration of human arterial smooth muscle cells via signaling pathways that are distinct from those of proliferation. J Clin Invest. 1994;93:1266-1274.

328. Delafontaine P, Song YH, Li Y. Expression, regulation, and function of IGF-1, IGF-1R, and IGF-1 binding proteins in blood vessels. Arterioscler Thromb Vasc Biol. 2004;24:435-444.

329. Kielty CM, Sherratt MJ, Shuttleworth CA. Elastic fibres. J Cell Sci. 2002;115:2817-2828.

330. Mecham RP, Davis EC. Elastic fiber structure and assembly. In Extracellular matrix assembly and structure (eds P. D. Yurchenco, D. E. Birk & R. P. Mecham). 1994; New York: Academic Press:281–314.

331. Csiszar K. Lysyl oxidases: a novel multifunctional amine oxidase family. Prog Nucleic Acid Res Mol Biol. 2001;70:1-32.

332. Gacheru S, Trackman PC, Shah MA, O'Gara CY, Spacciapoli P, Greenaway FT, Kagan HM. Strucutural and catalytic properties of copper in lysyl oxidase. J Biol Chem. 1990;265:19022-19027.

333. Eyre D. Collagen crosslinking amino-acids. Methods Enzymol. 1987;144:115-139.

334. Kagan HM, Li W. Lysyl oxidase: properties, specificity, and biological roles inside and outside of the cell. J. Cell. Biochem. 2003;88:660–672.

335. Hunsaker HA, Morita M, Allen KG. Marginal copper deficiency in rats. Aortal morphology of elastin and cholesterol values in firstgeneration adult males. Atherosclerosis. 1984;1:1-19.

336. Tinker D, Romero-Chapman N, Reiser K, Hyde D, Rucker RB. Elastin metabolism during recovery from impaired crosslink formation. Arch Biochem Biophys. 1990;278:326-332.

337. Allen KG, Klevay LM. Cholesterolemia and cardiovascular abnormalities in rats caused by copper deficiency. Atherosclerosis. 1978;29:81-93.

338. Giavaresi G, Torricellia P, Fornasaric PM, Giardinoa R, Barbuccib R, Leoneb G. Blood vessel formation after soft-tissue implantation of hyaluronanbased hydrogel supplemented with copper ions. Biomaterials. 2005;26:3001-3008.

339. Dahl SLM, Rucker RB, Niklason LE. Effects of copper and cross-linking on the extracelluar matrix if tissue-engineered arteries. Cell Transplantation. 2005;14:367-374.

340. Sorenson JRJ. Use of essential metalloelement complexes or chelates in biological studies. Free Radic Biol Med. 1992;13:593-594.

341. Hu GF. Copper Stimulates Proliferation of Human Endothelial Cells Under Culture. J Cell Biochem. 1998;69:326-335.

342. Halliwell B, Gutteridge JM. The importance of free radicals and catalytic metal ions in human diseases. Mol Aspects Med. 1985;8:89-193.

343. Rowley D, Halliwell B. Superoxide-dependent and ascorbate-dependent formation of hydroxyl radicals in the presence of copper salts: A physiologically significant reaction? Arch Biochem Biophys. 1983;225:279-284.

344. Gacheru SN, Thomas KM, Murray SA, Csiszar K, Smith-Mungo LI, Kagan HM. Transcriptional and post-transcriptional control of lysyl oxidase expression in vascular smooth muscle cells: Effects of TGF-b1 and serum deprivation. J Cell Biochem. 1997;65:395–407.

345. Solchaga LA, Tognana E, Penick K, Baskaran H, Goldberg VM, Caplan AI, Welter JF. A rapid seeding technique for the assembly of large cell/scaffold composite constructs. Tissue Eng. 2006;12:1851.

346. Majors AK, Ehrhart LA. Cell density and proliferation modulate collagen synthesis and procollagen mRNA levels in arterial smooth muscle cells. Exp Cell Res. 1992;200:168.

347. Augsburger PB, Tisdale C, Broekelmann T, Sloan C, Mecham RP. Identification of an Elastin Cross-linking Domain That Joins Three Peptide Chains. J Biol Chem. 1995;270:17778.

348. Kothapalli CR, Ramamurthi A. Benefits of concurrent delivery of hyaluronan and IGF-1 cues to regeneration of crosslinked elastin matrices by adult rat vascular cells. J Tissue Eng Regen Med. 2008;2:106-116.

349. Kishimoto T, Fukuzawa Y, Abe M, Hashimoto M, Ohno M, Tada M. Injury to cultured human vascular endothelial cells by copper (CuSO4). Nippon Eiseigaku Zasshi. 1992;47(5):965-970.

350. Cortizo MC, Fernandez Lorenzo de Mele M. Cytotoxicity of copper ions released from metal: variation with the exposure period and concentration gradients. Biol Trace Elem Res. 2004;102(1-3):129-141.

351. Kothapalli CR, Ramamurthi A. Biomimetic Regeneration of Elastin Matrix Structures Using Hyaluronan and Copper Ion Cues. Tissue Eng. 2008;In Press.

352. Ashworth JL, Murphy G, Rock MJ, Sherratt MJ, Shapiro SD, Shuttleworth CA. Fibrillin degradation by matrix metalloproteinases: implications for connective tissue remodelling. Biochem J. 1999;340:171-181.

353. Shapiro SD. Matrix metalloproteinase degradation of extracellular matrix: biological consequences. Curr Opin Cell Biol. 1998;10:602-608.

354. Jacob MP. Extracellular matrix remodeling and matrix metalloproteinases in the vascular wall during ageing and in pathological conditions. Biomed Pharmacol. 2003;57:195-200.

355. D'Armiento J. Decreased elastin in vessel walls puts the pressure on. J Clin Invest. 2003;112:1308-1310.

356. Safar ME, Levy BI, Struijker-Boudier H. Current perspectives on arterial stiffness and pulse pressure in hypertension and cardiovascular diseases. Circulation. 2003;107:2864-2869.

357. Franzblau C. Elastin. Comprehensive Biochem. 1971;26c:659-712.

358. Cleary EG, Gibson MA. Elastin-associated microfibrils and microfibrillar proteins. Int Rev Connect Tissue Res. 1983;10:97-209.

359. Opitz F, Schenke-Layland K, Cohnert TU, Starcher B, Halbhuber KJ, Martin DP, Stock UA. Tissue engineering of aortic tissue: dire consequence of suboptimal elastic fiber synthesis in vivo. Cardiovasc Res. 2004;63(4):719-730.

360. Kothapalli CR, Taylor PM, Smolenski RT, Yacoub MH, Ramamurthi A. TGF-β1 and Hyaluronan Oligomers Synergistically Enhance Elastin Matrix Regeneration by Vascular Smooth Muscle Cells. Tissue Eng. 2008;In Press.

361. Kagan HM, Cai P. Isolation of active site peptides of lysyl oxidase. Methods Enzymol. 1995;258:122-132.

362. Wills A, Thompson MM, Crowther M, Sayers RD, Bell PR. Pathogenesis of abdominal aortic aneurysms—cellular and biochemical mechanisms. Eur J Vasc Endovasc Surg. 1996;12:391-400.

363. Juvonen J, Surcel HM, Satta J, Teppo AM, Bloigu A, SyrjalaH et al. Elevated circulating levels of inflammatory cytokines in patients with abdominal aortic aneurysm. Arterioscler Thromb Vasc Biol. 1997;17:2843–2847.

364. Werb Z, Bainton DF, Jones PA. Degradation of connective tissue matrices by macrophages. J Exp Med. 1989;152:1340-1356.

365. Senior RM, Cornelly NL, Cury JD. Elastin degradation by human alveolar macrophages: a prominent role of metalloproteinase activity. Am Rev Respir Dis. 1989;139:1251-1256.

366. Hinek A, Wrenn DS, Mecham RP, Barondes SH. The elastin receptor: a galactoside-binding protein. Science. 1988;239:1539-1541.

367. Bostrom K. Insights into the mechanism of vascular calcification. Am J Cardiol. 2001;88:20E-22E.

368. Proudfoot D, Shanahan CM. Biology of calcification in vascular cells: intima versus media. Herz. 2001;26:245-251.

369. Niederhoffer N, Lartaud-Idjouadiene I, Giummelly P, Duvivier C, Peslin R, Atkinson J. Calcification of medial elastic fibers and aortic elasticity. Hypertension. 1997;29:999-1006.

370. Ross R. The pathogenesis of atherosclerosis: a perspective for the 1990s. Nature. 1993;362:801-809.

371. Libby P. Inflammation in atherosclerosis. Nature. 2002;420:868-874.

372. Dollery CM, Libby P. Atherosclerosis and proteinase activation. Cardiovasc Res. 2006;69:625-635.

373. Kahari VM, Chen YQ, Bashir M, Rosenbloom J, Uitto J. Tumor necrosis factor-α down-regulates human elastin gene expression. J Biol Chem. 1992;267:26134−26141.

374. Galis ZS, Khatri JJ. Matrix metalloproteinases in vascular remodeling and atherogenesis: the good, the bad, and the ugly. Circ Res. 2002;90(3):251-262.

375. Hiraga S, Kaji T, Ueda Y, Zisaki F, Iwata I, Koizumi F, Okada Y, Katsuda S, Nakanishi I. Modulation of Collagen Synthesis by Tumor Necrosis Factor Alpha in Cultured Vascular Smooth Muscle Cells. Life Sciences. 2000;66(3):235-244.

376. Solis-Herruzo JA, Brenner DA, Chojkier M. Tumor necrosis factor alpha inhibits collagen gene transcription and collagen synthesis in cultured human fibroblasts. J Biol Chem. 1988;263:5841-5845.

377. Blum A, Miller H. Role of cytokines in heart failure. Am Heart J. 1998;135:181-186.

378. Mann DL, Young JB. Basic mechanisms in congestive heart failure: Recognizing the role of proinflammatory cytokines. Chest. 1994;105:897-904.

379. Rabinovitch M. Elastase and cell matrix interactions in the pathobiology of vascular disease. Acta Paediatr Jpn. 1995;36(6):657-666.

380. Micheau O, Tschopp J. Induction of TNF receptor I-mediated apoptosis via two sequential signaling complexes. Cell. 2003;114:181-190.

381. Wang Z, Rao PJ, Castresana MR, Newman WH. TNF-a induces proliferation or apoptosis in human saphenous vein smooth muscle cells depending on phenotype. Am J Physiol Heart Circ Physiol. 2005;288:H293-H301.

382. Mariani TJ, Arikan MC, Pierce RA. Fibroblast tropoelastin and alpha-smooth-muscle actin expression are repressed by particulate-activated macrophage-derived tumor necrosis factor-alpha in experimental silicosis. Am J Respir Cell Mol Biol. 1999;21(2):185-192.

383. Solis-Herruzo JA, Brenner DA, Chojkier M. Tumor necrosis factor alpha inhibits collagen gene transcription and collagen synthesis in cultured human fibroblasts. J Biol Chem. 1988;263:5841-5845.

384. Matsuoka M, Pham NT, Tsukamoto H. Differential effects of interleukin-1 alpha, tumor necrosis factor alpha, and transforming growth factor beta 1 on cell proliferation and collagen formation by cultured fat-storing cells. Liver. 1989;9:71-78.

385. Evanko SP, Angello JC, Wight TN. Formation of hyaluronan- and versican-rich pericellular matrix is required for proliferation and migration of vascular smooth muscle cells. Arterioscler Thromb Vasc Biol. 1999;19(4):1004-1013.

386. Diehm N, Dick F, Schaffner T, Schmidli J, Kalka C, Di Santo S, Voelzmann J, Baumgartner I. Novel Insight Into the Pathobiology of Abdominal Aortic Aneurysm and Potential Future Treatment Concepts. Prog Cardiovasc Dis. 2007;50(3):209-217.

387. Pearce WH, Shively VP. Abdominal aortic aneurysm as a complex multifactorial disease: interactions of polymorphisms of inflammatory genes, features of autoimmunity, and current status of MMPs. Ann N Y Acad Sci. 2006;1085:117-132.

388. Kanno Y, Into T, Lowenstein CJ, Matsushita K. Nitric oxide regulates vascular calcification by interfering with TGF- signalling. Cardiovasc Res. 2008;77(1):221-230.

389. Longo GM, Xiong W, Greiner TC, Zhao Y, Fiotti N, Baxter BT. Matrix metalloproteinases 2 and 9 work in concert to produce aortic aneurysms. J Clin Invest. 2002;110:625-632.

390. Chiou AC, Chiu B, Pearce WH. Murine aortic aneurysm produced by periarterial application of calcium chloride. J Surg Res. 2001;99:371-376.

391. Powell J. Models of arterial aneurysm: for the investigation of pathogenesis and pharmacotherapy-a review. Atherosclerosis. 1991;87(2-3):93-102.

392. Wills A, Thompson MM, Crowther M, Brindle NP, Nasim A, Sayers RD, Bell PR. Elastase-induced matrix degradation in arterial organ cultures: an in vitro model of aneurysmal disease. J Vasc Surg. 1996;24(4):667-679.

393. Anidjar S, Salzmann JL, Gentric D, Lagneau P, Camilleri JP, Michel JB. Elastase-induced experimental aneurysms in rats. Circulation. 1990;82:973-981.

394. Gertz SD, Kurgan A, Eisenberg D. Aneurysm of the rabbit common carotid artery induced by periarterial application of calcium chloride in vivo. J Clin Invest. 1988;81:649-656.

395. Isenburg JC, Simionescu DT, Starcher BC, Vyavahare NR. Elastin stabilization for treatment of abdominal aortic aneurysms. Circulation. 2007;115(13):1729-1737.

396. Kondo S, Hashimoto N, Kikuchi H, Hazama F, Kataoka H. Apoptosis if medial smooth muscle cells in the development of saccular cerebral aneurysms in rats. Stroke. 1998;29(1):181-188.